Electric Motor Control

Electric Motor Control

DC, AC, and BLDC Motors

Sang-Hoon Kim

Department of Electrical & Electronics Engineering,
Kangwon National University



elsevier.com

Hesai Exhibit 1030, page 2

Elsevier
Radarweg 29, PO Box 211, 1000 AE Amsterdam, Netherlands
The Boulevard, Langford Lane, Kidlington, Oxford OX5 1GB, United Kingdom
50 Hampshire Street, 5th Floor, Cambridge, MA 02139, United States

Copyright © 2017 Elsevier Inc. All rights reserved.

No part of this publication may be reproduced or transmitted in any form or by any means, electronic or mechanical, including photocopying, recording, or any information storage and retrieval system, without permission in writing from the publisher. Details on how to seek permission, further information about the Publisher's permissions policies and our arrangements with organizations such as the Copyright Clearance Center and the Copyright Licensing Agency, can be found at our website: www.elsevier.com/permissions.

This book and the individual contributions contained in it are protected under copyright by the Publisher (other than as may be noted herein).

Notices
Knowledge and best practice in this field are constantly changing. As new research and experience broaden our understanding, changes in research methods, professional practices, or medical treatment may become necessary.

Practitioners and researchers must always rely on their own experience and knowledge in evaluating and using any information, methods, compounds, or experiments described herein. In using such information or methods they should be mindful of their own safety and the safety of others, including parties for whom they have a professional responsibility.

To the fullest extent of the law, neither the Publisher nor the authors, contributors, or editors, assume any liability for any injury and/or damage to persons or property as a matter of products liability, negligence or otherwise, or from any use or operation of any methods, products, instructions, or ideas contained in the material herein.

Library of Congress Cataloging-in-Publication Data
A catalog record for this book is available from the Library of Congress

British Library Cataloguing-in-Publication Data
A catalogue record for this book is available from the British Library

ISBN: 978-0-12-812138-2

For Information on all Elsevier publications
visit our website at https://www.elsevier.com/books-and-journals



Publisher: Joe Hayton
Acquisition Editor: Lisa Reading
Editorial Project Manager: Edward Payne
Production Project Manager: Anusha Sambamoorthy
Cover Designer: Greg Harris

Typeset by MPS Limited, Chennai, India

Preface

Owing to rapidly increasing energy costs and global interest in reducing carbon dioxide emissions, electric motors have recently become one of the most important prime movers that produce mechanical power. Recently, in many mechanical systems, traditional prime movers such as a hydraulic system, a steam turbine, a gas turbine, and an internal combustion engine are being rapidly replaced by electric motor drive systems, which are more efficient, controllable, and environment-friendly. Currently, electric motor drive systems are playing an important role in improving convenience in many areas of our lives including home appliances, office machines, transportation, and industrial machines.

The main aim of this book is to introduce practical drive techniques of electric motors for supporting stable, efficient control of such application systems, covering basic principles to high-performance motor control techniques.

Nowadays, the most widely used motors are classic direct current (DC) and alternating current (AC) motors (induction motor and synchronous motor). Besides these motors, there is a brand new brushless direct current (BLDC) motor. To control these motors efficiently, we will do a comprehensive study of fundamental operating principles, driving methods of electric motors, related control theories, and power converters for driving a motor. Many people do not have the background knowledge in these areas and may need to obtain these contents from various books. Therefore, this book is designed optimally for studying these contents at once and easy learning of difficult control principles. Furthermore, this book provides simulation examples for key subjects using MATLAB/Simulink tool and offers practical control techniques for industrial motor drive applications currently in use.

This book is the English version of my book titled *DC, AC, BLDC Motor Control*, which was first published in August 2007, in Korean. This book is based on my wide research experience in the electric motor control field over the past 20 years. During 20 years of teaching at my university, I realized that many students struggled with mastering the control of electric motors due to the complexity and difficulty of existing textbooks. Therefore, the main goal of this textbook was to address this issue by presenting the material in a straightforward way for the students to understand. As a result, this book gained popularity, and I received many appreciation letters from students and engineers after publishing the book, expressing gratitude for presenting the material well. I have also been invited many times to speak at seminars regarding the materials presented in the book.

The contents of this book are as follows.

Chapter 1, Fundamentals of electric motors, introduces the fundamental operating principle needed to understand electric motors and describes clear differences among the motors by comparing their operating principles.

Chapter 2, Control of direct current motors, describes DC motors, which used to be the typical motor for speed control and torque control, and the concept of

Hesai Exhibit 1030, page 4

torque control for DC motors, which will be helpful for understanding the vector control for torque control of AC motors. Furthermore, this chapter goes into detail about the design of the current and speed controllers of DC motors, which is readily applicable to the current and speed controllers of AC motors.

Chapter 3, Alternating current motors: synchronous motor and induction motor, discusses the basic characteristics of AC motors, including synchronous and induction motors, which are widely used for industrial motors. These characteristics can provide a basis for studying high-performance motor control, which will be described later in the book.

Chapters 4−8 discuss the high-performance motor control systems of AC motors for industrial motor drive applications as follows:

Chapter 4, Modeling of alternating current motors and reference frame theory—the modeling of AC motors and $d-q$ reference frame theory for control of AC motors,

Chapter 5, Vector control of alternating current motors—the concept of the vector control and its implementation for AC motors,

Chapter 6, Current regulator of alternating current motors—the design of current controller for the vector control system,

Chapter 7, Pulse width modulation inverter—the PWM inverter and its various techniques for AC motor drives,

Chapter 8, High-speed operation of alternating current motors—the field-weakening control for high-speed operations of AC motors.

Chapter 9, Speed estimation and sensorless control of alternating current motors, describes the position/speed sensors and speed estimation required for the motor control. In additional, sensorless control, which is a state-of-the-art technique in the motor control area, is explored briefly.

Chapter 10, Brushless direct current motors) deals with BLDC motors, which are not classical motors but mostly used in small motor drive systems. The operation principle, drive methods, PWM methods, and sensorless control schemes of BLDC motors are also explored in detail.

Chapters 1−3, and 10 will be adequate for providing technical background of motor control for undergraduates in a one-semester course, while Chapters 4−9 will be suitable for graduate students and engineers with the necessary background for understanding high-performance motor control systems.

I am certain that this book will be able to equip one with complete techniques for controlling electric motors required for industrial applications.

The companion web site of the book can be found at: https://www.elsevier.com/books-and-journals/book-companion/9780128121382

Sang-Hoon Kim
Seoul, November 2016

Hesai Exhibit 1030, page 5

CHAPTER

1 Fundamentals of electric motors

A moving object that has either a linear motion or rotary motion is powered by a prime mover. A prime mover is an equipment that produces mechanical power by using thermal power, electricity, hydraulic power, steam, gas, etc. Examples of the prime mover include a gas turbine, an internal combustion engine, and an electric motor. Among these, the electric motors have recently become one of the most important prime movers and their use is increasing rapidly. Nearly 70% of all the electricity used in the current industry is used to produce electric power in the motor-driven system [1].

Electric motors can be classified into two different kinds according to the type of the power source used as shown in Fig. 1.1: direct current (DC) motor and alternating current (AC) motor. The recently developed *brushless DC motor* is hard to be classified as either one of the motors since its configuration is similar to that of a permanent magnet synchronous motor (AC motor), while its electrical characteristics are similar to those of a DC motor.

The first electric motor built was inspired by Michael Faraday's discovery of electromagnetic induction. In 1831, Michael Faraday and Joseph Henry simultaneously succeeded in laboratory experiments in operating the motor for the first time. Later in 1834, M. Jacobi invented the first practical DC motor. The DC motor is the prototype of all motors from the viewpoint of torque production. In 1888, Nikola Tesla was granted a patent for his invention of AC motors, which include a synchronous motor, a reluctance motor, and an induction motor. By 1895, the three-phase power source, distributed stator winding, and the squirrel-cage rotor had been developed sequentially. Through these developments, the three-phase induction motors were finally made available for commercial use in 1896 [2].

Traditionally among the developed motors, DC motors have been widely used for speed and position control applications because of the ease of their torque control and excellent drive performance. On the other hand, induction motors have been widely used for a general purpose in constant-speed applications because of their low cost and rugged construction. Induction motors account for about 80% of all the electricity consumed by motors.

Until the early 1970s, major improvement efforts were made mainly toward reducing the cost, size, and weight of the motors. The improvement in magnetic material, insulation material, design and manufacturing technology has played a

Electric Motor Control. DOI: http://dx.doi.org/10.1016/B978-0-12-812138-2.00001-5
© 2017 Elsevier Inc. All rights reserved.

Hesai Exhibit 1030, page 6

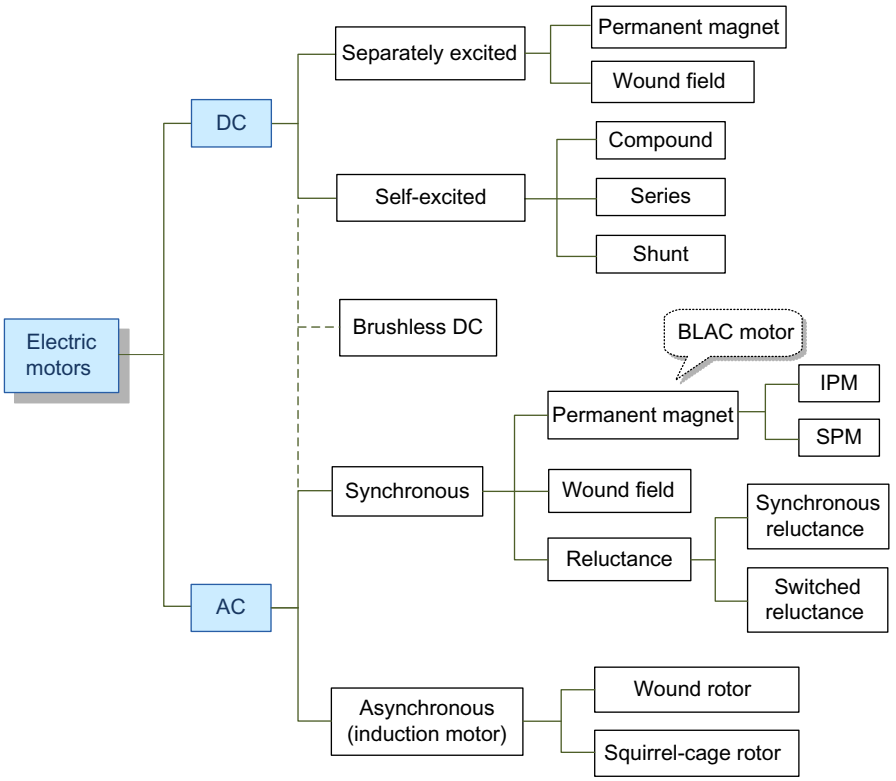


FIGURE 1.1

Classification of electric motors: AC motor and DC motor.

major role and made a big progress. As a result, a modern 100-hp motor is the same size as a 7.5-hp motor used in 1897. With the rising cost of oil price due to the oil crisis in 1973, saving the energy costs has become an especially important matter. Since then, major efforts have been made toward improving the efficiency of the motors. Recently, rapidly increasing energy costs and a strong global interest in reducing carbon dioxide emissions have been encouraging industries to pay more attention to high-efficiency motors and their drive systems [1].

Along with the improvement of motors, there have been many advances in their drive technology. In the 1960s, the advent of power electronic converters using power semiconductor devices enabled the making of motors with operation characteristics tailored to specific system applications. Moreover, using microcontrollers with high-performance digital signal processing features allowed the engineers to apply advanced control techniques to motors, greatly increasing the performance of motor-driven systems.

1.1 FUNDAMENTAL OPERATING PRINCIPLE OF ELECTRIC MOTORS

1.1.1 CONFIGURATION OF ELECTRIC MOTORS

An electric motor is composed of two main parts: a stationary part called the *stator* and a moving part called the *rotor* as shown in Fig. 1.2. The air gap between the stator and the rotor is needed to allow the rotor to spin, and the length of the air gap can vary depending on the kind of motors.

The stator and the rotor part each has both an electric and a magnetic circuit. The stator and the rotor are constructed with an iron core as shown in Fig. 1.3, through which the magnetic flux created by the winding currents will flow and which plays a role of supporting the conductors of windings. The current-carrying

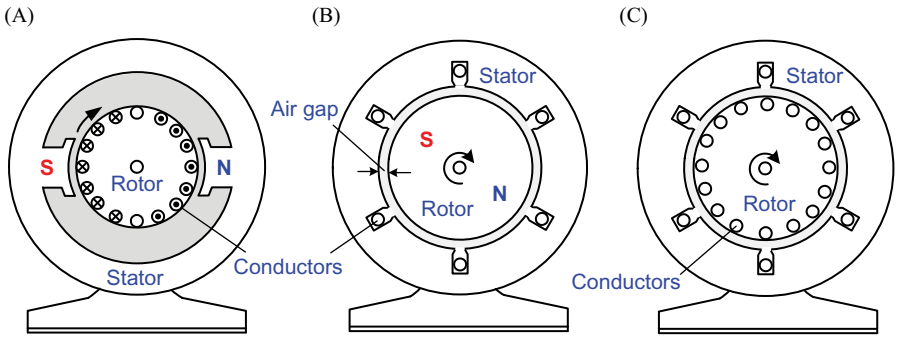


FIGURE 1.2

Configuration of electric motors. (A) DC motor, (B) AC synchronous motor, and (C) AC induction motor.

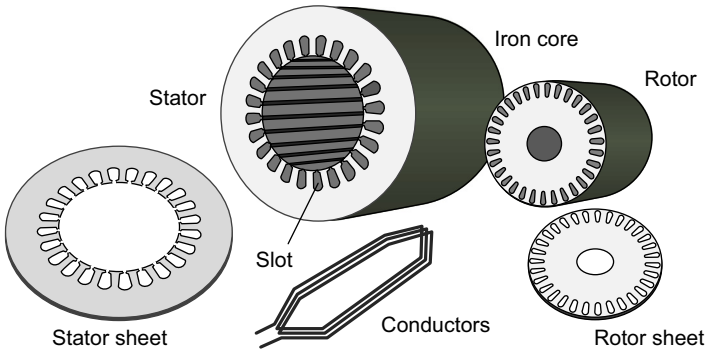


FIGURE 1.3

Electric and magnetic parts of electric motors.

conductors inserted into slots in the iron core form the electric circuit. When the current flows in these conductors, a magnetic field is created through the iron core, and the stator and the rotor each becomes an electromagnet.

To obtain a greater magnetic flux for a given current in the conductors, the iron core is usually made up of ferromagnetic material with high magnetic permeability, such as silicon steel. In some cases, the stator or the rotor creates a magnetic flux by using a permanent magnet.

1.1.2 BASIC OPERATING PRINCIPLE OF ELECTRIC MOTORS

All electric motors are understood to be rotating based on the same operating principle. As shown in Fig. 1.4A, there are generally two magnetic fields formed inside the motors. One of them is developed on the stationary stator and the other one on the rotating rotor. These magnetic fields are generated through either energized windings, use of permanent magnets, or induced currents. A force produced by the interaction between these two magnetic fields gives rise to a torque on the rotor and causes the rotor to turn. On the other hand, some motors, such as the reluctance motor, use the interaction between one magnet field and a magnetic material, such as iron, but they cannot produce a large torque (Fig. 1.4B). Most motors in commercial use today including DC, induction, and synchronous motors exploit the force produced through the interaction between two magnetic fields to produce a larger torque.

The torque developed in the motor must be produced continuously to function as a motor driving a mechanical load. Two motor types categorized according to the used power source, i.e., DC motor and AC motor, have different ways of achieving a continuous rotation. Now, we will take a closer look at these methods for achieving a continuous rotation.

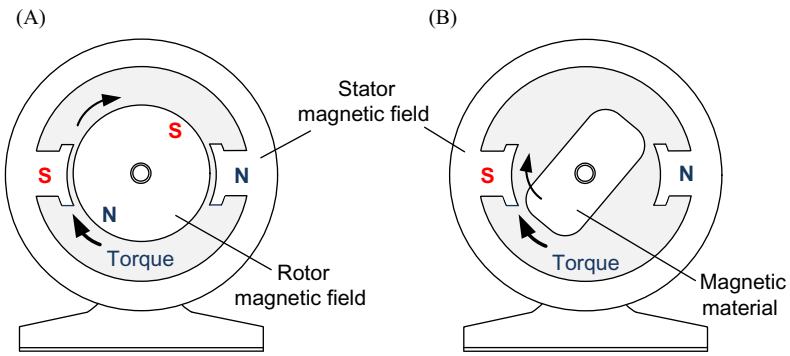


FIGURE 1.4

Rotation of electric motors. (A) Two magnetic fields and (B) one magnetic field and magnetic material.

1.1.2.1 Direct current motor

The simple concept for the rotation of a DC motor is that the rotor rotates by using the force produced on the current-carrying conductors placed in the magnetic field created by the stator as shown in Fig. 1.5A. Alternatively, we can consider the operating principle of a DC motor from the viewpoint of two magnetic fields as shown in Fig. 1.4A as follows.

There are two stationary magnetic fields in a DC motor as shown in Fig. 1.5B. One stationary magnetic field is the stator magnetic field produced by magnets or a field winding. The other is the rotor magnetic field produced by the current in the conductors of the rotor. It is important to note that the rotor magnetic field is also stationary despite the rotation of the rotor. This is due to the action of brushes and commutators, by which the current distribution in the rotor conductors is always made the same regardless of the rotor's rotation as shown in Fig. 1.5A. Thus the rotor magnetic field will not rotate along with the rotor. A consistent interaction between these two stationary magnetic fields produces a torque, which causes the rotor to turn continuously. We will study the DC motor in more detail in Chapter 2.

1.1.2.2 Alternating current motor

Unlike DC motors that rotate due to the force between two stationary magnetic fields, AC motors exploit the force between *two rotating magnetic fields*. In AC motors both the stator magnetic field and the rotor magnetic field rotate, as shown in Fig. 1.6.

As it will be described in more detail in Chapter 3, these two magnetic fields always rotate at the same speed and, thus, are at a standstill relative to each other and maintain a specific angle. As a result, a constant force is produced between them, making the AC motor is to run continually. The operating principle of the

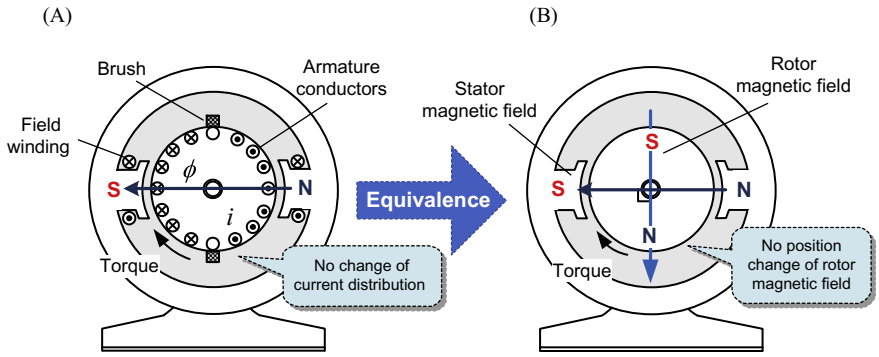


FIGURE 1.5

Operating principle of the DC motor. (A) Rotor current and stator magnetic field and (B) two magnetic fields.

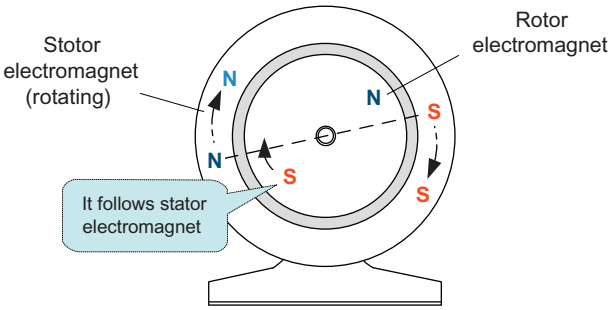


FIGURE 1.6

Operating principle of the AC motor.

AC motor is that the force produced by the interaction between the two rotating magnetic fields causes the rotor to turn.

In AC motors, the rotating magnetic field on the stator is created by three-phase currents. When a three-phase AC power source is applied to the three-phase stator windings of the AC motor, the three-phase currents flowing in these windings create a rotating magnetic field. We will examine the rotating magnetic field in more detail in Chapter 3.

There are two kinds of AC motors: a *synchronous motor* and an *induction (asynchronous) motor*. They generate the rotor magnetic field differently, whereas they generate the stator magnetic field in the same way. In a synchronous motor as depicted in Fig. 1.2B, the magnetic field on the rotor is generated either by a permanent magnet or by a field winding powered by a DC power supply separated from the stator AC power source. In this motor, the rotor magnetic field is stationary relative to the rotor. Hence, to produce a torque, the rotor should rotate at the same speed as the stator rotating magnetic field. This speed is called the *synchronous speed*. This is why this motor is referred to as the *synchronous motor*.

On the other hand, in an induction motor as shown in Fig. 1.2C, the rotor magnetic field is generated by the AC power. The AC power used in the rotor excitation is transferred from the stator by electromagnetic induction. Because of this crucial feature, this motor is referred to as the *induction motor*. In an induction motor, the rotor magnetic field rotates relative to the rotor at some speed. To produce a torque, the stator and the rotor rotating magnetic fields should rotate at the same speed. This requires that the rotor itself rotate at the speed difference between the stator and rotor rotating magnetic fields. More precisely, the rotor rotating magnetic field rotates at the speed difference between the stator rotating magnetic field and the rotor. To use the rotor excitation by electromagnetic induction, the rotor speed should always be less than the synchronous speed. Thus the induction motor is also called the *asynchronous motor*.

Among the motors, DC motors have largely been used for speed and torque control because of their simplicity. Their simplicity comes from the fact that the speed of a DC motor is proportional to the voltage, and its torque is proportional

to the current. However, since DC motors require periodic maintenance of the brushes and commutators, the trend has recently moved toward employing maintenance-free AC motors as they can offer high performance at a reasonable price.

As mentioned earlier, electric motors can operate on the fundamental principle that the torque produced from the interaction between the magnetic fields generated in the stator and the rotor causes the motor to run. Now, we will take a look at the requirements that ensure continuous torque production by the motor.

1.2 REQUIREMENTS FOR CONTINUOUS TORQUE PRODUCTION [3]

An electric motor is a type of electromechanical energy conversion device that converts electric energy into mechanical energy. The principle of torque production in a motor can be understood by analyzing its energy conversion process. Electromechanical energy conversion devices normally use the magnetic field as an intermediate in their energy conversion processes. Thus an electromechanical energy conversion device is composed of three different parts: the *electric system*, *magnetic system*, and *mechanical system* as shown in Fig. 1.7.

Now, we will examine the mechanism of torque production of a motor by looking at how the force (or torque) is being produced inside the electromechanical energy conversion device.

To evaluate the force (or torque) produced inside the energy conversion devices, we will apply the law of conservation of energy: "within an isolated system, energy can be converted from one kind to another or transferred from one place to another, but it can neither be created nor destroyed." Therefore the total amount of energy is constant. Fig. 1.8 shows an application of the law of conservation of energy when the electromechanical energy conversion device is acting as a motor.

Suppose that electric energy dW_e is supplied to the energy conversion device during the differential time interval dt. The supplied electric energy dW_e is converted to field energy dW_f in the magnetic system, and to mechanical energy dW_e in the mechanical system.

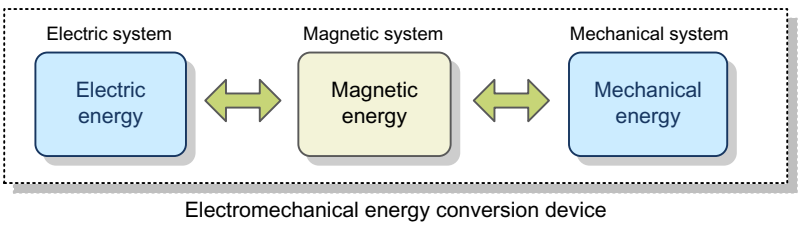


FIGURE 1.7

Electromechanical energy conversion.

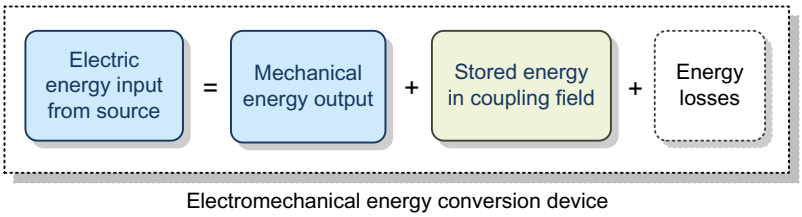


FIGURE 1.8

Equation of energy conservation for a motor.

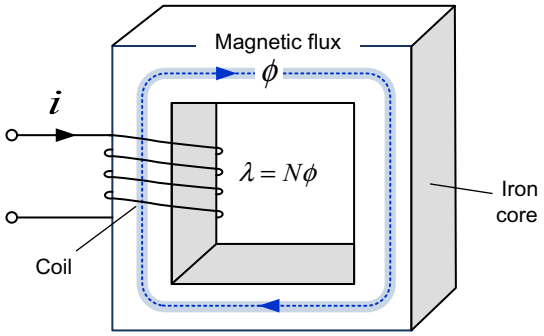


FIGURE 1.9

Coil wound on an iron core.

In addition a small amount of electric energy dW_e is converted into losses in each of the three parts: copper losses in an electric system, core losses such as hysteresis and eddy current losses in a magnetic system, and mechanical losses such as friction and windage losses. Since these losses may be dissipated in the form of heat or noise, we can leave out these losses in the process of evaluating the force or torque production in the energy conversion process. Therefore the energy conversion equation in Fig. 1.8 may be written as

$$dW_e = dW_f + dW_m \tag{1.1}$$

1.2.1 MAGNETIC ENERGY

In electric machines, including a motor, the magnetic flux is normally produced by the coil wound on an iron core as shown in Fig. 1.9. Because ferromagnetic materials such as an iron core have high permeability, much greater magnetic flux can be developed in the iron core for a given current than when the magnetic flux is developed in the air. Now, we will take a look at magnetic energy W_f stored in the magnetic system, where magnetic flux ϕ is developed in the iron core as shown in Fig. 1.9.

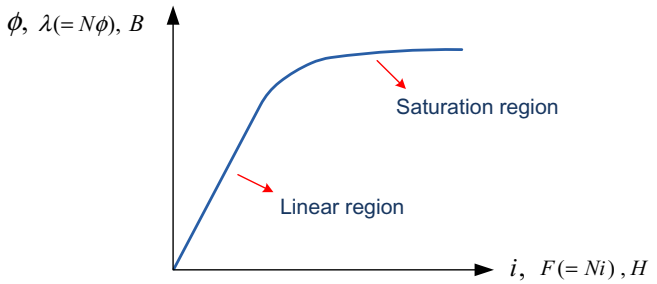


FIGURE 1.10

Flux–current characteristic.

First, we need to know the relationship between the magnetic flux ϕ produced in the core and the coil current i in this magnetic system. Fig. 1.10 demonstrates this relationship, which is the *B-H* characteristic called *magnetization curve*. In the beginning of the curve, the magnetic flux ϕ increases rapidly in proportion to the increase in the coil current i until it reaches a certain value. The region where the magnetic flux is linearly related to the applied current like this is called the *linear region* or *unsaturated region*.

However, above that certain value, further increases in the current produce relatively smaller increases in the magnetic flux. Eventually an increase in the current will produce almost no change at all in the magnetic flux. The region where the curve flattens out is called the *saturation region*, and the iron core is said to be saturated. When the saturation occurs, any further increase in the current will have little or no effect on the increase of the flux. In electric machines, the magnetic flux is designed to be produced as much as possible because their torque is directly proportional to the magnetic flux. Thus most electric machines normally operate near the knee of the magnetization curve, which is the transition range between the two regions.

Electric machines produce the magnetic flux by using coils, which normally consist of many turns. Thus, instead of the magnetic flux ϕ, the concept of flux linkage λ as a product of the number of turns N and the magnetic flux ϕ linking each turn is introduced. The flux linkage of N-turn coil can be given by

$$\lambda = N\phi \quad \text{(Wb-turns)} \tag{1.2}$$

The flux linkage λ can also be related to the coil current i by the definition of inductance L through the following relation.

$$L = \frac{\lambda}{i} = N\frac{\phi}{i} \quad \text{(H or Wb/A)} \tag{1.3}$$

A larger inductance value of the magnetic system implies that the same current can produce a larger flux linkage. Eq. (1.3) shows that the slope of the curve in Fig. 1.10 is the inductance of this magnetic system as shown in Fig. 1.11.

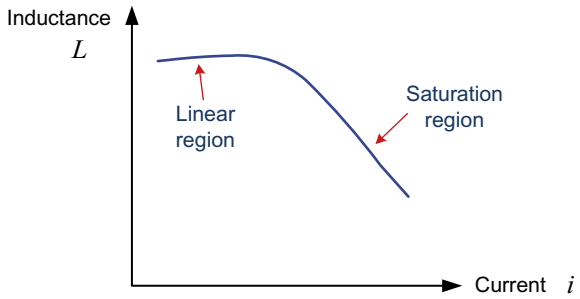


FIGURE 1.11

Inductance of the coil.

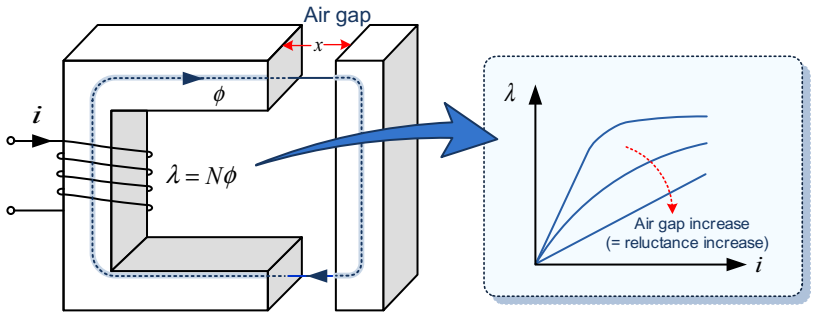


FIGURE 1.12

Flux–current characteristic according to the variation of an air-gap length.

The inductance is large and relatively constant in the unsaturated region but gradually drops to a very low value as the core becomes heavily saturated.

Now, we will take a look at magnetic energy W_f stored in the magnetic system, where magnetic flux ϕ is developed in the iron core as shown in Fig. 1.12.

The $\lambda - i$ characteristic of the magnetic system varies with the air-gap length x. Thus the inductance $L(x)$ of the coil is expressed as a function of the air-gap length x. As the air-gap length x increases, the slope of the $\lambda - i$ curve becomes smaller and results in smaller inductance as shown in Fig. 1.12.

The inductance L of the magnetic system is inversely related to its *reluctance* $\mathfrak{R}$, which is defined as the ratio of *magnetomotive force* (mmf) $F(=Ni)$ to magnetic flux ϕ, as in the following relation.

$$L = \frac{\lambda}{i} = \frac{N\phi}{i} = \frac{N^2}{\mathfrak{R}} \propto \frac{1}{\mathfrak{R}} \quad (F = \mathfrak{R}\phi = Ni) \tag{1.4}$$

Now, assume that the source voltage v is applied to the terminals of the N-turn coil on the iron core during dt as shown in Fig. 1.13. Then, the current i

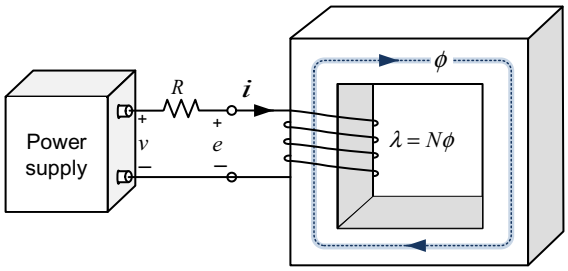


FIGURE 1.13

Magnetic system connected to source voltage.

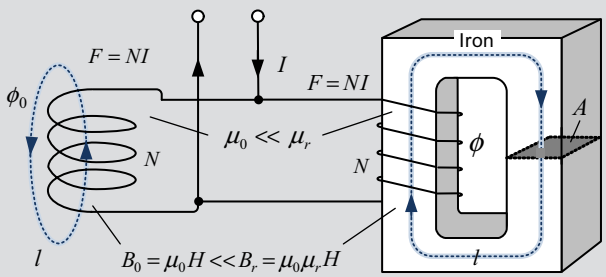
will flow in that coil. The resulting mmf $F(=Ni)$ will produce a magnetic flux ϕ in the core and establish flux linkage $\lambda(=N\phi)$ in the coil. Now, we will discuss the energy stored in the magnetic system.

MAGNETOMOTIVE FORCE (MMF) AND MAGNETIC FLUX

Magnetic flux ϕ is indispensable in producing torque in motors. The force that is capable of producing a magnetic flux is called magnetomotive force or mmf F. In general, mmf is generated by current, so the source of magnetic flux is the current. When the current I is flowing through an N-turn coil, the mmf F is expressed by NI (A-turn), i.e., $F = NI$. For a given mmf, the magnitude of the developed flux depends on the length of the closed-path through which the flux passes. The longer the length, the lower the flux density will be. Thus the magnetic field intensity H, which represents mmf per length, will be used instead of the mmf.

$$mmf = F = NI = \oint Hdl \rightarrow H = \frac{mmf}{l} = \frac{NI}{l} \quad (\text{A/m})$$

Also, for a given magnetic field intensity, the flux density will be different depending on the material through which the flux passes. For example, high flux density can be created in iron or steel but not in air gap as in the following figure.



This magnetic characteristic can be described in terms of relative permeability μ_r in reference to permeability μ_0 of free space. Thus the magnetic flux density B produced by the current can be represented as

$$B = \mu_0 \mu_r H \quad (\text{Wb/m}^2)$$

(*Continued*)

MAGNETOMOTIVE FORCE (MMF) AND MAGNETIC FLUX (CONTINUED)

The total magnetic flux flowing through the cross section A of a magnetic circuit in an uniform magnetic flux density B can be expressed as

$$\phi = \int_A B \cdot ndA = BA\cos\theta \quad \text{(Wb)}$$

where θ is the angle between the magnetic field lines and the surface A. Similar to the relation between the current and the voltage by Ohm's law in the electric circuit, there is a following relationship between the mmf F and the flux ϕ in the magnetic circuit.

$$F = \mathfrak{R}\phi$$

where $\mathfrak{R}$ is called reluctance and is inversely proportional to permeability.

In the system of Fig. 1.13, the electric energy dW_e supplied during the differential time interval is expressed from input power $P(=vi)$ as

$$dW_e = Pdt = vidt \tag{1.5}$$

The supplied electric energy after subtracting the copper loss produced by current in the coil is stored as the magnetic field energy. i.e.

$$dW_f = (vi - Ri^2)dt = (vi - Ri)dt = eidt \tag{1.6}$$

where e is back-EMF voltage induced in the coil.

Since the back-EMF voltage e on the N-turn coil is proportional to the rate of change of flux linkage λ with time, i.e., $e = d\lambda/dt$, Eq. (1.5) can be given by

$$dW_f = eidt = id\lambda \tag{1.7}$$

When the flux linkage is increased from zero to λ, the total energy stored in the magnetic system is

$$dW_f = \int_0^{\lambda} id\lambda \tag{1.8}$$

This magnetic energy is the area to the left of the $\lambda - i$ curve as shown in Fig. 1.14. On the other hand, the area to the right of $\lambda - i$ curve is known as *coenergy* W'_f, which is a useful quantity for the calculation of force and can be expressed as

$$W'_f = \int_0^{\lambda} \lambda di \tag{1.9}$$

For the linear system in which the $\lambda - i$ curve is a straight line, the magnetic energy is equal to the coenergy. The magnetic system that has an air gap in the flux path becomes a linear system.

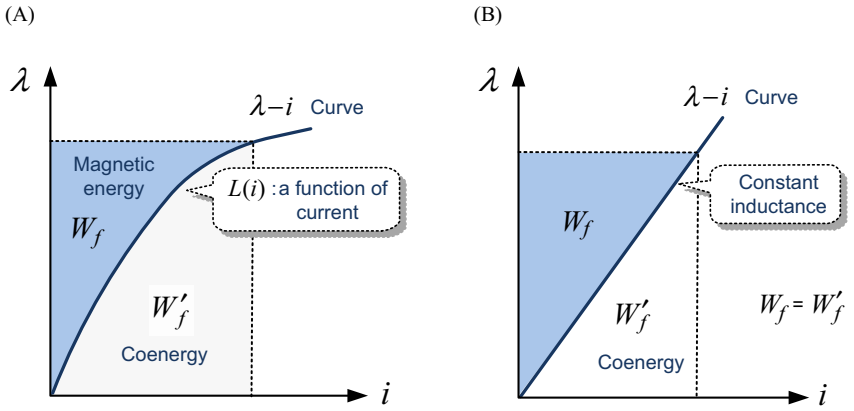


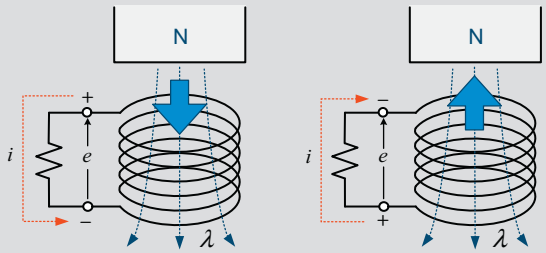
FIGURE 1.14

Magnetic energy in the flux–current characteristic. (A) Linear system and (B) nonlinear system.

BACK-ELECTROMOTIVE FORCE (BACK-EMF), OR INDUCED VOLTAGE *e*

Faraday's law states that the voltage e induced in the turn of a coil is directly proportional to the rate of change in the flux ϕ passing through that turn with respect to time. If there are N turns in the coil and the same flux passes through each turn of the coil, then the total voltage induced on the coil is given by

$$e = N\frac{d\phi}{dt} = \frac{d\lambda}{dt}$$



According to Lenz's law, the direction of the induced voltage opposes the change of the flux that causes it, and thus a minus sign is included in the equation above.

1.2.2 LINEAR MOTION DEVICE

Now, we will look at the force developed inside a movable energy conversion device. Before looking into rotating machines, we will first study the linear motion device, which consists of a fixed part (also called *stator*) and a moving part as shown in Fig. 1.15.

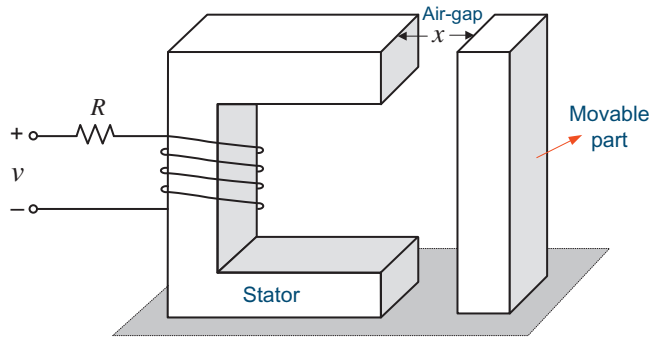


FIGURE 1.15

Linear motion device.

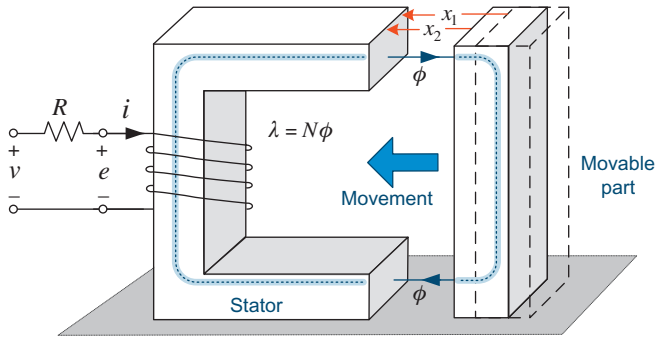


FIGURE 1.16

Movement of the movable part.

If a magnetic flux is produced by the current flowing through the coil of N turns in this device, then, as seen in everyday experiences, we can easily know that the movable part will move toward the stator as shown in Fig. 1.16. Now, we will discuss the force that causes this motion.

The current I of the coil is assumed to remain the same before and after the movable part moves. Suppose that the movable part moves from position x_1 to position x_2. The length of the air gap is changed as a result of the movement. This also changes the $\lambda - i$ characteristic of the system as shown in Fig. 1.17. The air gap decreases according to the movement, resulting in a decrease of reluctance so that the flux linkage increases from λ_1 to λ_2. The operating point will move from A to B. The trajectory of the movement depends on the moving speed. So, we will find the force acting on the movable part for the two extreme moving speeds.

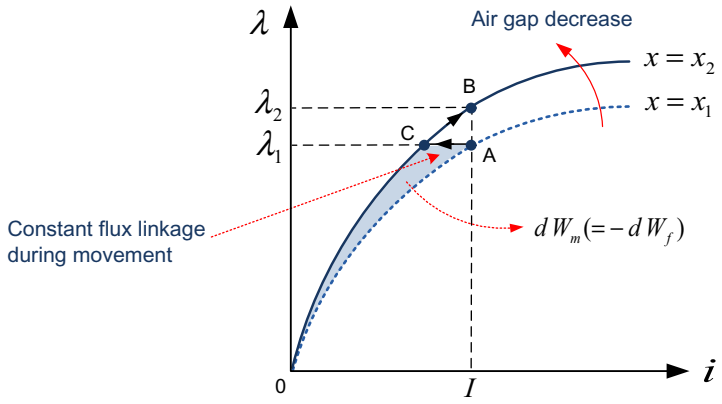


FIGURE 1.17

Flux linkage–current characteristic (rapid movement of the movable part).

First, suppose that the movement occurs very rapidly. In this case, the movement is so rapid that it may be completed before any significant change has occurred in flux linkage λ. Thus, during the movement, the flux linkage λ_1 remains constant so that the operating point moves from A to C as shown in Fig. 1.17.

After the completion of the movement, the flux linkage will be changed from λ_1 to λ_2 and the operating point will move from C to B. During the movement, the flux linkage does not change and this results in zero back-EMF, so the electrical energy input will be zero, i.e. $dW_e = eidt = id\lambda = 0$. Therefore Eq. (1.1) can be written as

$$dW_m = -dW_f \tag{1.10}$$

This equation indicates that the mechanical energy needed for the movement is supplied entirely by the magnetic energy. The amount of the reduced magnetic energy for the movement corresponds to the shaded area OAC of the $\lambda - i$ characteristic.

Considering the force to be defined as the mechanical work done dW_m per displacement dx, the developed force during this movement from Eq. (1.10) is

$$f_m = \frac{dW_m}{dx} = -\frac{dW_f(i,x)}{dx}\bigg|_{\lambda=\text{constant}} \tag{1.11}$$

This implies that the force acts in the direction at which the magnetic energy of the system is decreasing.

Now, we will express the force of Eq. (1.11) in terms of the coil current. Assume for simplicity that the $\lambda - i$ characteristic is linear. The magnetic energy of Eq. (1.8) can be expressed as

$$W_f = \int id\lambda = \int \frac{\lambda}{L(x)} d\lambda = \frac{\lambda^2}{2L(x)} = \frac{1}{2} L(x) i^2 \tag{1.12}$$

By substituting Eq. (1.12) into the force of Eq. (1.11), we obtain

$$f_m = -\left.\frac{dW_f(i,x)}{dx}\right|_{\lambda=\text{constant}} = -\left.\frac{d}{dx}\left(\frac{\lambda^2}{2L(x)}\right)\right|_{\lambda=\text{constant}} = \frac{\lambda^2}{2L^2(x)}\frac{dL(x)}{dx} = \frac{1}{2}i^2\frac{dL(x)}{dx} \tag{1.13}$$

Eq. (1.18) indicates that *the force acts in the direction that increases the inductance of the magnetic system*. Since the direction that increases the inductance is the direction that decreases the length of the air gap, the force is exerted on the movable part moving toward the stator.

From this, we can explain the attractive force between an electromagnet (or magnet) and magnetic materials. When an electromagnet and a magnetic material cling to each other without an air gap, the system has the greatest inductance. Thus an attractive force between the two objects is developed to move them toward each other.

Next, suppose that the movable part moves very slowly. In this case, the current $i = (v - e)/R$ remains constant during the movement. This is because the back-EMF $e(= d\lambda/dt)$ is negligibly small. Therefore the operating point on the $\lambda - i$ characteristic moves upward from A to B as shown in Fig. 1.18.

During this movement the change in the electric energy is given by

$$dW_e = eidt = id\lambda = i(\lambda_2 - \lambda_1) \tag{1.14}$$

This corresponds to the area *ABEF*. In this case, the amount of change in the stored magnetic energy from Eq. (1.8) is given by

$$dW_f = \int_0^{\lambda_2} id\lambda - \int_0^{\lambda_1} id\lambda = \text{Area } OBE - \text{Area } OAF \tag{1.15}$$

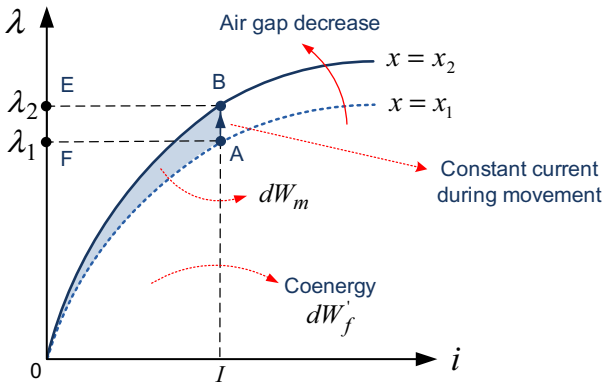


FIGURE 1.18

Flux linkage–current characteristic (very slow movement of the movable part).

Therefore, from Eq. (1.1), the mechanical energy required for the movement is

$$dW_m = dW_e - dW_f \tag{1.16}$$

By substituting Eqs. (1.14) and (1.15) into Eq. (1.16), it can be readily seen that the mechanical energy corresponds to the shaded area OAB of the $\lambda - i$ characteristic and is equal to the increments of coenergy dW'_f. Consequently, the used mechanical energy for the movement is equal to the increments of coenergy dW'_f during the movement as shown in the following.

$$dW_m = dW'_f \tag{1.17}$$

Therefore the developed force during this movement is

$$f_m = \frac{dW_m}{dx} = \left.\frac{dW'_f(i,x)}{dx}\right|_{i=\text{constant}} \tag{1.18}$$

This force acts in the direction of the increasing coenergy of the system.

The force for a slow movement is expressed in the same way as for a rapid movement. For a linear system $dW_f = dW'_f$, by substituting Eq. (1.12) into (1.18), we obtain

$$\begin{aligned} f_m &= \left.\frac{dW'_f(i,x)}{dx}\right|_{i=\text{constant}} = \left.\frac{dW_f(i,x)}{dx}\right|_{i=\text{constant}} \\ &= \left.\frac{d}{dx}\left(\frac{1}{2}L(x)i^2\right)\right|_{i=\text{constant}} = \frac{1}{2}i^2\frac{dL(x)}{dx} \end{aligned} \tag{1.19}$$

This is the same conclusion as was reached in Eq. (1.13), meaning that the force is the same regardless of the moving speed.

This force can also be expressed in terms of the *reluctance* $\mathfrak{R}$. The magnetic energy of Eq. (1.8) expressed as a function of reluctance $\mathfrak{R}$ is

$$W_f = \int_0^{\lambda} id\lambda = \int_0^{\phi} Fd\phi = \int_0^{\phi} \mathfrak{R}\phi d\phi = \frac{1}{2}\mathfrak{R}(x)\phi^2 \tag{1.20}$$

From Eq. (1.20), the force of Eq. (1.11) is

$$f_m = -\frac{d}{dx}\left(\frac{1}{2}\mathfrak{R}(x)\phi^2\right)\Big|_{\phi=\text{constant}} = -\frac{1}{2}\phi^2\frac{d\mathfrak{R}(x)}{dx} \tag{1.21}$$

This means that *the force acts in the direction that decreases the reluctance of the magnetic system*. Since the decrease in the air-gap length causes the reluctance to decrease, the force is exerted on the movable part moving toward the stator. Next, we will discuss the torque production in rotating machines.

1.2.3 ROTATING MACHINE

We will first start examining the machine in Fig. 1.19, which produces a rotational motion. The rotating machine consists of a fixed part (called *stator*) and a moving part (called *rotor*).

The rotor is mounted on a shaft and is free to rotate between the poles of the stator.

The force that causes a rotor to rotate can be expressed as torque, which is the mechanical work done per rotational distance or angle θ as follows:

$$T = \frac{dW_m}{d\theta} \tag{1.22}$$

In the machine shown in Fig. 1.18, when current i_s flows in the stator coil, a magnetic flux is produced, and the developed torque from Eqs. (1.12) and (1.22) acting on the rotor can be expressed as

$$T = \frac{1}{2} i_s^2 \frac{dL(\theta)}{d\theta} = -\frac{1}{2}\phi^2 \frac{d\Re(\theta)}{d\theta} \tag{1.23}$$

This torque results from the variation of reluctance (or inductance) with rotor position, and thus is called the *reluctance torque*. A machine using this torque is known as the *reluctance motor*. For motors of a cylindrical rotor configuration, since the reluctance does not vary with the rotor position, the reluctance torque cannot be produced.

Now, we will take a look at the necessary condition for ensuring that this machine continuously rotates to serve as a motor. First of all, it is not hard to consider that, if there is a DC current flowing in the coil, this machine never operates as a continuously rotating motor. Therefore we will consider the case in which the winding is excited from an AC current $i_s(=I_m\cos\omega_s t)$. In this case, the torque of Eq. (1.23) can be expressed in terms of the stator current i_s and the stator self-inductance L_{ss} as

$$T = \frac{1}{2} i_s^2 \frac{dL_{ss}(\theta)}{d\theta} \tag{1.24}$$

where the inductance $L_{ss}(=\lambda_s/i_s)$ is defined as the ratio of the total flux linkage λ_s in the stator coil to the stator current i_s generating the flux.

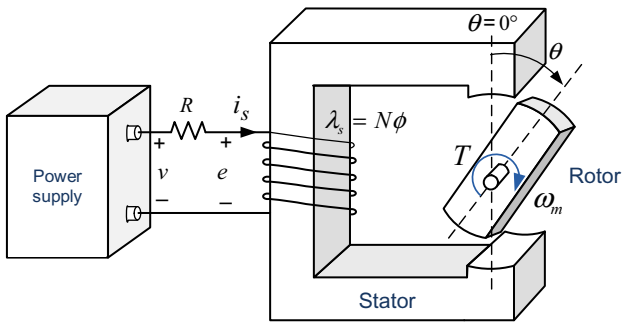


FIGURE 1.19

Rotating machine.

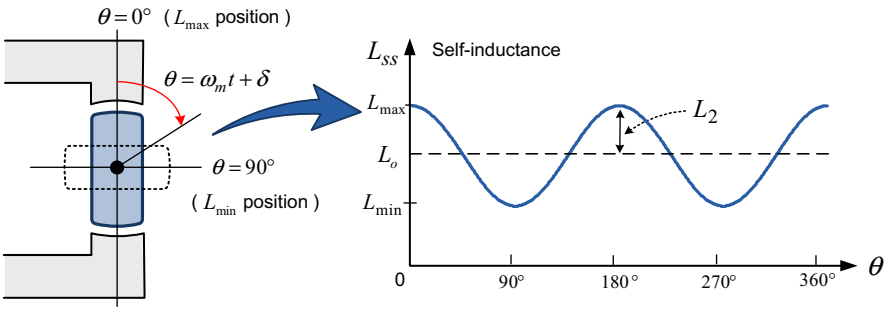


FIGURE 1.20

Self-inductance L_{ss} profile with respect to the rotor position.

The self-inductance L_{ss} in the machine of Fig. 1.19 varies with the angular position θ of the rotor as shown in Fig. 1.20.

There are two cycles of inductance during one revolution of a rotor. When $\theta = 0^\circ$, the air gap is the smallest and the inductance L_{ss} becomes the maximum value $L_{\max}$. When $\theta = 90^\circ$, the air gap is the largest and the inductance becomes the minimum value $L_{\min}$. In this way, the stator self-inductance L_{ss} varies with the rotor position θ in a sinusoidal manner and can be expressed as

$$L_{ss}(\theta) = L_0 + L_2 \cos 2\theta \tag{1.25}$$

where $L_0 = (L_{max} + L_{min})/2, \quad L_2 = (L_{max} - L_{min})/2.$

Substitution of Eq. (1.25) into Eq. (1.24) yields

$$T = \frac{1}{2} i_s^2 \frac{dL_{ss}(\theta)}{d\theta} = -I_m^2 L_2 \sin 2\theta \cos^2 \omega_s t \tag{1.26}$$

If the rotor is rotating at a constant angular velocity ω_m, then the angular position θ of the rotor can be given by

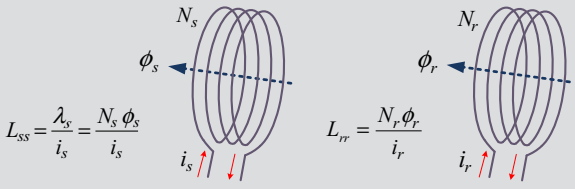
$$\theta = \omega_m t + \delta \tag{1.27}$$

where δ is the initial angular position of the rotor.

SELF-INDUCTANCE AND MUTUAL-INDUCTANCE

The inductance L of a coil is defined as the flux linkage per ampere of current in the coil.

- Self-inductance: Self-inductance is the flux linkage produced in the winding by the current in that same winding divided by that current.

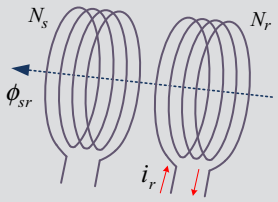


(Continued)

SELF-INDUCTANCE AND MUTUAL-INDUCTANCE (CONTINUED)

- Mutual-inductance: Mutual-inductance is the flux linkage produced in one winding by the current in the other winding divided by that current.

$$L_{sr} = \frac{N_s \phi_{sr}}{i_r}, \quad L_{rs} = \frac{N_r \phi_{rs}}{i_s}$$



Also, we consider ω_m to be positive when the position θ is increasing (clockwise motion). Substitution of Eq. (1.27) into Eq. (1.26) yields

$$\begin{aligned} T &= -I_m^2 L_2 \sin 2(\omega_m t + \delta) \frac{1 + \cos 2\omega_s t}{2} \\ &= -\frac{1}{2} I_m^2 \left\{ L_2 \sin 2(\omega_m t + \delta) + \frac{1}{2} \sin 2([\omega_m + \omega_s]t + \delta) + \frac{1}{2} \sin 2([\omega_m - \omega_s]t + \delta \right\} \end{aligned} \tag{1.28}$$

The three sin terms on the right side of Eq. (1.28) are functions of time t whose average value is zero. The average value of this torque is, therefore, zero.

This means that a constant torque cannot be developed in this machine for any direction. Therefore this machine cannot operate as a continuously rotating motor. However, if $\omega_m = 0$ or $\omega_m = \pm \omega_s$, then a nonzero average torque can be produced. The case of $\omega_m = 0$ will be excluded since this indicates nonrotating. Consequently the requirement for a continuous rotation is $\omega_m = \omega_s$. This requires that the rotor must rotate at the speed equal to the angular frequency ω_s of the exciting current, which is also called *synchronous speed*. In this case this machine can operate as a continuously rotating motor and its average torque becomes

$$T_{avg} = -\frac{1}{4} I_m^2 L_2 \sin 2\delta = -\frac{1}{8} I_m^2 (L_{max} - L_{min}) \sin 2\delta \tag{1.29}$$

The average developed torque depends on the inductance difference $(L_{max} - L_{min})$ and the initial rotor position δ. The maximum torque occurs when $\delta = -45^\circ$. Since the torque in this motor caused by the variation of reluctance (or inductance) with rotor position can be developed only at the synchronous speed, this motor is called *synchronous reluctance motor*.

Next, we will examine the necessary condition for a continuous rotation of the *doubly fed machine* in which both the stator and the rotor have windings carrying currents as shown in Fig. 1.21. Typical electric motors such as a DC motor, an induction motor, and a synchronous motor belong to the doubly fed machine.

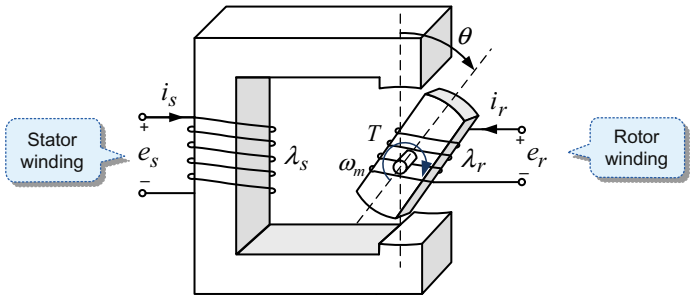


FIGURE 1.21

Doubly fed machine.

Modified from G.R. Slemon, A. Straughen, Electric Machines, Addison-Wesley, 1980 (Chapter 3); P.C. Sen, Principles of Electric Machines and Power Electronics, John Wiley & Sons, 1996.

Assume that this machine is a linear system, in which the magnetic energy and the coenergy are the same, i.e., $W_f = W'_f$. Similar to the force of Eq. (1.19), the torque of this machine can be obtained from

$$T = \frac{dW'_f(i,\theta)}{d\theta}\bigg|_{i=\text{constant}} = \frac{dW_f(i,\theta)}{d\theta}\bigg|_{i=\text{constant}} \tag{1.30}$$

To evaluate this torque, we need to obtain the magnetic energy W_f in this machine. When the magnetic field is established by winding currents i_s and i_r, the stored magnetic energy W_f can be easily derived by locking the rotor at an arbitrary position, which makes it produce no mechanical output. If there is no mechanical output, then the magnetic field energy increment during dt is

$$dW_f = dW_e = e_s i_s dt + e_r i_r dt = i_s d\lambda_s + i_r d\lambda_r \tag{1.31}$$

Here, the stator flux linkage λ_s consists of λ_{ss} produced by the stator current i_s and λ_{sr} produced by the rotor current i_r. This stator flux linkage can be expressed as functions of currents and inductances of windings as

$$\lambda_s = \lambda_{ss} + \lambda_{sr} = L_{ss} i_s + L_{sr} i_r \tag{1.32}$$

where $L_{ss}(= \lambda_{ss}/i_s)$ is the self-inductance of the stator winding, and $L_{sr}(= \lambda_{sr}/i_r)$ is the mutual-inductance between the stator and rotor windings.

The flux linkage λ_r in the rotor winding also consists of λ_{rr} produced by the rotor current i_r and λ_{rs} produced by the stator current i_s. This rotor flux linkage λ_r is expressed by

$$\lambda_r = \lambda_{rr} + \lambda_{rs} = L_{rr} i_r + L_{rs} i_s \tag{1.33}$$

where $L_{rr}(= \lambda_{rr}/i_r)$ is the self-inductance of the rotor winding, and $L_{rs}(= \lambda_{rs}/i_s)$ is the mutual-inductance between the stator and rotor windings. For a linear magnetic system, $L_{sr} = L_{rs}$.

In the doubly fed machine in Fig. 1.21, both self-inductances L_{ss}, L_{rr} and mutual-inductances L_{sr}, L_{rs} vary with the rotor position θ. For example, when $\theta = 0^\circ$, at which the length of the air gap is the minimum, the reluctance of the system is the minimum and the inductance becomes the largest. Thus λ_s and λ_r are functions of rotor position θ.

Substitution of Eqs. (1.32) and (1.33) into Eq. (1.31) yields

$$\begin{aligned} dW_f &= i_s d(L_{ss} i_s + i_r dL_{sr} i_r) + i_r d(L_{sr} i_s + i_r dL_{rr} i_r) \\ &= L_{ss} i_s di_s + L_{rr} i_r di_r + L_{sr} d(i_s i_r) \end{aligned} \tag{1.34}$$

Assuming that the rotor current is increased from zero to i_r after the stator current is increased from zero to i_s, the total stored magnetic energy will be

$$\begin{aligned} W_f &= L_{ss} \int_o^{i_s} i_s di_s + L_{rr} \int_0^{i_r} i_r di_r + L_{sr} \int_0^{i_s, i_r} d(i_s i_r) \\ &= \frac{1}{2} L_{ss} i_s^2 + \frac{1}{2} L_{rr} i_r^2 + L_{sr} i_s i_r \end{aligned} \tag{1.35}$$

By substituting Eq. (1.35) into Eq. (1.30), the torque is expressed by

$$\begin{aligned} T &= -\left. \frac{dW_f(i, \theta)}{d\theta} \right|_{i=\text{constant}} \\ &= \frac{1}{2} i_s^2 \frac{dL_{ss}}{d\theta} + \frac{1}{2} i_r^2 \frac{dL_{rr}}{d\theta} + i_s i_r \frac{dL_{sr}}{d\theta} \end{aligned} \tag{1.36}$$

This torque expression is derived in the condition in which the rotor is locked to produce no mechanical output. Even if the rotor is rotating, we can obtain the same torque expression [3].

In Eq. (1.36), the first two terms on the right side represent reluctance torques involving a change of self-inductances according to the rotor position θ. The last term involving a change of mutual-inductance expresses the electromagnetic torque formed by the interaction of two fields produced by the stator and rotor currents i_s and i_r. Typical rotating motors such as a DC motor, an induction motor, and a synchronous motor are based on this torque.

In the previous section, we saw that the reluctance motor must run at the speed equal to the angular frequency of the exciting current for developing an average torque. In the doubly fed machine, if the stator and the rotor currents differ in their operating frequency, then the motor will need to be synchronized at two different speeds for producing an average torque. Only one of the two can be satisfied at a time, and the other torque term will be oscillatory. This will result in an unwanted speed oscillation. However, we can solve this problem by eliminating one or both of the reluctance torque terms in Eq. (1.36).

First, we will eliminate the reluctance torque term involving a change in the stator self-inductance. We can realize this by making the rotor configuration cylindrical as shown in Fig. 1.22.

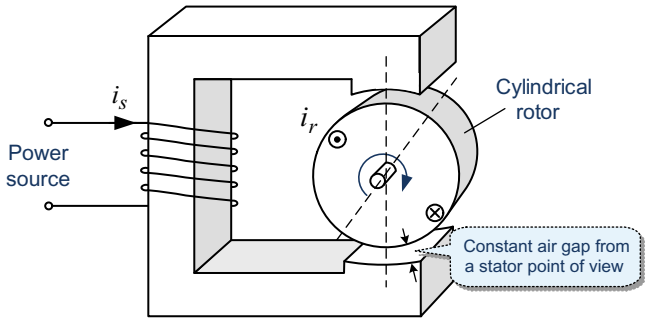


FIGURE 1.22

Cylindrical rotor configuration.

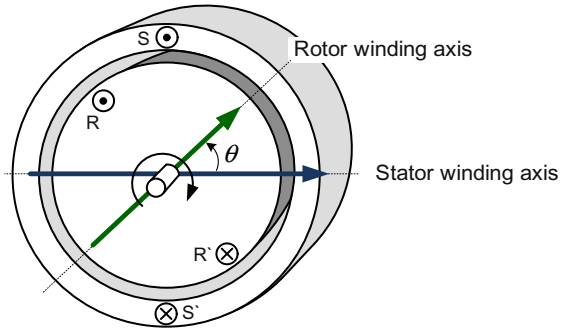


FIGURE 1.23

Cylindrical stator and rotor configurations.

In the cylindrical rotor configuration, the stator self-inductance L_{ss} becomes constant since the magnetic path becomes constant for the flux produced by the stator winding regardless of the rotor position. Thus

$$\frac{dL_{ss}}{d\theta} = 0 \tag{1.37}$$

Therefore the reluctance torque term due to the stator excitation will disappear from Eq. (1.36).

Furthermore, if we make the stator into a hollow cylinder coaxial with the rotor as shown in Fig. 1.23, then the rotor self-inductance L_{rr} becomes constant regardless of the rotor position. Thus

$$\frac{dL_{rr}}{d\theta} = 0 \tag{1.38}$$

This will lead to a disappearance of the second reluctance torque term due to rotor excitation.

We can see that no reluctance torque production results in a cylindrical machine that has both the stator and the rotor in the cylindrical configuration. This cylindrical machine produces only the torque involving a change of mutual-inductance between the stator and the rotor windings as given by

$$T = i_s i_r \frac{dL_{sr}}{d\theta} \tag{1.39}$$

Even in the cylindrical machine, this mutual-inductance can be varied by changing the relative positions of the stator and the rotor windings according to the rotor position.

Now, we will look at the necessary condition for the cylindrical machine to produce a torque continuously. Suppose that the currents in the stator and the rotor windings are

$$i_s = I_{sm}\cos\,\omega_s t \tag{1.40}$$

$$i_r = I_{rm}\cos\,(\omega_r t + \alpha) \tag{1.41}$$

If the axes of the two windings are aligned, i.e., when $\theta = 0^\circ$ as in Fig. 1.23, then the linking flux of the two windings will become a maximum, which will make the mutual-inductance its maximum as well. Thus the mutual-inductance according to the position of the rotor can be expressed as

$$L_{sr} = L_m\cos\,\theta \tag{1.42}$$

where L_m is the maximum mutual-inductance and θ is the angle between the stator and the rotor winding axes. The position of the rotor at instant t with the angular velocity ω_m of the rotor is

$$\theta = \omega_m t + \delta \tag{1.43}$$

where δ is the initial rotor position at $t = 0$.

Substitution of Eqs. (1.40), (1.41) and (1.42) into Eq. (1.39) yields

$$\begin{aligned} T &= i_s i_r \frac{dL_{sr}}{d\theta} \\ &= -I_{sm}I_{rm}L_m\cos\,\omega_s t\cdot\cos\,(\omega_r t + \alpha)\cdot\sin\,(\omega_m t + \delta) \\ &= -\frac{I_{sm}I_{rm}L_m}{4}\left[\sin\left\{(\omega_m + (\omega_s + \omega_r))t + \alpha + \delta\right\}\right. \\ &\quad +\sin\left\{(\omega_m - (\omega_s + \omega_r))t + \alpha + \delta\right\} \\ &\quad +\sin\left\{(\omega_m + (\omega_s - \omega_r))t + \alpha + \delta\right\} \\ &\quad \left.+\sin\left\{(\omega_m - (\omega_s - \omega_r))t + \alpha + \delta\right\}\right] \end{aligned} \tag{1.44}$$

Since averaging over one period of the sinusoidal function is zero, the average torque of Eq. (1.44) will also be zero. However, an average torque can be developed if the coefficient of t in sinusoidal terms of Eq. (1.44) is zero. This needs to satisfy the following condition.

$$|\omega_m| = |\omega_s \pm \omega_r| \tag{1.45}$$

Typical electric motors such as a DC motor, an induction motor, and a synchronous motor meet this condition in different ways, and thus, can rotate continuously.

Now, we will take a look at how each of these three motors meets this requirement for the average torque production. First, we will neglect the case in which both the stator and the rotor windings are excited by the DC ($\omega_s = \omega_r = 0$), because Eq. (1.45) results in $\omega_m = 0$, which indicates the state of nonrotating.

1.2.3.1 Direct current motor

If the stator is excited with a DC power ($\omega_s = 0$) and the rotor is excited with an AC power of an angular frequency ω_r, then the necessary condition of Eq. (1.45) for the development of an average torque is

$$|\omega_m| = |\omega_r| \tag{1.46}$$

This implies that the rotor needs to rotate at the same frequency as the frequency ω_r of the rotor current. A DC motor as shown in Fig. 1.24A is the one that satisfies this condition. In the DC motor, by the action of the commutator and brush, a rotor current becomes an AC, whose angular frequency is naturally equal to the rotor speed. Thus, the DC motor has a special mechanical structure, which allows it to always meet the condition of Eq. (1.46). From Eqs. (1.44) and (1.46), the average torque in this motor is

$$T_{avg} = -\frac{I_{sm} I_{rm}}{2} L_m \sin\delta \tag{1.47}$$

In the DC motor, δ, which indicates the angle between the stator field flux and the rotor mmf, is always 90° electric angle structurally, so the maximum torque per ampere can be obtained as

$$T_{avg} = -\frac{L_m}{2} I_{sm} I_{rm} \tag{1.48}$$

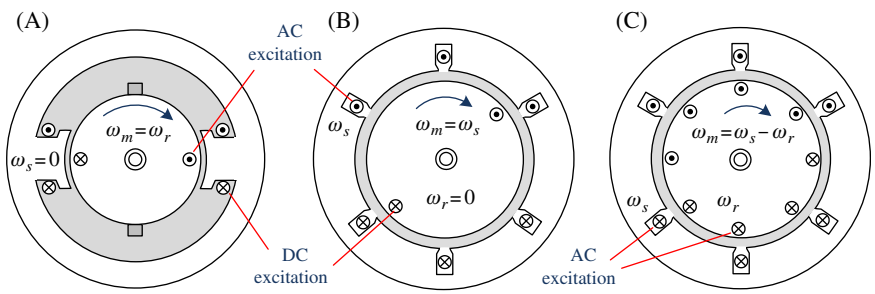


FIGURE 1.24

Doubly fed motors. (A) DC motor, (B) synchronous motor, and (C) induction motor.

1.2.3.2 Synchronous motor

If the stator is excited with an AC power source of an angular frequency ω_s and the rotor is excited with a DC power as shown in Fig. 1.24B, then Eq. (1.45) can only be satisfied if

$$|\omega_m| = |\omega_s| \tag{1.49}$$

To achieve this, the rotor must rotate at an angular frequency synchronized to the frequency ω_s of the stator current. A motor satisfying this condition becomes a synchronous motor. The name "*synchronous motor*" is due to this fact. From Eq. (1.44), the average torque in this motor can be given as

$$T_{avg} = -\frac{I_{sm}I_{rm}}{2}L_m \sin\delta \tag{1.47}$$

Unlike in the DC motor, the average torque in this motor varies according to the angle δ between the stator and the rotor field fluxes even though the same currents are flowing. We can easily see that a synchronous motor has no starting torque because it cannot meet the requirement of $\omega_m \neq \omega_s$ when starting.

1.2.3.3 Induction motor

When the stator and the rotor windings are excited with AC power of different frequencies ω_s and ω_r, respectively, a necessary condition should be

$$\omega_m = \omega_s - \omega_r \tag{1.50}$$

This means that the rotor has to rotate at the angular frequency of $\omega_s - \omega_r$. This can be achieved in an induction motor as shown in Fig. 1.24C. In an induction motor, the frequency ω_r of the currents induced in the rotor windings by electromagnetic induction becomes naturally $\omega_s - \omega_m$, which is the difference between the stator current and the rotor speed in the angular frequency. Thus, an induction motor always satisfies Eq. (1.51). From Eq. (1.44), the average torque in this motor can be given as

$$T_{avg} = -\frac{I_{sm}I_{rm}}{2}L_m \sin(\alpha + \delta) \tag{1.51}$$

Unlike in the DC motor, the average torque in the induction motor varies according to the angle δ between the stator and the rotor field fluxes even though the same currents are flowing.

As we saw previously, electric motors can be classified into cylindrical motors and reluctance motors. Cylindrical motors exploit the torque produced by varying the mutual-inductance between the windings as mentioned before. These cylindrical motors with windings on both the stator and the rotor can produce a larger torque even though they are more complex in construction. Therefore, most motors are of the cylindrical type. In comparison, reluctance motors of noncylindrical configuration utilize the torque produced by the variation of inductance (or reluctance) of the magnetic path. Reluctance motors are simple in construction, but the torque developed in these motors is small.

1.3 MECHANICAL LOAD SYSTEM

An electric motor is an electromechanical device that converts electrical energy into mechanical torque. When the torque developed by the motor is transferred to the load connected to it, the load variables such as speed, position, air-flow, pressure, and tension will be controlled. Now, we will discuss the characteristics of the load connected a motor and the mathematical representation that describes the motor-driven system.

1.3.1 DYNAMIC EQUATION OF MOTION

Consider that a driving force F_M acts on an object of mass M as shown in Fig. 1.25A, so that the object moves at a speed v[4]. From Newton's second law, which states that the rate of change of momentum of an object is directly proportional to the applied force, we have

$$F_M - F_L = \frac{d}{dt}(Mv) = M\frac{dv}{dt} + v\frac{dM}{dt} \tag{1.53}$$

where F_L is the load force, which acts in a direction opposite to F_M, and Mv is the object's momentum.

If the mass M of the load is constant, then the second term of the derivative in Eq. (1.53) is zero. Thus, Eq. (1.53) is given by a well-known equation derived from Newton's second law as

$$F_M - F_L = M\frac{dv}{dt} = Ma \tag{1.54}$$

where $a(=dv/dt)$ is the object's acceleration.

Next, for a rotational motion in Fig. 1.25B, the rotational analogue of Eq. (1.53) is given by

$$T_M - T_L = \frac{d}{dt}(J\omega) = J\frac{d\omega}{dt} + \omega\frac{dJ}{dt} \tag{1.55}$$

where T_M and T_L are driving and load torque, respectively, and ω is the angular speed of the rotating object. J denotes the moment of inertia of the rotating object and $J\omega$ is the object's angular momentum.

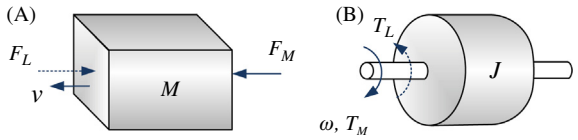


FIGURE 1.25

(A) Linear motion and (B) rotational motion objects.

When the moment of inertia J is assumed to be constant, we can rewrite Eq. (1.55) as

$$T_M - T_L = J\frac{d\omega}{dt} = J\alpha \tag{1.56}$$

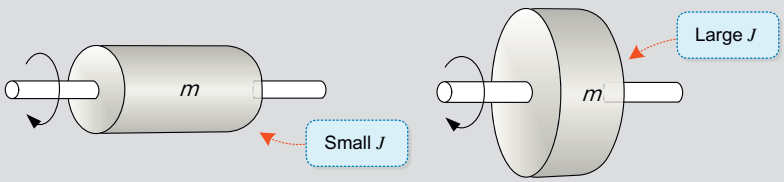
where $\alpha(=d\omega/dt)$ is the object's angular acceleration.

We can see that if $T_M > T_L$, then the object will accelerate, and if $T_M < T_L$, then it will decelerate. In the case of $T_M = T_L$, the speed will not be changed. Thus, when driving a load, to keep the load speed constant, the motor torque must be equal to the load torque.

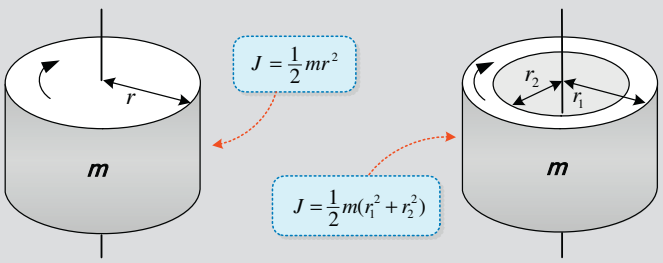
MOMENT OF INERTIA: J (kg m^2)

The tendency of a rotating object to continue in its original state of rotary motion is referred to as the *moment of inertia* J. The rotational kinetic energy of a rigid object with angular velocity ω is expressed as $\frac{1}{2}J\omega^2$ in terms of its moment of inertia. The moment of inertia of an object is also the measure of how fast the object can be accelerated or decelerated.

The moment of inertia in a rigid object is related to the distribution of mass as well as the mass m of the object. Therefore the moment of inertia of an object can depend on its shape. For example, if two objects have the same mass but are different in radius as shown in the following figure, then they may have different moments of inertia.



If the radius of an object is larger, then the moment of inertia is larger. The reason for this is as follows. A rotating object consists of many small particles at various distances from the axis of rotation. When the object is rotating, the particles which are far away from the axis of rotation will move faster than the ones which are located near the axis of rotation. Thus, the particles which are far away from the axis of rotation require more kinetic energy for a rotation. The moment of inertia I for each particle is defined as its mass multiplied by the square of the distance r from the axis of rotation to the particle, i.e., $I = mr^2$. Thus, for the same object mass, the further out from the axis of rotation its mass is distributed, the larger the moment of inertia of the object is. For solid or hollow cylinders, the moment of inertia can be calculated by the equations shown in the next figures.



(Continued)

MOMENT OF INERTIA: J (kg m^2) (Continued)

Instead of J, $GD^2 (= 4J)$, also known as *flywheel effect*, is generally used in industrial applications. Here, G is the mass (kg) and D is the diameter (m).

There is maximum permissible load inertia to a motor. It is important to ensure that the inertia of the motor matches the inertia of the driven load. Ideally, it is desirable to have a 1:1 inertia ratio between the load and the motor. For traction motors, the motor inertia should be large enough to drive the load of a large inertia. To have a large inertia, the motor will be designed with a rotor configuration of a large diameter and a short axial length. On the other hand, for servo motors operated in frequent acceleration/deceleration, the inertia of the rotor should be small. Thus, the rotor will be designed to have a small diameter and a long axial length.

Fig. 1.26 shows a simplified configuration of a motor drive system consisting of a driving motor and a driven mechanical load, in which the torque of the motor is transferred to the load through the shaft and coupling.

From the motor's viewpoint, a mechanical load can be seen as a load torque T_L connected to its shaft. Thus, from Eq. (1.56), the equation of motion of a motor drive system can be expressed as

$$T_M = (J_M + J_L)\frac{d\omega}{dt} + T_L \tag{1.57}$$

where J_M and J_L are the motor inertia and the load inertia, respectively.

When the motor is driving a mechanical load, the torque required to run the load is the load torque T_L, which varies with the type of load.

In addition to Eq. (1.57), when a load begins to move and is in motion, a friction force occurs, resisting the motion. Therefore, the equation of motion needs to include the friction force T_F as

$$T_M = (J_M + J_L)\frac{d\omega}{dt} + T_F + T_L \tag{1.58}$$

The friction force is usually proportional to the speed, given by $T_F = B\omega$, where B is the coefficient of friction. Finally, we have an equation of motion, which expresses the dynamic behavior of a motor drive system as

$$T_M = J\frac{d\omega}{dt} + B\omega + T_L \tag{1.59}$$

where $J = J_M + J_L$.

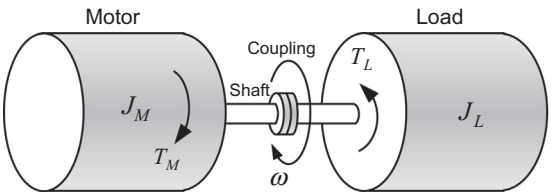


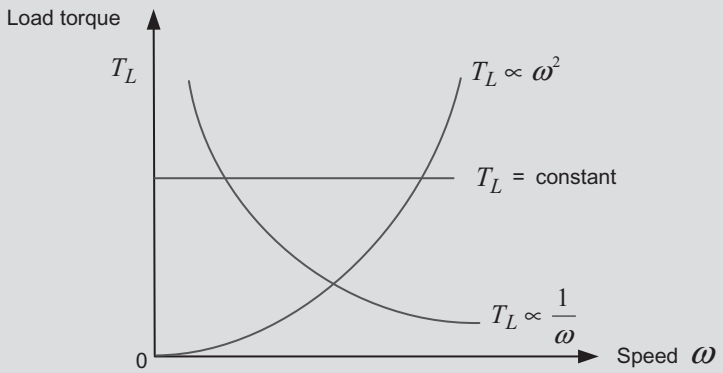
FIGURE 1.26

Simplified motor drive system.

A motor-driven system has mechanical transmission devices such as shaft, gearbox, or coupling to connect the motor and the load. In a real system, the stiffness of these components is limited, and the transmissions are flexible. Therefore, if the coupling or shaft between the motor and the load is long or elastic, then it may be subjected to torsion. In this case, we need to add the torque term $K_{sh}\theta$ produced by torsional deformation of the shaft to Eq. (1.59), where K_{sh} (Nm/rad) is the coefficient of stiffness.

LOAD TORQUE T_L

There are several types of loads driven by a motor. In most loads, the required torque is normally a function of speed. There are three typical loads whose speed-torque characteristics are shown in the following figure.



1. Constant torque load

   The torque required by this type of load remains constant regardless of the speed. Loads such as elevators, screw compressors, conveyors, and feeders have this type of characteristic.

2. Constant power load ($T_L \propto 1/\omega$)

   This load requires a torque, which is inversely proportional to the speed, so this load is considered a constant power load. This type is most often found in machine tool industry and drilling, milling industry.

3. Load proportional to the square of the speed ($T_L \propto \omega^2$)

   The torque of this load increases in proportion to the square of the speed. This is a typical characteristic of a fan, blower, and pump, which are the most commonly found in industrial drive applications.

The load in traction drives such as electric locomotives and electric vehicles shows the combined characteristic of a constant torque load in low speeds and a constant power load in high speeds.

1.3.1.1 Combination system of translational motion and rotational motion

Many motions in the industry such as an elevator, a conveyor, or electric vehicles are a combination of translational motion and rotational motion as shown in Fig. 1.27. In this case, we need to convert the load parameters such as load inertia to the motor shaft.

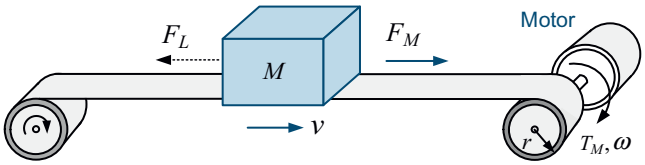


FIGURE 1.27

Combination system of translational motion and rotational motion.

The expression for the translational motion in Fig. 1.27 is given by

$$F_M - F_L = M\frac{dv}{dt} \tag{1.60}$$

The relationships between force and torque, and velocity and angular velocity are

$$T_M = rF_M \tag{1.61}$$

$$T_L = rF_L \tag{1.62}$$

$$\omega = \frac{v}{r} \tag{1.63}$$

By substituting Eqs. (1.61)–(1.63) into Eq. (1.60), we obtain

$$T_M - T_L = Mr^2\frac{d\omega}{dt} = J_e\frac{d\omega}{dt} \tag{1.64}$$

where $J_e = Mr^2$ represents the equivalent moment of inertia, which is reflected to the motor shaft side of the mass M in translational motion.

1.3.1.2 System with gears or pulleys

Often, the speed required by the load is too low compared to the nominal speed of the motor. Gears or pulleys between the motor and the load being driven are most often used to change the speed. In this case, we need to know how the load will be seen through the gears or pulleys at the motor side.

We will look at an example of two meshed gears as shown in Fig. 1.28.

The equation of motion at the load side is given by

$$T_L = J_L\frac{d\omega_L}{dt} + B\omega_L \tag{1.65}$$

Because the two gears will travel at an equal distance, we have

$$\omega_L = \frac{N_1}{N_2}\omega_M \tag{1.66}$$

where N_1 and N_2 are the number of teeth on the gears of the motor and load sides, respectively.

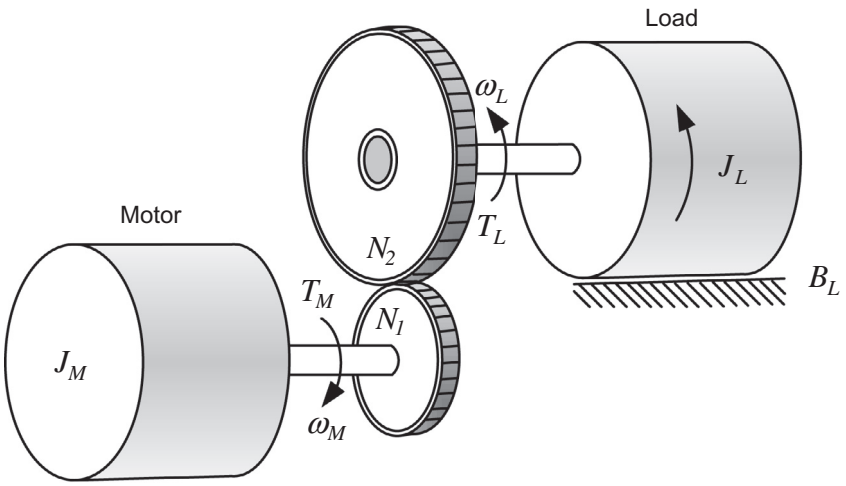


FIGURE 1.28

System with gears.

When neglecting friction and losses of the gears, the power is the same at the input and at the output of the gear, i.e.,

$$P = T_L\omega_L = T_M\omega_M \quad \rightarrow \quad T_L = \frac{N_2}{N_1}T_M \tag{1.67}$$

Substituting Eqs. (1.65) and (1.66) in Eq. (1.65) yields

$$T_L = J_L\left(\frac{N_1}{N_2}\right)\frac{d\omega_L}{dt} + B_L\left(\frac{N_1}{N_2}\right)\omega_L = \left(\frac{N_2}{N_1}\right)T_M \tag{1.68}$$

Finally, the equation of motion at the motor side is given by

$$\begin{aligned} T_M &= J_L\left(\frac{N_1}{N_2}\right)^2\frac{d\omega_M}{dt} + B_L\left(\frac{N_1}{N_2}\right)^2\omega_M \\ &= (J_M + J)\frac{d\omega_M}{dt} + B\omega_M \end{aligned} \tag{1.69}$$

where $J = J_L(N_1/N_2)^2$ and $B = B_L(N_1/N_2)^2$ are the load inertia J_L and the friction coefficient B_L converted to the motor side, respectively. It can be seen that the load parameters reflected back to the motor are a squared function of the gear ratio N_1/N_2.

1.3.2 OPERATING MODES OF AN ELECTRIC MOTOR

Operation of a motor can be divided into two modes according to the direction of the energy transfer.

When the motor rotates in the same direction as its developed torque in Fig. 1.29A, the motor will supply mechanical energy to the load. In this case, the motor operates as a typical *motoring mode*. On the other hand, when the

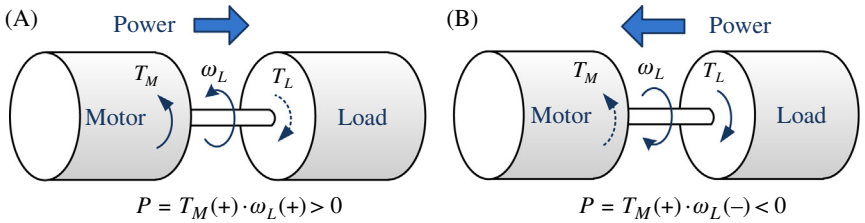


FIGURE 1.29

Operation mode of the motor. (A) Motoring mode and (B) generating (braking) mode.

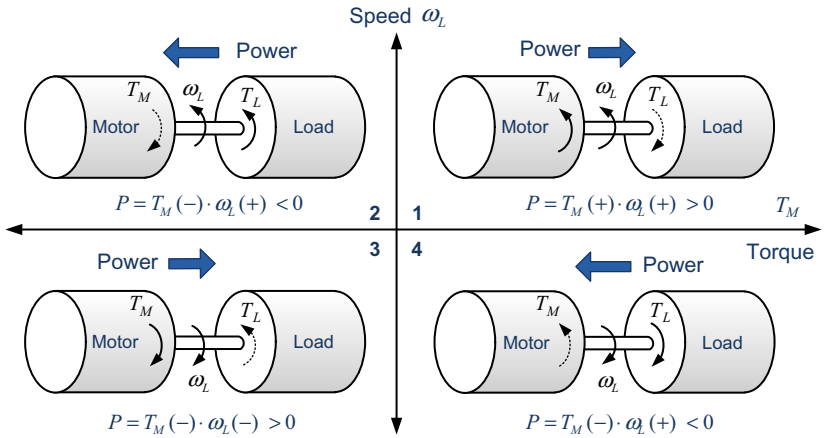


FIGURE 1.30

Four-quadrant operation modes.

motor is rotating in a direction opposite to its developed torque in Fig. 1.29B, the mechanical energy of the load is supplied to the motor. In this case, the motor is acting as a generator. It corresponds to the *generating mode*, in which the motor absorbs the load energy, providing a braking action.

When braking, the mechanical energy of the load is converted into electrical energy through the motor, and the generated electrical power can be returned to the power source. This method called *regenerative braking* is the most efficient braking method, but it requires a high-cost power converter. An alternative method for dealing with the generated electrical power is to dissipate it as heat in the resistors. This is called *dynamic braking*, which is inefficient but inexpensive.

Similarly, there are also operation modes of motoring and generating in the reverse driving. Consequently, four-quadrant operation modes are available in variable speed drive systems as shown in Fig. 1.30. Quadrants 1 and 2 are the motoring and generating operation modes, respectively, in the forward drive, while Quadrants 3 and 4 are the two operation modes in the reverse drive. Braking occurs

in Quadrants 2 and 4. To achieve the four-quadrant operation modes in motor drive systems, the torque should be controlled in the positive and negative direction, and the speed should be controlled in the forward and reverse direction.

As an example of the four-quadrant operation, let us take a look at an elevator drive system as shown in Fig. 1.31. In an elevator system, the car carrying people or goods is connected to and is driven by a traction motor through ropes and gears. As a traction motor, induction motors are most widely used. In recent times, however, permanent magnet synchronous motors are used as well.

A counterweight attached to the opposite side of the ropes reduces the amount of power required to move the car. The weight of the counterweight is typically equal to the weight of the car plus 40−50% of the capacity of the elevator. When the car goes up or down, we can see the four-quadrant operation of the driving motor occurring due to the weight difference between the car and the counterweight as follows:

- Quadrant 1 operation: the forward motoring mode $(+T, +\omega)$

  When the car carrying people goes up and is heavier than the counterweight, the traction motor is needed to produce the forward direction torque, so it operates in the *forward motoring mode*.

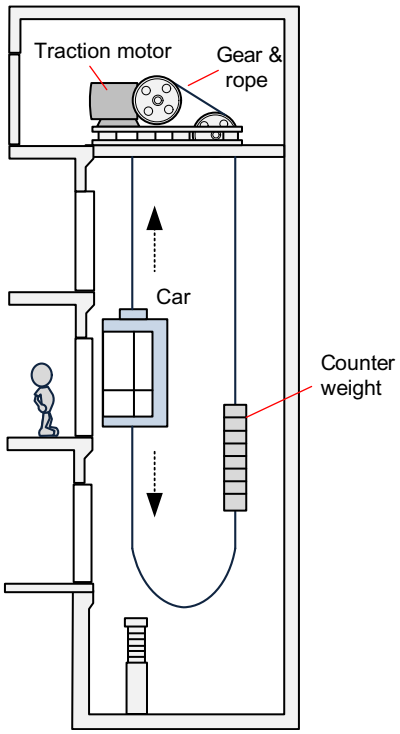


FIGURE 1.31

Four-quadrant operation in an elevator drive.

- Quadrant 2 operation: the forward braking mode $(-T, +\omega)$
  When an empty car goes up and is lighter than the counterweight, the traction motor is needed to produce the braking torque of the reverse direction, so it operates in the *forward braking (generating) mode*.
- Quadrant 3 operation: the reverse motoring mode $(-T, -\omega)$
  When an empty car goes down and is lighter than the counterweight, the traction motor is needed to produce the reverse direction torque, so it operates in the *reverse motoring mode*.
- Quadrant 4 operation: the reverse braking mode $(+T, -\omega)$
  When the car carrying people goes down and is heavier than the counterweight, the traction motor is needed to produce the braking torque of the forward direction, so it operates in the *reverse braking (generating) mode*.

Here, the going-up of the car is assumed as the forward direction.

1.4 COMPONENTS OF AN ELECTRIC DRIVE SYSTEM

For a given mechanical load, an adequate design of the motor drive system is essential to meet its required performance criteria such as speed-torque characteristic, operation speed range, speed regulation, efficiency, cost, duty cycle, etc.

A motor drive system consists normally of five parts as shown in Fig. 1.32. Within the available power supply, we have to choose these components appropriately to achieve the requirements of the drive performance. We will now briefly take a look at these five parts.

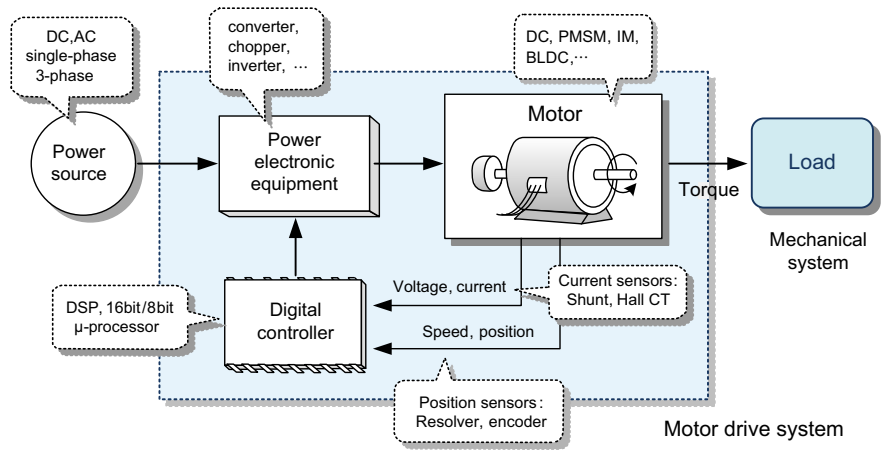


FIGURE 1.32

Configuration of a motor drive system.

1.4.1 POWER SUPPLY

Single-phase or three-phase AC voltage sources are most commonly used as a power supply that provides electric energy for motor drives. The three-phase AC voltage source is generally used for motors of several kilowatts or higher. In many cases, the AC voltage sources are converted into a DC source, which is converted into the form of power needed by a motor through using power electronic converters such as an inverter or a chopper. Recently, DC power has often been provided by renewable energy sources such as solar cells and fuel cells.

1.4.2 ELECTRIC MOTORS

For driving motors, we have to choose the one that meets the required speed-torque characteristic of the driven mechanical load. In addition, important performance criteria like efficiency, size, cost, duty cycle, and operating environment need to be considered. As mentioned earlier, there are two basic types of a driving motor: DC motor and AC motor. Some applications use special types such as a BLDC motor or a stepping motor, which cannot be classified into the basic types.

DC motors have an advantage of a simple speed/torque control for their excellent drive performance. However, due to the wear associated with their commutators and brushes, DC motors are less reliable and unsuitable for a maintenance-free operation. On the other hand, AC motors are smaller, lighter, and have more power density than DC motors. AC motors also require virtually no maintenance and thus are better suited for high speeds. However, AC drives with a high performance capability are more complex and expensive than DC drives.

1.4.3 POWER ELECTRONIC CONVERTERS

Power electronic converters play the role of taking electrical energy from the power system and turning it into a suitable form needed by a motor. The power electronic converter may be determined according to the given power source and the driving motor.

For DC drives, power electronic converters such as a controlled rectifier or a chopper can be used to adjust the DC power, which will be described in more detail in Chapter 2. In contrast, AC drives mostly use an inverter to adjust the voltage and frequency in the AC power, which will be also described in more detail in Chapter 7. In this case, a rectifier is often included to convert the AC power in the mains power system into the DC power.

These power electronic converters use power semiconductor devices such as gate turn-off (GTO) thyristor, integrated gate-commutated thyristor (IGCT), insulated gate bipolar transistor (IGBT), power metal oxide semiconductor field effect transistor (MOSFET), and power bipolar junction transistor (BJT). These switching devices are determined according to their power handling capability and their switching speed. The power handling capability can be ranked in an increasing order of

MOSFET, IGBT, and GTO thyristor, while the switching speed can be ranked in an increasing order of GTO thyristor, IGBT, and MOSFET. All these switching devices described above are based on the silicon (Si) semiconductor material. Recently, switching devices based on wide bandgap materials such as silicon carbide (SiC) or gallium nitride (GaN) are being recognized as a promising future device.

1.4.4 DIGITAL CONTROLLERS

The controller in charge of executing algorithms to control the motor is the most important part in the motor drive systems. This controller manipulates the operation of the power electronic converter to adjust the frequency, voltage, or current provided to the motor. Nowadays, digital controllers are usually used. A digital controller is based on microprocessor, microcontroller, or digital signal processor (DSP), which can be a 16-bit or 32-bit, and also either a fixed-point or floating-point.

There is a trade-off between the control performance and the cost. DC motor and BLDC motor drives requiring relatively simple controls may use 16-bit processors, while AC motor drives requiring complex controls such as a vector controlled induction or synchronous motors may need high-performance 32-bit processors or DSP.

1.4.5 SENSORS AND OTHER ANCILLARY CIRCUITS

To achieve a high-performance motor drive, a closed-loop control of position, speed or current is often adopted, and in this case, speed/position or current information is required.

Sensors are essential for obtaining this information. Shunt resistances, Hall effect sensors, or current transformers are mainly used as the current sensor. The shunt resistance is more cost effective, while the Hall effect sensors can usually give a high resolution and isolation between the controller and the system. Encoders and resolvers are widely used as speed/position sensors, which will also be discussed in Chapter 9.

In addition to these components, several circuits for protection, filtering, power factor correction, or harmonics reduction may be necessary to improve the reliability and quality of the drive system.

REFERENCES

[1] P.E. Scheihing, et al., United States Industrial Motor-Driven Systems Market Assessment: Charting a Road map to Energy Savings for Industry,' U.S. Department of Energy, April 2007.
[2] S.J. Chapman, Electric Machinery Fundamentals, third ed., McGrawHill, Boston, MA, 1999.
[3] G.R. Slemon, A. Straughen, (Chapter 3) Electric Machines, Addison-Wesley, 1980.
[4] W. Leonhard, Control of Electrical Drives, second ed., Springer-Verlag, Berlin Heidelberg New York, 1996.

CHAPTER

Control of direct current motors

2

Direct current (DC) motors have been widely used in adjustable speed drives or variable torque controls because their torque is easy to control and their range of speed control is wide. However, DC motors have a major drawback in which they need mechanical devices such as commutators and brushes for a continuous rotation. These mechanical parts require regular maintenance and hinder high-speed operations. Recently due to a major development in alternating current (AC) motor control technology, power electronics technology, and microprocessors, AC motors have been used instead of DC motors, but DC motors are still used in lower power ratings below several kilowatts.

In this chapter, we will study the current and the speed control of DC motors. Understanding the current and speed control techniques for DC motors is very important because these techniques are directly applicable to the AC motor control, which will be discussed in Chapter 6.

2.1 CONFIGURATION OF DIRECT CURRENT MOTORS

A DC motor has two windings as shown in Fig. 2.1. One is found in the stator and produces a field flux. This winding is called a *field winding*. The other one resides in the rotor and is called an *armature winding*. The armature current interacts with the stator field flux to produce torque on the rotor shaft. Small DC motors commonly have a permanent magnet instead of a field winding to produce the stator flux. A DC motor also has a mechanical commutation device consisting of brushes and commutators, which converts the DC current given from the DC power supply to AC current in the armature winding.

The DC motors can be mainly classified into two different categories: a *separately excited DC motor* and a *self-excited DC motor*. In a separately excited DC motor, the armature winding and field winding each have separate DC power supplies, while in a self-excited DC motor, the two windings share one DC power supply.

The self-excited DC motors can also be categorized into a *shunt motor*, *series motor*, and *compound motor* depending on the ways in which the two windings are connected to the DC power supply. Nowadays the DC motors mostly use a

Electric Motor Control. DOI: http://dx.doi.org/10.1016/B978-0-12-812138-2.00002-7
© 2017 Elsevier Inc. All rights reserved.

Hesai Exhibit 1030, page 43

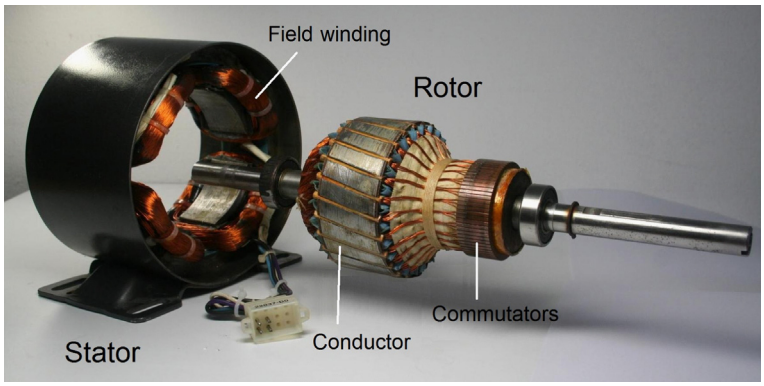


FIGURE 2.1

DC motor configuration.

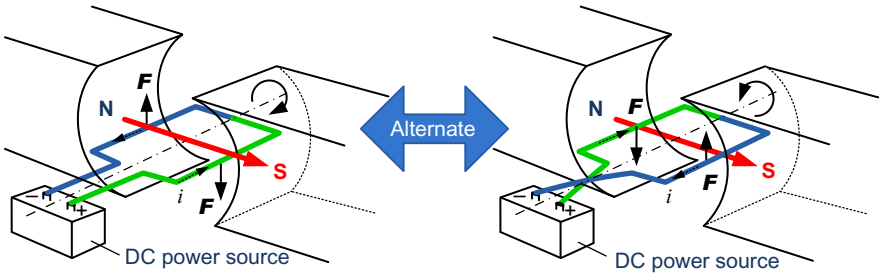


FIGURE 2.2

Force on a one-turn coil.

permanent magnet to produce the field flux and the DC power supply thus applies only to the armature winding.

Now we will learn about the roles of brushes and commutators, which are essential for the continuous rotation of DC motors. First, we will take a look at Fig. 2.2, which shows a one-turn coil in a rotor winding. When the coil is connected to the DC power supply, a current flows in the coil. We will assume that, in the initial stage, the flux distribution and the current flowing in the coil are formed like the figure on the left. In this condition, the force on the conductors on both sides makes the coil rotate in the clockwise direction according to the direction of the force given by *Fleming's left-hand rule*.

When the coil rotates and comes to the position as in the figure on the right, the force produced on the conductors on both sides will return the coil again to its initial position as shown in the left side of Fig. 2.2. Since the force produced on the coil is not produced continuously in one direction, the

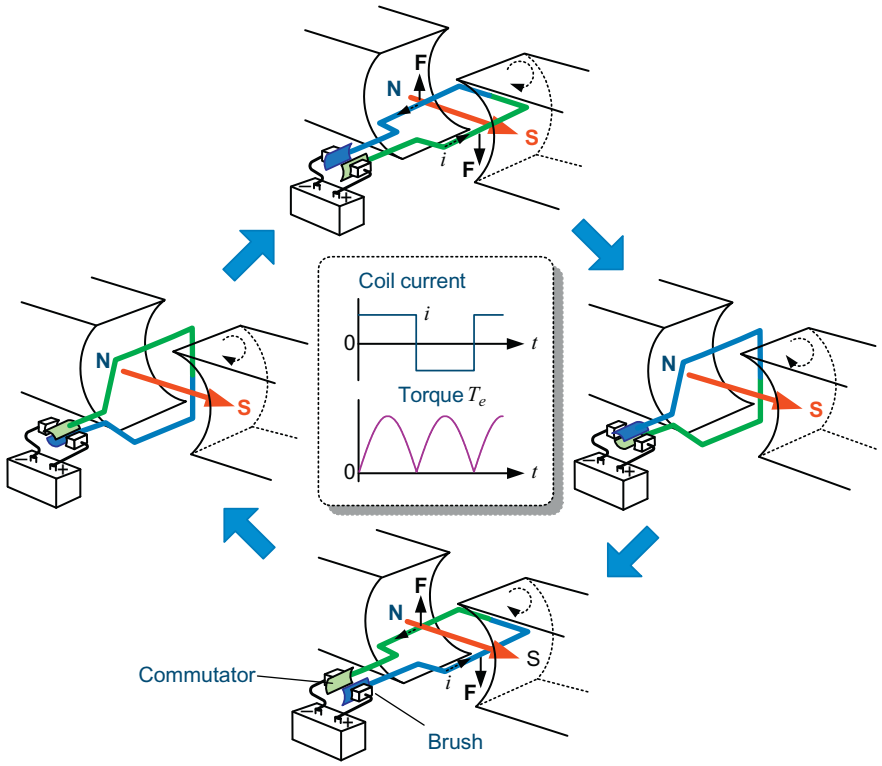


FIGURE 2.3

Continuous rotation by the use of brushes and commutators.

coil also cannot rotate in the same direction continuously. However, when the coil is at the position shown on the right, if the direction of its current is reversed, then the force produced on the conductors on both sides is reversed and thus, the force on the coil will remain in the same direction of clockwise. Thus the coil will rotate continuously in that direction. By the commutation actions of the brush and the commutator, the coil current can be reversed as shown in Fig. 2.3. It should be noted that the current that flows in the coil must be an alternating current in DC motors. The frequency of this alternating current is always the same as the angular velocity of the coil, which indicates the speed of the rotor. In Section 1.2.3, we have already seen that this meets the necessary condition for the continuous torque production in the doubly fed machine.

The armature winding of the DC motor has many coils to increase the average torque and reduce torque ripple as shown in Fig. 2.4. Each coil is connected to the DC power supply through a brush and its own isolated commutator.

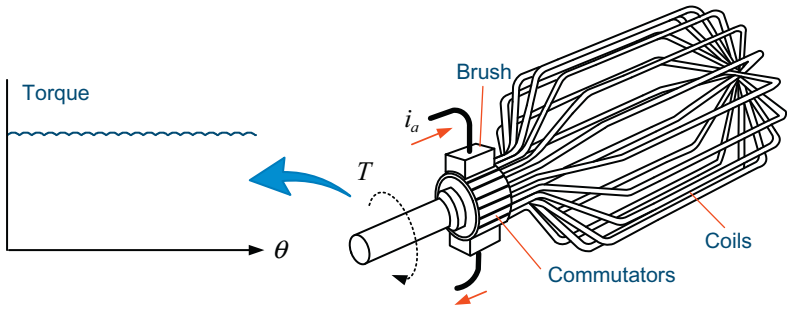


FIGURE 2.4

Armature winding.

As described earlier, in order for a DC motor to rotate continuously, it must have brushes and commutators in its structure. However, due to the wear and the arcing associated with their brushes and commutators, DC motors require much more maintenance and are limited in high-speed operation.

2.2 MODELING OF DIRECT CURRENT MOTORS

A complete dynamic model of the DC motor drive system can be expressed as the following four equations: *armature circuit*, *back-electromotive force (back-EMF)*, *torque*, and *mechanical load system*.

2.2.1 ARMATURE CIRCUIT

The voltage equation for the armature winding of a DC motor is given by

$$V_a = R_a i_a + L_a \frac{di_a}{dt} + e_a \tag{2.1}$$

where i_a is winding current, L_a is winding inductance, R_a is winding resistance, and e_a is back-EMF induced by the rotation of the armature winding in a magnetic field. The equivalent circuit of a DC motor derived from Eq. (2.1) is shown in Fig. 2.5.

We need a back-EMF e_a to obtain the current flowing through the armature winding for a voltage V_a applied to a DC motor from Eq. (2.1).

2.2.2 BACK-ELECTROMOTIVE FORCE

As shown in Fig. 2.6, when a conductor of length l meters is moving with a constant velocity v in the presence of a uniform magnetic field B, a voltage $e = Blv$ (called back-EMF) will be induced in the conductor. Similarly, in a DC motor, when the conductors of the armature winding with an angular velocity ω_m

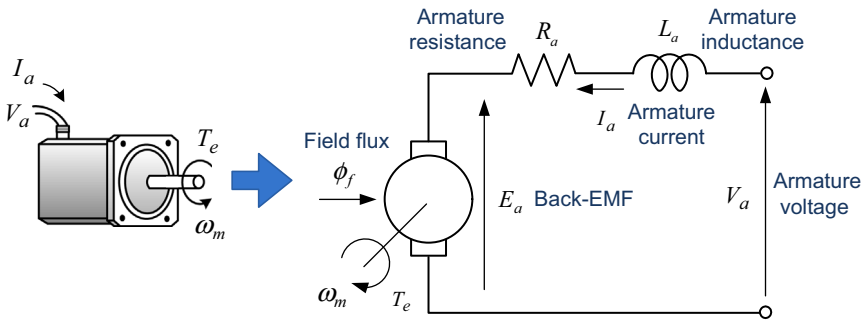


FIGURE 2.5

Equivalent circuit of a DC motor.

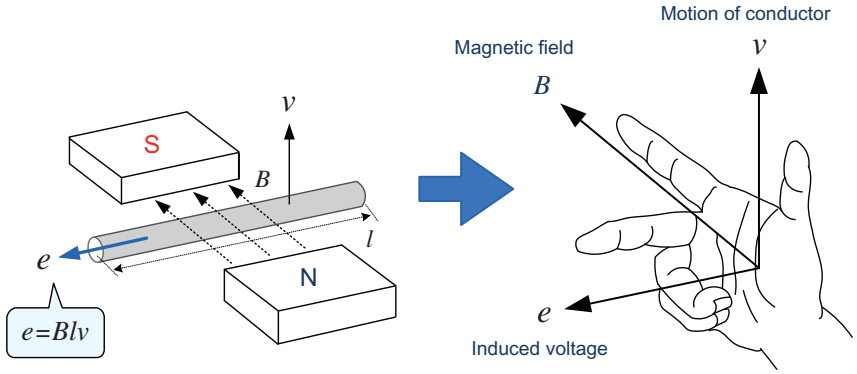


FIGURE 2.6

Induced voltage for a moving conductor.

are moving in the presence of the uniform stator magnetic flux ϕ_f, the back-EMF in the armature winding will be expressed as

$$e_a = k_e \phi_f \omega_m \quad (\leftarrow e = Blv) \tag{2.2}$$

where k_e is the back-EMF constant (Vs/rad/Wb). Commonly, since the flux remains constant, the back-EMF is proportional to the angular velocity.

With the armature current i_a calculated from the applied input voltage V_a and the back-EMF e_a, we can obtain the developed torque of a DC motor as the following.

2.2.3 TORQUE

As shown in Fig. 2.7, when a conductor of length l meters carrying a current of i amps is placed in a uniform magnetic field B, the force acting on the conductor

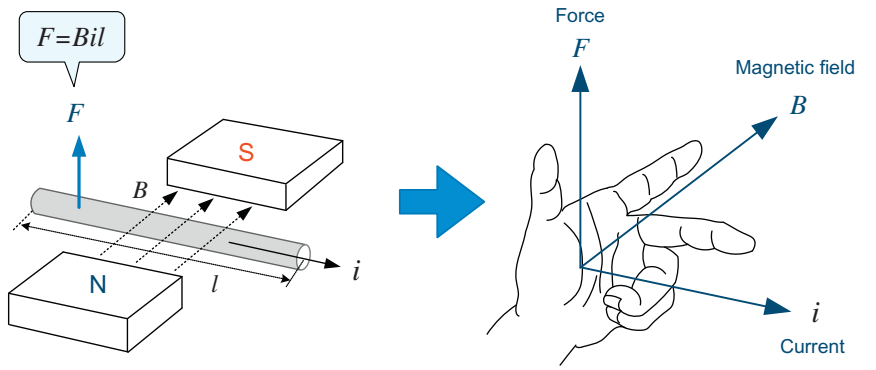


FIGURE 2.7

Force for a current carrying conductor.

will be $F = Bli$. Similarly, in a DC motor, the torque experienced by the conductors of the armature winding carrying a current i_a in the uniform stator magnetic flux ϕ_f is given by

$$T_e = k_T \cdot \phi_f \cdot i_a \quad (\leftarrow F = Bli) \tag{2.3}$$

where k_T is the torque constant (Nm/Wb/A). The numerical values of k_T and k_e constants are equal in SI units (the International System of Units), i.e., $k_T = k_e$.

It is interesting to note that the torque of a DC motor can be expressed as a simple arithmetical product of the stator magnetic flux ϕ_f and the armature current i_a. This is because the stator magnetic flux ϕ_f and the conductors carrying current i_a are always perpendicular to each other. Thus the DC motors inherently have a maximum torque per ampere characteristic.

The speed of a rotor can be determined by the developed torque as the following.

2.2.4 MECHANICAL LOAD SYSTEM

When a DC motor with the output torque in Eq. (2.3) is driving a mechanical load system, the rotor speed can be determined from the equation of motion in Eq. (2.4) as mentioned in Chapter 1.

$$T_e = J\frac{d\omega_m}{dt} + B\omega_m + T_L \tag{2.4}$$

where ω_m is the angular velocity of the rotor, T_L is the load torque, J is the moment inertia and B is the friction coefficient of the DC motor drive system, respectively.

From the above dynamic model represented by Eqs. (2.1)–(2.4), we can understand the steady-state as well as the transient characteristics of the current and the speed in the DC motor drive system. First, on the basis of this model, we will examine the speed–torque characteristic of the DC motor in the steady-state condition.

2.3 STEADY-STATE CHARACTERISTICS OF DIRECT CURRENT MOTORS

The term "steady-state" refers to a condition that exists after all initial transients or fluctuating conditions have damped out. The steady-state behavior of the DC motor is easily determined by making the time derivatives of the variables in Eqs. (2.1) and (2.4) zero, i.e., $di_a/dt = 0$, $d\omega_m/dt = 0$. From the steady-state equations, the speed−torque relation may be written as

$$\omega_m = \frac{V_a}{k\phi_f} - \frac{R_a}{(k\phi_f)^2} T_L \quad (k = k_T = k_e) \tag{2.5}$$

Here, the friction coefficient B is neglected.

We can see that, from this torque−speed relation, the speed of the DC motor decreases steadily with increasing load torque (or armature current) as shown in Fig. 2.8. Here, N is the speed expressed in terms of revolution per minute (r/min) for angular speed ω_m. From the curve, we can find the speed and the current at a certain load.

Eq. (2.5) implies that the steady-state speed of a DC motor can be adjusted by the armature voltage V_a or the stator field flux ϕ_f. Thus there are two speed control methods for the DC motor: *armature voltage control* and *field flux control.* In addition to the two methods, we can see from Eq. (2.5) that the speed can be controlled by varying the armature resistance R_a. However, this inefficient method is no longer in use.

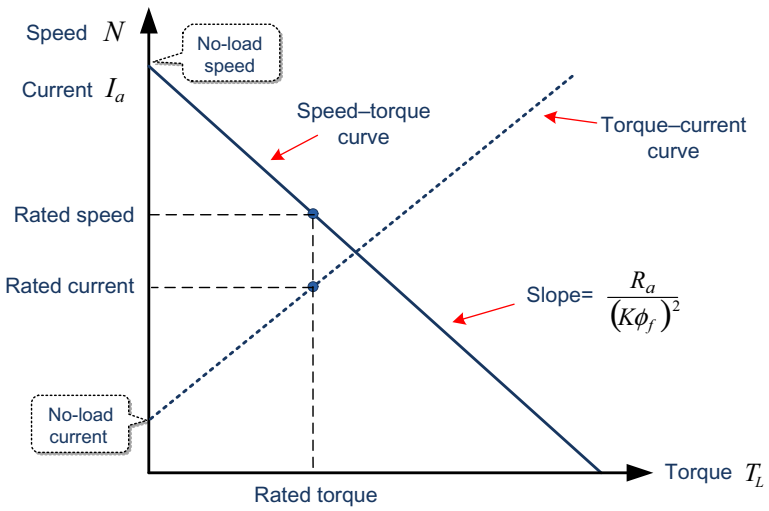


FIGURE 2.8

Speed−torque characteristic of a DC motor in the steady-state.

Now, we will take a look at the speed control characteristics of the DC motor by armature voltage control and field flux control.

2.3.1 ARMATURE VOLTAGE CONTROL

With a constant stator field flux, Eq. (2.5) expressing the torque−speed characteristic can be reduced to

$$\omega_m = \frac{V_a}{k\phi_f} - \frac{R_a}{(k\phi_f)^2} T_L = K_1 V_a - K_2 T_L \tag{2.6}$$

where $K_1 = V_a/k\phi_f$ and $K_2 = R_a/(k\phi_f)^2$

From this expression, we can see that the speed ω_m of the DC motor changes linearly with the armature voltage V_a. Thus, for a constant torque load such as elevators and cranes, the speed of the load can be controlled linearly by adjusting the armature voltage V_a of the DC motor as shown in Fig. 2.9.

To employ the armature voltage control, variable DC power supplies such as phase-controlled rectifiers or choppers are needed. Because a voltage higher than the rated voltage should not be applied to the motor, this armature voltage control method can provide a speed control range only up to the rated speed. To operate in a speed range above the rated speed, the DC motor has to adopt the field flux control, which will be described later. Permanent magnet DC motors, however, cannot use the field flux control method, so they are incapable of an operation above the rated speed.

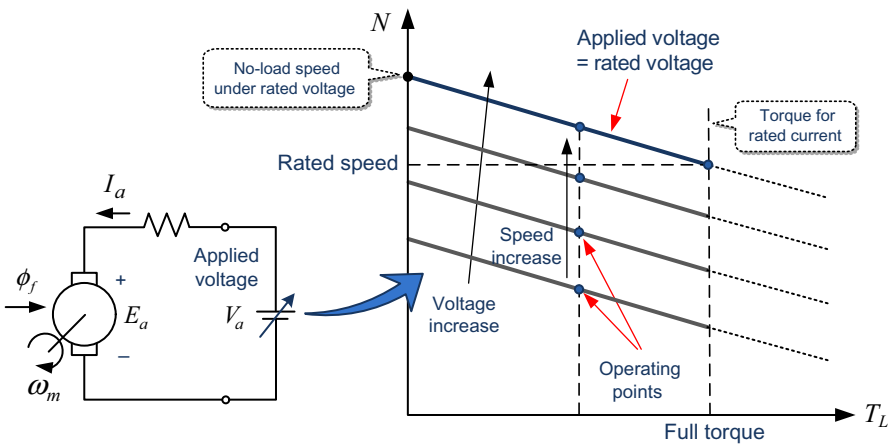


FIGURE 2.9

Armature voltage control.

2.3.2 FIELD FLUX CONTROL

Under a constant armature voltage, Eq. (2.5) can be rewritten as a function of field flux:

$$\omega_m = \frac{V_a}{k\phi_f} - \frac{R_a}{(K\phi_f)^2} T_L = \frac{K_1}{\phi_f} - \frac{K_2}{\phi_f^2} T_L \tag{2.7}$$

where $K_1 = V_a/k$ and $K_2 = R_a/k^2$.

From Eq. (2.7), we can see that the speed of the DC motor varies inversely with the field flux. Fig. 2.10 shows the torque−speed characteristic of the DC motor using the field flux control. When using this field flux control method, the field flux has to be controlled below the rated value to avoid magnetic saturation of iron core because the rated flux is commonly given as a value near the knee of the magnetization curve as shown in the left side of Fig. 2.10. If the field flux is reduced below the rated value, then the speed can increase above the rated speed.

When the speed of the DC motor can be controlled above the rated value by adjusting the field flux control, there are potential problems that can arise. When the field flux is reduced to increase the speed, the developed torque will also be reduced for the same armature current. If the armature current is increased to produce the same torque, then the efficiency will be lowered due to the increased copper losses. The armature current also may not be fully increased due to the thermal limit and the capacity of the DC power supply. Moreover the inductance of the field winding is normally designed to be large to produce the flux effectively. Thus the field flux cannot be changed rapidly, and this will result in a slow response of the speed regulation. In addition, in a high-speed range, the speed regulation will be poor for the applied load, and the resultant lower field

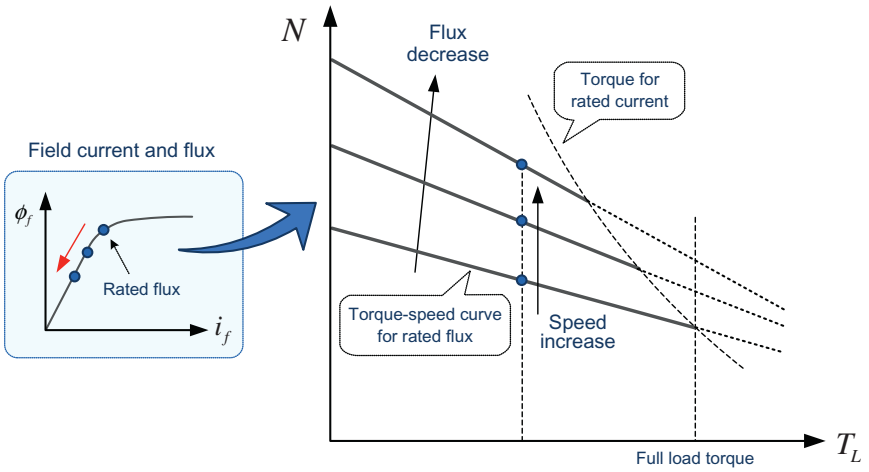


FIGURE 2.10

Field flux control.

flux will be easily influenced by the armature reaction. Besides these electrical problems, the DC motors also suffer from speed limitations due to mechanical commutation devices. On this account, the achievable speed range of this field flux control is generally limited up to three times the rated speed.

2.3.3 OPERATION REGIONS OF DIRECT CURRENT MOTORS

The operating speed range of the DC motor is divided into two regions as follows: *constant torque region* and *constant power region*. The operation in these two regions can be achieved through the armature voltage control and the field flux control.

2.3.3.1 Constant torque region ($0 \leq \omega_m \leq$ base speed ω_b)

In the operating region below the rated speed, the field flux is maintained at a constant and the torque production is controlled only by the armature current I_a. This region is called the *constant torque region* because the same torque can be developed by the same armature current at any speed within this region.

As the operating speed is increased, the back-EMF is increased. Thus the applied motor voltage should also be increased to maintain the same armature current, i.e., the same torque. Like this, in this region, the terminal voltage of the DC motor varies with its speed. Because the voltage applied to the motor should not exceed the rated value, the range of this region is normally limited to the speed at which the terminal voltage of the DC motor reaches the rated value. This speed may be different from the rated speed depending on the operating conditions. Thus it is usually referred to as the base speed ω_b.

2.3.3.2 Constant power region ($\omega_m \geq$ base speed): field-weakening region

Once the motor voltage reaches the rated value, the speed can no longer be controlled by the voltage. At speeds higher than the base speed, the applied voltage remains constant. Thus, instead of the voltage control, the speed can be increased by the reduction of the field flux (is called *field-weakening operation*). The reduction of the field flux can make the back-EMF constant regardless of the speed increase. This allows the armature current, which produces a torque, to flow. However, even though the same current is flowing, the output torque will be decreased with the operating speed due to the reduced field flux. Because the terminal voltage and the current remain constant in this region, the motor operates in a constant power, $P = (V_a \cdot I_a = T_e \cdot \omega_m)$. Thus this speed region is called the *constant power region*.

Fig. 2.11 shows the speed−torque characteristic of the DC motor, which is commonly called the *capability curve*. The capability curve demonstrates the achievable speed range and the output torque of a motor under the available voltage and current. For DC motor drives with the four-quadrant operation modes as described in Section 1.3.2, this speed−torque characteristic appears in all four quadrants. Considering the voltage drop in armature resistance and losses, the output torque in Quadrants 2 and 4 are somewhat larger than those in Quadrants 1

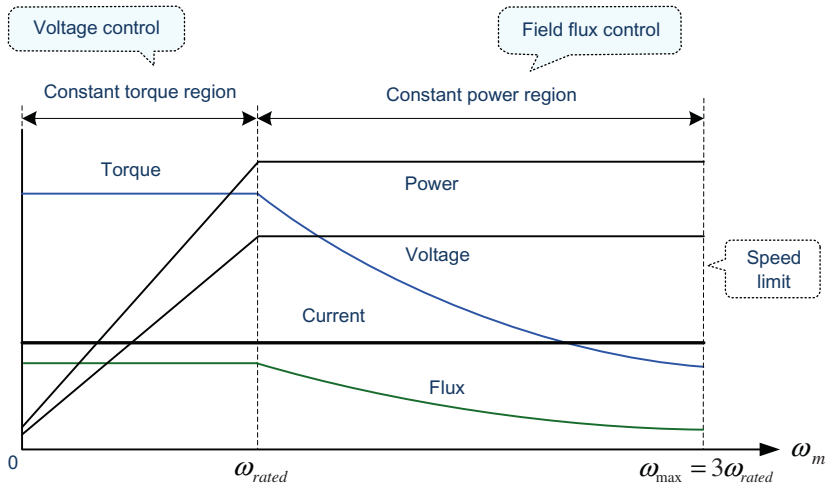


FIGURE 2.11

Capability curve of the DC motor.

and 3. For the four-quadrant operation, the direction of the output torque needs to be reversed to change the direction of the rotor rotation. In this case, changing the polarity of the armature current will be more effective. Even though the direction of the torque may be changed by reversing the polarity of field flux, its response is slow due to a large inductance of the field winding, and thus the stability of the drive system may be deteriorated.

EXAMPLE 1

The rated values for a separately excited DC motor are 5 kW, 140 V, 1800 r/min and the efficiency η is 91% (the losses such as mechanical losses and iron losses are ignored). The armature resistance is 0.25 Ω. Evaluate the following questions.

1. the armature current and the rated torque
2. the speed at full-load when the armature voltage is reduced by 10%
3. the speed at full-load current when the flux is reduced by 10% and the output torque available by armature current at this speed

Solution

1. From the relation of the input and output powers as

$$P_{out} = \frac{P_{in}}{\eta} = \frac{V_a \cdot I_a}{\eta}.$$

the armature current is

$$I_a = \frac{P_{out}}{V_a \cdot \eta} = \frac{5\ \text{kW}}{125\ \text{V} \cdot 0.91} = 44.96\ \text{A}.$$

From the output power $P_{out} = T_e \cdot \omega_m$, the rated torque is

$$T_e = \frac{P_{out}}{\omega_m} = \frac{3150\ \text{W}}{\left(\frac{3000 \cdot 2\pi}{60}\right)} = 26.5\ \text{N m}.$$

2. The armature voltage reduced by 10%, V_{new}, is 112.5V. At this voltage, the speed is

$$\omega_m = \frac{E_a}{k\phi_f} = \frac{V_{new} - R_a I_a}{k\phi_f} = \frac{101.25}{0.60344}. = 167.8\ \text{rad/s}\ (= 1602.2\ r/\text{min})$$

Here, $k\phi_f = E_a/\omega_m = (V_{new} - R_a I_a)/\omega_m = 0.60344$.

3. The speed at the flux reduced by 10% is

$$\omega_m = \frac{E_a}{0.9k\phi_f} = \frac{(V_{new} - R_a I_a)}{0.9k\phi_f} = \frac{113.75}{(0.9 \cdot 0.60344)} = 209.44\ \text{rad/s}(= 2000\ \text{r/min})$$

At this speed, the output torque available by armature current is

$$T_{e@2000} = 0.9k\phi_f I_a = 23.87\text{N m}.$$

2.4 TRANSIENT RESPONSE CHARACTERISTICS OF DIRECT CURRENT MOTORS

In Section 2.3, we studied the steady-state characteristics of DC motors, which demonstrate the speed control by the armature voltage or the field flux. The steady-state characteristic shows what the final speed is, whereas the transient response shows how to reach the final speed. In addition to the steady-state characteristic, the transient characteristic is very important for high-performance motor drives. This is because the transient response characterizes the dynamics of the drive system. As an example, transient responses to a step speed command are shown in Fig. 2.12.

Even though all three responses reach the same final speed, their response times and moving trajectories to reach the final speed are different. Although an oscillatory or slow response can ultimately achieve the speed command, it has no practical use. Therefore we need to take into account the transient characteristic as well as the steady-state characteristic for high-performance motor drives.

Now, let us take a look at the transient response of reaching the final speed by the applied armature voltage for a DC motor. An easy way to examine the transient response is to use the transfer function of the system. We can obtain the

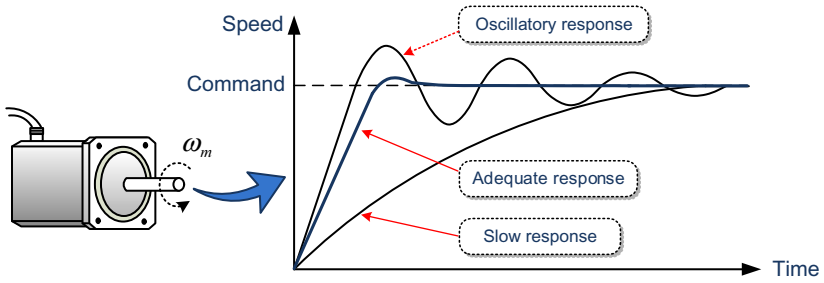


FIGURE 2.12

Transient response to a step speed command.

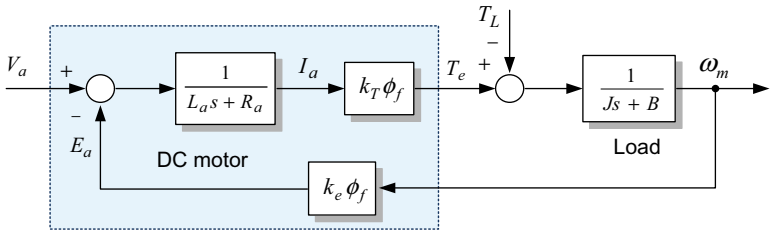


FIGURE 2.13

Block diagram for a DC motor.

transfer function for the DC motor drive system by taking the *Laplace* transform of the differential equations of Eq. (2.1) and (2.4) as follows.

$$v_a = R_a i_a + L_a \frac{di_a}{dt} + e_a \rightarrow V_a(s) = (R_a + sL_a)I_a(s) + E_a(s) = (R_a + sL_a)I_a(s) + k_e \phi_f \omega_m(s) \tag{2.8}$$

$$T_e = J\frac{d\omega_m}{dt} + B\omega_m + T_L \rightarrow T_e(s) = (Js + B)\omega_m(s) + T_L = k_T \phi_f I_a(s) \tag{2.9}$$

Here, s denotes the *Laplace* operator. Eqs. (2.8) and (2.9) together can be represented by the closed-loop block diagram as shown in Fig. 2.13.

From the block diagram in Fig. 2.13, the transfer function from the input armature voltage $V_a(s)$ to the output angular velocity $\omega_m(s)$ is given by

$$\frac{\omega_m(s)}{V_a(s)} = \frac{\frac{1}{L_a s + R_a} \cdot k_e \phi_f \cdot \frac{1}{Js + B}}{1 + \left(\frac{1}{L_a s + R_a} \cdot k_e \phi_f \cdot \frac{1}{Js + B} k_T \phi_f\right)} = \frac{\frac{k}{JL_a}}{s^2 + \left(\frac{R_a}{L_a} + \frac{B}{J}\right)s + \left(\frac{R_a}{L_a}\frac{B}{J} + \frac{k^2}{JL_a}\right)} \quad (k = k_T \phi_f = k_e \phi_f) \tag{2.10}$$

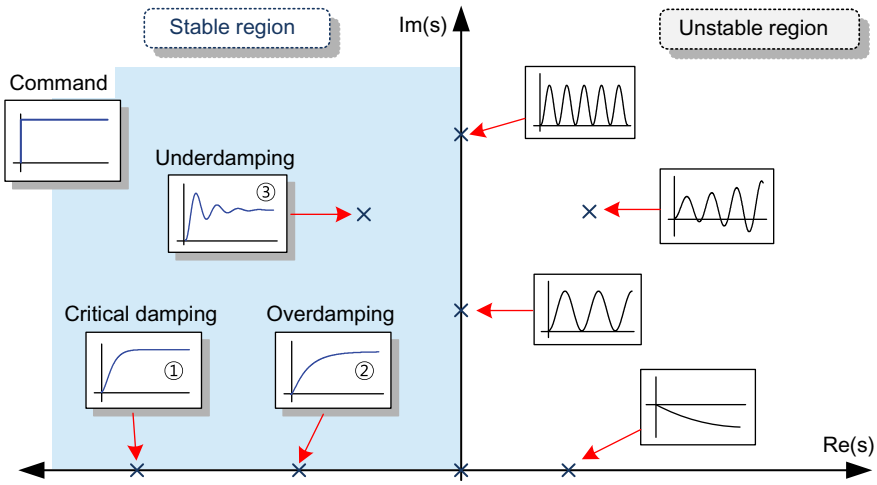


FIGURE 2.14

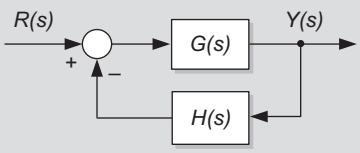
System pole locations and the corresponding transient responses.

This transfer function is a second-order system including two poles, which are important factors in determining the transient response of the system. Fig. 2.14 shows the pole locations of a system in the *s*-plane and the corresponding transient responses. The imaginary axis location of the pole determines the frequency of oscillations in the response. Thus, if the poles are complex roots, the response is oscillatory. The real axis location of the pole determines the speed of the exponential decay of the transient situation. Therefore, the farther the distance of the pole from the origin is to the left in the *s*-plane, the faster the transient situation disappears, i.e., the system reaches the final value faster.

CLOSED-LOOP TRANSFER FUNCTION

A system with a feedback loop has the following transfer function:

$$\frac{Y(s)}{R(s)} = \frac{G(s)}{1 + G(s)H(s)}$$



From the locations of the two poles in Eq. (2.10), we can predict the transient response of the speed to the applied armature voltage. Thus the transient response depends heavily on the system parameters such as motor parameters R_a and L_a and mechanical parameters J and B, as shown in the following.

Assuming that $B = 0$ in Eq. (2.10) to analyze the system easily, we can obtain a simplified transfer function as

$$\frac{\omega_m}{V_a} = \frac{\dfrac{k}{JL_a}}{s^2 + \left(\dfrac{R_a}{L_a}\right)s + \left(\dfrac{k^2}{JL_a}\right)} = \frac{\dfrac{1}{k}\left(\dfrac{R_a}{L_a} \cdot \dfrac{k^2}{JR_a}\right)}{s^2 + \left(\dfrac{R_a}{L_a}\right)s + \left(\dfrac{R_a}{L_a} \cdot \dfrac{k^2}{JR_a}\right)} \tag{2.11}$$

Letting the electromechanical time constant $T_m = JR_a/k^2$ and the electrical time constant $T_a = L_a/R_a$, Eq. (2.11) can be rewritten as

$$\frac{\omega_m}{V_a} = \frac{\dfrac{1}{k}\left(\dfrac{1}{T_m T_a}\right)}{s^2 + \dfrac{1}{T_a}s + \dfrac{1}{T_m T_a}} \tag{2.12}$$

The poles can be obtained from the roots of the denominator (also called the characteristic equation) of Eq. (2.12) as

$$s_{1,2} = -\frac{1}{2T_a} \pm \frac{1}{T_a}\sqrt{\frac{1}{4} - \frac{T_a}{T_m}} \tag{2.13}$$

If $T_m \geq 4T_a$, then the characteristic equation has two real roots. A DC motor drive system with a large J or R_a corresponds to this case, and its response is either ① or ② in Fig. 2.14. If $T_m < 4T_a$, then the characteristic equation has two complex roots. In this case, the system response is oscillatory such as ③ in Fig. 2.14.

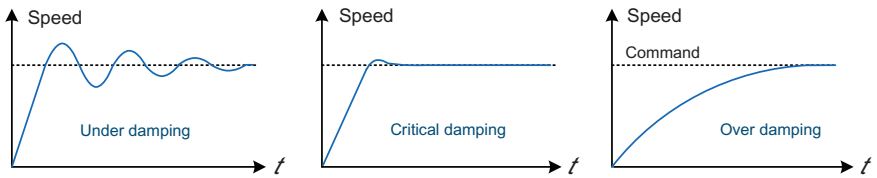
We can also find out the response characteristic from the damping ratio for this second-order system. To do so, we compare this equation with the following prototype of the second-order system.

$$G(s) = \frac{\omega_n^2}{s^2 + 2\zeta\omega_n s + \omega_n^2} \tag{2.14}$$

Given Eq. (2.14), the undamped natural frequency ω_n and the damping ratio ζ for the DC motor drive system are given by

$$\omega_n = \frac{1}{\sqrt{T_a T_m}} = \frac{k}{\sqrt{JL_a}} \tag{2.15}$$

$$\zeta = \frac{1}{2}\sqrt{\frac{T_m}{T_a}} = \frac{1}{2}\frac{R_a}{k}\sqrt{\frac{J}{L_a}} \tag{2.16}$$



(A) Underdamping (ζ<1) (B) Critical damping (ζ=1) (C) Overdamping (ζ>1)

FIGURE 2.15

System responses according to the damping ratio. (A) Underdamping ($\zeta < 1$), (B) critical damping ($\zeta = 1$), and (C) overdamping ($\zeta > 1$).

There are three typical responses of the system according to the value of the damping ratio ζ: *underdamping* ($0<\zeta<1$), *critical damping* ($\zeta = 1$), or *overdamping* ($\zeta>1$) [1]. As shown in Fig. 2.15, in the case of underdamping ($0<\zeta<1$), the system comes rapidly to equilibrium but has a slight oscillatory response. As ζ is increased, the oscillation is reduced. In the case of overdamping ($\zeta>1$), the system is not oscillatory but has a very slow response. A critically damped system response ($\zeta=1$), which comes to equilibrium as fast as possible without oscillating, is the most desirable.

Eq. (2.16) implies that the damping ratio ζ, which implies the dynamic performance of the speed to the applied armature voltage, depends on the electromechanical time constant value T_m and the electrical time constant value T_a. If $T_m<4T_a$, then $\zeta<1$ and its speed response will be oscillatory. By contrast, in the case of $T_m \geq 4T_a$, the system will have a stable speed response without oscillation.

Normally, small motors have $T_m>4T_a$, while servo motors or high power motors have $T_m<4T_a$, resulting in an oscillatory response. Even though the system response is inherently oscillatory, we can achieve the desired response by adopting an adequate controller, which will be described later.

In most motor drive systems, the time response of an electric system is faster than that of a mechanical system. In that case, we can ignore the transient of the electric circuit so that $L_a = 0$. Thus Eq. (2.11) can be written as

$$\frac{\omega_m}{V_a} = \frac{k}{R_a J s + K^2} = \frac{1}{k}\frac{\omega_c}{s+\omega_c}\left(\omega_c = \frac{k^2}{R_a J}\right) \tag{2.17}$$

This equation implies that, in a DC motor, the relationship between the speed ω_m and the armature voltage V_a can be considered as a first-order, low-pass filter with a cut-off frequency ω_c. This means that the speed ω_m is directly proportional to the armature voltage V_a with its changing rate below the ω_c, though there is a time delay between the two. Generally it can be assumed that the rotational speed of a DC motor is proportional to the voltage applied to it.

EXAMPLE 2

Consider a separately excited DC motor with the following parameters. The armature resistance is 0.28 Ω, the armature inductance is 1.7 mH, the inertia of moment J of this motor is 0.00252, and $k\phi_f = 0.4078$.

1. Calculate the locations of the two poles and predict the transient response of the speed to an armature voltage at no-load.
2. Predict the transient response when this motor is driving the load with the inertia of moment of $6J$.

Solution

1. From Eq. (2.13), the two poles are

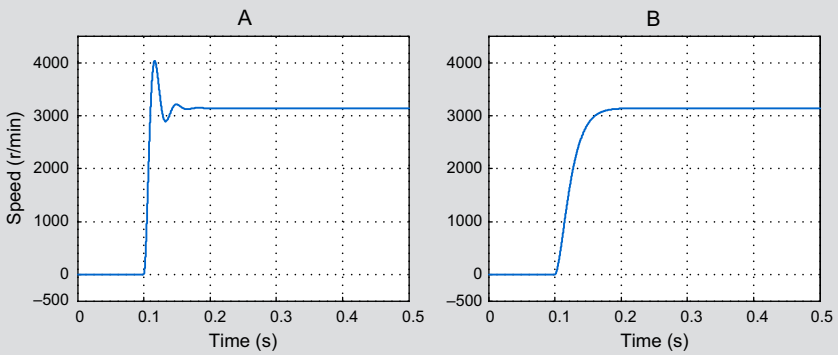
$$s_{1,2} = -\frac{1}{2T_a} \pm \frac{1}{T_a}\sqrt{\frac{1}{4} - \frac{T_a}{T_m}} = -76.47 \pm j181.57.$$

Since the system has two complex poles, we can expect an oscillatory system response. Also, from Eq. (2.16), the damping ratio is

$$\zeta = \frac{1}{2}\sqrt{\frac{T_m}{T_a}} = \frac{1}{2}\frac{R_a}{k}\sqrt{\frac{J}{L_a}} = 0.3881.$$

Because $\zeta < 1$, we can expect the system to have an under-damped response and an overshoot. From Figure A, we can see the oscillatory speed response of this system to the step applied voltages.

2. When this motor is driving the load with the inertia of moment of $6J$, the system has two real poles of -152 and -0.0002. Thus the system response is not oscillatory. Also, since $\zeta = 1.0269$, we can expect the critically damped system response to be as Figure B.



2.5 MOTOR CONTROL SYSTEM

An electric motor is an electromechanical device that converts electrical energy into mechanical torque. As a torque-producing device, the electric motor needs to have its torque controlled as a priority. When the torque produced by the motor is applied to a mechanical load, the torque will change the speed ω_m of the driven load and, in turn, change its position θ_m as shown in Fig. 2.16.

Therefore, in motor drives, the most effective way for controlling the position or speed of the load connected to the motor is to control the torque of the motor directly. However, the torque control is expensive due to the high cost of the torque sensor for motor torque feedback. We can see from Eq. (2.3) that the torque is directly proportional to the current under a constant field flux. This tells us that we can control the torque by using the current instead of the torque itself. Thus the current control is important for the speed or position control of a motor.

2.5.1 CONFIGURATION OF CONTROL SYSTEM

Fig. 2.17 illustrates the typical configuration of controllers in the motor drive systems, in which the controllers required for position, speed and current control are usually connected in a cascade.

Among these, the current controller must be placed at the most inner loop and has the widest bandwidth. As mentioned above, since the speed and position can be controlled through the current control, the response time for the current control must be the fastest among the three. Likewise, the response for the control of the inner loop should be sufficiently faster than that of the outer loop to improve the response performance and the stability of the outer control loop. For example, the bandwidth of the current loop needed to be at least five times wider than that of the speed loop to ensure that the current control will not have any influence on the speed control performance.

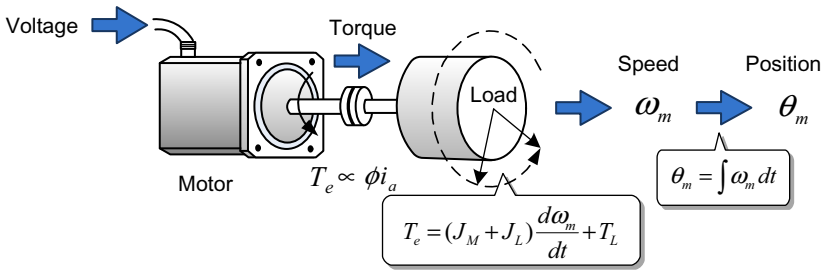


FIGURE 2.16

The motor drive system.

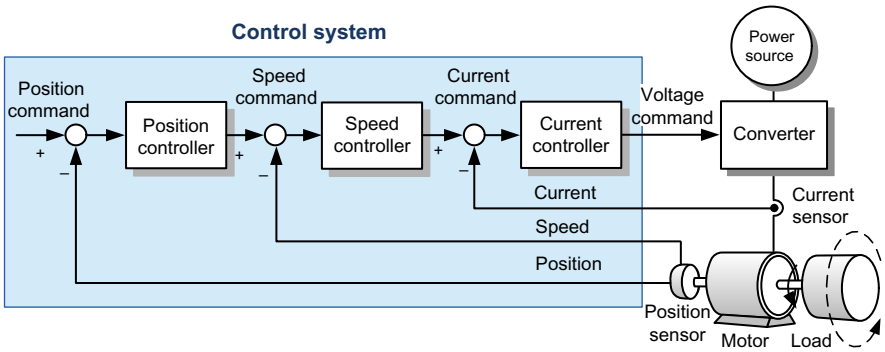


FIGURE 2.17

Configuration of the motor control system.

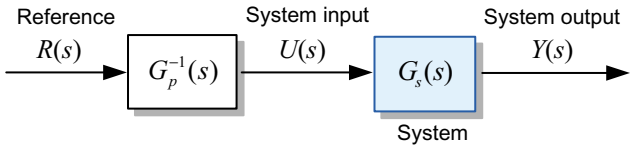


FIGURE 2.18

Open-loop control.

2.5.2 TYPES OF CONTROL

The aim of control is to adjust the control input so that the state or output of the system reaches the required goal. In the motor drive systems, the state or output may be the current, flux, speed, position, or torque, while the control input is only the input voltage. For control performance, the ability of reference tracking, i.e., the system output follows the reference input as accurately as possible, is the most important factor. The control system is also needed to have the disturbance rejection capability while tracking the reference input. This means that no disturbance can affect the system tracking the reference input as much.

There are two basic types of control: *open-loop control* and *closed-loop control*, also known as *nonfeedback* and *feedback*, respectively.

2.5.2.1 Open-loop control (or nonfeedback control)

Open-loop control is a type of control that determines the control input $U(s)$ of a system by using the system model $G_s(s)$ as shown in Fig. 2.18.

A drawback of the open-loop control is that it requires perfect knowledge of the system. Since the open-loop control does not use the feedback of the system output $Y(s)$, the error between the reference $R(s)$ and the output $Y(s)$ cannot be reflected in determining its control input $U(s)$. Therefore its output may be

different from the desired goal due to the change in system parameters or disturbances.

Because of its simplicity and low cost, the open-loop control is often used in systems where it has the well-defined relationship between input and output and are not influenced by disturbances. However, this open-loop control is inadequate for the high-performance motor drive systems, which are easily affected by parameter variations and disturbances such as the back-EMF and load torque.

2.5.2.2 Closed-loop control (or feedback control)

Closed-loop control is a type of control that adjusts the control input $U(s)$ by the feedback of the output $Y(s)$, as shown in Fig. 2.19. The closed-loop control is generally used to control the position, speed, current, or flux in the motor drive systems.

The controller $G_c(s)$ adjusts its control input $U(s)$ to reduce the error between the output and the desired goal. Thus the role of the controller $G_c(s)$ in the closed-loop control is very critical to the system's performance. There are several types of widely used types of the feedback controller in the motor drive systems as follows.

2.5.2.2.1 Feedback control

Proportional controller (P controller)

In this type of controller, which is illustrated in Fig. 2.20, the controller output is proportional to the present error $e(t)(= r(t) - y(t))$ as given by

$$U(t) = K_p e(t) \tag{2.18}$$

where K_p represents the proportional gain.

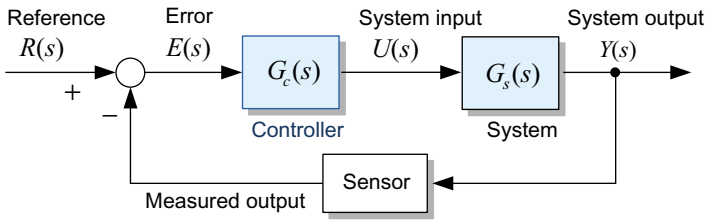


FIGURE 2.19

Closed-loop control.

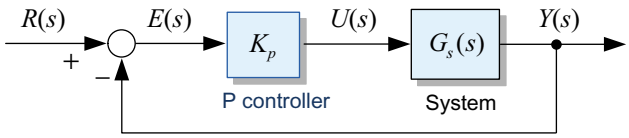


FIGURE 2.20

Proportional control.

An advantage of the proportional control is its immediate response to errors. The larger the proportional gain is, the faster the response is. Thus it should be noted that the proportional gain determines the control bandwidth. However, there is a limit to increasing the proportional gain because a large gain can lead to system instability or may require unrealizable control input. A drawback of the proportional control is that the error can never be zero. In other words, there exists a steady-state error in the P control. This is because when the error comes to zero, the output of the P controller becomes zero. Thus the system will have an error again. We can evaluate the steady-state error of the P controller from its close-loop transfer function of the block diagram in Fig. 2.20 as,

$$\frac{R(s)}{Y(s)} = \frac{G^o(s)}{1 + G^o(s)} = \frac{K_p G_p(s)}{1 + K_p G_p(s)} \tag{2.19}$$

where $G^o(s)(= K_p G_p(s))$ is the open-loop transfer function of the system including the proportional controller.

From Eq. (2.19), if the proportional gain K_p is very large, then $R(s)/Y(s)$ will be close to one and the error will be very small, but it will never reach zero.

Integral controller (I controller)

In this type of controller, the controller output is the integral of the error as shown in Fig. 2.21, so the past errors as well as the present error have an effect on the control input as given by

$$U(t) = K_i \int e(t)dt = \frac{K_p}{T_{pi}} \int e(t)dt \tag{2.20}$$

where K_i represents the integral gain and $T_{pi}(= K_p/K_i)$ represents the integral time constant.

The integral controller can remove the steady-state error completely for the non-time varying reference $R(s)$. This is because it continuously produces nonzero control input from the accumulated past errors even though the present error is zero. However, due to the accumulated errors in the integral term, it responds slowly to change in errors. For this reason, the integral controller is not normally used alone but is combined with the P controller.

Proportional–integral controller

A widely used controller in motor drive systems is the proportional–integral controller (PI controller), which is a combination of a proportional controller and an integral controller to achieve both a fast response and a zero steady-state error. The block diagram of a proportional–integral controller is shown in Fig. 2.22.

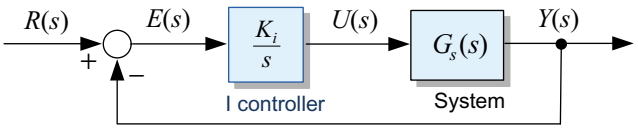


FIGURE 2.21

Integral control.

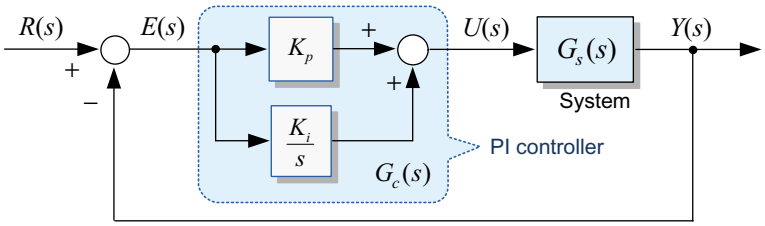


FIGURE 2.22

Proportional–integral control.

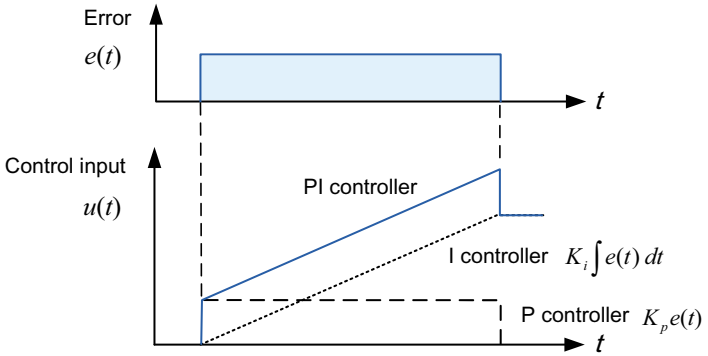


FIGURE 2.23

Control inputs for an error.

Fig. 2.23 compares the control inputs for an error in the three controllers described earlier.

2.5.2.3 Feedforward control

Disturbances are always present in the control process. In motor drive systems, e.g., the back-EMF acts as a disturbance on the current control, and the load torque acts as a disturbance on the speed and position control. We can see from the Section 2.5.2.2.1 that the feedback control operates to reduce the error between the output and the desired goal. Thus the feedback control can react to the disturbance only after the disturbance has an effect on the output. Accordingly, the feedback control cannot achieve a fast response to the disturbance.

Feedforward control is an effective way to rapidly eliminate the effect of the disturbance on the output. The feedforward control predicts and compensates for the disturbance by adding it to the control input in advance.

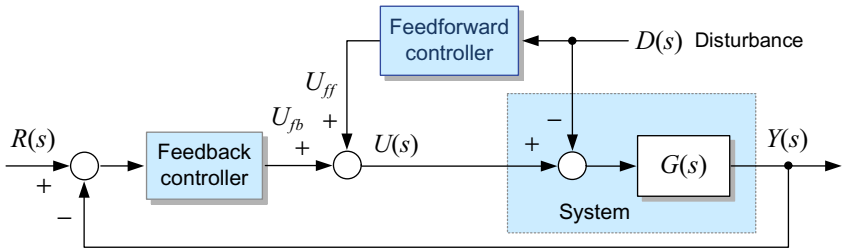


FIGURE 2.24

Feedforward control.

The feedforward control is always used along with the feedback control. Fig. 2.24 shows the block diagram of a typical system with the feedback control and the feedforward control. This control system can reduce the effect of the disturbance $D(s)$ on the output $Y(s)$ more than the system with the feedback control alone. For the feedforward control, accurate system parameters are required to predict the disturbance correctly.

In motor current control systems, the performance of the current control could be significantly improved by the feedforward control, which compensates for the back-EMF that acts as a disturbance on the current control. This feedforward control for current control of DC motors and AC motors will be described in detail later. For motor speed control, the performance of the speed control could also be significantly improved by feedforward control for the load torque.

2.5.3 DESIGN CONSIDERATION OF CONTROL SYSTEM

The PI controller has been widely used in motor drive systems as the controller for the current, speed, or flux linkage control because it could give a satisfactory performance. The performance of the PI controller depends heavily on its selected gains. Thus it is very important to select appropriate gains of the PI controller for obtaining a satisfactory performance in a given system.

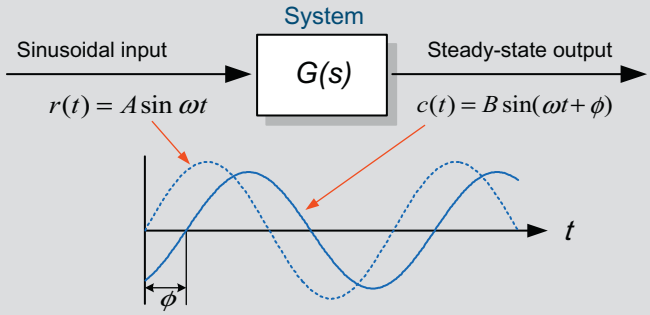
Now, we will discuss the gain selection method for the current and speed PI controllers. Through the frequency response of the whole system including the PI controller, we will determine the P and I gains for achieving the desired transient and steady-state characteristics.

WHAT IS FREQUENCY RESPONSE?

The output of a linear system to a sinusoidal input is a sinusoid of the same frequency but with a different amplitude and phase. The *frequency response* refers to a system's open-loop responses at the steady state to sinusoidal inputs at varying frequencies as shown in the following figure.

(*Continued*)

WHAT IS FREQUENCY RESPONSE? (CONTINUED)



The frequency response is used to characterize the dynamics of a system and measure the ability of the system following an input reference. The frequency response is characterized by the magnitude and phase of the system's response as a function of frequency, which are calculated from the transfer function $G(s)$ of the system as

$$\left.\frac{C(s)}{R(s)}\right|_{s=j\omega} = G(s)\big|_{s=j\omega} = |G(j\omega)| \angle \phi(j\omega)$$

where $|G(j\omega)|$ and $\angle \phi(j\omega)$ represent the amplitude and phase angle between the input and output signals, respectively.

We can easily see the frequency response of a dynamic system through a *Bode plot*, which displays the magnitude (in dB) and the phase (in degrees) of the system response as a function of frequency.

When designing a control system, we should consider the three specifications: *stability, response time*, and *steady-state error*. We will begin with briefly reviewing these specifications.

2.5.3.1 Stability

First of all, the whole system, including the controller, must be stable. Therefore the stability is the most important requirement for the design of a control system. The response of an unstable system to a bounded input signal will continue to oscillate, but the magnitude of this oscillation will never diminish or get larger.

The stability of linear systems can be assessed by checking the poles of the transfer function of the system, i.e., the roots of the characteristic equation in the s-plane as we already saw in Fig. 2.14. A linear system is stable if *all* the poles lie in the left-half s-plane.

However, merely knowing whether a system is stable or unstable is not sufficient. We need to find out how stable the system is. We can measure the relative stability of a system by examining the *gain margin* and the *phase margin* obtained from the Bode plot of the frequency response. A brief description of the gain margin and the phase margin is presented below.

2.5.3.1.1 Gain margin and phase margin

Phase margin and gain margin are the measures of closed-loop control systems stability. They are illustrated in Fig. 2.25.

1. Gain margin
   Gain margin is defined as the amount of change in open-loop gain needed to make a closed-loop system unstable. The gain margin is the difference between 0 dB and the gain at the phase cross-over frequency that gives a phase of $-180°$. If the gain $|GH(j\omega)|$ at the frequency of $\angle GH(j\omega) = -180°$ is greater than 0 dB as shown in the left of Fig. 2.25, meaning a positive gain margin, then the closed-loop system is stable.
2. Phase margin
   Phase margin is defined as the amount of change in open-loop phase needed to make a closed-loop system unstable. The phase margin is the difference in phase between $-180°$ and the phase at the gain cross-over frequency that gives a gain of 0 dB. If the phase $\angle GH(j\omega)$ at the frequency of $|GH(j\omega)| = 1$ is greater than $-180°$ as shown in the left of Fig. 2.25, meaning a positive phase margin, the closed-loop system is stable.

In general, as the gain of a system increases, the system becomes less stable. The gain margin and the phase margin indicate how much the gain increases until the system becomes unstable.

Let us take a look at the relationship between the gain and phase margins and the stability of a system. For example, assume that the phase margin of a system is zero degree, i.e., $\angle GH(j\omega) = 180°$ at a frequency ω of $|G(j\omega)| = 1$ dB. In this case, as shown in Fig. 2.26, the phase difference between $Y(s)$ and $R(s)$ is 180°,

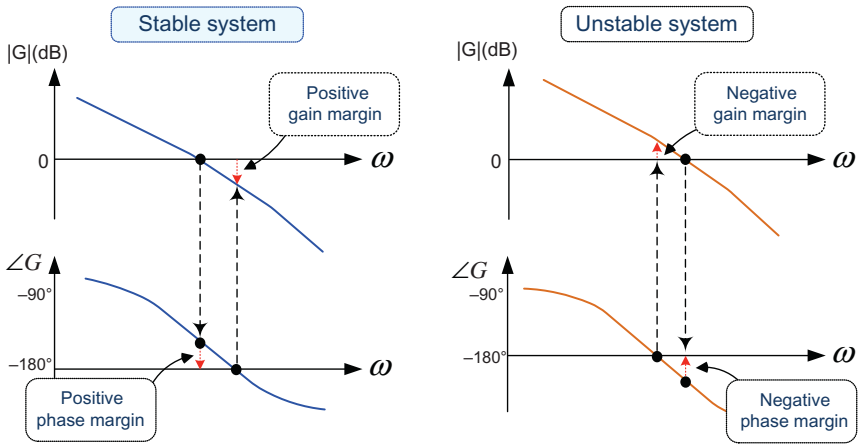


FIGURE 2.25

Gain margin and phase margin.

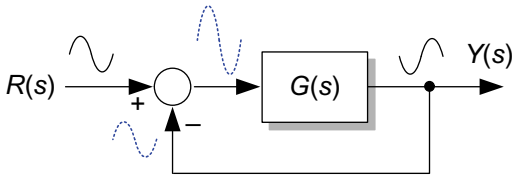


FIGURE 2.26

Example of an unstable system.

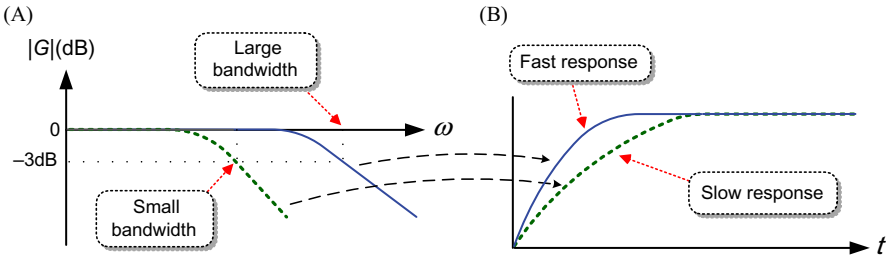


FIGURE 2.27

Speed of response versus system bandwidths. (A) Frequency responses and (B) step responses.

and this closed-loop system thus becomes a positive feedback system. This system will continue to amplify its output and become unstable.

If a closed-loop system is stable, both the gain margin and the phase margin need to be positive. In general, the phase margin of 30−60 degrees and the gain margin of 2−10 dB are desirable in the closed-loop system design. A system with a large gain margin and phase margin is stable but has a sluggish response, while the one with a small gain margin and phase margin has a less sluggish response but is oscillatory.

2.5.3.2 Response time/speed of response

How quickly a system responds to the change in input is an important measure of the system's dynamic performance. The speed of response of a closed-loop system may be proportional to its control bandwidth. Thus the control bandwidth is a measure of the speed of response.

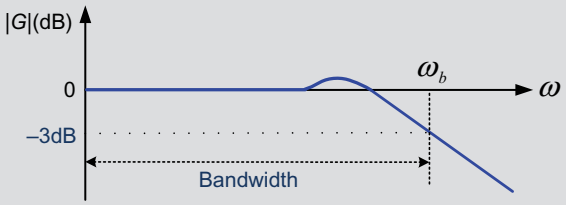
We can see the system responds according to its control bandwidth from Fig. 2.27, which is showing the responses to a step command versus system bandwidths. Generally, the wider the system's control bandwidth, the faster the speed of response is. However, if the control bandwidth of a system is too large, the system may be sensitive to noise and become unstable.

This control bandwidth is mainly dependent on the proportional gain of the controller. Thus we need to adjust the P gain to obtain the desired response speed.

WHAT IS BANDWIDTH?

Bandwidth describes how well a system follows a sinusoidal input. We can easily find the bandwidth from the system's closed-loop frequency response. As in the following figure, the bandwidth is the range of frequencies for which the magnitude $|G|$ of the frequency response is greater than 3 dB, i.e., $0 \leq \omega \leq \omega_b$.

The bandwidth is a measure of the feedback system's ability to follow the input signal. Sinusoidal inputs with a frequency less than the bandwidth frequency ω_b are followed reasonably well by the system, whereas sinusoidal inputs with a frequency greater than the bandwidth frequency are attenuated in magnitude by a factor of 1/10 or greater (and are also shifted in phase). The concept of the bandwidth is very important in control systems because it describes how quickly a system follows its command.



2.5.3.3 Steady-state error

A steady-state error is defined as the difference between the desired value and the actual value of a system when the response has reached the steady state. We can calculate the steady-state error of the system using the *final value theorem*. This theorem is given for the unit feedback system in Fig. 2.28 as

$$\text{Final value theorem: } e_\infty = \lim_{t\to\infty} e(t) = \lim_{s\to 0} sE(s) = \lim_{s\to 0} \frac{s}{1+G(s)} R(s) \tag{2.21}$$

$$\left(\text{Error: } E(s) = R(s) - Y(s) = \frac{R(s)}{1+G(s)}\right)$$

As an example, let us evaluate the steady-state error for a step input command in the control system for a DC motor, where the speed or current command is

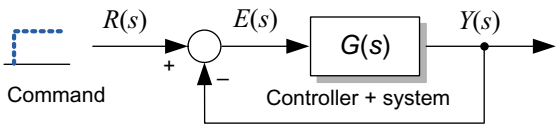


FIGURE 2.28

Unit feedback system.

generally given as a step signal. Assume that the control system for the DC motor is a unit feedback system as in Fig. 2.28, and the transfer function of the current control system is $G(s)$. For the unit step input ($r(t) = 1 \rightarrow R(s) = 1/s$) to this system, the steady-state error is given from the final value theorem by

$$e_\infty = \lim_{s\to 0} \frac{s}{1+G(s)} R(s) = \lim_{s\to 0} \frac{s}{1+G(s)} \frac{1}{s} = \lim_{s\to 0} \frac{1}{1+G(s)} \tag{2.22}$$

The steady-state error depends on the system type (0, I, or II).

First, suppose a control system of type 0 expressed as $G(s) = K/(Ts+1)$. In this system the steady-state error is given as

$$e_\infty = \frac{1}{1+G(0)} = \frac{1}{1+K} \tag{2.23}$$

The magnitude of the error depends on the system gain K and will be never zero.

Next, suppose a type I system of $G(s) = K/s(Ts+1)$. This control system has no steady-state error as

$$e_\infty = \frac{1}{1+G(0)} = \frac{1}{1+\infty} = 0 \tag{2.24}$$

From this, it can be seen that if a control system includes an integrator $1/s$, then the steady-state error to a step reference will be zero.

2.6 CURRENT CONTROLLER DESIGN

The PI controller is the most commonly used in the DC motor drive systems for current control. In this section we will introduce how to design a current controller, i.e., how to select the P and I gains of a PI current controller for the desired performance.

The PI controller consists of a proportional term, which depends on the present error, and an integral term, which depends on the accumulation of past and present errors as follows:

$$G_{pi}(s) = K_p + \frac{K_i}{s} \tag{2.25}$$

where K_p and K_i are the proportional and integral gain, respectively.

Fig. 2.29 shows the frequency response of the PI controller. The PI controller has an infinite DC gain (i.e., gain when $\omega = 0$) due to an integrator.

The transfer function of Eq. (2.25) can be rewritten as

$$G_{pi}(s) = K_p\left(1 + \frac{1}{T_{pi}s}\right) = K_p \frac{\left(s + \frac{1}{T_{pi}}\right)}{s} \tag{2.26}$$

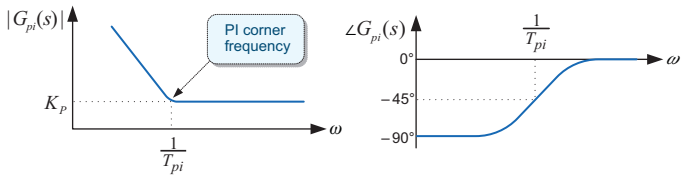


FIGURE 2.29

Frequency response of the PI controller.

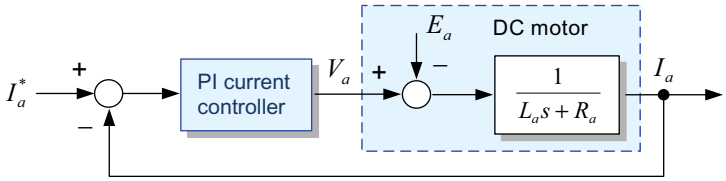


FIGURE 2.30

Block diagram of the DC motor including a current controller.

where $T_{pi} = K_p/K_i$ is the integral time constant of the PI controller and $1/T_{pi}$ is called the corner frequency of the PI controller.

From Eq. (2.26), we can see that the PI controller can add one pole at $s = 0$ and one zero at $s = -K_i/K_p$ to the transfer function of the system. The location of this zero has a strong influence on the system performance, which will be described in detail later. If the zero is correctly placed, then the damping of the system can be improved. As mentioned earlier, the pole at $s = 0$ of the PI controller causes the system type to be increased by adding an integrator $1/s$ to the transfer function, improving the steady-state error. However, the increased system type may make the system unstable when gains are large. In general, the PI controller can improve the steady-state error but at the expense of stability. In addition, the PI controller can reduce the maximum overshoot and improve the gain and phase margins as well as the resonant peak, but it reduces the bandwidth and extends the rise time. The PI controller also has a characteristic of a low-pass filter that reduces the noise.

Now, let us evaluate the performance of the PI controller for current control of a DC motor. The transfer function of a DC motor system that includes a PI current controller as shown in Fig. 2.30 is given as

$$I(s) = \frac{K_{pc}s + K_{ic}}{L_a s^2 + (R_a + K_{pc})s + K_{ic}} I^*(s) - \frac{s}{L_a s^2 + (R_a + K_{pc})s + K_{ic}} E(s) \qquad (2.27)$$

where K_{pc} and K_{ic} represent the proportional and integral gains of the current controller, respectively.

We can see from Eq. (2.27) that the back-EMF $E(s)$ of the DC motor will act as a disturbance to the current control system. If the current reference of the

DC motor remains a constant value (i.e., $s = 0$), then $E(s)$ will have no influence on the current control performance. However, when the current reference $I^*(s)$ is changed, $E(s)$ may have an influence on the dynamic performance of the actual current $I(s)$ following its reference.

For a large system inertia, the effect of $E(s)$ on the current control can be ignored since the variation of $E(s)$ due to the speed variation is very small. However, for servo motors designed with a small inertia for a fast speed response, the effect of $E(s)$ cannot be ignored. To obtain a good performance of the current control by eliminating this undesirable effect of the back-EMF, we can adopt the feedforward control as described in the Section 2.5.2.3. Since the back-EMF of a DC motor is $e_a = k_e \phi_f \omega_m$, we can easily estimate it from the speed information. When the disturbance $E(s)$ is compensated by the feedforward control as in Fig. 2.31A, the DC motor will be simplified as a R-L circuit shown in Fig. 2.31B.

For the case of Fig. 2.31B, the current control will be easier and its performance will be improved. In this case, Eq. (2.27) becomes

$$\frac{I(s)}{I^*(s)} = \frac{K_{pc}s + K_{ic}}{L_a s^2 + (R_a + K_{pc})s + K_{ic}} \tag{2.28}$$

From Eq. (2.28), it can be seen that the current control characteristic depends on the performance of the current controller, which will be determined by the P and I gains selected for the PI controller.

Now, we will look at how the proper gains are selected to achieve the desired performance of the current control. Here, we will introduce a gain selection method based on the frequency response of the system.

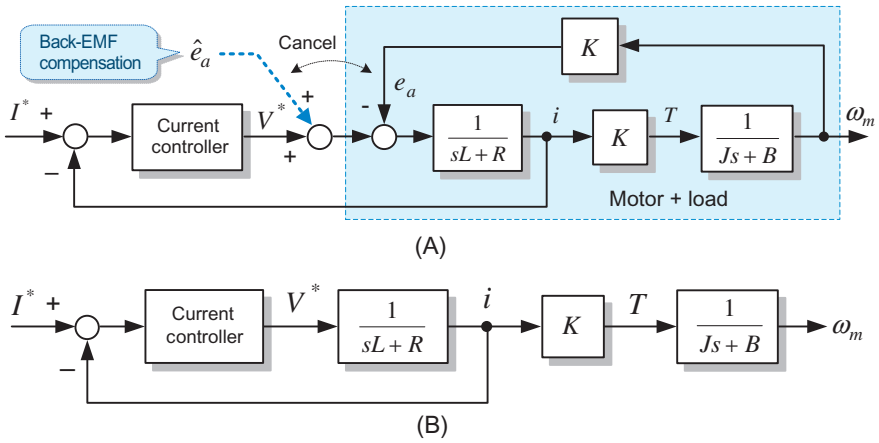


FIGURE 2.31

Current control system. (A) Feedforward control of the back-EMF and (B) system after compensating the back-EMF.

2.6.1 PROPORTIONAL–INTEGRAL CURRENT CONTROLLER

A current control system containing a PI controller is shown in Fig. 2.32. Here, assume that the feedforward control compensates the back-EMF of the DC motor perfectly.

In this PI current controller, the relationship between the current error and its output voltage is given as

$$V_a = K_{pc}\left(1 + \frac{1}{T_{pi}s}\right)\left(I_a^* - I_a\right) \tag{2.29}$$

where $T_{pi}(= K_{pc}/K_{ic})$ is the integral time constant of the PI current controller and K_{ic} is the integral gain.

There are several PI gain tuning rules such as the famous Ziegler–Nichols method. Here, we will adopt the technique called the *pole-zero cancellation method.* By using the pole-zero cancellation, we can remove the current control characteristic of the DC motor itself so that the PI controller may determine the performance of the current control.

The open-loop transfer function $G_c^o(s)$ of this system is given by

$$G_c^o(s) = K_{pc}\left(\frac{s + \frac{1}{T_{pi}}}{s}\right)\cdot\frac{1}{L_a s + R_a} = K_{pc}\frac{\left(s + \frac{K_{ic}}{K_{pc}}\right)}{s}\cdot\frac{\frac{1}{L_a}}{\left(s + \frac{R_a}{L_a}\right)} \tag{2.30}$$

If the zero $(-K_{ic}/K_{pc})$ of the PI controller is designed to cancel the pole $(-R_a/L_a)$ of the DC motor by the pole-zero cancellation method, i.e.

$$\frac{1}{T_{pi}} = \frac{K_{ic}}{K_{pc}} = \frac{R_a}{L_a} \tag{2.31}$$

then, Eq. (2.30) becomes

$$G_c^o(s) = \frac{1}{\left(\frac{L_a}{K_{pc}}\right)s} \tag{2.32}$$

Fig. 2.33 shows the bode plot of the open-loop frequency response from $G_c^o(s)$. The phase is -90° at the gain cross-over frequency ω_{cc} where the magnitude $\left|G_c^o(j\omega)\right| = 0$ dB. Thus the gain margin is positive and the system will be

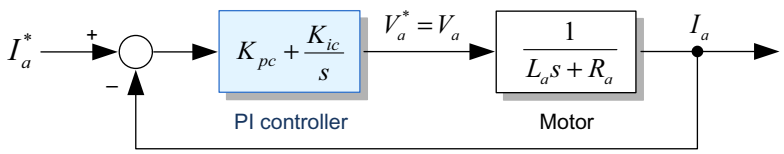


FIGURE 2.32

PI current control system.

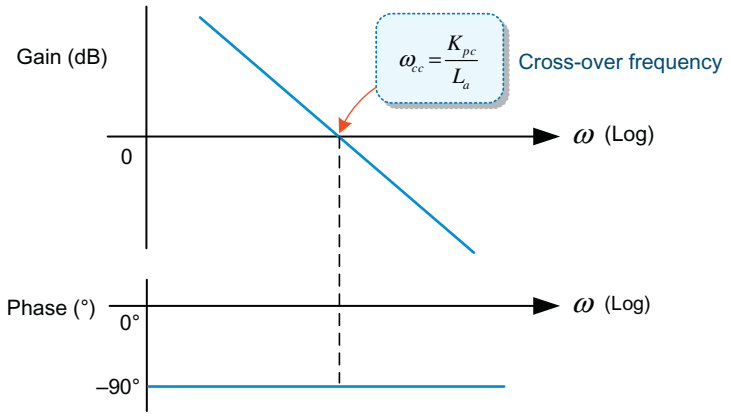


FIGURE 2.33

Open-loop frequency response.

stable. Also, in this case, the transfer function of Eq. (2.32) becomes the system of type = 1 and, thus, we can expect the steady-state error to be zero as

$$e_\infty = \lim_{s\to 0} \frac{1}{1 + G_c^o(s)} = \frac{1}{1 + \infty} = 0 \tag{2.33}$$

From Eq. (2.32), the gain cross-over frequency ω_{cc} can be determined by

$$\left|G_c^o(j\omega_{cc})\right| = \frac{1}{\left|\frac{L_a}{K_{pc}} j\omega_{cc}\right|} = 1 \rightarrow \omega_{cc} = \frac{K_{pc}}{L_a} \tag{2.34}$$

The gain cross-over frequency ω_{cc} of the open-loop frequency response is equal to the gain cut-off frequency of the close-loop frequency response, which indicates the bandwidth of the current control system. Let us check the bandwidth of this current control system.

The closed-loop transfer function of this system is given by

$$\frac{I(s)}{I^*(s)} = G_c^c(s) = \frac{G_c^o(s)}{1 + G_c^o(s)} = \frac{1}{\left(\frac{L_a}{K_{pc}}\right)s + 1} = \frac{\omega_{cc}}{s + \omega_{cc}} \tag{2.35}$$

Its frequency response is shown in Fig. 2.34. We can see that the bandwidth of this system is given as ω_{cc} by letting $\left|G_c^c(j\omega)\right|$ equal to $1/\sqrt{2}(= -3$ dB) as

$$\left|G_c^c(j\omega)\right| = \left|\frac{\omega_{cc}}{j\omega + \omega_{cc}}\right| = \frac{1}{\sqrt{2}} \tag{2.36}$$

Thus the bandwidth is equal to the gain cross-over frequency of the open-loop frequency response.

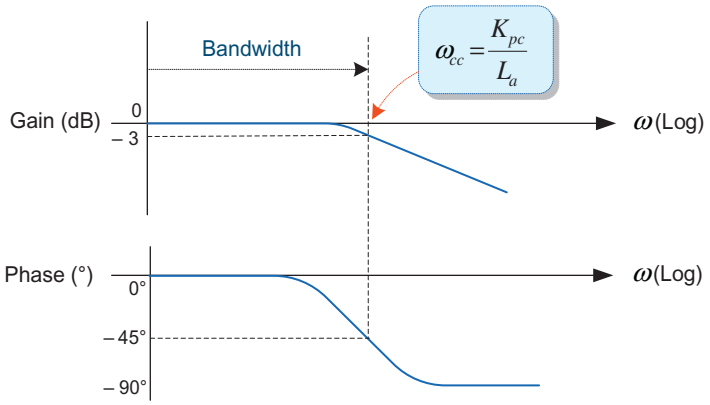


FIGURE 2.34

Closed-loop frequency response.

Like this, if the zero of the PI controller is designed to cancel the pole of the system, the current control system is expressed simply as a first-order system with a cut-off frequency ω_{cc}, which is stable. In this case, there will be no overshoot in the response and the time required for the response to reach the final value will be about four times the time constant of the system.

Based on the explanation given above, the proportional and integral gains of the current controller needed to achieve the required bandwidth can be determined as follows.

If the required control bandwidth is ω_{cc}, then the proportional gain K_{pc} can be obtained from Eq. (2.34) and the integral gain K_{ic} can be obtained from Eq. (2.31) as

$$\text{Proportional gain: } K_{pc} = L_a \cdot \omega_{cc} \tag{2.37}$$

$$\text{Integral gain: } K_{ic} = \frac{R_a}{L_a} K_{pc} = R_a \cdot \omega_{cc} \tag{2.38}$$

It is important to note that the gains of the controller depend on the motor parameters L_a and R_a. Therefore the gain values to achieve the same current control performance may differ from motor to motor. For example, a motor with a large value of winding inductance, whose current is difficult to change, needs a larger proportional gain to obtain an equal bandwidth of the current control than that with a small value of winding inductance, whose current is easy to change. Therefore, accurate information about the motor parameters is essential to achieve the required current control performance.

2.6.1.1 Selection of the bandwidth for current control

The value of the proportional gain K_{pc} determines how fast the system responds, whereas the value of the integral gain K_{ic} determines how fast the steady-state

error is eliminated. When the value of these gains is larger, the control performance is better. However, large gains may lead to an oscillatory response and result in an unstable system. As can be seen in Eq. (2.37) and (2.38), since the gains of a current controller are determined by its bandwidth ω_{cc}, we first need to select an appropriate bandwidth ω_{cc} for the target current control system. A wider bandwidth will lead to a faster response but an unstable system.

The bandwidth ω_{cc} of a current controller is limited by the following two factors: the switching frequency of the power electronic converter realizing the output of the current controller and the sampling period for detecting an actual current for feedback in the digital controller. Since a motor current cannot change faster than the switching frequency of the power electronic converter, the switching frequency limits the bandwidth of the current control. If the current is sampled twice every switching period, as a rule of thumb, the maximum available bandwidth can be up to 1/10 of the switching frequency. On the other hand, if it is sampled once every switching period, the maximum available bandwidth can be up to 1/20 of the switching frequency. For this case, it is desirable to restrict the bandwidth to 1/25 of the sampling frequency [1,2].

As an example, suppose that the switching frequency of a chopper, which provides the voltage applied to a DC motor, is 5 kHz. In this case, the maximum available bandwidth of the current controller can be up to at most 1/10 of the switching frequency, i.e., 5 kHz/10 = 500 Hz($\approx$ 3100 rad/s). However, for a stable current control or if the current is sampled once every switching period, it is better to restrict to 1/20 of the switching frequency, i.e., 5 kHz/20 = 250 Hz ($\approx$ 1550 rad/s).

Fig. 2.35 compares the current control performances according to the gains, which are determined by the gain selection method as described earlier. We can identify the different responses according to the control bandwidth.

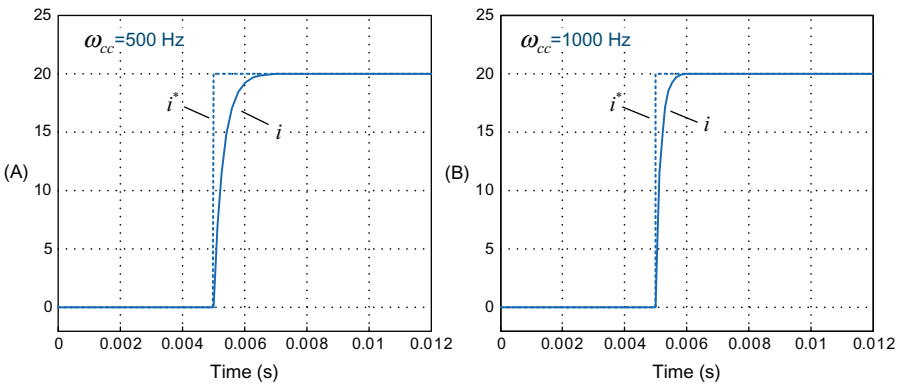


FIGURE 2.35

Current control performance according to the control bandwidth.

2.6.2 ANTI-WINDUP CONTROLLER

As stated before, we can see that the integral controller can effectively eliminate the steady-state error. This is because of the nature of the integral controller producing its output from the accumulated past errors. However, this nature is often the cause of control performance degradation in cases where the output of the controller is limited.

The output of the PI current controller, which indicates the voltage reference applied to a DC motor, should be limited to a feasible value by the following reasons. First, a voltage exceeding its rated value should not be applied to a motor. Furthermore, power electronic converters, which produce the voltage applied to the motor, normally have a restricted output voltage due to the limited availability of the input voltage and the voltage rating of switching devices.

Once the output of the PI controller exceeds its limit due to sustained error signals for a significant period of time, the output will be saturated, but the integrator in the controller may have a large value by its continual integral action. This phenomenon is known as *integral windup*. When the windup occurs, the controller is unable to immediately respond to the changes in the error due to a large accumulated value inside the integrator. It is required that the error have an opposite sign for a long time until the controller returns to the normal state. This system becomes an open-loop system because the output remains at its limit irrespective of the error. As a result, the system will exhibit a large overshoot and a long setting time. To avoid such integrator windup, the magnitude of the integral term should be kept at a proper value when the saturation occurs, so that the controller can resume the action as soon as the control error changes.

There are several methods to avoid the integrator windup such as *back calculation, conditional integration*, and *limited integration* [3,4]. The anti-windup scheme of back calculation as shown in Fig. 2.36 is widely used because of its satisfactory dynamic characteristic.

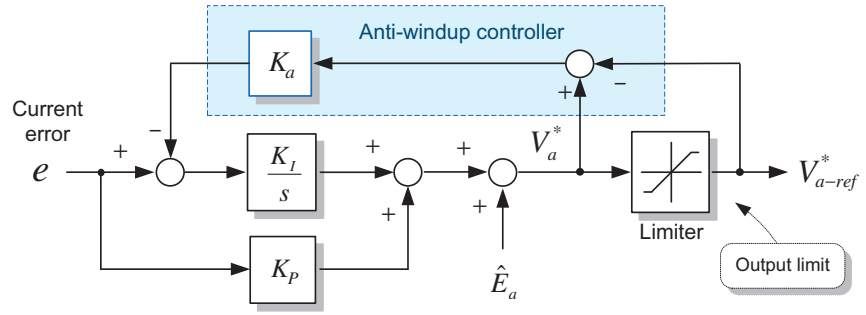


FIGURE 2.36

Anti-windup control by the back calculation method.

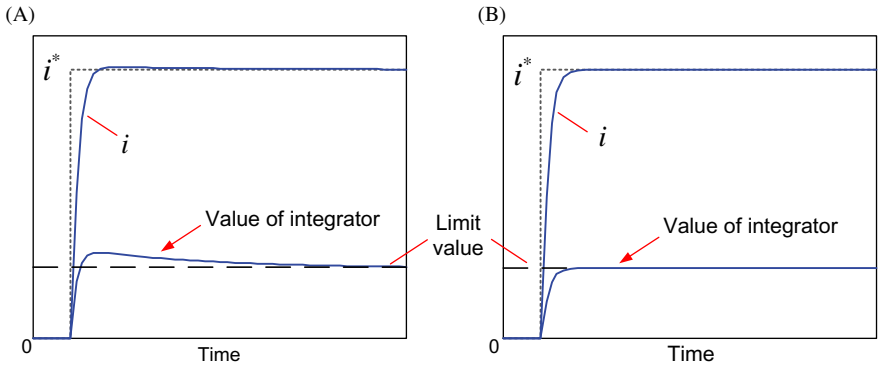


FIGURE 2.37

Anti-windup control. (A) Without anti-windup control and (B) with anti-windup control.

In this scheme, when the output is saturated, the difference between the controller output and the actual output is fed back to the input of the integrator with a gain of K_a so that the accumulated value of the integrator can be kept at a proper value. The gain of an anti-windup controller is normally selected as $K_a = 1/K_p$ to eliminate the dynamics of the limited voltage.

Fig. 2.37 shows the phenomenon of integrator windup for a PI current controller, which is generated by a large change in the reference value. Fig. 2.37A shows the performance of a current controller without an anti-windup control. Due to its saturated output voltage, the actual current exhibits a large overshoot and a long setting time. On the other hand, Fig. 2.37B shows a current controller with an anti-windup control. When the output is saturated, the accumulated value of the integrator can be kept at a proper value, resulting in an improved performance.

2.6.2.1 Gains selection procedure of the proportional–integral current controller

1. Find the switching frequency f_{sw} of the system.
2. Select the control bandwidth ω_{cc} of the current controller to be within 1/10–1/20 of the switching frequency f_{sw} and below 1/25 of the sampling frequency.
3. Calculate the proportional and integral gains from the selected bandwidth ω_{cc} as

$$\text{Proportional gain: } K_{pc} = L_a \cdot \omega_{cc}$$

$$\text{Integral gain: } K_{ic} = R_a \cdot \omega_{cc}$$

4. Select the gain of the anti-windup controller as $K_a = 1/K_{pc}$.

The procedures **1** and **2** are interchangeable with each other, i.e., the switching frequency can be determined by the required bandwidth ω_{cc} for current control.

2.7 SPEED CONTROLLER DESIGN

When controlling the speed of a motor, the speed controller must be placed in the outer loop of the current controller as shown in Fig. 2.38. In this case, if the bandwidth of current control is chosen to be sufficiently wider than that of speed control, then the current control will not have any influence on the speed control performance, and the stability of the speed control will be improved.

Like the current controller, a PI controller is widely used for speed control. Now, we will explain how the PI speed controller is designed, i.e., how to select the proper gains to achieve the desired speed control performance.

2.7.1 PROPORTIONAL–INTEGRAL SPEED CONTROLLER [5]

The transfer function of a PI speed controller is given by

$$G_{pi}(s) = K_{ps} + \frac{K_{is}}{s} \tag{2.39}$$

where K_{ps} and K_{is} are the proportional and integral gains of a PI speed controller, respectively.

From the block diagram in Fig. 2.38, the open-loop transfer function of the speed control system is given by

$$G_s^o(s) = G_{pi}(s)G_c^c(s)\cdot\frac{K_T}{Js} = \left(K_{ps} + \frac{K_{is}}{s}\right)\cdot\frac{\omega_{cc}}{s+\omega_{cc}}\cdot\frac{K_T}{Js} \tag{2.40}$$

This open-loop characteristic is the sum of the frequency responses of three parts: a PI speed controller, a PI current controller, and a mechanical system of a motor and a load. Here, we assume that the current controller is a first-order system with a bandwidth of ω_{cc}. Also, the load torque T_L is neglected and $K_T = k_T\phi_f$.

The bode plot of the open-loop frequency responses for a speed control system is shown in Fig. 2.39. Here, ω_{cs} is the gain cross-over frequency, which is equal to the bandwidth of the speed controller, and $\omega_{pi}(=K_{is}/K_{ps})$ is the PI corner frequency. As a rule of thumb, ω_{pi} is selected as one-fifth of ω_{cs}. If ω_{pi} is too small, the

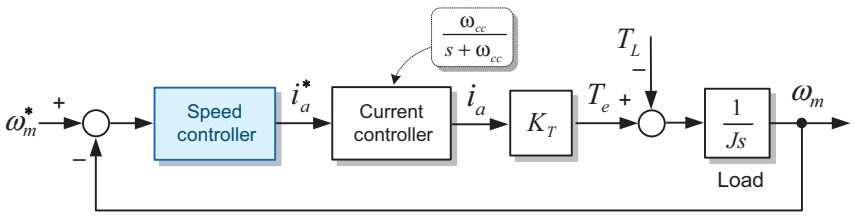


FIGURE 2.38

The speed control system.

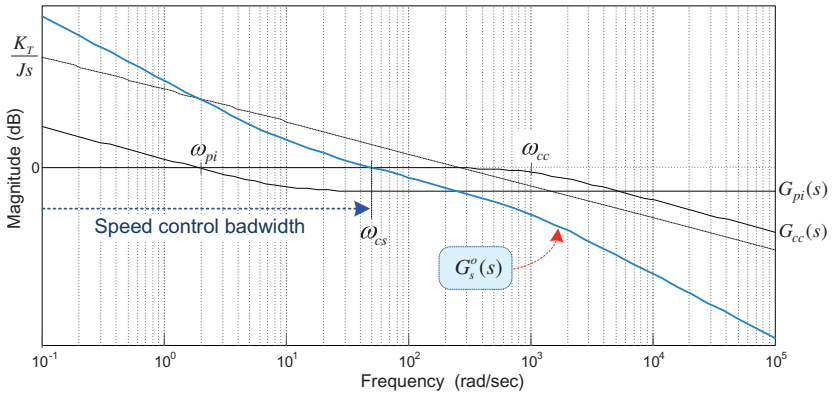


FIGURE 2.39

Bode plot of the open-loop frequency responses for a speed control system.

steady-state performance will be degraded, but if it is too large, the system will exhibit an overshoot.

As stated before, in order for current control to not exert any influence on speed control, the current control bandwidth ω_{cc} should be at least five times wider than the speed control bandwidth ω_{cs}. Under this condition, the gain of the current controller around the cross-over frequency ω_{cs} becomes almost one, i.e.,

$$G_c^c(s) = \frac{\omega_{cc}}{s + \omega_{cc}} \approx 1 \tag{2.41}$$

Also, if the PI corner frequency ω_{pi} is much smaller than the speed control bandwidth ω_{cs}, then the transfer function of the PI current controller around ω_{cs} can be reduced as

$$G_{pi}(s) = K_{ps} + \frac{K_{is}}{s} \approx K_{ps} \tag{2.42}$$

Consequently the open-loop transfer function of Eq. (2.40) around the cross-over frequency ω_{cs} can be simplified as

$$G_s^o(s) \approx K_{ps} \cdot \frac{K_T}{Js} \tag{2.43}$$

The gain of this open-loop transfer function at frequency ω_{cs} is 0 dB, i.e.,

$$\left|G_s^o(j\omega_{cs})\right| = 0 \text{ dB} \tag{2.44}$$

From this, we can obtain the proportional gain K_{ps} and the integral gain K_{is} as

$$\text{Proportional gain: } K_{ps} = \frac{J\omega_{cs}}{K_T} \tag{2.45}$$

$$\text{Integral gain: } K_{is} = K_{ps} \cdot \omega_{pi} = K_{ps} \cdot \frac{\omega_{cs}}{5} = \frac{J\omega_{cs}^2}{5K_T} \tag{2.46}$$

It is important to note that the gains of a speed controller depend on the system inertia J and the torque constant K_T of the target motor. Since J and K_T can be different from each system, the gains of a speed controller may vary with the applied system. From Eq. (2.45), it can be seen that, to achieve an equal bandwidth of speed control, the value of the proportional gain needs to be large for a large J and small for a large K_T.

Like the current controller, the PI speed controller needs to include an anti-windup controller to prevent integrator saturation.

2.7.1.1 Selection of the bandwidth of speed control

The speed control bandwidth ω_{cs} that determines the dynamic performance of the speed controller is limited by the bandwidth of the current controller and the sampling frequency of speed (i.e., the period of the speed control). As mentioned before, the bandwidth of speed control should be five times less than that of current control, and the sampling frequency of speed should also be considered. It is natural that the bandwidth of a speed controller cannot be larger than the frequency measuring the speed. We can select the speed control bandwidth within the limit of 1/10 or 1/20 of the sampling frequency.

As an example, suppose that the bandwidth of a current controller is 500 Hz and the sampling period to measure the speed is 2 ms. In this case, the available bandwidth of the speed controller can be up to one-fifth of the current controller, i.e., 500 Hz/5 = 100 Hz($\approx$628 rad/s). However, since the sampling frequency of speed is 500 Hz(=1/2 ms), it is desirable that the bandwidth of the speed controller be less than 50 Hz (=500/10).

Gains selection procedure of the proportional–integral speed controller

1. Identify the bandwidth of the current controller.
2. Select the bandwidth ω_{cs} of speed control to be five times less than the bandwidth of current control and ten times less than the sampling frequency of speed.
3. Calculate the proportional and integral gains from the selected bandwidth ω_{cs} as

   Proportional gain: $K_{ps} = \dfrac{J\omega_{cs}}{K_T}$

   Integral gain: $K_{is} = K_{ps} \cdot \omega_{pi} = K_{ps} \cdot \dfrac{\omega_{cs}}{5} = \dfrac{J\omega_{cs}^2}{5K_T}$
4. Select the gain of an anti-windup controller as $K_a = 1/K_{ps}$

We can normally obtain appropriate gains of the speed controller using the design method as stated just above. However, inaccurate information of the system parameters, J and K_T, may lead to incorrect gains for achieving the required bandwidth, so we may need to adjust additionally the gains by monitoring the transient response as shown in Fig. 2.40. If the system has an oscillatory response, we need to decrease the gains. On the other hand, if the system has a very slow response, we need to increase the gains.

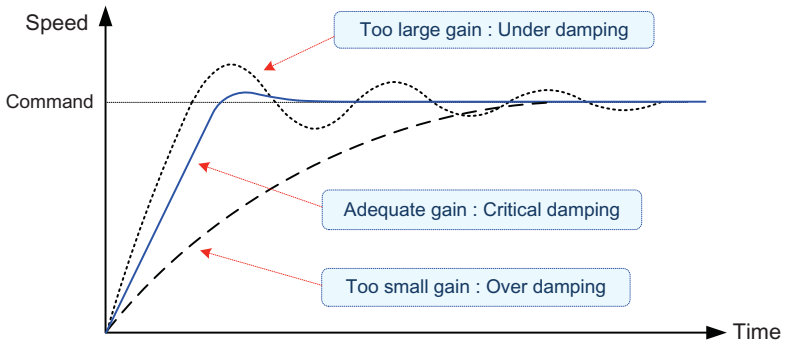


FIGURE 2.40

Transient responses according to different controller gains.

2.7.1.3 Drawback of a proportional–integral speed controller

From the open-loop transfer function $G_s^o(s)$of Eq. (2.40), the closed-loop transfer function $G_s^c(s)$ of the speed control system is given by

$$G_s^c(s) = \frac{G_c^o(s)}{1 + G_c^o(s)} = \frac{\left(\frac{K_T K_{ps}}{J}\right)s + \left(\frac{K_T K_{is}}{J}\right)}{s^2 + \left(\frac{K_T K_{ps}}{J}\right)s + \left(\frac{K_T K_{is}}{J}\right)} \tag{2.47}$$

Here, the gain of the current controller is assumed to be 1.

By comparing this transfer function with the prototype form, $s^2 + 2\zeta\omega_n s + \omega_n^2$, of the second-order system, the damping ratio ζ can be obtained as

$$\zeta = \frac{1}{2}\sqrt{\frac{K_T K_{is}}{J} \cdot \frac{K_{ps}}{K_{is}}} = \frac{1}{2}\sqrt{\frac{\omega_{cs}}{\omega_{pi}}} \tag{2.48}$$

We can see that the damping ratio ζ depends on the ratio of ω_{cs} to ω_{pi}. The condition of $\omega_{pi} = \omega_{sc}/5$ given in the Section 2.7 results in $\zeta = \sqrt{5}/2$. Because ζ is greater than 1, we expect the system response by the PI controller to be over-damped and have no overshoot. However, the zero of $s = -K_{is}/K_{ps}$ in the PI controller causes an overshoot in the system response. The closer the zero is located to the imaginary axis in the s-plane, the greater its effects will be [1]. We can easily see the effect of this zero by dividing Eq. (2.47) into two parts as:

$$\begin{aligned} &\frac{\frac{K_T K_{is}}{J}}{s^2 + \left(\frac{K_T K_{ps}}{J}\right)s + \left(\frac{K_T K_{is}}{J}\right)} + \frac{\left(\frac{K_T K_{ps}}{J}\right)s}{s^2 + \left(\frac{K_T K_{ps}}{J}\right)s + \left(\frac{K_T K_{is}}{J}\right)} \\ &\rightarrow \frac{\omega_n^2}{s^2 + 2\zeta\omega_n s + \omega_n^2} + \frac{2\zeta\omega_n s}{s^2 + 2\zeta\omega_n s + \omega_n^2} \end{aligned} \tag{2.49}$$

The responses of these two parts to a unit step command are shown in Fig. 2.41. It can be seen that the second term of Eq. (2.49) gives an overshoot to the system response. It is interesting to note that, in current control, this zero has no effect on the system response because the zero is canceled out by the system pole.

The overshoot problem by the zero in the PI controller can be solved by an *integral and proportional (IP) controller*.

2.7.2 INTEGRAL-PROPORTIONAL CONTROLLER

We can remove the zero from Eq. (2.47) by adjusting the position of the P control part in the PI controller as shown in Fig. 2.42. This controller is known as the *IP controller*.

The transfer function of the IP control system is given as

$$\frac{\omega_m}{\omega_m^*} = \frac{\dfrac{K_T K_{is}}{Js}}{s^2 + \left(\dfrac{K_T K_{ps}}{J}\right)s + \dfrac{K_T K_{is}}{J}} \tag{2.50}$$

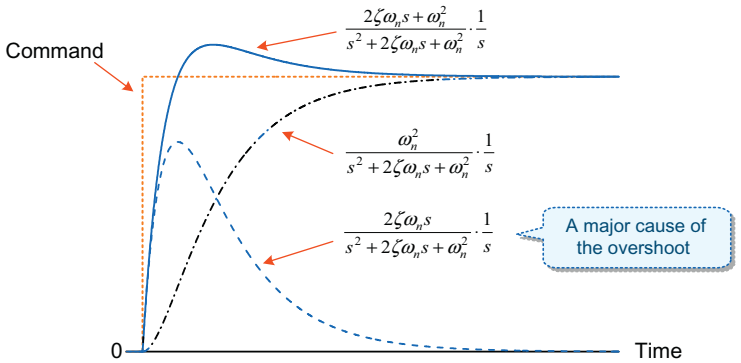


FIGURE 2.41

Response to a unit step command.

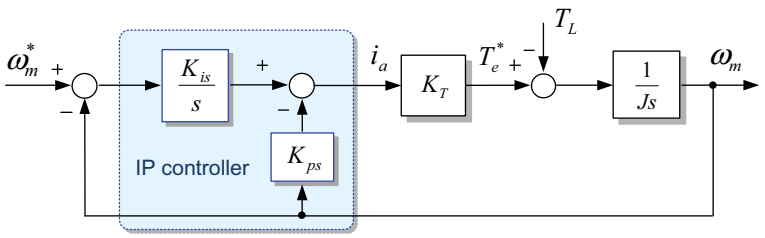


FIGURE 2.42

Block diagram of the IP controller.

The poles of this transfer function are the same as those of the PI controller but this transfer function has no zero. Thus the IP controller has no problem with the overshoot caused by the zero.

In the IP controller, the system response to the speed reference depends only on the damping ratio in Eq. (2.50). The critical damped response (i.e., $\zeta = 1$) is obtained by allowing $\omega_{pi} = \omega_{sc}/4$.

From reconstructing Fig. 2.42 as Fig. 2.43, we can see that an IP controller is equivalent to a PI controller except for the first-order, low-pass filter with the time constant of K_{ps}/K_{is} on the input side. Therefore, an IP controller exhibits no overshoot due to low-pass filtering of its input command, but its response will be slower than that of a PI controller.

Although the speed responses to speed reference of PI and IP controllers are different from each other, the speed responses to disturbance torque are the same. The transfer function of the speed response to a disturbance torque T_L for an IP controller can be obtained from Fig. 2.42 as

$$\frac{\omega_m}{T_L} = -\frac{s}{Js^2 + K_T K_{ps} s + K_T K_{ps}} \tag{2.51}$$

It is not hard to ascertain that the transfer function of the PI controller is the same as Eq. (2.51). Therefore the speed responses to a disturbance torque for the two controllers are identical. The speed responses of the PI and IP controllers under an equal control bandwidth are shown in Fig. 2.44A. It can be seen that the IP controller exhibits no overshoot, but its response is slower than that of the PI controller. On the other hand, the speed responses to a disturbance torque for the two controllers are the same, as we would expect. If the bandwidths are adjusted for the two controllers to have the same overshoot in their response to speed reference, the IP controller can achieve a larger bandwidth than the PI controller. For the same overshoot, the bandwidth of the IP controller can be set as 5.44 times larger than that of the PI controller. In this condition, the IP controller will exhibit an improved speed response to the disturbance torque as shown in Fig. 2.44B.

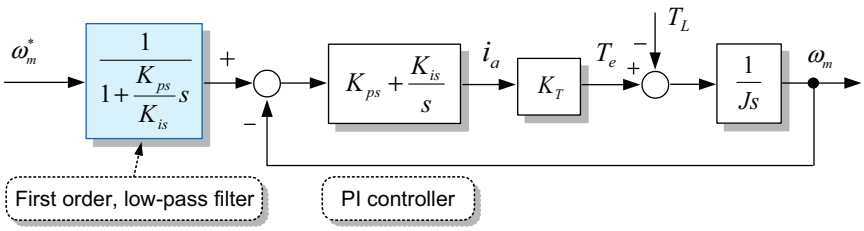


FIGURE 2.43

Equivalent block diagram of the IP controller.

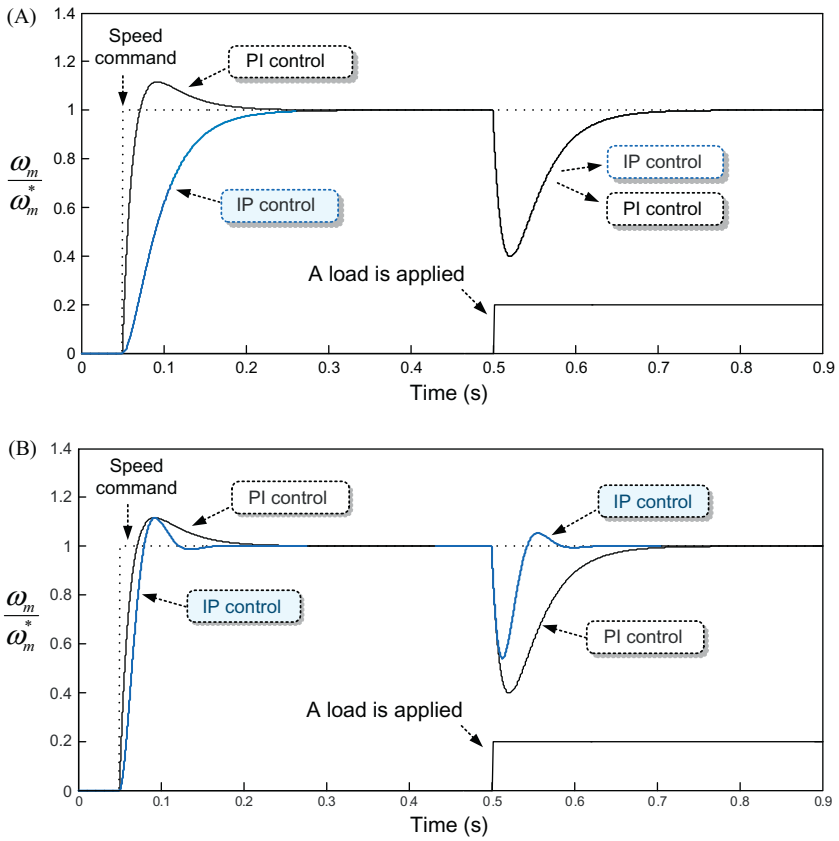


FIGURE 2.44

Speed responses of PI and IP controllers. (A) Same bandwidth and (B) same overshoot.

By combining these two controllers, we can make a compromise between the response to speed reference and the response to disturbance torque. This combined controller is shown in Fig. 2.45. The characteristic of the combined controller depends on the control variable α. When $\alpha = 0$, it becomes an IP controller, whereas if $\alpha = 1$, it becomes a PI controller. In case of $0 < \alpha < 1$, a combined characteristic of the two controllers can be obtained.

A PI speed controller will exhibit a satisfactory performance if its bandwidth is large enough. In many applications such as elevators that are susceptible to mechanical resonance and flexible joint robots, a speed controller often cannot have a large enough bandwidth, so we cannot expect a satisfactory response. In this case, we need to improve the control performance by combining a PI controller with other control schemes such as acceleration feedforward compensation or Fuzzy algorithm [6].

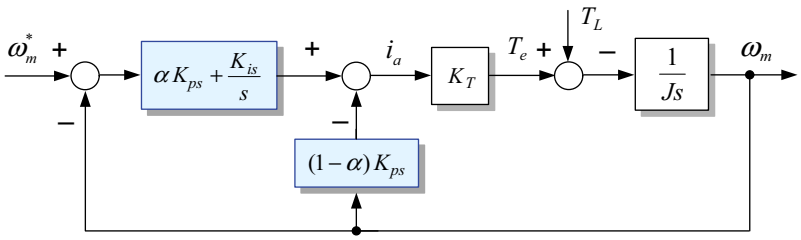


FIGURE 2.45

Combined controller.

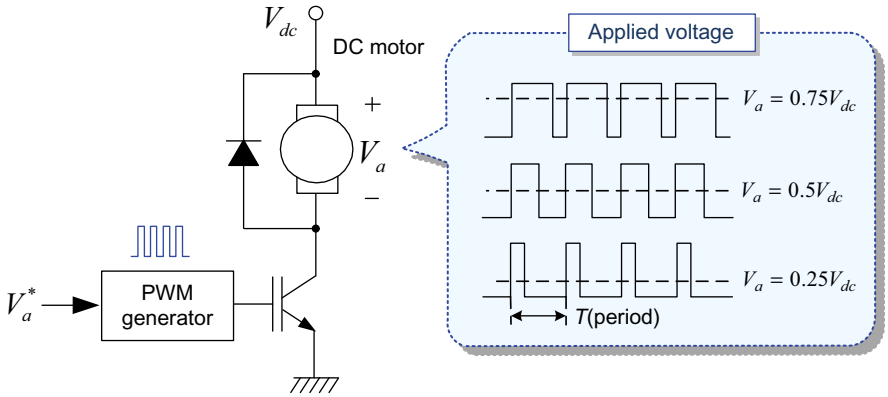


FIGURE 2.46

Simple driving circuit for a DC motor.

2.8 POWER ELECTRONIC CONVERTER FOR DIRECT CURRENT MOTORS

The voltage applied to a DC motor can be controlled by using a power electronic converter. Fig. 2.46 shows a simple driving circuit for the forward motoring mode operation. Commonly, in a driving circuit, the switching states of the power devices are determined by the pulse width modulation (PWM) technique to achieve the required voltage command. The voltage command is given by the current controller as described earlier.

A four-quadrant chopper (or H-bridge circuit) is often used to operate a DC motor in both motoring and braking modes for both forward and reverse directions. The H-bridge circuit is implemented with four power switching devices as shown in Fig. 2.47.

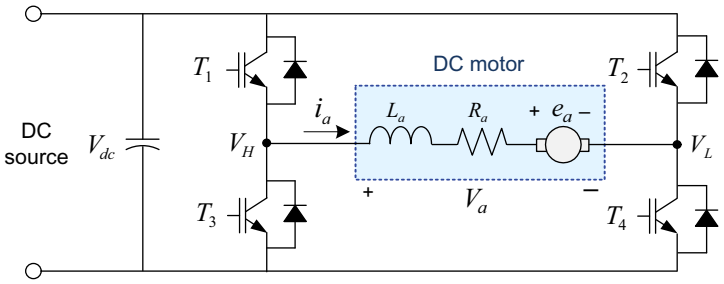


FIGURE 2.47

H-bridge circuit.

This circuit is widely used in DC servo drive systems because it can provide high-performance current control with a bandwidth up to several thousand (rad/s). In this circuit, there are two PWM techniques for adjusting the output voltage: *bipolar* and *unipolar switching schemes*.

2.8.1 SWITCHING SCHEMES

2.8.1.1 Bipolar switching scheme

The switching states of devices are determined by comparing the voltage reference V_a^* with the triangular carrier wave as shown in Fig. 2.48.

In this scheme, if the voltage reference V_a^* is larger than the triangular carrier wave, then both T_1 and T_4 will be turned on, and the output V_a will become $+V_{dc}$. On the other hand, if the reference voltage V_a^* is less than the triangular carrier wave, both T_2 and T_3 will be turned on, and the output V_a will become $-V_{dc}$. In this manner, two switching devices (T_1 and T_4, T_2 and T_3) placed diagonally will be turned on or off simultaneously. Since these switching actions give an output voltage of either positive or negative DC voltage (i.e., $+V_{dc}$ and $-V_{dc}$), this scheme is called the bipolar switching scheme.

In this scheme, the switching frequency equals to the frequency $(1/T_s)$ of the triangular carrier wave. This scheme has an advantage of smoothly changing the average output voltage from $+V_{dc}$ to $-V_{dc}$ as shown in Fig. 2.49. However, the instantaneous output voltage becomes as wide as $2V_{dc}$, resulting in a large current ripple of the motor.

2.8.1.2 Unipolar switching scheme

In this scheme, the switching of the devices is also determined by comparing the voltage reference with the triangular carrier wave as in the bipolar switching scheme, but the switching in the H-pole and the L-pole is performed independently according to its own reference as shown in Fig. 2.50. The reference voltage V_H of the H-pole is given as V_a^*. Meanwhile, the reference voltage V_L of the L-pole is given as $-V_a^*$. The output voltage (i.e., the motor voltage) V_a is given by the voltage difference between the H-pole and the L-pole, i.e., $V_H - V_L$. Since

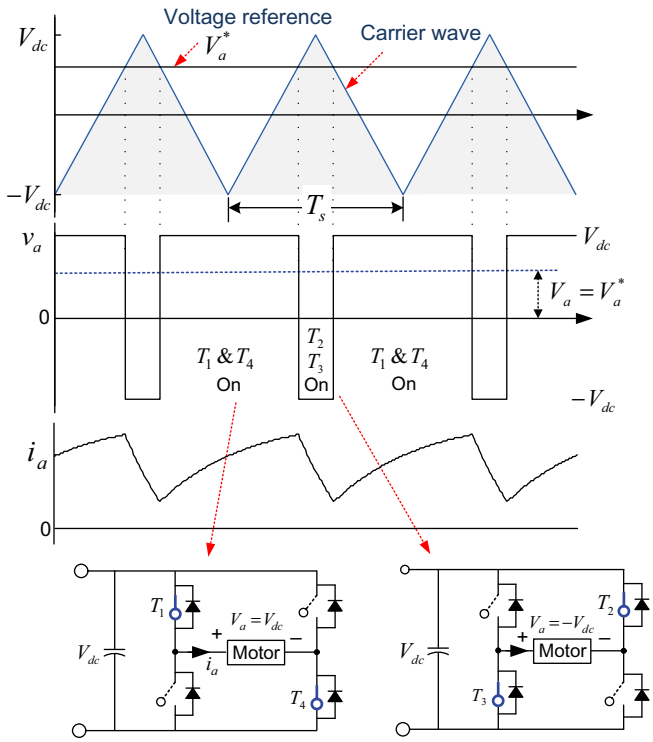


FIGURE 2.48

Bipolar switching scheme.

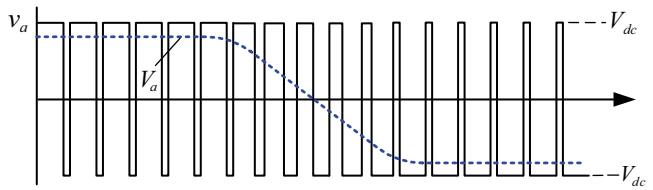


FIGURE 2.49

Output voltage of bipolar switching.

this switching action gives an output voltage of 0 and $+V_{dc}$ or 0 and $-V_{dc}$, this scheme is called the unipolar switching scheme.

In this scheme, the output voltage fluctuates by V_{dc}, so the current ripple of the motor will be two times smaller than that of the bipolar switching scheme and the torque ripple will also be smaller as shown in Fig. 2.51. Furthermore, the output voltage changes effectively with the doubling of the switching frequency. However, since this scheme is difficult to provide a small average voltage, the sign transition of the average voltage may be discontinuous as described in Fig. 2.52. As a result, it is difficult to change the rotational direction of the motor smoothly.

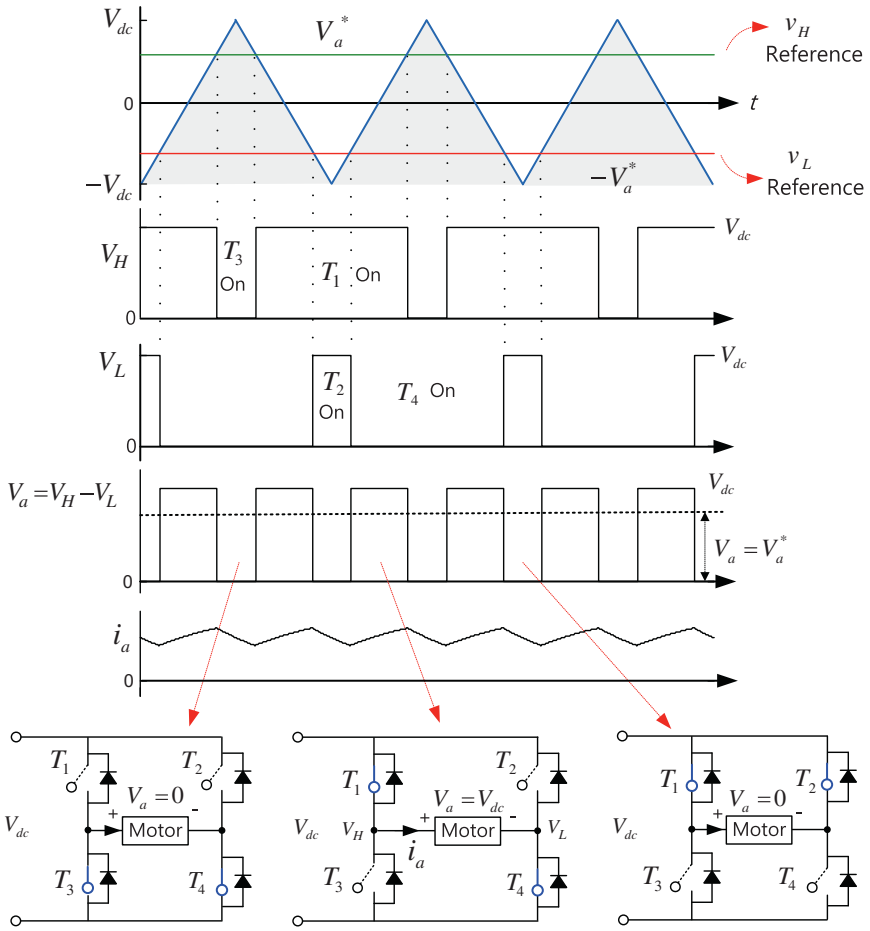


FIGURE 2.50

Unipolar switching scheme.

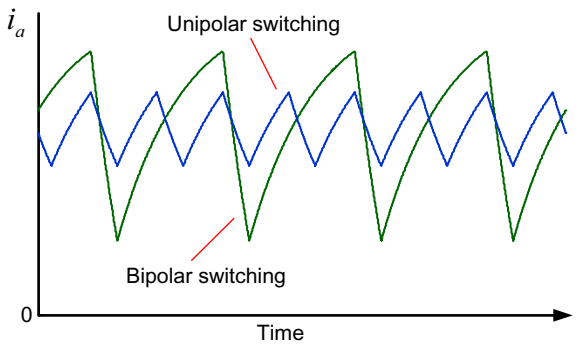


FIGURE 2.51

Comparison of the current ripple for the two switching schemes.

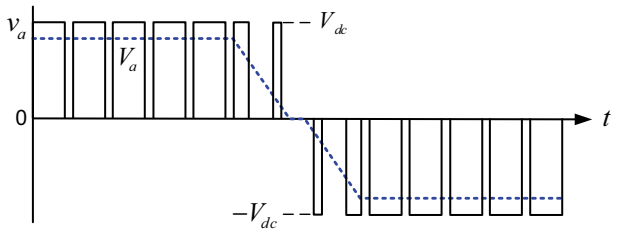


FIGURE 2.52

Output voltage of unipolar switching.

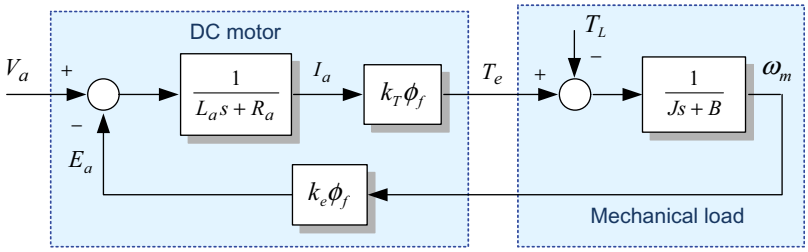


FIGURE 2.53

Block diagram of a permanent magnet DC motor drive system.

2.9 SIMULATION OF DIRECT CURRENT MOTOR DRIVE SYSTEM: MATLAB/SIMULINK

Now, we will examine the performance of the current and speed controllers as mentioned in the Sections 2.6 and 2.7 through a simulation of a DC motor drive system using MATLAB/Simulink.

A block diagram of a DC motor drive system is shown in Fig. 2.53. The system consists of a DC motor part and a mechanical load part.

The modeling of these parts for MATLAB/Simulink simulation is as follows:

2.9.1 DIRECT CURRENT MOTOR MODELING

In the electric circuit of a DC motor, the input is the applied armature voltage, and the output is the armature current. Thus, to obtain the armature current, the voltage equation of Eq. (2.1) can be rewritten as

$$V_a = R_a i_a + L_a \frac{di_a}{dt} + e_a$$

$$\rightarrow i_a(t) = \frac{1}{L_a}\int [V_a(\tau) - R_a i_a(\tau) - e_a(\tau)]d\tau \tag{2.52}$$

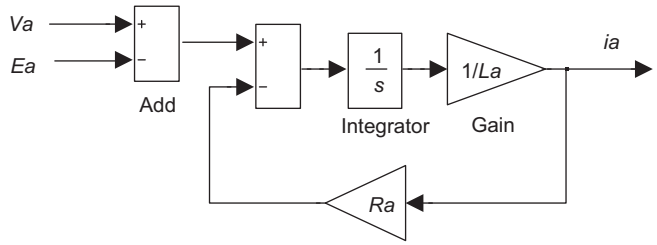


FIGURE 2.54

Simulink block diagram of the electric circuit in a DC motor.

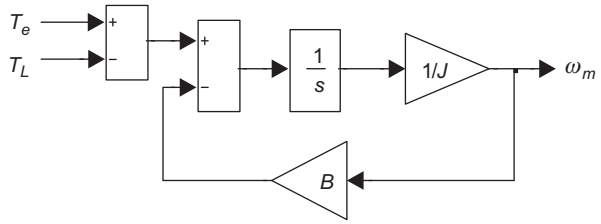


FIGURE 2.55

Simulink block diagram of the mechanical load system.

From this equation, the simulation model of the electric circuit of a DC motor is given as Fig. 2.54.

2.9.2 MECHANICAL SYSTEM MODELING

In the mechanical system, the input is the developed torque of the DC motor, and the output is the speed of the load. To obtain the speed, the motion equation of Eq. (2.4) can be rewritten as

$$T_e = k_T \phi i_a = J\frac{d\omega_m}{dt} + B\omega_m + T_L$$

$$\rightarrow \omega_m(t) = \frac{1}{J}\int [T_e(\tau) - B\omega_m(\tau) - T_L(\tau)]d\tau \tag{2.53}$$

From this equation, the simulation model of the mechanical load system is given as Fig. 2.55.

Fig. 2.56 shows a complete model for a DC motor drive system, which combines the electric circuit, mechanical system, torque, and back-EMF equations.

Here, we assume $K = k_e\phi = k_T\phi$ and $T_L = 0$. To apply a step input voltage to a DC motor, the step block (V_a) is added to the simulation model.

Now, we will carry out a simulation by using this complete model. The parameters and the rating of the DC motor used for simulations are listed as M-file in Fig. 2.57. We can set the simulation time and the solver option by using the *simulation/configuration parameters* menu.

First, we will examine the speed response to a step input voltage. Fig. 2.58 compares the speed responses of this system to two different step input voltages. The final speed depends on the voltage applied to the motor. The rotational speed

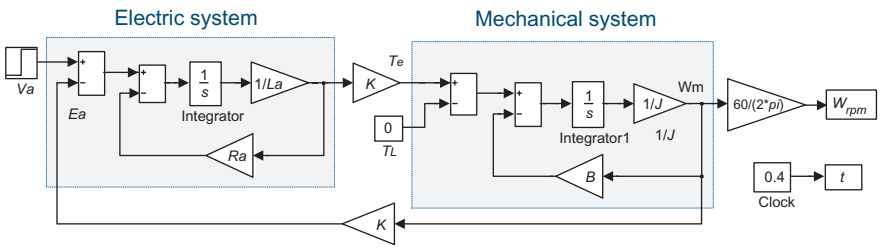


FIGURE 2.56

Complete Simulink model for a DC motor drive system.

```
%-- DC Motor Parameters ---------------------------------------------------
Power=3336;                % Power[W]
Va_rated=140;              % Rated Voltage [V]
Ia_rated=25;               % Rated Current [A]
Wm_rated=3000*2*pi/60;     % Rated Angular Velocity[rad/s]
Te_rated=Power/Wm_rated;   % Rated Torque [Nm]

Ra=0.26;                   % Amature Resistance [Ohm]
La=1.7e-3;                 % Amature Inductance [H]
J=.00252;                  % Moment of Inertia [kg-m^2]
B=.0;                      % Coefficient of Viscous Friction [kgm^2/sec]

Kt=Te_rated/Ia_rated;
```

FIGURE 2.57

M-file for simulation.

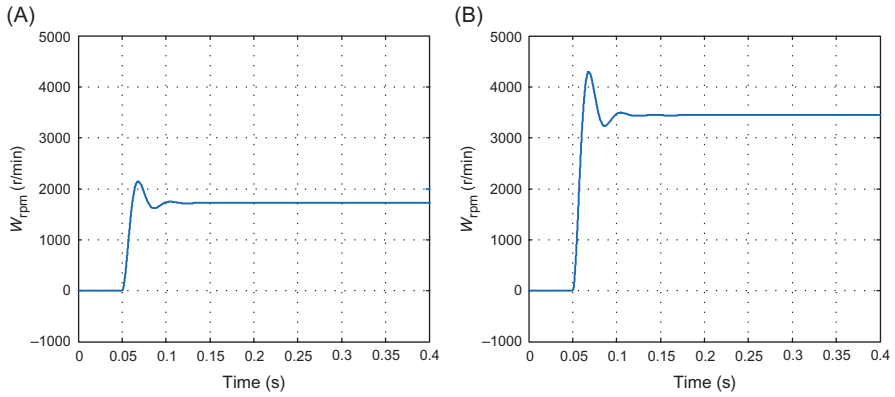


FIGURE 2.58

Speed response to a step input voltage. (A) $V_a = 70$ V and (B) $V_a = 140$ V.

W_{rpm} of the DC motor is proportional to the armature voltage V_a, as can be expected. The parameters of the motor give a damping ratio ζ of 0.37. Because $\zeta < 1$, we can expect the system to have an under-damped response and an overshoot. This is verified by this simulation results.

Next, we will model a PI current controller and then connect it with the DC motor drive system.

2.9.3 PROPORTIONAL–INTEGRAL CURRENT CONTROLLER MODELING

The entire system containing a PI current controller is shown in Fig. 2.59.

The subsystem "PMDC" represents all the blocks in Fig. 2.56. This system also includes an anti-windup controller, back-EMF feedforward compensation, and a limiter. The limiter restricts the output of the current controller to the rated voltage of the motor. The proportional and integral gains can be obtained from Eqs. (2.37) and (2.38), and the anti-windup gain is $K_a = 1/K_p$.

Fig. 2.60 compares the responses to the step current command ($i_a^* = 20$A) for gains according to the control bandwidths of 500 and 1000 Hz. As we have expected, the PI current controller does not give a steady-state error, and a larger bandwidth can improve the response time.

The two responses show that the actual currents reach their references at 2 and 1 ms, respectively. This indicates that the current control system has bandwidths of 500 and 1000 Hz, respectively, as designed.

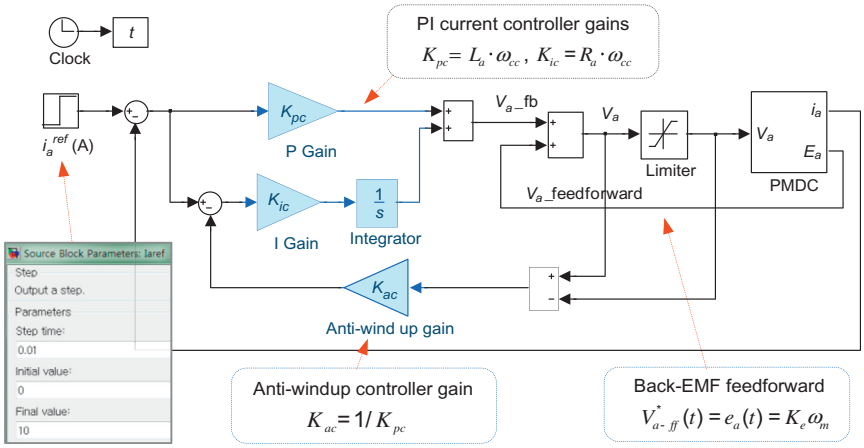


FIGURE 2.59

System containing a PI current controller.

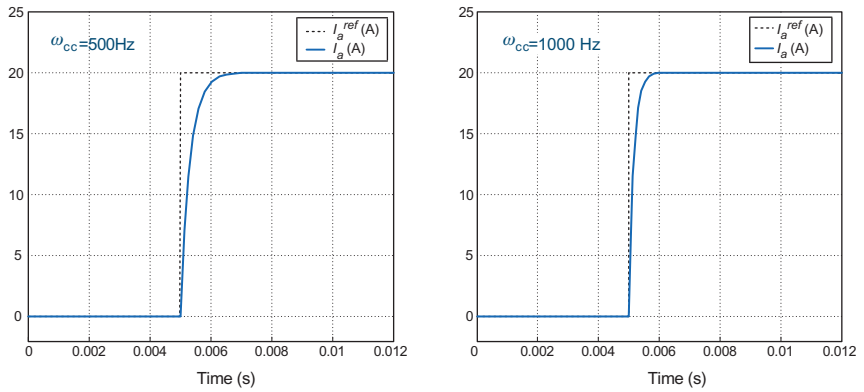


FIGURE 2.60

Step response according to control bandwidth.

2.9.4 PROPORTIONAL–INTEGRAL SPEED CONTROLLER MODELING

The entire DC motor drive system containing a PI speed controller is shown in Fig. 2.61. The subsystem "PMDC with CC" represents all the blocks in Fig. 2.59. This controller also has an anti-windup controller.

The system responses to the step speed command of 2500 r/min according to two different bandwidths are shown in Fig. 2.62. Again, we can make sure that a larger bandwidth can lead to a faster response.

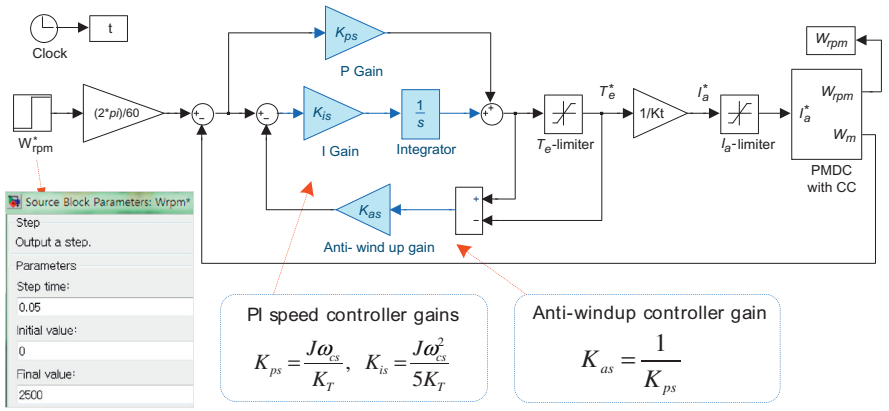


FIGURE 2.61

DC motor drive system block containing a PI speed controller.

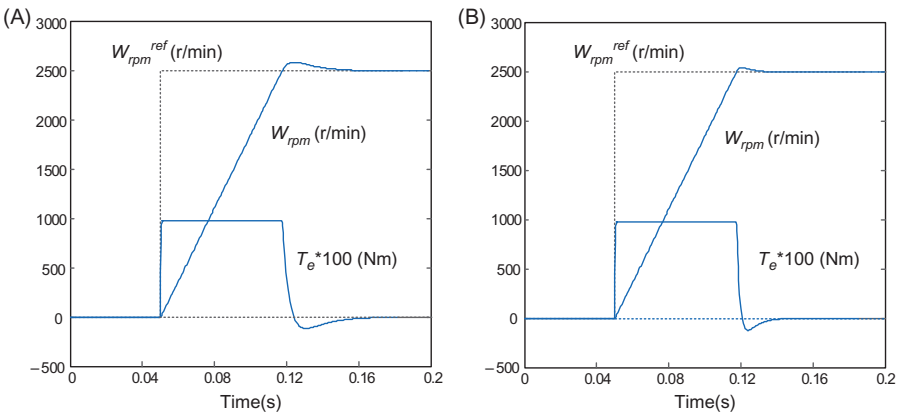


FIGURE 2.62

System responses according to two different bandwidths. (A) $\omega_{cs} = 50$ Hz and (B) $\omega_{cs} = 100$ Hz.

2.9.5 FOUR-QUADRANT CHOPPER MODELING

The simulation block containing a four-quadrant chopper, which generates the voltage applied to the DC motor, is shown in Fig. 2.63. We assume that this chopper adopts a unipolar switching scheme with a switching frequency of 5 kHz.

The switching signals produced by the unipolar switching scheme are shown in Fig. 2.64A. The PWM output voltage of the chopper and the current of the motor are shown in Fig. 2.64B.

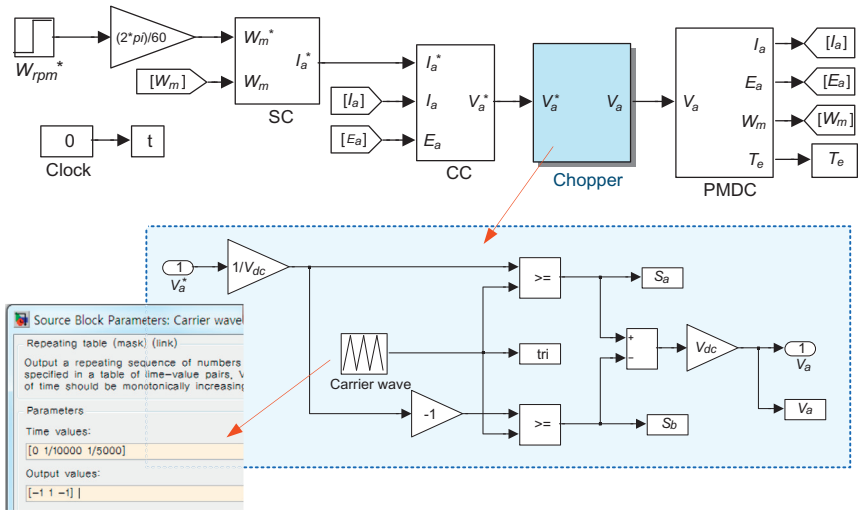


FIGURE 2.63

Simulation block containing a four-quadrant chopper.

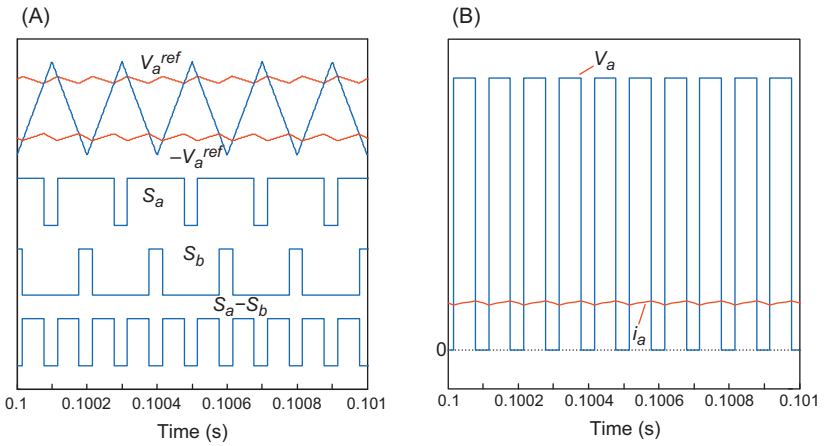


FIGURE 2.64

Unipolar switching scheme. (A) Switching signals and (B) PWM output voltage and current.

For the step speed reference of 2500 r/min, the speed and torque of the motor are shown in Fig. 2.65. When compared with Fig. 2.61, the current and torque waveforms powered by the chopper exhibit ripple components due to PWM switching.

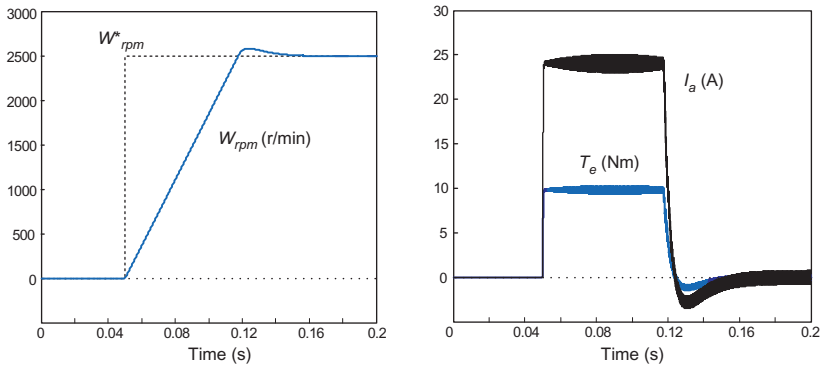


FIGURE 2.65

Speed, current, and output torque.

REFERENCES

[1] G. Franklin, J.D. Powell, A. Emami-Naeini, Feedback Control of Dynamic Systems, fifth ed., Prentice Hall, Upper Saddle River, NJ, 2006.

[2] Y. Peng, D. Vrancic, R. Hanus, Design and analysis of pulsewidth-modulated amplifiers for DC servo systems, IEEE Trans. Ind. Electron. Control Instr. IECI-23 (1) (1976) 47–55.

[3] Y. Peng, D. Vrancic, R. Hanus, Anti-windup, bumpless, and conditioned transfer techniques for PID controllers, IEEE Control Syst. Mag. 16 (2) (1996) 48–57.

[4] H.-B. Shin, New antiwindup PI controller for variable-speed motor drives, IEEE Trans. Ind. Electron. 45 (3) (1998) 445–450.

[5] H. Sugimoto, M. Koyama, S. Tamai, Practical Theory and Design of an AC Servo System, ISBN-10: 4915449580 (in Japanese) (Chapter 7), Tokyo, 1990.

[6] J.S. Yu, S.H. Kim, B.K. Lee, C.Y. Won, J. Hur, Fuzzy-logic-based vector control scheme for permanent-magnet synchronous motors in elevator drive applications, IEEE Trans. Ind. Electron. 54 (4) (2007) 2190–2200.

CHAPTER

3 Alternating current motors: synchronous motor and induction motor

The rotation of alternating current (AC) motors exploits the force developed by the interaction between two magnetic fields rotating at the same speed as stated in Chapter 1. There are two classifications of an AC motor: *synchronous motor* and *asynchronous motor*. An asynchronous motor is more commonly known as an *induction motor*.

Synchronous and induction motors have the same stator configuration for producing the rotating magnetic field. However, they have different rotor constructions due to the difference in their ways of generating the rotor magnetic field. In synchronous motors, typically, the rotor magnetic field is generated from the field winding excited by a direct current (DC) power source. For small- to medium-sized synchronous motors, permanent magnets are commonly used for generating the rotor magnetic field. On the other hand, in induction motors, the rotor magnetic field is produced by an AC power. It is interesting to note that this AC power is transferred from a stator by electromagnetic induction.

Induction motors have several advantages such as simple construction, reliability, ruggedness, low maintenance, low cost, high-speed operation capability, and the ability to be operated by a direct connection to an AC power source. On the other hand, synchronous motors are superior to induction motors in efficiency, power density, dynamic response, and power factor.

In this chapter, we will study the basic operation principle and characteristics of AC motors in more detail. We will begin by examining the more general type of motor, the induction motor.

3.1 INDUCTION MOTORS

The fundamental principle of induction motors was first demonstrated by the experiment known as Arago's Disk in 1824. From this experiment, it was found that, when a magnet rotates along the rim of a copper disk (a nonmagnetic substance), the disk rotates in the direction of the magnet at a smaller speed (Fig. 3.1). In 1832, Faraday demonstrated that this phenomenon is due to the currents induced in the copper disk. The discovery of this phenomenon ultimately led to the development of the fundamental concept of an induction motor. When a magnet passes along the rim of a copper disk, an electromotive force (EMF) is

Electric Motor Control. DOI: http://dx.doi.org/10.1016/B978-0-12-812138-2.00003-9
© 2017 Elsevier Inc. All rights reserved.

Hesai Exhibit 1030, page 98

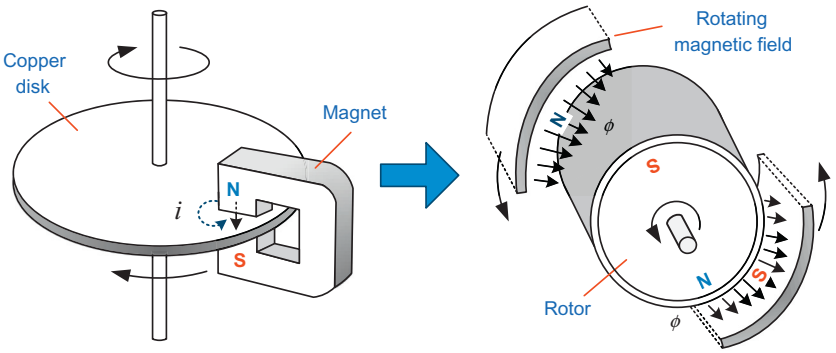


FIGURE 3.1

Arago's disk and the fundamental concept of an induction motor.

induced at the part in the disk that experiences a changing magnetic field. The induced voltage causes an eddy current to flow in the disk. As a result, since the current-carrying part is built under the magnetic field of the magnet, a force (known as *Lorentz force*) is created on the current-carrying part. The direction of the force is the same as that of the magnet's movement, and this force makes the copper disk to rotate along with the magnet.

In an induction motor based on this fundamental concept, such rotating magnet is realized by a rotating magnetic field generated from three-phase stator windings connected to a three-phase AC power source. The rotor, then, follows this rotating magnetic field.

Induction motors are most widely used as general-purpose motors in many industrial applications because of their low cost and rugged construction. Traditionally, induction motors had been connected directly to the line voltage of 60 or 50 Hz and operated at a nearly constant speed. However, recently, variable speed drives have been made possible by power electronic converters such as inverter, so induction motors are widely used in many applications requiring speed control.

3.1.1 STRUCTURE OF INDUCTION MOTORS

The structure of a typical induction motor is shown in Fig. 3.2. An induction motor has cylindrical stator and rotor configurations, which are separated by a uniform radial air gap. The stator and the rotor are made up of an iron core, which has windings inserted inside. The iron core is not a single solid lump but consists of a stack of insulated laminations of silicon steel, usually with a thickness of about 0.3−0.5 mm to reduce eddy current losses. The iron core is made from a ferromagnetic material such as steel, soft iron, or various nickel alloys to produce magnetic flux efficiently and reduce hysteresis losses.

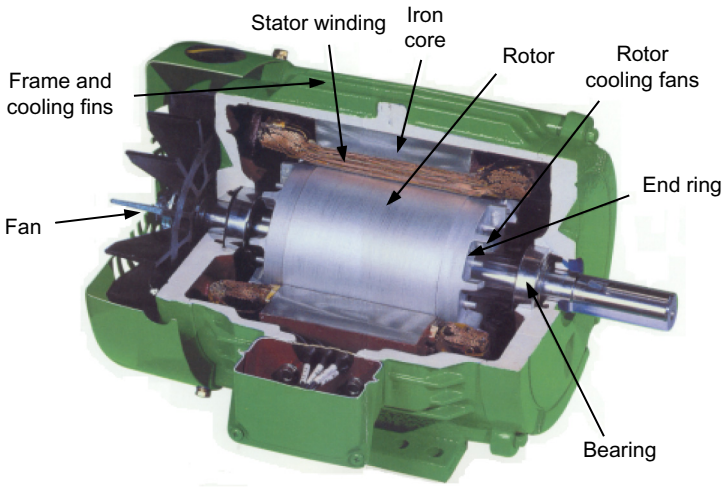


FIGURE 3.2

Structure of a typical induction motor.

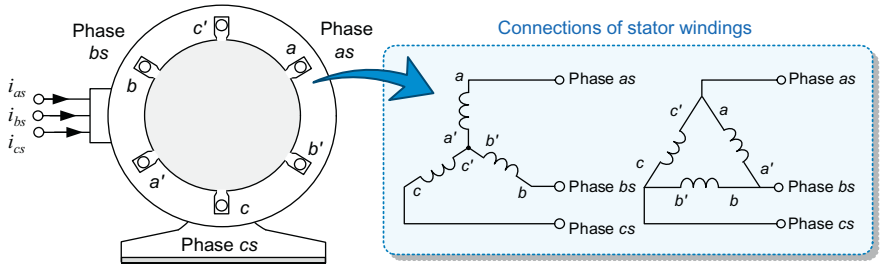


FIGURE 3.3

Stator windings.

3.1.1.1 Stator

In an induction motor, only the stator windings are fed by the three-phase AC power supply. It should be noted that the three-phase stator windings perform the roles of both the armature and field windings of a DC motor. These three-phase windings are placed in the slots that are axially cut along the inner periphery of the iron core as shown in Fig. 3.3. They are displaced from each other by 120 electrical degrees along the periphery and are typically connected in delta for low-supply voltage or in wye for high-supply voltage.

All turns in each winding are continuously distributed in the numerous slots spread around the periphery, such that the winding density can be sinusoidal as shown in Fig. 3.4. The purpose of this arrangement is to establish a sinusoidal flux distribution in the air gap when currents flow through them. This winding

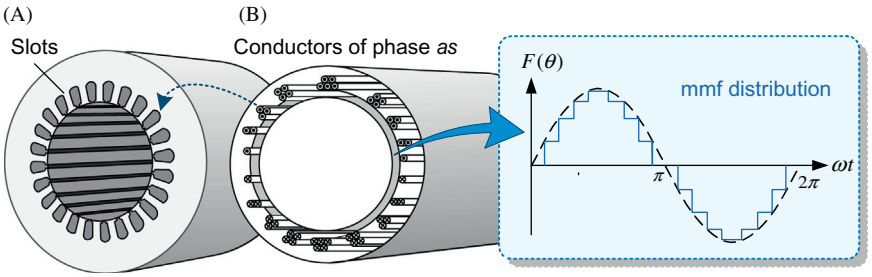


FIGURE 3.4

Stator phase winding. (A) Stator core and (B) sinusoidally distributed winding and mmf.

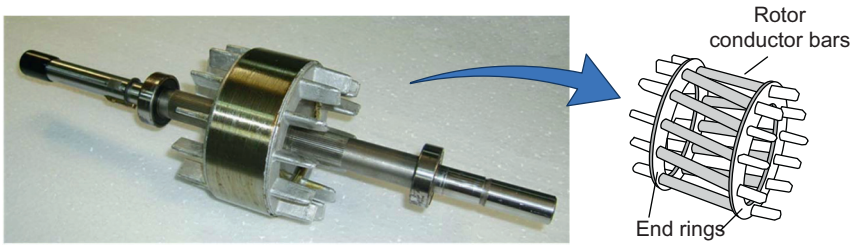


FIGURE 3.5

Squirrel-cage rotor.

type is called *distributed winding*. The distributed winding configuration increases the utilization of the iron core and reduces magnetomotive force (mmf) space harmonics, resulting in a lower torque ripple compared to that of the *concentrated winding*, in which all coils of the phase winding are placed in one slot under a pole.

3.1.1.2 Rotor

Similar to the stator, a rotor has a cylindrical iron core that consists of silicon steel laminations. It should be noted that the electric circuit (windings or conductors) in the iron core of the rotor is not fed by an external power source but its current flows by the induced EMF.

There are two types of a rotor used in induction motors: *squirrel-cage rotor* and *wound rotor*.

3.1.1.2.1 Squirrel-cage type

A squirrel-cage rotor has a laminated iron core with slots for placing skewed conductors, which may be a copper, aluminum, or alloy bar. These rotor bars are short-circuited at both ends through end rings as shown in Fig. 3.5.

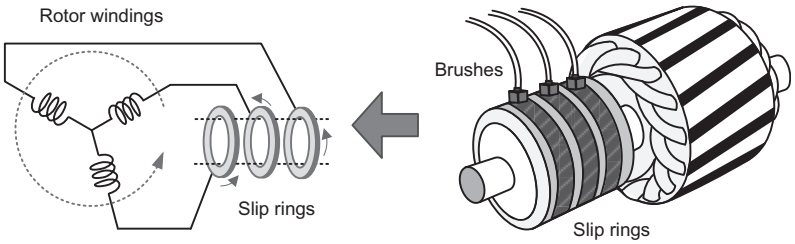


FIGURE 3.6

Wound-rotor.

This rotor gets its name from its structure's resemblance to a squirrel cage. The rotor conductors are not placed exactly parallel to the shaft but are skewed by one slot-pitch to reduce cogging torque, and this allows the motor to run quietly. Because of its simple and rugged construction, about 95% of the induction motors use the squirrel-cage rotor.

3.1.1.2.2 Wound-rotor type

Similar to the windings on a stator, a wound-rotor as shown in Fig. 3.6 has a set of three-phase windings, which are usually Y-connected. The rotor windings are tied to the slip rings on the rotor's shaft and thus can be accessible through the brushes. Due to this configuration, in a wound-rotor type induction motor, the rotor resistance can be varied by connecting external resistors to the rotor windings via the brushes. This allows the torque−speed characteristics of the induction motor to be varied as needed.

Now, we will discuss in detail the squirrel-cage induction motor, which is the most common type of an induction motor.

3.1.2 FUNDAMENTALS OF INDUCTION MOTORS

In an induction motor, when a three-phase AC voltage source is applied to the stator windings, which are displaced by 120 electrical degrees in space with respect to each other, the three-phase currents flowing in these windings will produce a rotating magnetic field in the air gap as shown in Fig. 3.7. The speed of this magnetic field is directly proportional to the frequency of the applied AC source voltage.

When the rotating magnetic field is linking to the conductors in the rotor, EMFs based on Faraday's law are induced in the conductors. The induced voltages cause currents in the shorted conductors. Torque is produced on the current-carrying conductors in the rotating magnetic field. Through this developed torque, the rotor will then start rotating in the same direction as the rotating magnetic field.

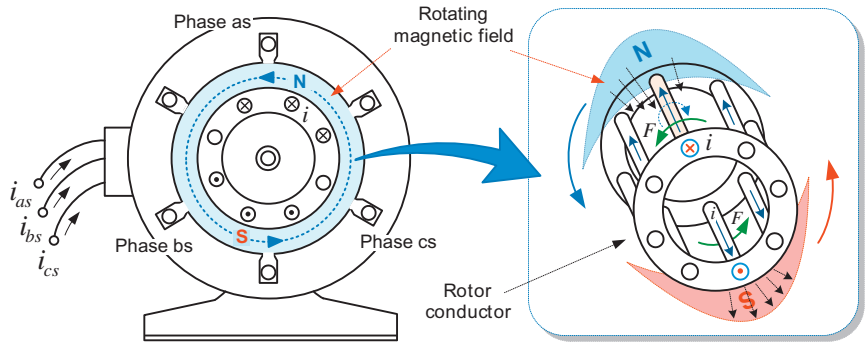


FIGURE 3.7

Rotation of an induction motor [1].

C.I. Hubert, Electric Machines, Theory, Operation, Applications, Adjustment, and Control, second ed., Prentice Hall, 2002, p. 135.

Supposing that the rotating magnetic field is moving counterclockwise, the induced voltages make the currents in the shorted conductors to flow in the direction as depicted in Fig. 3.7 [1]. This is because the induced currents will establish a flux that opposes the change imposed by the rotating magnetic field, in accordance with Lenz's law. When applying Fleming's left-hand rule to the induced currents and the rotating magnetic field, the force on the conductor is developed in the same direction as the rotating magnetic field.

As explained above, an induction motor has no external source provided to its rotor winding but exploits the rotor currents produced by electromagnetic induction. This is why it is called *induction motor*. When an induction motor is running, the rotor speed is always slightly less than the speed of the rotating magnetic field, i.e., synchronous speed. If the rotor rotates in the same speed as the rotating magnetic field, there will be no induced voltage and current in the short-circuited rotor windings and thus no torque. In induction motors, the rotor speed is just slow enough to cause the proper amount of the rotor current to flow so that the developed torque may be sufficient to drive the load. Thus, an increase in load will cause the rotor to slow down.

Now, we will take a look at the rotating magnetic field, which is the basis for the rotation of AC motors.

3.1.2.1 Rotating magnetic field

The rotating mmf is created by three-phase currents flowing through three-phase stator windings. To begin with, consider an mmf resulting from a current flowing in the winding of phase *as* as shown in Fig. 3.8. We will consider only the centered coil on the magnetic axis of the phase *as* distributed winding for simplicity.

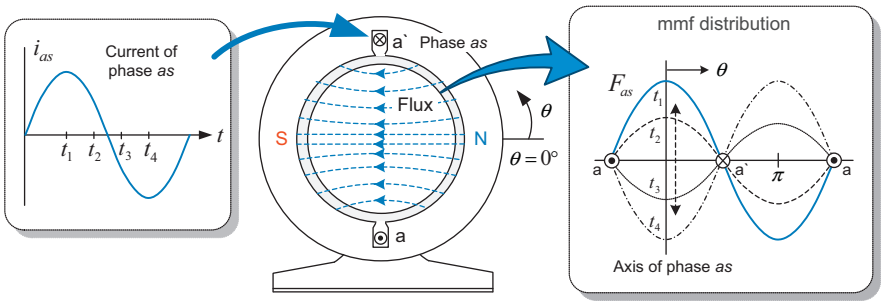


FIGURE 3.8

Phase *as* current and mmf.

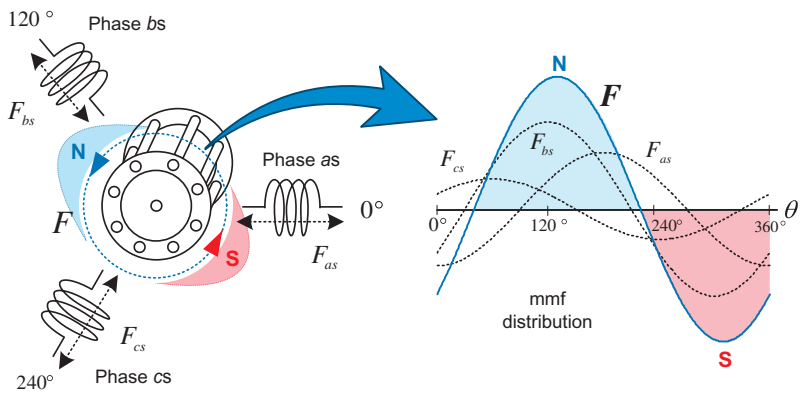


FIGURE 3.9

Resultant air-gap mmf.

Here, a sign of $\otimes$ indicates that the direction of the current is directed into the page, while a sign of $\odot$ indicates that the direction of the current is directed out of the page. Also, the current flowing into the page is assumed to be positive. When a current flows in the phase *as* winding, it will produce a sinusoidally distributed mmf F_{as} centered on its axis. The amplitude of the mmf F_{as} varies with the instantaneous value of the current as shown in Fig. 3.8.

Similarly, the windings of the phase *bs* and phase *cs* produce their own mmfs, pulsating along their axes according to their currents as shown in Fig. 3.9. If these windings are displaced from each other by 120 electrical degrees in space and are supplied by symmetric three-phase AC sine currents, the vector sum of the three mmfs of these windings becomes a single rotating mmf vector F in the air gap. This is called the *rotating magnetic field*, and its moving speed is directly proportional to the frequency of the currents.

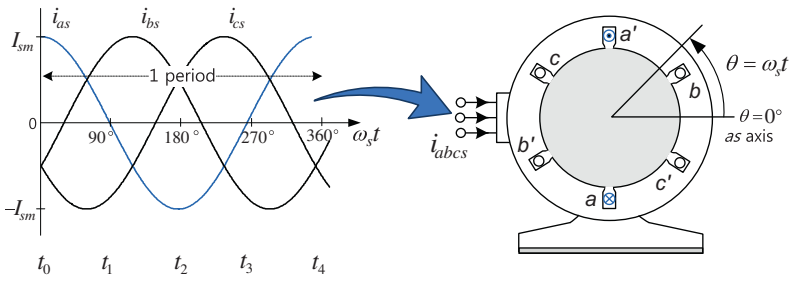


FIGURE 3.10

Three-phase windings and currents.

Let us describe mathematically this resultant air-gap mmf generated by the three-phase currents. The three-phase winding currents as shown in Fig. 3.10 are assumed as Eq. (3.1).

$$\begin{aligned} i_{as} &= I_{sm}\cos\omega_s t \\ i_{bs} &= I_{sm}\cos(\omega_s t - 120^\circ) \\ i_{cs} &= I_{sm}\cos(\omega_s t + 120^\circ) \end{aligned} \tag{3.1}$$

where $\omega_s (= 2\pi f_s)$ is the angular frequency of the currents and f_s is the frequency of the currents.

The mmfs resulting from the three-phase currents flowing in windings with a total number of turns N_s are given by

$$\begin{aligned} F_{as}(\theta) &= N_s i_{as}\cos\theta \\ F_{bs}(\theta) &= N_s i_{bs}\cos(\theta - 120^\circ) \\ F_{cs}(\theta) &= N_s i_{cs}\cos(\theta + 120^\circ) \end{aligned} \tag{3.2}$$

Here, the axis of phase *as* is chosen as $\theta = 0^\circ$.

From Eqs. (3.1) and (3.2), the resultant mmf is given as

$$\begin{aligned} F(\theta) &= F_{as}(\theta) + F_{bs}(\theta) + F_{cs}(\theta) \\ &= N_s I_{sm}\left[\cos\omega_s t\cos\theta + \cos(\omega_s t - 120^\circ)\cos(\theta - 120^\circ)\right] \\ &\quad + \cos(\omega_s t + 120^\circ)\cos(\theta + 120^\circ) \\ &= \frac{3}{2} N_s I_{sm}\cos(\omega_s t - \theta) \end{aligned} \tag{3.3}$$

Eq. (3.3) describes that the resultant mmf is rotating at the angular velocity ω_s over time with a constant amplitude $(\frac{3}{2}N_s I_{sm})$ and is sinusoidally distributed in the air gap as shown in Fig. 3.11.

Let us observe the movement of this resultant air-gap mmf according to the three-phase currents. Fig. 3.12 shows the locations of the resultant mmf produced

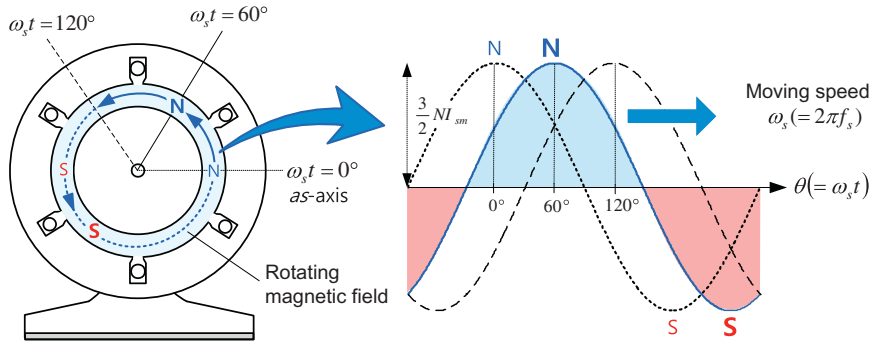


FIGURE 3.11

Resultant mmf.

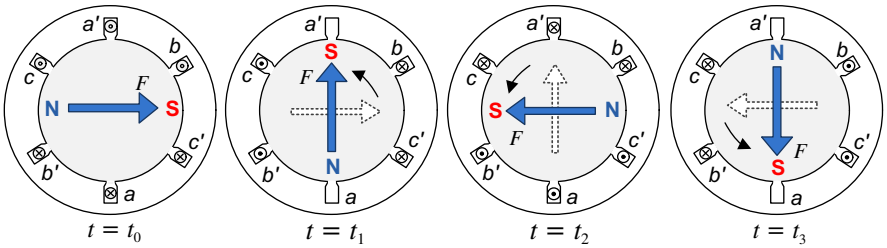


FIGURE 3.12

Movement of the resultant air-gap mmf per cycle of the current.

by the spatial distribution of the three-phase currents at four instants of time, which is shown in Fig. 3.10. Here, we will consider only the centered coils on the axes of the three-phase distributed windings for simplicity. We can see that the resultant air-gap mmf makes one revolution per cycle of the current. The direction of the rotation of the mmf can be reversed by reversing the phase sequence of the currents.

The resultant mmf produces one north magnetic pole and one south magnetic pole in the air gap, i.e., the number of magnetic poles is two. In this two-pole motor, the mmf makes one mechanical revolution per complete cycle of the current. In the four-pole motor that has two sets of three-phase windings, the mmf produces two north and south poles in the air gap as shown in Fig. 3.13. In this case, one cycle of the current corresponds to a half mechanical revolution of the mmf. Thus one revolution of the mmf needs two cycles of the current. The number of electrical cycles required to complete a mechanical rotation is

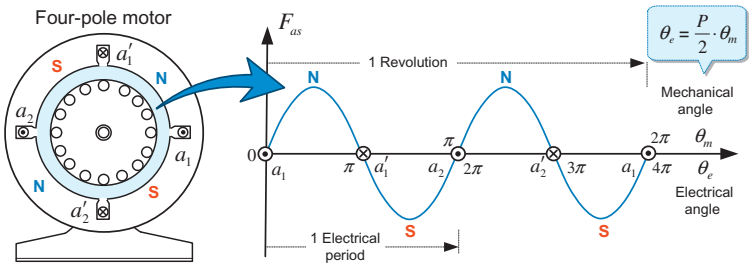


FIGURE 3.13

mmf Distribution by phase *as* current in the four-pole motor.

equal to the number of pole pairs. Thus, in a P-pole motor, there is a relationship between the mechanical angle θ_m and the electrical angle θ_e as

$$\theta_e = \frac{P}{2} \cdot \theta_m \tag{3.4}$$

When dealing with the performance of the motor, all calculations for electric quantities are carried out based on the electrical angle in radian. In a P-pole motor, the rotating speed n_s of the mmf by the three-phase currents with a frequency f is expressed in terms of revolution per minute (r/min) as

$$n_s = \frac{2}{P} \cdot f \cdot 60 = \frac{120f}{P} (r/\text{min}) \tag{3.5}$$

This speed of the rotating mmf is called the *synchronous speed*. For example, for a two-pole induction motor fed by currents of 60 Hz, the synchronous speed is 3600 r/min.

3.1.3 EQUIVALENT CIRCUIT OF INDUCTION MOTORS

To analyze the operating characteristic and performance of an induction motor, we usually use an equivalent circuit based on voltage equations that describe the behavior of the motor. In this section we will start with the steady-state equivalent circuit, and in Chapter 4, we will introduce the equivalent circuit that is useful for characteristics in the transient state as well as in the steady state.

Consider a two-pole, three-phase, wye-connected symmetrical induction motor as shown in Fig. 3.14.

It is assumed that the rotor windings, which may be a wound or a squirrel-cage type, are approximated as three-phase windings. Both the stator and rotor windings are distributed windings, but Fig. 3.14 shows only the centered coils on the axis of each phase. We will initially explore the voltage equations for the stator windings.

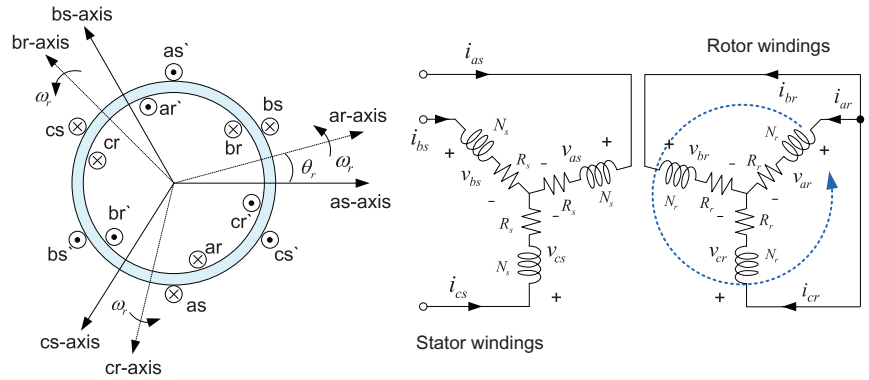


FIGURE 3.14

Two-pole, three-phase, wye-connected symmetrical induction motor.

3.1.3.1 Stator circuit

The voltage equation for the stator windings consists of the voltage drop of the winding resistance R_s and the induced voltage proportional to the rate of change over time of the stator flux linkage λ_s. Thus the voltage equation for the stator windings is written by

$$v_s = R_s i_s + \frac{d\lambda_s}{dt} \tag{3.6}$$

where R_s is the resistance of the stator winding and λ_s is the flux linkage of the stator winding.

When the stator voltage v_s is applied to the stator winding with the effective number of turns N_s, a stator current i_s flows in the winding. The current i_s produces a stator mmf $(N_s i_s)$ and in turn produces a stator flux ϕ_s in the air gap. Most of the stator flux ϕ_s crosses the air gap and links to the rotor winding. This air-gap flux is termed mutual flux, which is often called *magnetizing flux*. Only the mutual flux is contributed to energy conversion, i.e., torque production. However, a small portion of the stator flux cannot cross the air gap but links to only the stator winding itself. This is termed *leakage flux*. Thus the stator flux linkage λ_s will be expressed as

$$\lambda_s = N_s(\phi_{ls} + \phi) = N_s(\phi_{ls} + \phi) \tag{3.7}$$

where ϕ is the magnetizing flux and ϕ_{ls} is the leakage flux.
Here, the flux linkage may be written as

$$\lambda_s = L_{ls} i_s + L_m i_m \tag{3.8}$$

where L_{ls} is leakage inductance, L_m is magnetizing inductance, and i_m is magnetizing current.

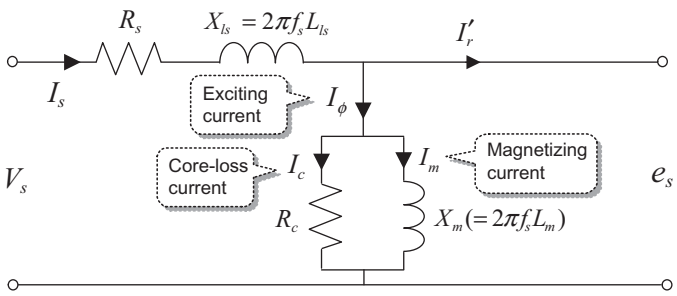


FIGURE 3.15

Equivalent circuit of the stator winding.

Substituting Eq. (3.8) into the voltage equation of Eq. (3.6) yields

$$v_s = R_s i_s + L_{ls}\frac{di_s}{dt} + L_m\frac{di_m}{dt} = R_s i_s + L_{ls}\frac{di_s}{dt} + e_s \tag{3.9}$$

Here, $e_s(=L_m(di_m/dt))$ is the induced voltage (called back-EMF) in the stator winding.

Based on Eq. (3.9), the equivalent circuit of the stator winding can be represented as shown in Fig. 3.15. Here, f_s is the frequency of the stator voltage.

To take into account the core loss such as eddy current loss and hysteresis loss, this circuit includes the equivalent resistance R_c representing the core loss. This resistance is connected in parallel with the magnetizing inductance. Accordingly, the exciting current i_ϕ to produce the flux is comprised of a magnetizing current i_m and a core loss current i_c.

Though an induction motor and a transformer have similar equivalent circuits as shown in Fig. 3.15, they differ in their value of parameters. Because there must be an air gap in induction motors, the magnetizing inductance L_m in induction motors will be a much smaller than that of a transformer. This means that a higher magnetizing current is required to achieve a given flux level. For transformers, the magnetizing current accounts for 1−5% of the rated current, while for induction motors it accounts for 30−50% of the rated current.

We need to know the induced voltage e_s to complete the voltage equation of Eq. (3.9). The induced voltage is proportional to the rate of change over time of the stator flux linkage. To obtain the induced voltage, we need to find out the stator flux, which also requires finding of the flux density.

The rotating magnetic field discussed in the Section 3.1.2.1 may be considered simply as a magnet rotating in the air gap as shown in Fig. 3.16.

The rotating magnetic field will induce voltages in both the stator and rotor windings. When the rotating magnetic field is aligned with the magnetic axis of phase *as* (i.e., $\theta = 0°$) as shown in Fig. 3.17, the flux density distribution in the air gap can be expressed as

$$B(\theta) = B_{max}\cos\theta \tag{3.10}$$

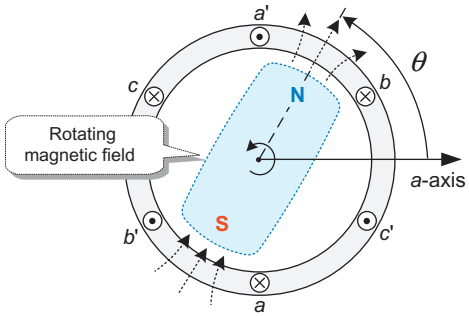


FIGURE 3.16

Rotating magnetic field.

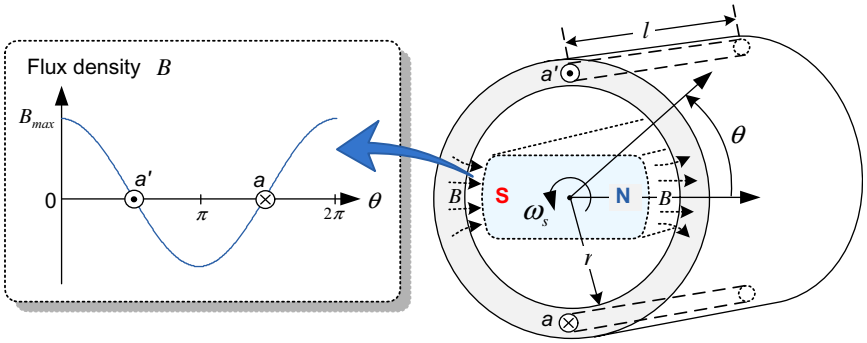


FIGURE 3.17

Flux density distribution in the air gap.

The air-gap flux per pole in the air gap is

$$\phi = \int_{-\pi/2}^{\pi/2} B(\theta) l r d\theta = 2B_{max} l r \tag{3.11}$$

where l is the axial length of the stator and r is the radius to the mean of the air gap.

As the rotating magnetic field moves along the air gap, the flux linking the windings will vary with its position as shown in Fig. 3.18.

The flux linkage λ_a for N_s-turn coils of phase as will be the maximum $N_s\phi$ at $\theta = 0^\circ$ and zero at $\theta = 90^\circ$. Thus λ_a will vary as the cosine of the position angle $\theta(= \omega_s t)$ as

$$\lambda_a = N_s \phi \cos \omega_s t \tag{3.12}$$

The voltage induced in the phase as winding is obtained from Faraday's law as

$$e_a = -\frac{d\lambda_a}{dt} = \omega_s N_s \phi \sin \omega_s t = E_{\max} \sin \omega_s t \tag{3.13}$$

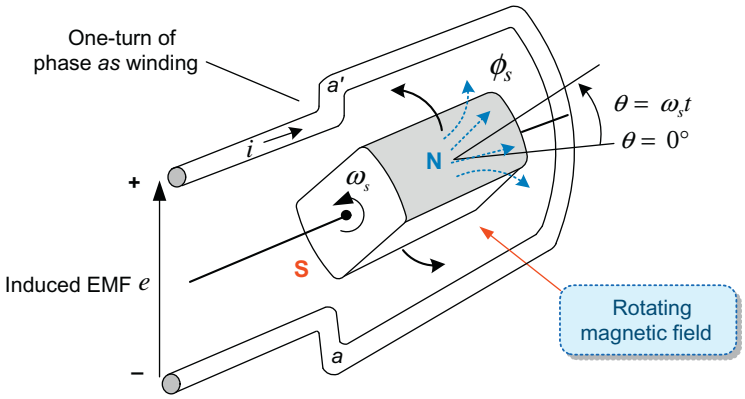


FIGURE 3.18

Flux linking the one-turn coil.

Similarly the voltages induced in the other windings are given by

$$e_b = E_{max} \sin(\omega_s t - 120°) \tag{3.14}$$

$$e_c = E_{max} \sin(\omega_s t + 120°) \tag{3.15}$$

The root mean square (rms) value of the induced voltage is

$$E_{rms} = \frac{E_{max}}{\sqrt{2}} = \frac{\omega_s N_s \phi}{\sqrt{2}} = 4.44 f_s N_s \phi \tag{3.16}$$

where N_s is the total number of the series turns per phase forming a concentrated full-pitch winding. A *full-pitch winding* means that the coil-pitch (i.e., the distance between two sides of a coil) is equal to the pole-pitch (i.e., the distance between two adjacent poles). If the coil-pitch is less than the pole-pitch, then it is called *fractional-pitch* or *short-pitch winding*. In an actual distributed winding, the voltages induced in coils placed in different slots are not in time phase, and therefore the phasor sum of the voltages is less than their numerical sum when all coils are connected in series for the phase winding. Considering this, a reduction factor, called the *winding factor* $K_{\omega s}$, is used. The winding factor $K_{\omega s}$ for most motors is about 0.85−0.95. Consequently, for a distributed winding, the rms-induced voltage per phase is

$$E_s = 4.44 f_s N_s \phi K_{\omega s} \tag{3.17}$$

It is important to note that the stator flux is directly proportional to the ratio of the induced voltage to the stator frequency, i.e., $\phi \propto E_s/f_s$. This fact gives a useful basis for the speed control of induction motors that will be described later.

Next, let us acquire the equivalent circuit of the rotor winding.

3.1.3.2 Rotor circuit

The rotating magnetic field in the air gap induces voltages in the rotor circuit as well as the stator circuit. This induced voltage becomes the source voltage applied to the rotor circuit. Similar to Eq. (3.17), the voltage induced in the rotor circuit can be expressed as

$$E_r = 4.44 N_r \phi K_{\omega r} f_r \tag{3.18}$$

where N_r is the total number of turns per phase, $K_{\omega r}$ is the winding factor for the rotor windings, and f_r is the frequency of the voltage induced in the rotor winding.

Since the rotor winding experiences a flux variation due to the difference in speed between the rotating magnetic field and the rotor, the frequency f_r of the induced voltage in the rotor circuit becomes the difference $f_s - f$ between the frequency f_s of the rotating magnetic field and the rotating frequency f of the rotor. Thus the induced voltage E_r depends on the rotor speed as

$$E_r = 4.44 N_r \phi K_{\omega r} \times f_r = 4.44 N_r \phi K_{\omega r} \times (f_s - f) \tag{3.19}$$

At standstill ($f = 0$), the frequency f_r is the same as the stator frequency f_s. Thus the induced voltage in the rotor winding will be the maximum as

$$E_{r0} = 4.44 N_r \phi K_{\omega r} f_s \tag{3.20}$$

In this case, similar to a transformer, the ratio of the voltages induced in the two windings is equal to the ratio of their number of turns.

The induced voltage in the shorted rotor winding produces a rotor current. Torque in the rotor winding is developed by the interaction between this rotor current and the stator rotating magnetic field. The rotor will then start rotating. Assume that the rotor eventually reaches a steady-state speed n (r/min). This rotor speed is always less than the speed of the stator rotating magnetic field (i.e., the synchronous speed). The difference between the synchronous speed n_s and the rotor speed n is called the *slip speed*. The slip speed expressed as a fraction of the synchronous speed is called the *slip s* and can be defined as

$$\text{Slip:} \quad s = \frac{n_s - n}{n_s} \tag{3.21}$$

It should be noted that the slip is a very important factor in the induction motor because most of its performance characteristics of an induction motor, such as the developed torque, current, efficiency and power factor, depends on the operating slip. The operating slip depends on the load. An increase in the load will cause the rotor to slow down and increase the slip. A decrease in the load will cause the rotor to speed up and decrease the slip. A typical induction

motor operates in the slip range of 0.01−0.05, i.e., 1−5%. For example, a four-pole motor operated at 60 Hz has a synchronous speed of 1800 r/min. If the rotor speed at full load is 1765 r/min, then the slip is 1.9%.

Now, let us examine the induced voltage in the rotor winding when the rotor is rotating at a speed n (slip s). The frequency f_r in the rotor circuit at the slip s is called the *slip frequency* and is given as

$$f_r = f_s - f = sf_s \tag{3.22}$$

From Eq. (3.20), the induced voltages in the rotor circuit at the slip s becomes

$$E_r = 4.44N_r\phi K_{\omega r} \times f_r = 4.44N_r\phi K_{\omega r} \times sf_s = sE_{r0} \tag{3.23}$$

We can see that the magnitude of the voltage induced in the rotor winding is directly proportional to the slip. When the rotor is stationary (i.e., $s = 1$), the largest voltage is induced in the rotor circuit. As the rotor speed is increased, the induced voltage is decreased. If the rotor speed is equal to the synchronous speed, then the induced voltage becomes zero.

Now, we are ready to discuss the equivalent circuit of the rotor winding. From Eq. (3.23), we can see that the source voltage in the rotor circuit is sE_{0r}. With the resistance R_r and the leakage inductance L_{lr} of the rotor circuit, the rotor equivalent circuit is depicted as Fig. 3.19A. The rotor equivalent circuit of Fig. 3.19A is at the rotor frequency f_r. Thus we cannot combine this rotor circuit with the stator equivalent circuit of Fig. 3.16 together in a single circuit because the two circuits differ in the operating frequency. Therefore, we need to adjust the rotor frequency to combine the two circuits. By dividing the voltage and the impedance of Fig. 3.19A by the slip s, we will obtain the rotor equivalent circuit of Fig. 3.19B. In the circuit, the rotor current is the same as in Fig. 3.19A, but its operating frequency is equal to the stator frequency f_s. Thus, this becomes the rotor equivalent circuit as seen from the stator. These two circuits can now be joined together by considering the turns ratio $a(= N_s/N_r)$ of the stator winding and the rotor winding.

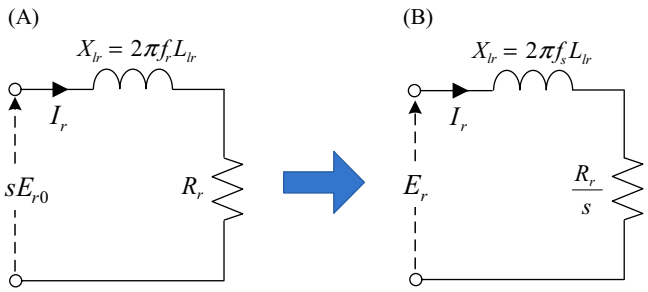


FIGURE 3.19

Rotor equivalent circuit. (A) Referred to rotor side and (B) referred to stator side.

The complete equivalent circuit per phase of a three-phase induction motor is shown in Fig. 3.20.

This equivalent circuit is similar to that of a transformer, except for the effects of varying speed. The quantities that are reflected from the rotor to the stator are denoted by the prime symbol ($'$). From this point on, we will skip the prime symbol.

Similar to the three-phase currents of the stator winding, the three-phase currents induced in the rotor winding also produce a rotating magnetic field F_r in the air gap as shown in Fig. 3.21A. From the rotor structure's point of view, this rotor rotating magnetic field F_r rotates at the speed $n_r(=n_s-n)$. Since the rotor itself is rotating at n, from the stator structure's point of view, the rotor rotating magnetic field rotates at the synchronous speed $n_s(=n_r+n)$. Thus, both the stator magnetic field and the rotor magnetic field always rotate in the air gap at

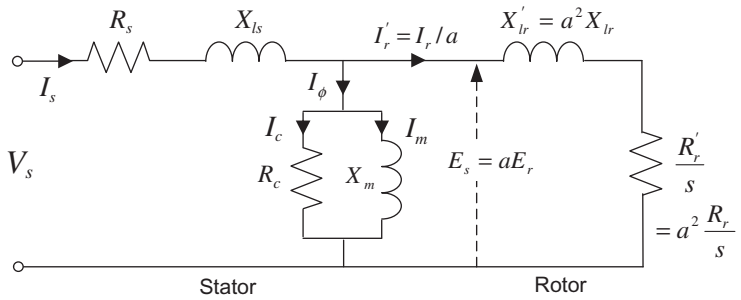


FIGURE 3.20

Complete per phase equivalent circuit of a three-phase induction motor.

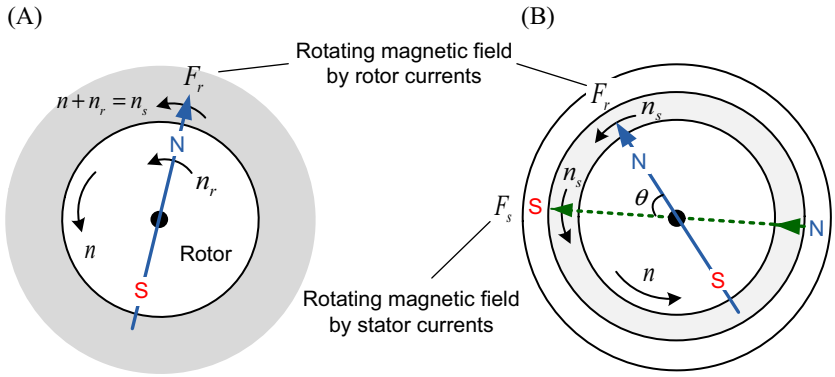


FIGURE 3.21

Rotating magnetic fields. (A) Magnetic field by rotor current and (B) magnetic fields by stator and rotor currents.

the same synchronous speed. These stator and rotor magnetic fields, therefore, remain stationary with respect to each other as shown in Fig. 3.21B. The interaction between these two fields is considered to produce the torque.

3.1.4 CHARACTERISTICS OF INDUCTION MOTORS

In this section, we will discuss the characteristics of an induction motor such as the current, input power factor, output torque, and efficiency from the equivalent circuit of Fig. 3.20. We will see that these characteristics depend on the slip, i.e., the operating speed.

3.1.4.1 Stator current

The stator current is the input current of an induction motor. From Fig. 3.20, neglecting the core losses, the input impedance as a function of slip is given as

$$Z_s = R_s + jX_{ls} + \left[X_m / \left(\frac{R_s}{s} + jX_{lr}\right)\right] = |Z_s| \angle \theta_s \tag{3.24}$$

where θ_s is input impedance angle.

From the applied stator voltage and the input impedance of Eq. (3.24), the stator current is given as

$$I_s = \frac{V_s}{Z_s} = I_\phi + I_r \tag{3.25}$$

The stator current is the sum of the exciting current I_ϕ and the rotor current I_r. With a constant stator voltage V_s, the stator current I_s as a function of speed (i.e., slip s) is shown in Fig. 3.22.

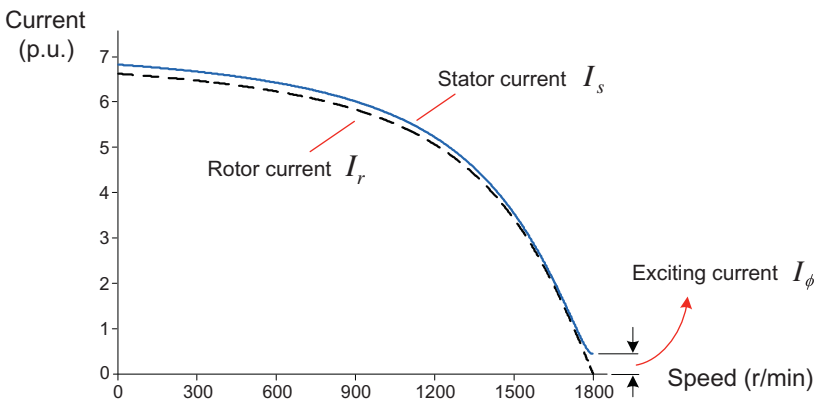


FIGURE 3.22

Stator current as a function of speed (5-hp, four poles).

At starting ($s = 1$), since the impedance is minimum, the stator current will be the maximum value, which may be 5−8 times larger than the rated current. As the speed increases, the slip s decreases. As the slip s decreases, the rotor current I_r decreases, and thus the stator current also decreases. At the synchronous speed, i.e., $s = 0$, $R_s/s \approx \infty$, so there is no rotor current, i.e., $I_r = 0$. Thus the stator current I_s will be equal to the exciting current I_ϕ.

3.1.4.2 Input power factor

From the input impedance angle θ_s of Eq. (3.24), the input power factor of an induction motor is written as

$$PF = \cos\theta_s \tag{3.26}$$

The power factor varies with speed as shown in Fig. 3.23. Since induction motors inherently draw a lagging current to produce the magnetic flux, the power factor is always smaller than one. The power factor also varies with the load applied to the motor. The power factor is minimum at no load, and it increases with the load. It usually reaches the peak at or near full load.

3.1.4.3 Output torque

We can derive a general expression for the output torque of an induction motor from the power-flow diagram as shown in Fig. 3.24.

The input power $P_{in}(= 3V_sI_s\cos\theta_s)$ to an induction motor, excluding the stator losses such as the stator copper loss and the core loss, will be transferred to the rotor across the air gap and then transformed to mechanical power P_{mech}. We can derive the output torque using the mechanical power P_{mech}.

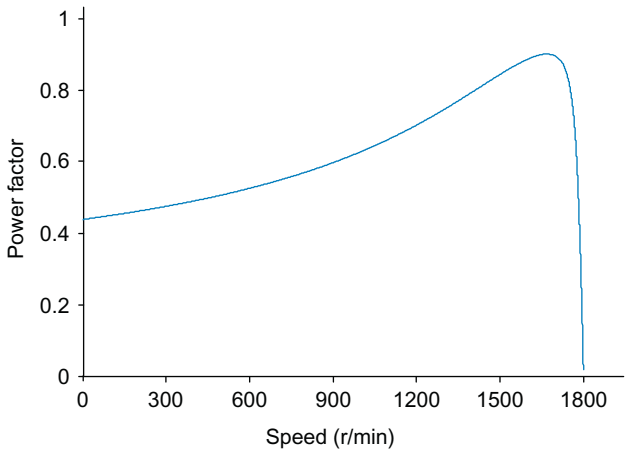


FIGURE 3.23

Input power factor (5-hp, four-pole motor).

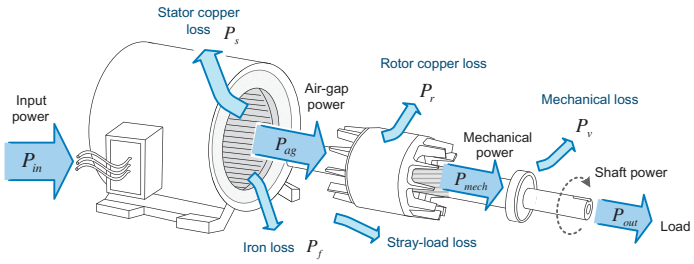


FIGURE 3.24

Power-flow diagram in an induction motor.

Redrawn from http://images.slideplayer.com/14/4186646/slides/slide_32.jpg.

The power delivered through the air gap from the stator to the rotor is called the *air-gap power* P_{ag}. Referring to the equivalent circuit given in Fig. 3.20, the air-gap power is written by

$$P_{ag} = I_r^2 \frac{R_r}{s} \tag{3.27}$$

Because the induction motors are operated typically at low slips of 0.01−0.05, the air-gap power is considerably large. This air-gap power P_{ag}, i.e., input power to the rotor, will be dissipated in the resistance R_r of the rotor circuit (i.e., rotor copper loss) and converted into a mechanical output. Thus, Eq. (3.27) can be divided into two components as

$$P_{ag} = \underbrace{I_r^2 R_r}_{\substack{\text{Rotor copper loss} \\ P_r}} + \underbrace{I_r^2 \frac{R_r}{s}(1-s)}_{\substack{\text{Mechanical output} \\ P_{mech}}} \tag{3.28}$$

$$P_r = I_r^2 R_r = s\, P_{ag} \tag{3.29}$$

$$P_{mech} = I_r^2 \frac{R_r}{s}(1-s) = (1-s)P_{ag} \tag{3.30}$$

The first term on the right-hand side of Eq. (3.28) represents the rotor copper loss P_r. The second term represents the mechanical output power P_{mech} that develops the output toque. Fig. 3.25 shows this power distribution in the rotor circuit based on Eq. (3.28).

We can see that the power distribution depends on the slip s. It is clear that the lower the slip of the motor, the lower the rotor copper loss and the higher the mechanical output power.

The mechanical power is equal to the output torque T_{mech} times the angular frequency ω_{mech} as

$$P_{mech} = I_r^2 \frac{R_r}{s}(1-s) = T_{mech} \cdot \omega_{mech} \tag{3.31}$$

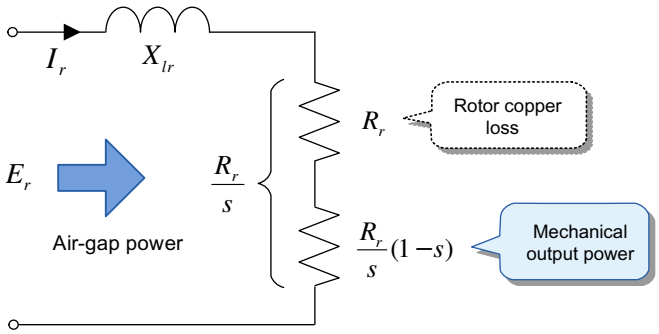


FIGURE 3.25

Distribution of the air-gap power.

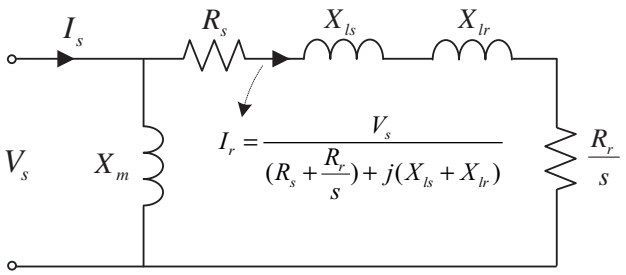


FIGURE 3.26

Approximated per phase equivalent circuit of an induction motor.

Thus the output torque of an induction motor is given by

$$T_{mech} = \frac{P_{mech}}{\omega_{mech}} = \frac{1}{\omega_{mech}} I_r^2 \frac{R_r}{s}(1-s) = \frac{1}{\omega_s} I_r^2 \frac{R_r}{s} \tag{3.32}$$

where $\omega_{mech} = (1-s)\omega_s$ and ω_s represents the synchronous angular frequency.

We need to express this torque equation in terms of the input voltage instead of a nonmeasurable rotor current. The rotor current can be easily obtained from the approximate equivalent circuit given in Fig. 3.26, in which the core loss resistance is ignored and the magnetizing inductance is shifted to the input side assuming $R_s + jX_{ls} \ll \omega_s L_m$.

From this circuit, the rotor current is given by

$$I_r = \frac{V_s}{\left(R_s + \frac{R_r}{s}\right) + j(X_{ls} + X_{lr})} \tag{3.33}$$

By substituting this rotor current into Eq. (3.32), the output torque (per phase) is expressed as

$$\text{Torque:}\quad T_{mech} = \frac{1}{\omega_s}\frac{V_s^2}{\left(R_s + \dfrac{R_r}{s}\right)^2 + j(X_{ls}+X_{lr})^2}\frac{R_r}{s} \tag{3.34}$$

This is the steady-state average torque per phase for a given input voltage V_s, which is a function of the slip. The torque for a given slip is proportional to the square of the stator input voltage. The torque calculated by using this approximate circuit varies within 5% from that of the full circuit [2]. The shaft torque, which is available to the load at the shaft of the motor, can be obtained by subtracting the friction and windage torques from this output torque.

Let us examine the speed−torque characteristics of an induction motor based on Eq. (3.34). In the low-slip region, which is the normal operating range of an induction motor, the impedance of equivalent circuit parameters shows the following relations as

$$R_s + \frac{R_r}{s} \gg X_{ls} + X_{lr} \quad \text{and} \quad \frac{R_r}{s} \gg R_s \tag{3.35}$$

Thus the torque of Eq. (3.34) can be simplified as

$$T_{mech} \approx \frac{1}{\omega_s}\frac{V_s^2}{R_r}s \;\rightarrow\; T_{mech} \propto s \tag{3.36}$$

In this case, it is noteworthy that the output torque increases linearly with the slip s. On the other hand, in the low-speed range with larger values of the slip,

$$R_s + \frac{R_r}{s} \ll X_{ls} + X_{lr} \tag{3.37}$$

Thus the torque varies almost inversely with the slip s as

$$T_{mech} = \frac{1}{\omega_s}\frac{V_s^2}{(X_{ls}+X_{lr})^2}\frac{R_r}{s} \;\rightarrow\; T_{mech} \propto \frac{1}{s} \tag{3.38}$$

There is a speed at which the maximum torque, often referred to as *pull-out torque* or *breakdown torque*, is developed. The slip at the maximum torque can be obtained by solving $dT_{mech}/ds = 0$ as

$$s_{max} = \frac{R_r}{\sqrt{R_r^2 + (X_{ls}+X_{lr})^2}} \tag{3.39}$$

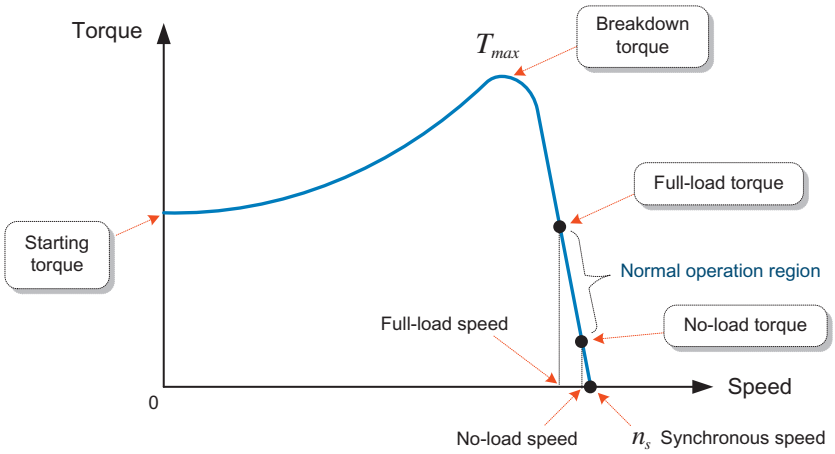


FIGURE 3.27

Speed versus torque curve for an induction motor.

It is important to note that the rotor resistance R_r is an important parameter in determining the slip at which the maximum torque occurs. From s_{max}, the maximum torque can be given as

$$T_{max} = \frac{1}{2\omega_s} \frac{V_s^2}{R_s + \sqrt{R_s^2 + (X_{ls} + X_{lr})^2}} \tag{3.40}$$

The value of the maximum torque is independent of the rotor resistance, which determines the maximum slip value. The speed−torque curve of a typical three-phase induction motor is shown in Fig. 3.27. This curve shows the speed versus the output torque when an induction motor is started with full voltage.

The normal operating range of an induction motor is near the synchronous speed, confined to less than 5% slip. In this low-slip region, the output torque increases linearly with the increasing slip. The slip increases approximately linearly with the increased load, and thus the rotor speed decreases approximately linearly with the load.

3.1.4.4 Stable operating point

When a motor is driving a mechanical load, the motor will operate in a steady state at a speed at which the torque developed by the motor is equal to the torque required by the load. As it can be seen from the motion equation in Eq. (3.41), when the motor torque T_{motor} exceeds the load torque T_{load}, the motor speed will increase. When the motor torque is less than the load torque, the motor speed will decrease. Thus the equilibrium point will be the speed at which the motor torque equals to the load torque.

$$T_{motor} - T_{load} = (J_{motor} + J_{load}) \frac{d\omega}{dt} \tag{3.41}$$

There are two kinds of an equilibrium operating point: *stable point* and *unstable point*. At the stable operating point, the speed will be restored after a small departure from the original equilibrium point due to a disturbance in the input voltage or load. However, at the unstable operating point, the speed will not be restored.

In the induction motor drives, a stable operating point is in the range above the speed at which the maximum torque occurs in the speed−torque curve. As an example, consider Fig. 3.28 that shows the speed−torque curve of the induction motor along with two different load curves.

There exist three equilibrium operating points. Among these, point A is an unstable operating point, whereas points B and C are stable operating points. At point A, the system will not be able to maintain its original equilibrium state when there is a disturbance in the drive system. For example, assume that, at point A, there is a reduction in speed caused by a disturbance. In this case, a decrease in the speed causes the motor torque to be less than the load torque. As a result, the system will decelerate and eventually come to a stop. Similarly, an increase in the speed caused by a disturbance will make the motor torque larger than the load torque. Thus the operating point will move from point A to point B. Therefore point A is an unstable operating point. On the contrary, points B and C are stable operating points. At these points, the speed will return to their original points after the deviation in speed by a disturbance. Criterion for the stability is given by

$$\frac{d(T_{load} - T_{motor})}{d\omega} > 0 \tag{3.42}$$

Hence a stable operation needs the following conditions: when the speed is decreased, the motor torque developed needs to be greater than the load torque,

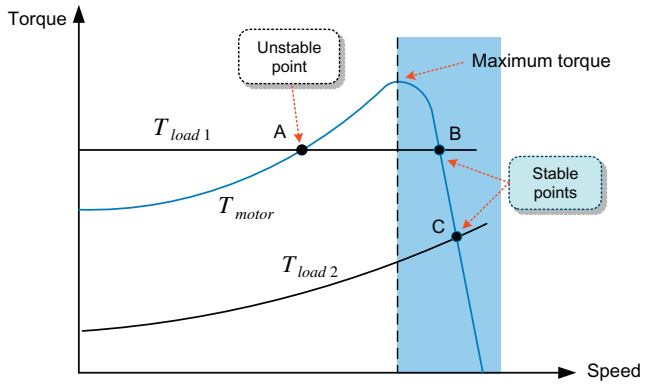


FIGURE 3.28

Operating points in motor drives.

whereas when the speed is increased, the motor torque needs to be less than the load torque.

3.1.4.5 Efficiency

Next, we will discuss the efficiency of an induction motor. Efficiency is defined as the ratio of the output power to the input power of the motor expressed as

$$\eta = \frac{P_{out}}{P_{in}} = \frac{P_{out}}{P_{out} + P_{Loss}} \cdot 100\,(\%) \tag{3.43}$$

As for a motor, the efficiency indicates how well the motor converts electrical power into mechanical power. The input power of an induction motor is given by

$$P_{in} = 3V_s I_s \cos\theta_s \tag{3.44}$$

As shown in Fig. 3.24, the losses in induction motors are typically grouped into five significant origins: the stator copper loss P_s, the core loss P_f, the rotor copper loss P_r, the windage and friction loss P_v, and the stray-load loss. The stray-load loss indicates residual losses that are difficult to determine by a direct measurement or a calculation. The stator copper loss accounts for a large part of the motor loss. Fig. 3.29 shows the loss distribution rating by rating [3].

The efficiency of induction motors is also dependent on the slip. If all the losses that have little or no relationship to the slip are neglected, then the efficiency can be expressed as a function of the slip as

$$\eta = \frac{P_{out}}{P_{in}} \rightarrow \frac{P_{mech}}{P_{ag}} = \frac{P_{ag} - P_r}{P_{ag}} = 1 - s \tag{3.45}$$

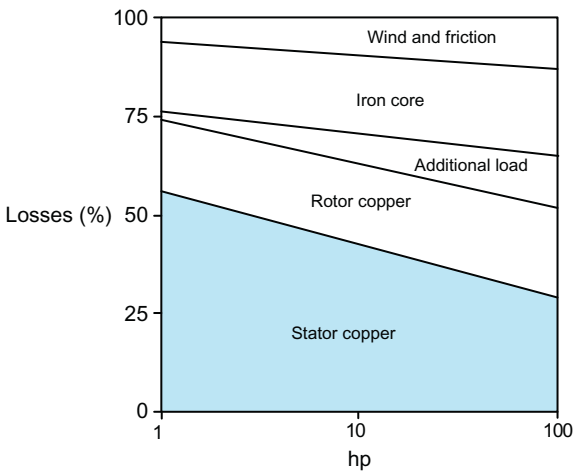


FIGURE 3.29

Loss distribution of induction motor.

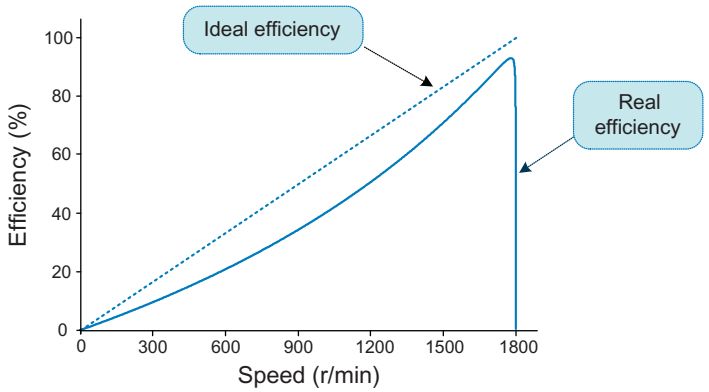


FIGURE 3.30

Actual efficiency and ideal efficiency.

This is called the ideal efficiency or the internal efficiency. The internal efficiency as a function of speed is shown in Fig. 3.30. The internal efficiency gives a measure of how much of the power delivered to the air gap is available for mechanical power. The lower slip operation leads to a higher efficiency because the rotor copper loss is directly proportional to the slip as we can see from Eq. (3.29). In general, larger motors are more efficient than smaller motors. Today's premium efficiency three-phase induction motors have efficiencies ranging from 86.5% at 1 hp to 95.8% at 300 hp.

EXAMPLE 1

A 5 hp, 220 V, 60 Hz, four-pole three-phase induction motor operates at 1740 r/min when fully loaded at its rated voltage and rated frequency. The motor parameters are $R_s = 0.295\ \Omega$, $R_r = 0.379\ \Omega$, $X_m = 22.243\ \Omega$, and $X_{ls} = X_{lr} = 0.676\ \Omega$. Evaluate the following:

1. the slip, power factor, stator current, exciting current, and developed torque when running at rated conditions;
2. the stator current and developed torque when starting at full voltage;
3. the slip at which maximum torque is developed.

Solution

1. The synchronous speed is

$$n_s = \frac{120 f_s}{P} = \frac{120 \cdot 60}{4} = 1800\,\text{r/min}$$

Thus the rated slip is

$$s = \frac{n_s - n}{n_s} = \frac{1800 - 1740}{1800} = 0.0333$$

From the equivalent circuit in Fig. 3.20, the rotor impedance is

$$Z_r = \frac{R_s}{s} + jX_{lr} = 11.37 + j0.679$$

The input impedance is

$$Z_s = R_s + jX_{ls} + \frac{Z \cdot jX_{lr}}{Z_r + jX_{lr}} = 8.887 + j5.599$$
$$= |Z_s| \angle \theta_s = 10.5 \angle 32.212$$

The power factor is

$$\cos \theta_s = 0.846$$

The stator current is

$$I_s = \frac{V_{phase}}{|Z_s|} = \frac{\left(\frac{220}{\sqrt{3}}\right)}{10.5} = 12.092 \text{ A}$$

The rotor current is

$$I_r = I_s \cdot \frac{jX_m}{Z_r + jX_m} = 10.512 \text{ A}$$

The torque is

$$T_{mech} = \frac{1}{\omega_s} I_r^2 \frac{R_r}{s} = \frac{1}{188.5} \cdot 10.512^2 \cdot \frac{0.379}{0.0333} = 20 \text{ Nm}$$

where

$$\omega_s = 2\pi f_s \left(\frac{2}{P}\right) = 188.5 \text{ rad/s}$$

2. Since $s = 1$ at start, the rotor impedance is

$$Z_r = \frac{R_s}{s} + jX_{lr} = 0.379 + j0.679$$

The input impedance is

$$Z_s = R_s + jX_{ls} + \frac{Z \cdot jX_{lr}}{Z_r + jX_{lr}} = 0.652 + j1.343$$

The stator current is

$$I_s = \frac{V_{phase}}{|Z_s|} = \frac{\left(\frac{220}{\sqrt{3}}\right)}{1.493} = 85.08\text{A}$$

and the starting current is seven times larger than the rated current.

The rotor current is

$$I_r = I_s \cdot \frac{jX_m}{Z_r + jX_m} = 82.557\text{A}$$

The starting torque is

$$T_{mech} = \frac{1}{\omega_s} I_r^2 \frac{R_r}{s} = \frac{1}{188.5} \cdot 82.557^2 \cdot \frac{0.379}{1} = 41.1\ \text{Nm}$$

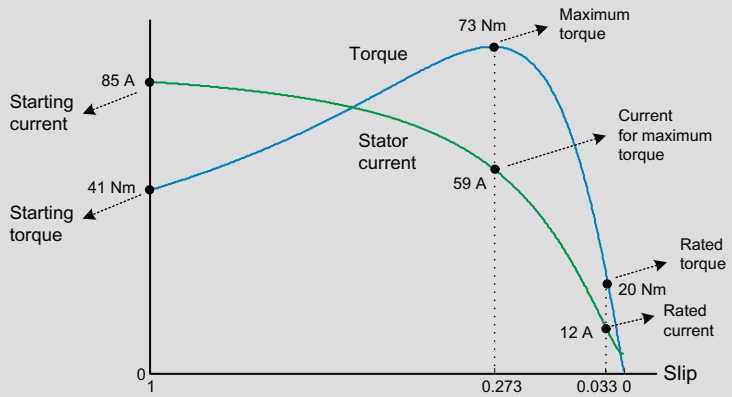
3. The slip at the maximum torque is

$$s_{max} = \frac{R_r}{\sqrt{R_r^2 + \left(X_{ls} + X_{lr}\right)^2}} = 0.273$$

The maximum torque developed is

$$T_{max} = \frac{3}{2\omega_s} \frac{V_s^2}{R_s + \sqrt{R_s^2 + \left(X_{ls} + X_{lr}\right)^2}} = 73.28$$

From the above results, the speed−torque curve of this induction motor is shown as



3.1.5 OPERATING MODES OF INDUCTION MOTORS

An induction motor can be operated in three modes according to its operating speed and rotation direction. Fig. 3.31 shows the power, operating speed, and torque in the available three operation modes of an induction motor.

First, a typical operation of an induction motor is the *motoring mode*, in which the rotor rotates in the same direction as the stator rotating magnetic field but at a somewhat slower speed. Thus the slip ranges between 0 and 1 ($0 < s \leq 1$), and both the air-gap power and the mechanical power are positive as

$$P_{ag} = I_r^2 \frac{R_r}{s} > 0, \quad P_{mech} = (1 - s)P_{ag} > 0 \tag{3.46}$$

This implies that, in the motoring mode, the induction motor converts the applied input power into mechanical power through the air gap.

If an induction motor is driven to a speed higher than the synchronous speed by an external prime mover, then the slip will be negative ($s < 0$) and both the air-gap power and the mechanical power are negative as

$$P_{ag} = I_r^2 \frac{R_r}{s} < 0, \quad P_{mech} = (1 - s)P_{ag} < 0 \tag{3.47}$$

This implies that the power from the mechanical system flows into the rotor circuit, then across the air gap to the stator circuit and the external electrical system. Thus the induction motor will operate in the *generation mode*.

This mode may occur when the stator frequency applied to an induction motor is lowered to reduce the speed of the rotor. In this process, the

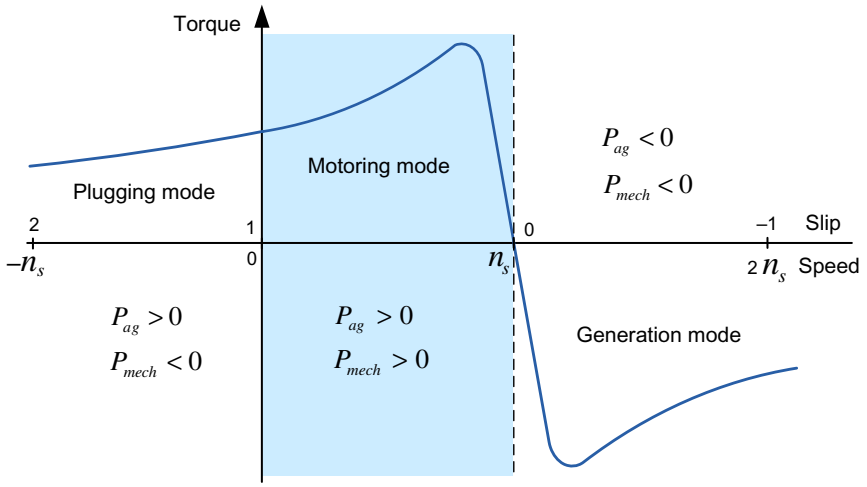


FIGURE 3.31

Three operation modes of an induction motor: plugging mode, motoring mode, and generation mode.

instantaneous speed of the rotor may be higher than the instantaneous synchronous speed because of the inertia of the drive system. This leads to a negative slip, and the direction of the torque developed in the motor will be opposite to the rotation of the rotor. This torque will act as a braking torque that slows down the rotor speed. In this case, the motor operates as a generator, and the generated power is fed back into the power source. This process is called *regenerative braking*.

The last operating mode is the *plugging mode*, in which the rotor rotates in the direction opposite to the stator magnetic field and thus, the slip $s > 1$. In this mode, the air-gap power and the mechanical power are given as

$$P_{ag} = I_r^2 \frac{R_r}{s} > 0, \quad P_{mech} = (1 - s)P_{ag} < 0 \tag{3.48}$$

Both powers flow into the rotor and are dissipated in the rotor as heat. Thus the rotor bar may be overheated. This mode can also be used for braking the motor to stop quickly. When an induction motor is running, the direction of the rotation of the stator magnetic field can be reversed by switching any two of the three-phase windings. In this case, the developed torque will be in the direction of the stator magnetic field but opposite to the rotation of the rotor, and the induction motor will operate in the plugging mode.

3.1.6 EFFECT OF ROTOR RESISTANCE

The resistance in the rotor circuit greatly influences the characteristics of an induction motor. This is because the speed at which the maximum torque occurs depends on the rotor resistance as shown in Eq. (3.4).

Fig. 3.32 shows the speed−torque characteristics for two different values of the rotor resistance. A high rotor resistance will provide a high starting torque, leading to a rapid acceleration of the mechanical load system. This is also desirable for a low starting current and a high power factor during starting. However a high rotor resistance results in a high slip during the normal running operation. This causes increased rotor loss and reduced efficiency. Therefore, during a normal operation, a low rotor resistance is desirable. This results in a lower slip and thereby a higher efficiency.

Therefore we can see that there are conflicting requirements of rotor resistance for a satisfactory performance, i.e., a high resistance at starting and low resistance at the normal operating speed. For this reason, different types of rotors have been developed to achieve a variation in rotor resistance with operating speed.

In a wound-rotor induction motor, external resistance can be connected to the rotor windings through slip rings as shown in Fig. 3.6. Thus a satisfactory performance in both the starting and running conditions can be obtained by varying the value of the external resistance with the rotor speed.

For squirrel-cage induction motors, the rotor resistance depends on the operating speed. This is because the effective resistance of the rotor conductor

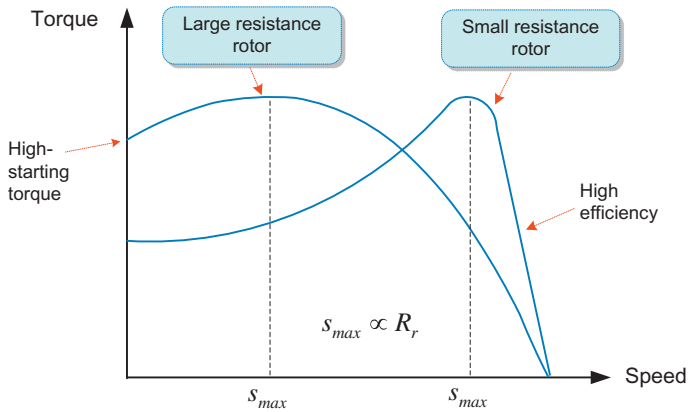


FIGURE 3.32

Torque–speed characteristics for different values of the rotor resistance.

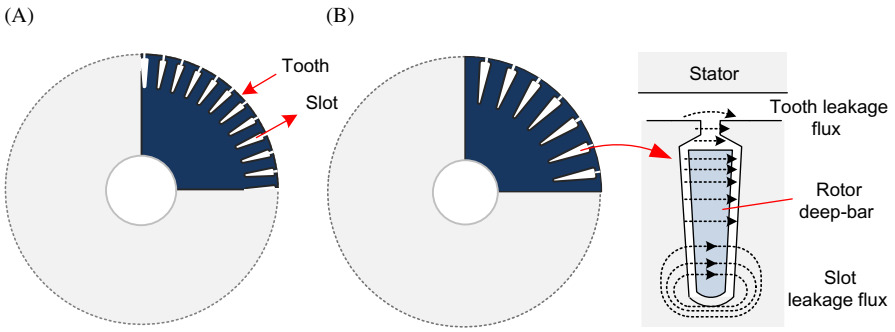


FIGURE 3.33

Comparison of rotor bars. (A) Normal rotor and (B) deep-bar rotor.

may be changed with the rotor frequency due to the skin effect. The skin effect is the tendency of AC current to flow near the surface of the conductor. The skin effect causes the effective area of the cross section of the conductor to reduce at higher frequencies, thus increasing the effective resistance of the conductor. At standstill, the rotor frequency is high since it equals to the stator frequency, whereas at a normal operating speed, it is low at about 1–3 Hz in a 60-Hz motor. As a result, the effective resistance of the rotor circuit decreases as the operating speed increases.

Besides the skin effect, the rotor conductor can be properly designed to have a higher resistance at the starting. In this case, the rotor conductor is made in the form of a *deep-bar* as shown in Fig. 3.33B. In the current-carrying deep-bar, the leakage flux surrounding the bottom part of the deep-bar conductor is greater

than that of the upper part. The leakage flux lines are shown by the *dotted lines* on the right of Fig. 3.33B. The leakage inductance of the conductor elements at the bottom part is larger than that of the conductor elements at the upper part. Therefore the AC current in the upper part of the conductor will flow more easily than in the bottom part with a large leakage reactance. This nonuniform current distribution makes the effective resistance of the bar to increase.

Since the leakage reactance is proportional to the frequency, this nonuniform current distribution is more pronounced at the starting of a high rotor frequency. At normal operating speeds, since the rotor frequency is low, the rotor current is almost uniformly distributed over the cross-sectional area of the rotor bar, and thus the effective resistance R_{eff} will be as low as the DC value R_{dc}. For a deep-bar rotor, its effective resistance at starting may be several times greater than at the rated speed as shown in Fig. 3.34.

As explained above, for induction motors with a deep-bar rotor, the rotor resistance varies according to the speed so that a satisfactory performance can be achieved both at the start and normal operations.

A double-cage rotor is another type of rotor whose effective resistance varies as shown in Fig. 3.35 [4]. It consists of two cages to exaggerate its variation more than the deep-bar. The upper cage has smaller cross-sectional areas than the lower cage. In addition, the upper cage is made up of a higher resistance material than the lower cage. Similar to a deep-bar rotor, the rotor bars in the lower cage have a greater leakage flux and thus, higher leakage inductance. At starting, since the rotor frequency is high, the division of the rotor current is mainly decided by the leakage reactance difference between the two cages. Most of the currents will flow in the upper cage that has a lower reactance, but a high resistance.

On the other hand, at a normal operating speed, since the rotor frequency is low, the division of the rotor current is mainly dependent on the resistance of the two cages. Most of the current will flow in the lower cage which has a lower resistance. Therefore, in a double-cage rotor, at the start-up, the current flows mainly in the upper cage which has a higher resistance, while at a normal operating speed, it flows in the lower cage which has a lower resistance.

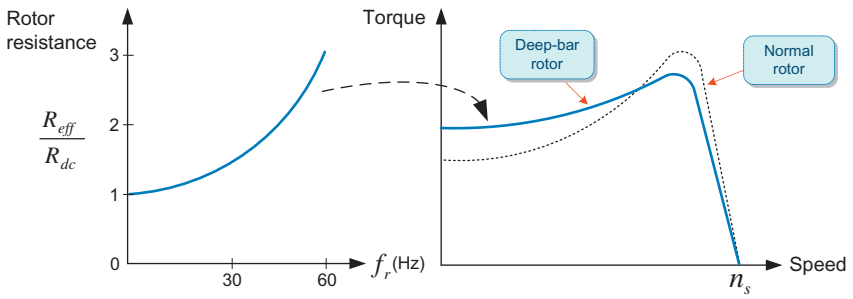


FIGURE 3.34

Effective resistance and output torque in the deep-bar rotor.

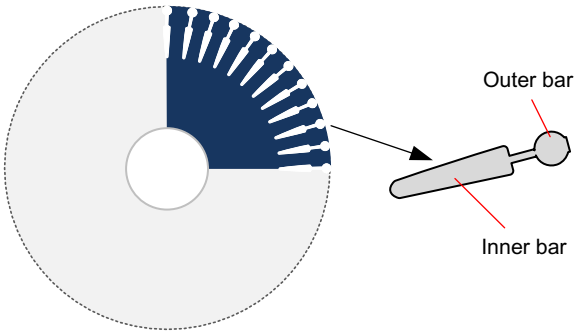


FIGURE 3.35

Double-cage rotor.

3.1.6.1 Design types of induction motors

As we discussed in Section 1.3, there are several types of loads. The required performance characteristics for a driving motor may be different according to the driven load. For example, the performance characteristics of motors for crane or hoist drives may be much different from those of motors for pump and blower drives.

Induction motors can be classified into different designs according to the starting and the normal operating characteristics. For classification of the motor, there are two most widely used standards: National Electrical Manufacture's Association (NEMA) and International Electrotechnical Commission (IEC). The NEMA standards mainly specify four design types: *Design A*, *B*, *C*, and *D*. Of these, the most widely used are Design B (normal torque) and Design C (high torque). Description on these four design types is summarized later.

Design A—It is characterized by normal starting torque (typically 150−170% of the rated), high starting current, low operating slip, and high-breakdown torque (the highest of all the NEMA types); common applications include fans, blowers, and pumps.

Design B—It is characterized by normal starting torque, low starting current, and low operating slip; common applications being the same as Design A. Design B is the most commonly used type for general-purpose applications.

Design C—It is characterized by high starting torque, low starting current, and higher operating slip than Designs A and B; common applications include compressors and conveyors.

Design D—It is characterized by high starting torque (higher than all the NEMA motor types), high starting current, high operating slip (5−13%), and inefficient operation efficiency for continuous loads; it is commonly used for intermittent loads such as a punch press.

Fig. 3.36 shows the speed−torque curve for the four NEMA designs [4].

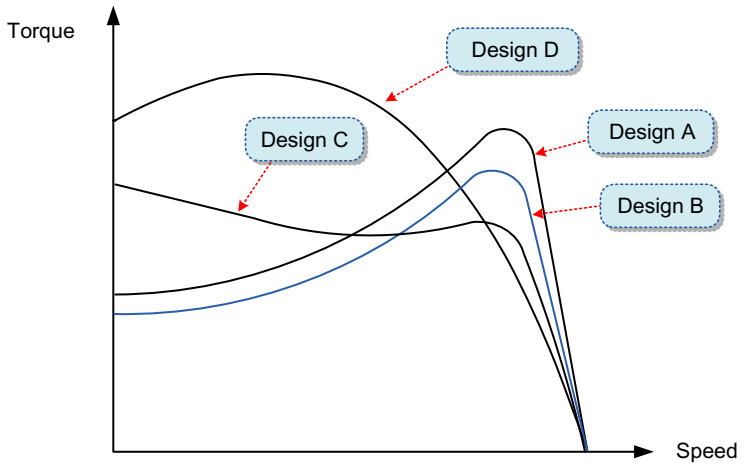


FIGURE 3.36

Torque characteristic according to design types of induction motors.

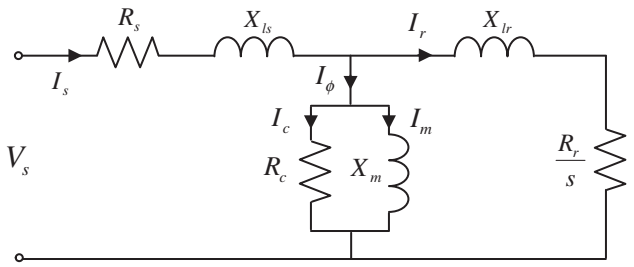


FIGURE 3.37

Equivalent circuit parameters for an induction motor.

3.1.7 DETERMINING EQUIVALENT CIRCUIT PARAMETERS

To analyze the operating and performance characteristics from the equivalent circuit of an induction motor as shown in Fig. 3.37, the parameters for the given induction motor should be determined. In addition, an accurate knowledge of motor parameters is essential for high-performance control of induction motors, which will be discussed in Chapter 5. Now, we will introduce specific tests on the induction motor to determine its equivalent circuit parameters.

3.1.7.1 Measurement of stator resistance R_s

The resistance R between any two terminals of three-phase windings, which may be connected in a delta or in a wye, can be directly measured. We can obtain the

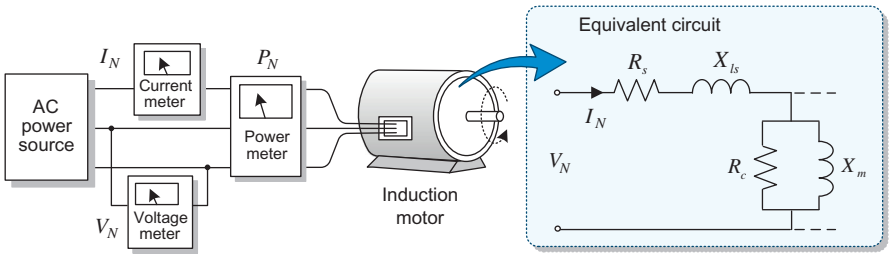


FIGURE 3.38

No-load test.

stator resistance as $R_s = R/2$ for a wye connection or as $R_s = 1.5R$ for a delta connection. This test must be performed with a precise instrument for large-sized motors because their resistance is very small. The stator resistance can be also obtained from the measured current after applying a DC voltage between the two windings.

3.1.7.2 No-load test

This test can determine the stator circuit parameter $L_{ls} + L_m$ and the parameter R_c. Here, R_c represents both the core loss and rotational loss. This test corresponds to the open-circuit test on a transformer. In this test, the rated voltage is applied to the stator terminals without any mechanical load. Then, the voltage V_N, current I_N, and input power P_N are measured at the motor input. The slip of an induction motor at no-load is almost zero, and thus $R_r/s \approx \infty$ and $I_r \approx 0$. Therefore the rotor branch of the equivalent circuit can be neglected as shown in Fig. 3.38.

At no-load test, the input power measured is equal to the losses, which consist of the stator copper loss, the core loss, and the rotational loss of friction and windage losses. The rotor copper loss can be negligible because the rotor current is extremely small. Here, the sum of the core loss and the rotational loss, which is normally almost constant at all operating conditions, is regarded as R_c. With the value of the premeasured stator resistance R_s, the value of R_c may be found by

$$P_N = 3I_N^2(R_s + R_c) \;\rightarrow\; R_c = \frac{\left(\frac{P_N}{3}\right)}{I_N^2} - R_s \tag{3.49}$$

From the measurement data P_N, V_N, and I_N, the equivalent impedance and resistance are

$$Z_N = \frac{\left(\frac{V_N}{\sqrt{3}}\right)}{I_N}, \quad R_N = \frac{P_N}{3I_N^2} \tag{3.50}$$

and the equivalent reactance is

$$X_N = \sqrt{Z_N^2 - R_N^2} = X_{ls} + X_m \tag{3.51}$$

The values of X_{ls} and X_m will be separately determined by the following blocked rotor test data.

3.1.7.3 Blocked rotor test

This test determines the rotor resistance R_r and the sum of the leakage inductances $L_{ls} + L_{lr}$, corresponding to the short-circuit test on a transformer. In this test, the rotor is locked so that it cannot rotate, and the current is maintained at the rated value by adjusting the applied voltage. Afterward, the resulting voltage V_B, current I_B, and power P_B are measured at the motor input. Since the rotor is not rotating, the slip $s = 1$, resulting in $X_m \gg R_r + jX_{lr}$. Thus the magnetizing X_m branch of the equivalent circuit can be neglected. The equivalent circuit for the block rotor test is reduced to the circuit as shown in Fig. 3.39.

In this case, the input power measured is equal to the sum of the stator and the rotor copper losses. Thus the rotor resistance is determined by

$$P_B = 3I_B^2(R_r + R_s) \;\rightarrow\; R_r = \frac{\left(\frac{P_B}{3}\right)}{I_B^2} - R_s \tag{3.52}$$

From the measurement data V_B and I_B, the equivalent impedance is

$$Z_B = \frac{\left(\frac{V_B}{\sqrt{3}}\right)}{I_B} \tag{3.53}$$

and the reactance X_B, which is the sum $X_{ls} + X_{lr}$ of the stator and rotor leakage reactances, is given by

$$X_B = \sqrt{Z_B^2 - (R_s + R_r)^2} = X_{ls} + X_{lr} \tag{3.54}$$

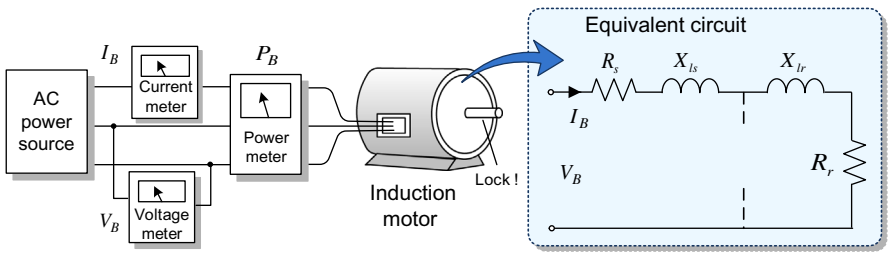


FIGURE 3.39

Blocked rotor test.

As for the proportion of the stator and rotor leakage reactances, empirically, $X_{ls} = X_{lr} = 0.5X_B$ for Design A and D types, $X_{ls} = 0.4X_B$, $X_{lr} = 0.6X_B$ for Design B type, and $X_{ls} = 0.3X_B$, $X_{lr} = 0.7X_B$ for Design C type [4].

Given the value of X_{ls}, the magnetizing reactance can be separated from Eq. (3.51) as

$$X_m = X_N - X_{ls} \tag{3.55}$$

In this test, since the rotor is locked, the rotor frequency is equal to the source frequency of 50 or 60 Hz. However, at normal operating conditions, the rotor frequency is in the range of 1−3 Hz. Since the resistance depends on the operating frequency, an incorrect rotor frequency can lead to misleading results in this test. A typical compromise is to use a frequency 25% or less of the rated frequency [2].

3.1.8 SPEED CONTROL OF INDUCTION MOTORS

Traditionally, induction motors have been used as nearly constant speed motors, which are operated by their direct connection to the power grid. However, because of their low cost and ruggedness, the induction motors are also being used for variable speed drives in many applications.

The operating speed of an induction motor depends on the slip or the synchronous speed of the given load. Therefore the speed control of an induction motor can be classified into two methods as follows:

- Slip control: inefficient, restricted speed control range
- Synchronous speed control: efficient, wide speed control range

3.1.8.1 Slip control

At a constant stator frequency, the speed of an induction motor can be varied according to the slip. The slip can be changed by varying the stator voltage or the rotor resistance.

First, let us take a look at the speed control by changing the stator voltage. As can be seen from Eq. (3.34), the torque developed by an induction motor is proportional to the square of the stator voltage as

$$T_{mech} = \frac{1}{\omega_s} \frac{V_s^2}{\left(R_s + \frac{R_r}{s}\right)^2 + j\left(X_{ls} + X_{lr}\right)^2} \frac{R_r}{s} \propto V_s^2 \tag{3.56}$$

Fig. 3.40 shows the variation of a speed−torque curve with respect to the stator voltage. We can see that the speed control by varying the stator voltage is available only for a limited range. The controllable speed range depends on the value of the slip (i.e., the maximum slip) at which the maximum torque occurs. By comparing Fig. 3.40A with B, we can see that the Design C or D motors have a wider speed control range than the Design A or B motors.

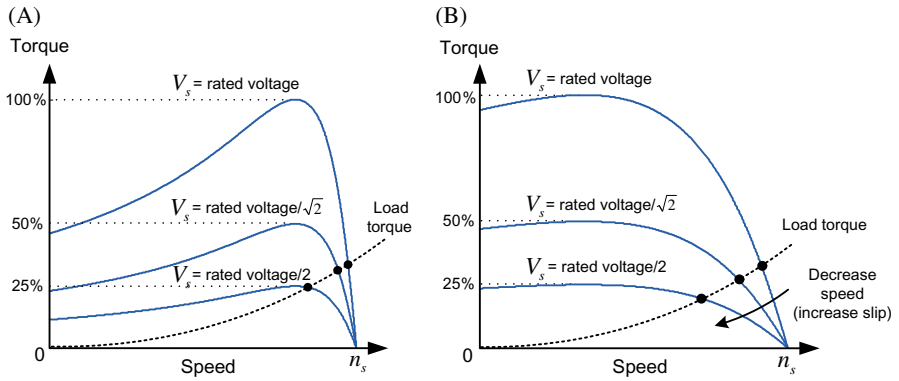


FIGURE 3.40

Torque characteristics according to the stator voltage variation. (A) Design A or B motor and (B) Design C or D motor.

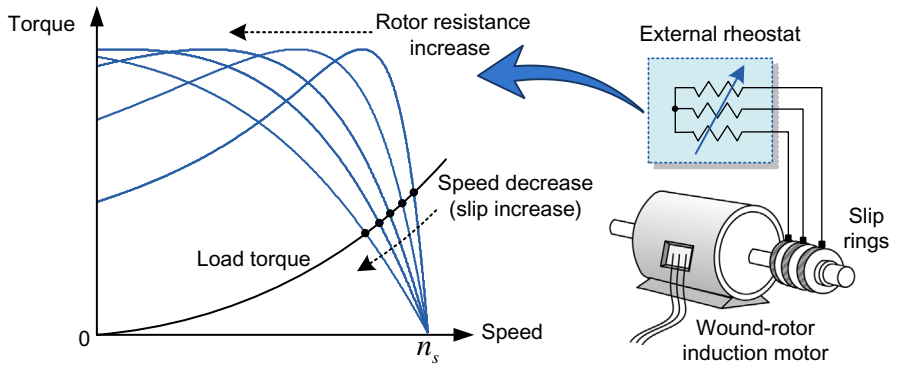


FIGURE 3.41

Speed control by changing the rotor resistance.

Next, let us examine the speed control by changing the rotor resistance. From the Section 3.1.4.3, we can see that the slip at which the maximum torque occurs is proportional to the rotor resistance R_r as

$$s_{max} = \frac{R_r}{\sqrt{R_s^2 + (X_{ls} + X_{lr})^2}} \propto R_r \tag{3.57}$$

Thus, changing the rotor resistance will alter the shape of the speed−torque curve and in turn, adjust the operating speed of the motor. Fig. 3.41 shows the speed−torque curves for different rotor resistances.

To adopt the speed control by changing the rotor resistance, we need to use the wound-rotor type induction motors. The rotor resistance in the wound-rotor type induction motors can be varied by adding an external rheostat or a resistor bank to the rotor windings via the slip rings. Changing the value of the rheostat will change the operating speed of the motor. Similar to the applied voltage

varying method, the rotor resistance varying method also gives a limited controllable speed range. Moreover, inserting extra resistances into the rotor circuit seriously reduces the efficiency of the drive.

In the speed control methods of varying the stator voltage or the rotor resistance, the speed is considered to be changed by varying the slip at a constant stator frequency. As we can see from Eq. (3.46), since the efficiency of induction motors depends on the operating slip, the speed reduction by these methods will lead to a reduction in efficiency. Nevertheless, these speed control methods are applicable to small-sized motors that drive loads requiring a torque proportional to the square of the operating speed such as fans or blowers. For such loads, since the power consumption is reduced significantly according to the reduction in the speed, the reduction in efficiency is relatively small.

Instead of wasting energy in the rotor resistance (referred to as the *slip energy*), there is a better approach to improve the efficiency, which is known as a *slip energy recovery system*. In the slip energy recovery system, the slip energy can be returned back to the electric power source. There are two types of the slip energy recovery system: *Kramer* drive system and *Scherbius drive systems*. These systems exploit a power electronic converter connected to the rotor circuit instead of external resistors. Such a system can recover the energy taken from the rotor through the slip rings to decrease the speed and feed it back into the power source.

3.1.8.2 Synchronous speed control

The rotor of an induction motor follows the stator magnetic field which rotates at the synchronous speed proportional to the applied stator frequency. Thus, changing the stator frequency is more fundamental to the speed control. The relationship between the synchronous speed n_s and the stator frequency f_s is

$$n_s = \frac{120 \cdot f_s}{P} \tag{3.58}$$

Though the synchronous speed can be altered by changing the number of poles, this requires a complex motor construction. Moreover, it is not possible to provide a continuous change in the synchronous speed. Thus, it is more effective to change the stator frequency. The speed−torque characteristics for a variation in the stator frequency at the rated stator voltage are shown in Fig. 3.42.

When changing the stator frequency to adjust the speed, if the stator voltage remains constant, then the stator frequency variations lead to the change of the developed torque as well as the operating speed as shown in Fig. 3.42. The explanation is as follows.

At normal operating conditions, since the voltage drop across the stator resistance and leakage reactance are negligible in comparison to the applied voltage, the torque of Eq. (3.34) can be simplified as

$$T_{mech} \cong \frac{V_s^2}{\left(\frac{R_r}{s}\right)^2 + (\omega_s L_{lr})^2} \cdot \frac{R_r}{\omega_s s} = \left(\frac{V_s}{\omega_s}\right)^2 \frac{R_r \omega_{sl}}{R_r^2 + (\omega_{sl} L_{lr})^2} \tag{3.59}$$

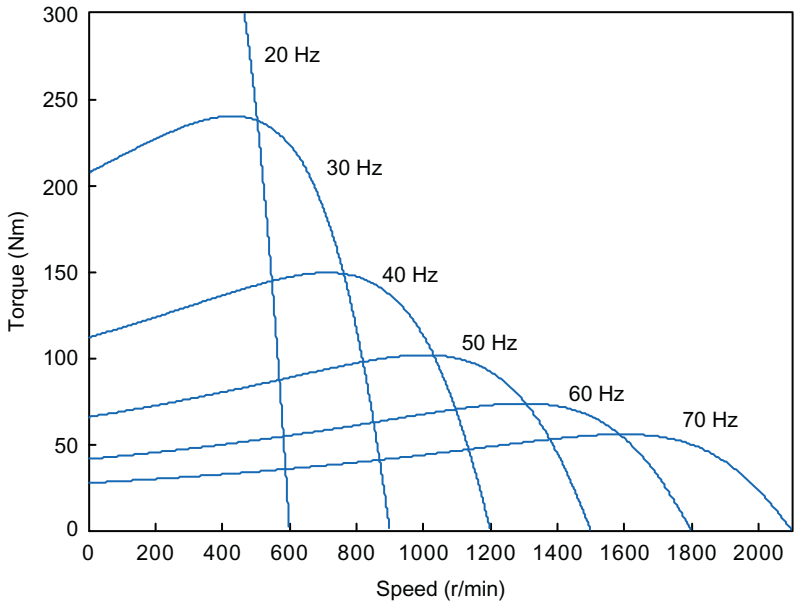


FIGURE 3.42

Speed–torque characteristic curves for several frequencies (5-hp, four-pole motor).

It can be seen that at a fixed stator voltage and slip frequency, the developed torque is inversely proportional to the square of the stator frequency. From Eq. (3.17), we can see that the air-gap flux depends on the ratio of the stator voltage V_s to the stator frequency f_s as

$$\phi \propto \frac{E_s}{f_s} \approx \frac{V_s}{f_s} \quad (\leftarrow E_s = 4.44 f_s N_s \phi K_{\omega s}) \tag{3.60}$$

Thus, under a fixed stator voltage, the air-gap flux varies inversely with the stator frequency. As can be seen from Eq. (3.59), the developed torque is proportional to the square of the air-gap flux and thus, is inversely proportional to the square of the stator frequency.

The rotor current is also influenced by the variation of the stator frequency. Assuming that at normal operating conditions, the stator resistance and leakage reactance are negligible, the rotor current varies inversely with the stator frequency as

$$I_r = \frac{V_s}{\sqrt{\left(\frac{R_r}{s}\right)^2 + (X_{lr})^2}} = \left(\frac{V_s}{\omega_s}\right) \frac{\omega_{sl}}{\sqrt{R_r^2 + (\omega_{sl} L_{lr})^2}} \propto \frac{1}{f_s} \tag{3.61}$$

When adjusting the operating speed by changing the stator frequency, if the stator voltage is varied linearly with the frequency as shown in Fig. 3.43, then the air-gap flux $\phi \approx V_s/f_s$ will remain constant and thus, the torque and rotor current will remain unchanged. This technique is called the *constant volts*

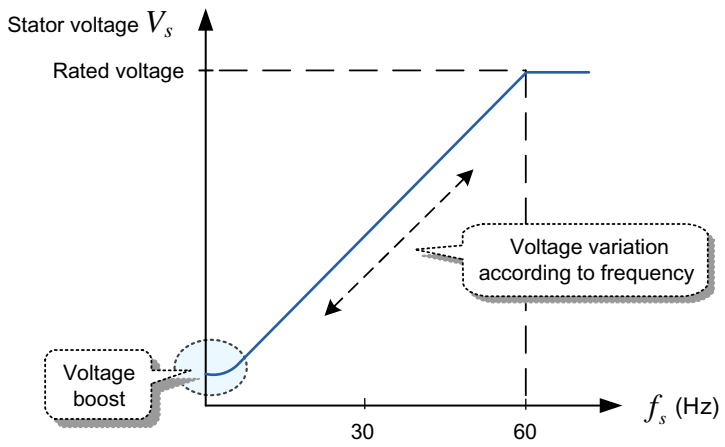


FIGURE 3.43

Constant volts per Hertz (*V/f*) control.

per Hertz (*V/f*) *control*, which has become a popular variable speed drive for induction motors in general-purpose applications today. The *V/f* ratio may be adjusted according to the driven load.

At low frequencies below a few Hertz, due to the influence from the voltage drop across the stator resistance and leakage reactance, the magnitude of the stator voltage determined by this linear *V/f* relationship will be insufficient to keep the magnitude of the air-gap flux constant. This is because the actual air-gap flux ϕ is not proportional to V_s/f_s, but E_s/f_s. This results in reduction of the air-gap flux and in turn, reduction of the output torque. Thus, for the constant *V/f* control at a low operating frequency, we have to boost the stator voltage to compensate for the voltage drop of the stator resistance and leakage reactance as shown in Fig. 3.43.

Fig. 3.44 shows the speed−torque characteristics curves for several frequencies under the constant *V/f* control. To summarize, under the constant *V/f* operation of an induction motor,

- Torque is independent of the stator frequency,
- Rotor current is independent of the stator frequency,
- Synchronous speed is proportional to the stator frequency.

The constant *V/f* control can be utilized for the speed control below the rated speed. If the stator frequency increases more than the rated frequency, the constant *V/f* ratio cannot be maintained due to the limitation of the applied voltage. Thus, for speeds higher than the rated speed, the maximum torque will be reduced due to the reduction in the air-gap flux. The control method for high speeds above the rated speed will be discussed in more detail in Chapter 8.

In the induction motor drives with the constant *V/f* control, it should be noted that the torque and the rotor current are determined only by the slip angular

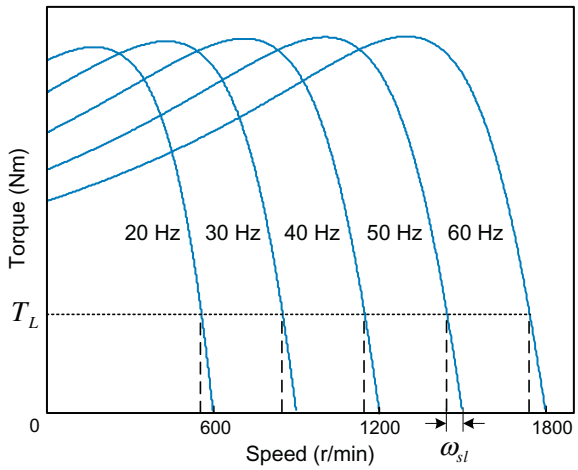


FIGURE 3.44

Speed–torque curves with constant volts per Hertz control (5-hp, four poles).

frequency $\omega_{sl}(=s\omega_s)$. We can see from Fig. 3.44 that the output torque can be produced equally at any speed for the same slip frequency. Thus, even though the speed is reduced by the stator frequency, the operating slip can be kept low so that the efficiency cannot be degraded unlike the slip control. Moreover, at start-up, a high starting torque can be achieved by applying a low stator frequency without requiring a high rotor resistance. After the starting, the stator frequency is increased along with the stator voltage according to the linear *V/f* relationship.

Up to this point, we have discussed the open-loop speed control by the stator frequency. In the open-loop speed control, however, the steady-state speed can be affected by the load variation because the operating slip frequency depends on the load. In particular, in the low-speed region, the variation of the operating slip frequency may bring about a large error in the steady-state speed. Thus this open-loop speed control needs a proper compensation to offset the speed error according to the load variation. More accurate speed control can be achieved by the closed-loop speed control, which adjusts the slip frequency under the constant *V/f* control as the following.

3.1.8.3 Closed-loop speed control by adjusting the slip frequency under constant V/f control

Under the constant *V/f* control, the torque of an induction motor can be controlled by adjusting the slip frequency f_r. The torque of Eq. (3.59) is rewritten in terms of the slip frequency f_r as

$$T_{mech} = \left(\frac{V_s}{\omega_s}\right)^2 \frac{2\pi f_r R_r}{R_r^2 + (2\pi f_r L_{lr})^2} \tag{3.62}$$

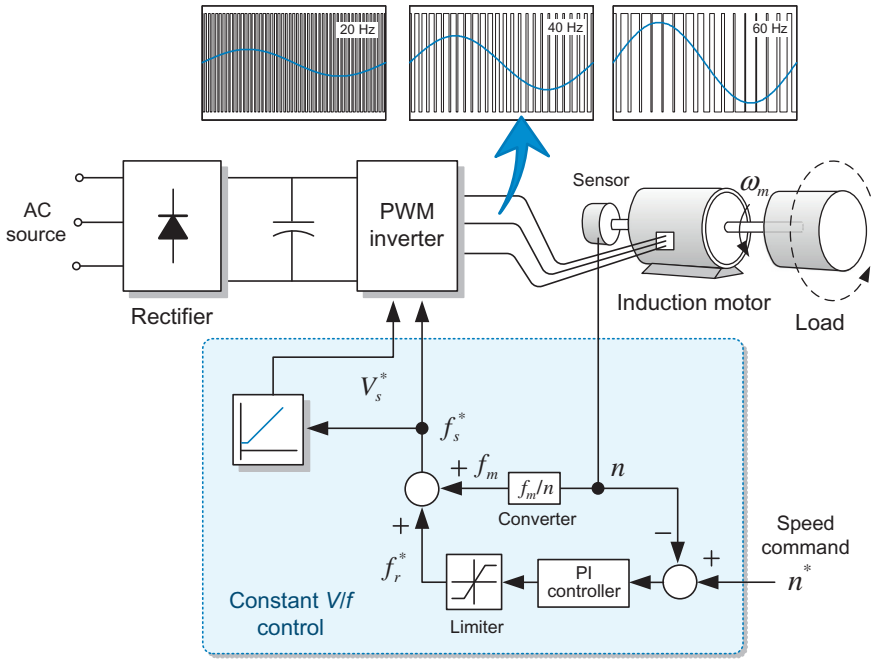


FIGURE 3.45

Speed control by adjusting the slip frequency with constant *V/f* control.

Since the standard induction motors normally have $R_r \gg 2\pi f_r L_{lr}$, if the air-gap flux is constant, then the torque is proportional to the slip frequency f_r as

$$T_{mech} \cong \left(\frac{V_s}{\omega_s}\right)^2 \frac{2\pi}{R_r} f_r \tag{3.63}$$

Fig. 3.45 shows the block diagram of the closed-loop speed control system based on Eq. (3.63).

In this speed control system, with the constant *V/f* operation, the slip frequency f_r is adjusted so that the actual speed n follows the command speed n^*. Since the developed torque of an induction motor can be adjusted by the slip frequency, if the actual speed of the motor is less than its command, then the controller increases the slip frequency to produce a larger torque. On the other hand, if the actual speed is higher than its command, then the controller decreases the slip frequency to reduce the developed torque. In this case, the variation range of the slip frequency should be limited within the maximum slip frequency, at which the breakdown torque occurs.

Once the required slip frequency f_r^* is determined in this manner, the stator frequency command can be determined by the sum of the slip frequency and the rotor speed f_m as

$$f_s^* = f_m \pm f_r^* \tag{3.64}$$

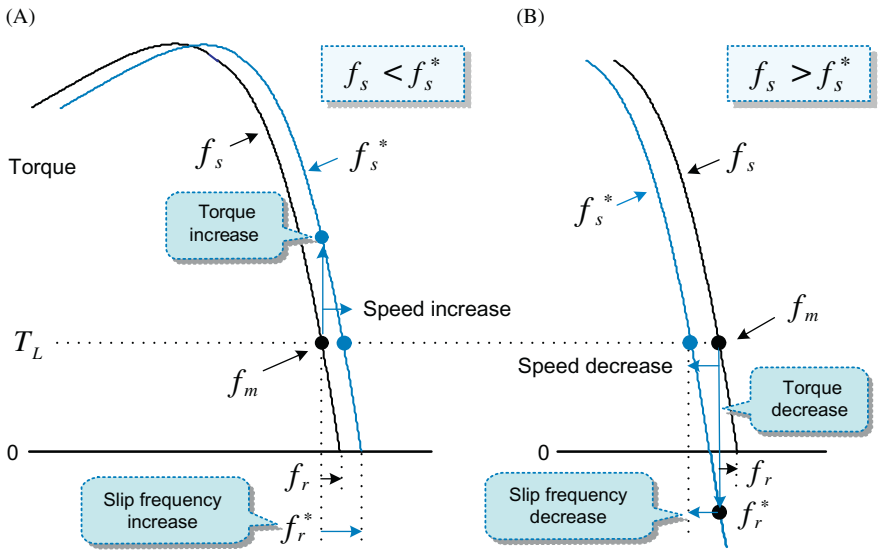


FIGURE 3.46

Operations in the closed-loop speed control system. (A) Speed increase and (B) speed decrease.

From this stator frequency command f_s^*, the voltage command applied to the motor should be determined according to the linear *V/f* relationship shown in Fig. 3.43. This voltage reference V_s^* with the stator frequency will generally be generated by using the PWM inverter, which will be described in Chapter 7. The inverter used for this purpose is called the *Variable Voltage Variable Frequency (VVVF) inverter*.

Fig. 3.46 describes the closed-loop speed control that was shown in Fig. 3.45. Fig. 3.46A shows the operation for the increase in speed. If the stator frequency is increased by the increased slip frequency, then the developed torque becomes greater than the load torque, and thus the speed is increased. On the other hand, Fig. 3.46B shows the operation for the decrease in speed. If the stator frequency is decreased by the decreased slip frequency, then the developed torque becomes smaller than the load torque, and thus the speed is reduced.

This speed control scheme for induction motors is widely used in general-purpose drives such as fans, pumps, and conveyors because it can improve the system efficiency and provide a satisfactory starting torque and a satisfactory steady-state performance. This control can give a speed regulation of 1−2%. However, this control scheme is insufficient to achieve a high dynamic performance. Therefore, we need an advanced control technique such as the *Vector control*, which will be described in Chapter 5.

3.1.9 OPERATION REGIONS OF INDUCTION MOTORS

Induction motors have been traditionally used as constant speed motors supplied by the AC power source. However, recently, it has been increasingly used as variable speed motors driven by an inverter. As stated in the Section 3.1.8.2, the variable speed induction motor drive can be achieved by controlling the frequency and voltage applied to the motor. The operation range of an induction motor can be divided into three regions according to the output torque capability as

- Constant torque region: speed range below the base speed
- Constant power region: speed range above the base speed
- Breakdown torque region: speed range above the base speed maintaining the maximum slip frequency

The speed range above the base speed can be further divided into two subregions: *constant power region* and *breakdown torque region*. Because the field flux is reduced for operation in these regions, they are called *field-weakening regions*. Fig. 3.47 illustrates the output toque characteristic in each region.

3.1.9.1 Constant torque region

In this region, the motor speed is increased by increasing the stator frequency. To maintain the air-gap flux at a constant value, the applied stator voltage will be increased with the stator frequency according to the linear *V/f* relationship. This is the constant *V/f* control as stated in the Section 3.1.8.2. In this control method, since the output torque is proportional to the slip frequency, the output torque can be produced equally at any speed for the same slip frequency as shown in Fig. 3.48. (The same slip frequency means the same stator current.) Hence, this speed range is called *constant torque region*. The maximum torque developed by the induction motor is limited only by the allowable current rating in this region.

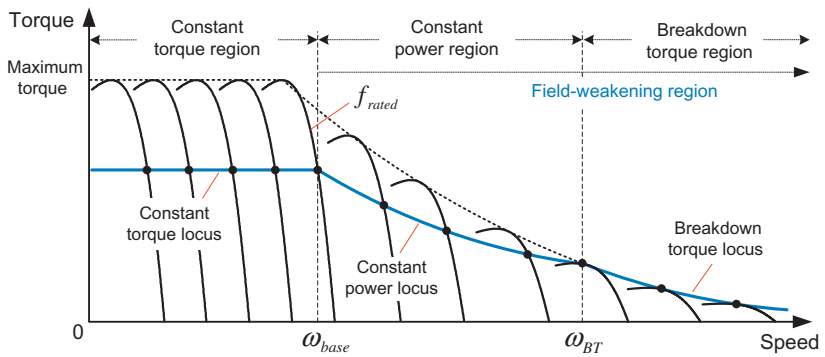


FIGURE 3.47

Operation regions of an induction motor.

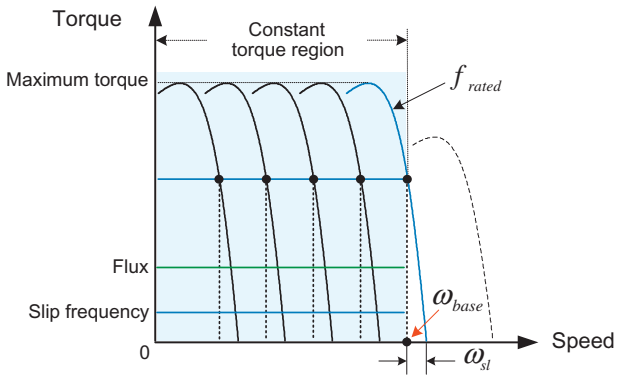


FIGURE 3.48

Operation characteristics in constant torque region.

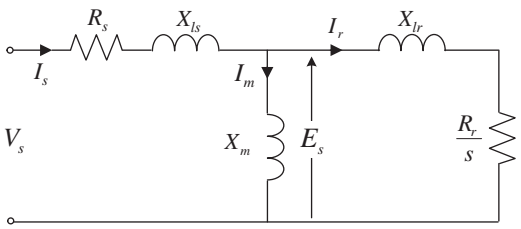


FIGURE 3.49

Steady-state equivalent circuit of an induction motor.

3.1.9.2 Constant power region

Since the back-electromotive force (back-EMF) of the induction motor increases with the speed, the voltage applied to the motor should also be increased with the speed for the stator current to flow properly. However, since the terminal voltage of the motor should not exceed the rated (or nominal) voltage, the stator voltage cannot be increased above the rated voltage despite the speed increase. The onset speed, at which the terminal voltage of the motor becomes the rated voltage, is called the *base speed*. Since the induction motor will be operated with a constant voltage in the speed region above the base speed, the air-gap flux as well as the rotor current will decrease as the operating speed increases.

The steady-state equivalent circuit in Fig. 3.49 implies that under a constant stator voltage V_s, an increase in the operating frequency causes the reactance to increase, resulting in a decrease of both the exciting current I_ϕ and rotor current I_r. Therefore the output torque of an induction motor in this region will be different from that in the constant torque region.

In the Section 3.1.4.3, the output torque and the rotor current of an induction motor were given as

$$T_e = 3\frac{1}{\omega_s} I_r^2 \frac{R_r}{s} \tag{3.65}$$

$$I_r = \frac{E_s}{\left(\frac{R_r}{s}\right) + jX_{lr}} = \left(\frac{E_s}{\omega_s}\right) \frac{\omega_{sl}}{\sqrt{R_r^2 + (\omega_{sl} L_{lr})^2}} \tag{3.66}$$

Substituting Eq. (3.66) into Eq. (3.65), the following torque expression as a function of air-gap flux and rotor current can be obtained.

$$T_e = 3\left(\frac{E_s}{\omega_s}\right) I_r \frac{R_r}{\sqrt{R_r^2 + (\omega_{sl} L_{lr})^2}} \cong K\phi I_r \quad \left(\phi = \frac{E_s}{\omega_s}\right) \tag{3.67}$$

Under a constant stator voltage, an increase in the stator frequency leads to a reduction in both the air-gap flux $\phi(\propto E_s/\omega_s)$ and the rotor current I_r. Therefore the output torque will decrease in proportion to $1/\omega_s^2$. However, if we make the slip frequency ω_{sl} increase as the stator frequency increases, then the rotor current will remain constant due to the reduced impedance R_r/s by the increase in the slip. This can be readily seen in Eq. (3.66) and Fig. 3.49. In this way, if the rotor current remains constant despite the stator frequency increase, then the developed torque decreases in proportion to $1/\omega_s$, not $1/\omega_s^2$, as shown in Fig. 3.50. Thus an enhanced output torque capability can be achieved.

Therefore for operation in this region, the slip frequency ω_{sl} should be increased as the stator frequency increases. In this case, since both the voltage and the current remain constant, this region is called the *constant power region* (strictly speaking, *constant VA*), which corresponds to the field-weakening region of a DC motor.

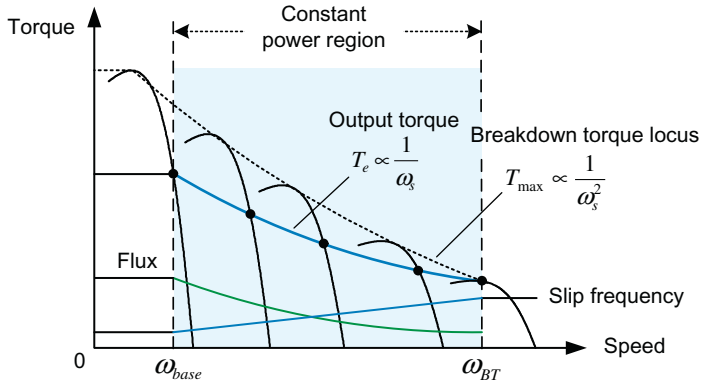


FIGURE 3.50

Operation of constant power regions.

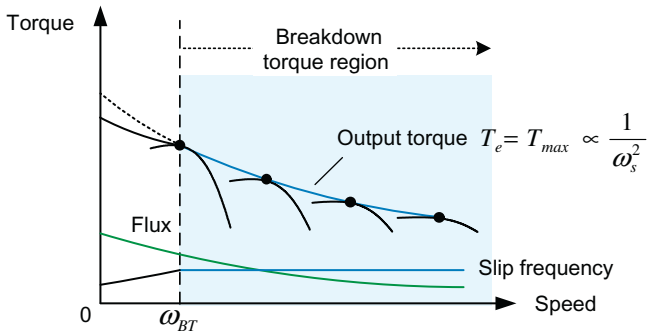


FIGURE 3.51

Operation of breakdown torque regions.

3.1.9.3 Breakdown torque region

In the constant power region, the slip frequency is increased with the speed increase to lower the reduction rate of the output torque. However, there is a limit to increasing the slip frequency because an induction motor has a maximum slip for the stable operation as

$$S_{max} = \frac{R_r}{\sqrt{R_s^2 + (X_{ls} + X_{lr})^2}} \tag{3.68}$$

Once the operating slip frequency reaches its maximum value, the rotor current will decrease and, in turn, the output torque will decrease in proportion to $1/\omega_s^2$ as the stator frequency increases as shown in Fig. 3.51. Since the current will be decreased, the input power will not remain constant. In this case, an induction motor will be operated at the maximum slip for producing the breakdown torque. Thus this region is called the *breakdown torque region*.

Fig. 3.52 depicts characteristics such as voltage, current, developed output torque, flux, and slip frequency over the overall speed range. The curve, which shows the output torque capability versus the speed, is called the *capability curve* of an induction motor.

The base speed, at which the constant power region starts, does not usually coincide with the rated speed and varies with the available voltage, operating current, flux level, and load condition. A detailed explanation on this will be given in Chapter 8. The range of the constant power region depends on the maximum value of the slip frequency. As can be seen from Eq. (3.68), this maximum slip frequency is a function of leakage inductance, and thus, its range depends on the total leakage inductance, $X_{ls} + X_{lr}$. For a standard induction motor, this value is normally 0.2 p.u., producing a constant power range up to two to three times the rated speed. By contrast, induction motors for high-speed drives often have a constant power region range over four times the rated speed.

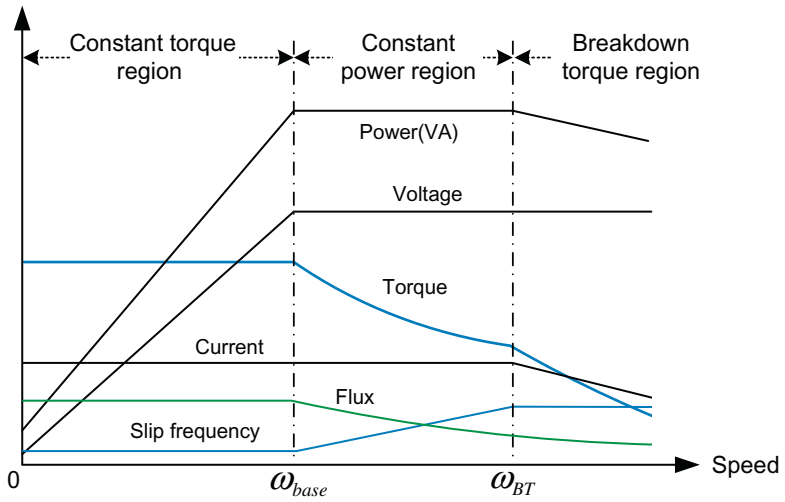


FIGURE 3.52

Capability curve of an induction motor.

3.2 SYNCHRONOUS MOTORS

As stated in Chapter 1, the name *synchronous motors* stems from its characteristic to develop the torque only when the rotor operates at the synchronous speed. Traditionally, large-sized synchronous machines have been mainly used as generators. As motors, they have been used to improve the power factor in the power grid by changing the field current, i.e., excitation. In this case, they are called synchronous condensers. In small sizes, they have been often used in applications requiring a constant speed operation.

However, recently, synchronous motors with a permanent magnet rotor are growing rapidly in use for variable speed drives instead of DC motors. This is because permanent magnet synchronous motors (PMSMs) have many advantages over other motors such as high efficiency, high power density, high dynamic response, and high power factor. However, one disadvantage is its higher cost in comparison to an induction motor. In this section, we will study the basic performance characteristics of the synchronous motor under steady-state conditions, and in Chapter 4 and Chapter 5, we will learn about its dynamic characteristics.

The structure of the stator and rotor of a synchronous motor is shown Fig. 3.53. A synchronous motor has the same stator configuration as an induction motor, but a different rotor structure. Unlike an induction motor, a synchronous motor has independent excitations for the stator and rotor windings,

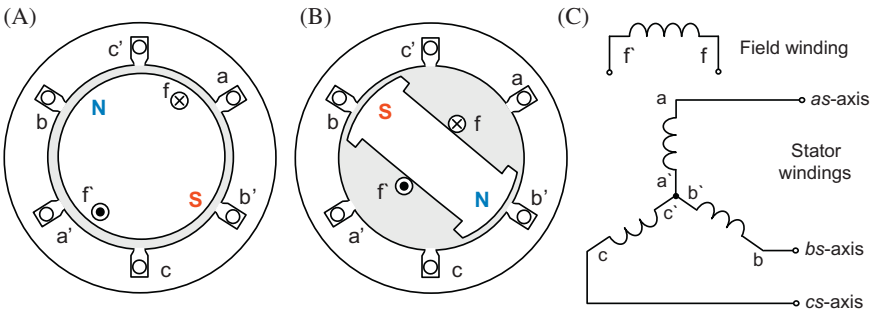


FIGURE 3.53

Stator and rotor structure of a synchronous motor. (A) Cylindrical type, (B) salient pole type, and (C) stator windings.

i.e., AC excitation to the stator winding and DC excitation to the rotor winding. The function of the stator winding, which is commonly called an *armature winding*, is to generate a rotating magnet field through its connection to a three-phase AC power source such as an induction motor. The rotor winding, which is called the *field winding*, generates a field flux with a DC excitation or by a permanent magnet.

There are two types of rotor construction: *cylindrical* (or *nonsalient pole*) *type* and *salient pole type*. A salient pole rotor is normally used for low-speed applications such as hydroelectric generators, while a cylindrical rotor is normally used in high-speed applications such as steam or gas turbine generators. Now, we will explore the steady-state equivalent circuit and the output torque of a synchronous motor.

3.2.1 CYLINDRICAL ROTOR SYNCHRONOUS MOTORS

Since the rotor winding with a DC excitation can be represented as a simple R-L circuit without back-EMF, we need to discuss an equivalent circuit for only the stator winding.

The stator windings of a synchronous motor are the same as those of an induction motor. Thus, from Eq. (3.6), the stator voltage equation of a synchronous motor is given as

$$v_s = R_s i_s + \frac{d\lambda_s}{dt} \tag{3.69}$$

However, since the stator flux linkage of a synchronous motor is different from those of an induction motor, we need to examine the stator flux linkage λ_s.

A synchronous motor has independent excitations for the stator and rotor windings. In the air gap, these excitations generate two magnetic fields which

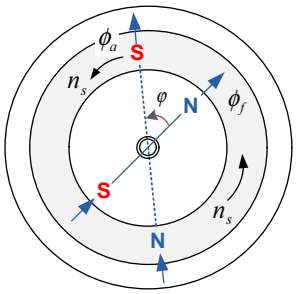


FIGURE 3.54

Rotating field flux of stator and the field flux of rotor.

rotate at the synchronous speed as shown in Fig. 3.54. One is generated by the stator winding currents as in an induction motor, and the other is generated by the field winding current. In synchronous motors, the torque is produced by the interaction of these two magnetic fields.

The rotating field flux ϕ_a generated by the three-phase AC currents I_s flowing in the stator winding consists of the armature reaction flux ϕ_{ar} and the leakage flux ϕ_{al} as

$$\phi_a = \phi_{ar} + \phi_{al} \tag{3.70}$$

The armature reaction flux ϕ_{ar} corresponds to the magnetizing flux in the induction motor. The field flux ϕ_f generated in the field winding is also a rotating magnetic field rotating at the synchronous speed because the rotor itself rotates at the synchronous speed. In the air gap, there is a resultant of these two field fluxes as

$$\phi_s = \phi_f + \phi_{ar} \tag{3.71}$$

Thus the flux linkage λ_s of the stator winding with an effective number of turns N_s will be expressed as

$$\lambda_s = N_s(\phi_f + \phi_{ar}) \tag{3.72}$$

In the stator winding, the voltage is induced by these two fluxes. The voltage E_f induced by the field flux ϕ_f is called the *excitation voltage* as shown in Fig. 3.55. The magnitude of the excitation voltage is proportional to the field current and the rotor speed.

The voltage E_{ar} induced by the armature reaction flux ϕ_{ar} is called the *armature reaction voltage*, whose equation is the same as the Eq. (3.18) of the induced voltage for an induction motor.

The total induced voltage in the stator winding is the sum of these two induced voltages as

$$E_s = E_f + E_{ar} \tag{3.73}$$

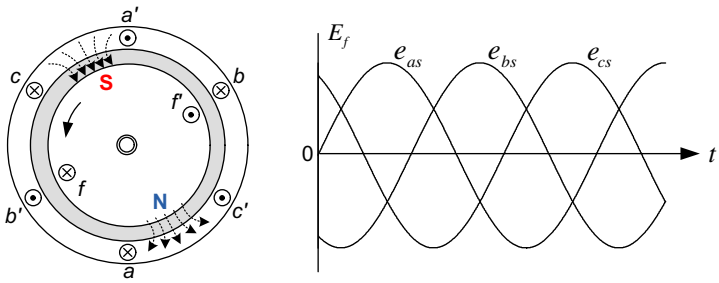


FIGURE 3.55

Excitation voltage induced by the field flux.

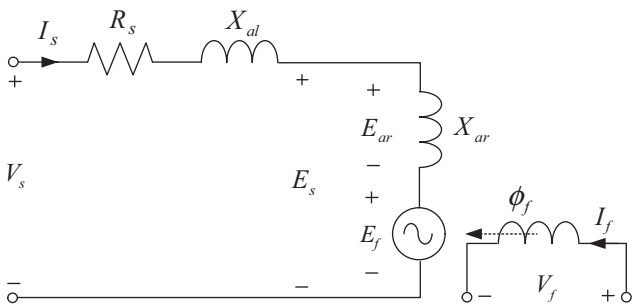


FIGURE 3.56

Per phase equivalent circuit of a cylindrical rotor synchronous motor.

Here, the armature reaction voltage E_{ar} lags the armature reaction flux ϕ_{ar} by 90°, so it can be expressed in terms of the armature reaction reactance X_{ar} as

$$E_{ar} = I_a j X_{ar} \tag{3.74}$$

Considering the total induced voltage, the voltage drop of the stator resistance R_s, and leakage reactance X_{al}, the stator voltage equation of Eq. (3.69) can be expressed as the phasor representation by

$$\begin{aligned} V_s &= I_s R_s + I_s j X_{al} + E_s \\ &= I_s R_s + I_s j X_{al} + I_s j X_{ar} + E_f \\ &= I_s R_s + I_s j X_s + E_f = I_s Z_s + E_f \end{aligned} \tag{3.75}$$

where, $X_s (= X_{ar} + X_{al})$ is the synchronous reactance and $Z_s (= R_s + jX_s)$ is the synchronous impedance.

By using Eq. (3.75), the complete per phase equivalent circuit of a cylindrical rotor synchronous motor under the steady-state condition is shown in Fig. 3.56.

3.2.1.1 Torque of a cylindrical rotor synchronous motor

The torque of a cylindrical rotor synchronous motor is obtained by dividing the output power by the synchronous speed ω_s. The input power of a synchronous motor is given by

$$P = 3V_s I_s \cos\theta \tag{3.76}$$

where θ is the phase angle between the stator voltage V_s and the stator current I_s.

Eq. (3.75) of a synchronous motor can be represented by the phasor diagram as shown in Fig. 3.57. The phase angle δ between the stator voltage V_s and the excitation voltage E_f is an important factor of power transfer and stability in synchronous machines and is usually termed the *power angle* (or *load angle*). For motoring operation, this angle δ is also called the *torque angle*, and the stator voltage V_s is ahead of the excitation voltage E_f. The angle δ acts as the slip in an induction motor. The angle δ increases with the increased load. This angle can also be regarded as the difference angle between the stator and the rotor rotating magnetic fields. In motoring operation, the stator magnetic field is ahead of the rotor magnetic field. The power and torque for synchronous machines are usually expressed as a function of the stator voltage, excitation voltage and their angle δ.

Now, we will derive the output torque from the equivalent circuit. From the phasor diagram shown in Fig. 3.57, we have

$$V_s\cos\delta = E_f + I_s X_s \sin(\theta-\delta) + I_s R_s \cos(\theta-\delta) \tag{3.77}$$

$$V_s\sin\delta = I_s X_s \cos(\theta-\delta) - I_s R_s \sin(\theta-\delta) \tag{3.78}$$

If the stator winding resistance R_s is neglected, then we can readily obtain

$$I_s\cos\theta = \frac{E_f \sin\delta}{X_s} \tag{3.79}$$

By substituting this into Eq. (3.76), the power is expressed by

$$P = 3\frac{V_s E_f}{X_s}\sin\delta = P_{max}\sin\delta \tag{3.80}$$

Since the stator losses are neglected by assuming $R_s = 0$, the power of Eq. (3.80) is considered as the output power. Thus the developed torque is obtained by dividing the output power by the synchronous speed ω_s as

$$\text{Torque:}\quad T = \frac{P}{\omega_s} = 3\frac{V_s E_f}{\omega_s X_s}\sin\delta = T_{max}\sin\delta \tag{3.81}$$

Eqs. (3.80) and (3.81) indicate that the output power and the torque vary as a sine of the torque angle δ as shown in Fig. 3.58. The maximum torque occurs at a torque angle of 90 electrical degrees. This is called the *pull-out torque*, which indicates the maximum value of torque that a synchronous motor can develop without pulling out of synchronism. In general, its value varies from 1.25 to 3.5 times the full-load torque. In actual practice, however, the motor will never

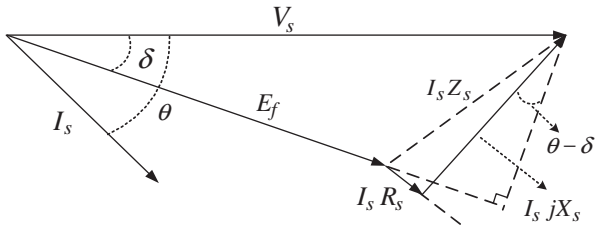


FIGURE 3.57

Phasor diagram for a synchronous motor.

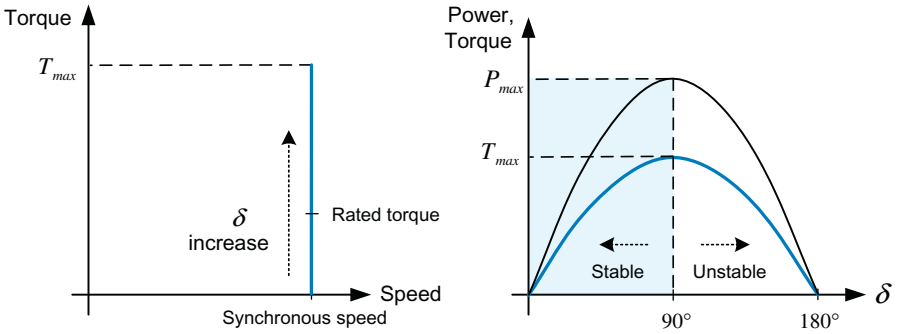


FIGURE 3.58

Output power and torque for a cylindrical rotor synchronous motor.

operate at a torque angle close to 90 electrical degrees because the stator current will be many times its rated value at this operation.

Next, we will discuss the salient pole rotor synchronous motor.

3.2.2 SALIENT POLE ROTOR SYNCHRONOUS MOTORS

As we can see in Fig. 3.59, a salient pole synchronous motor has a nonuniform air gap due to the protruding rotor poles. In this type of motor, the amount of the flux produced by the stator current varies according to the position of the rotor. A higher flux is generated along the poles in comparison to between the poles because the reluctance of the flux path is low along the poles and high between the poles.

To consider the saliency of the rotor in a synchronous motor model, we need to define the d and q axes as the following. The d-axis is defined as the axis along the poles, which is also the direction of the rotor flux produced by the field winding. The reluctance of the d-axis path is low due to the small air gap, and thus the inductance L_d of the d-axis is large. On the other hand, the q-axis is defined as the axis between the poles, which is also the direction of the excitation voltage. The reluctance of the q-axis path is large due to the large air gap, and so the inductance L_q of the q-axis is small. Thus, $L_d > L_q$.

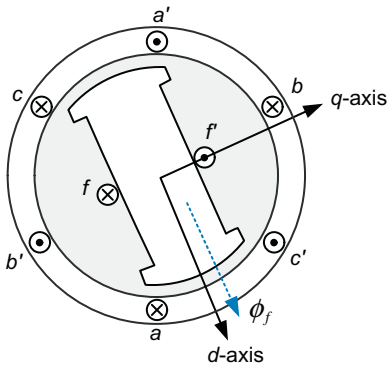


FIGURE 3.59

Salient pole rotor synchronous motor.

In order to consider the flux variation with the position of the rotor, it is more effective to analyze the saliency of the rotor by using the divided stator current into two components of the current I_d aligned with the d-axis and the current I_q aligned with the q-axis. Thus the stator current I_s is expressed as

$$I_s = I_q - jI_d \tag{3.82}$$

where $I_q = I_s\cos\varphi$, $I_d = I_s\sin\varphi$, and φ is the phase angle between I_q and I_a.

According to the d and q axes currents, the armature reaction flux ϕ_{ar} is also divided into two components: the d-axis flux ϕ_d produced by the d-axis current I_d and the q-axis flux ϕ_q by the q-axis current I_q. The relation between ϕ_d and I_d is expressed by the d-axis armature reactance X_{ad}, whereas the relation between ϕ_q and I_q is expressed by the q-axis armature reactance X_{aq}. The d and q axes synchronous reactances are given by

$$X_d = X_{ad} + X_{al} \tag{3.83}$$

$$X_q = X_{aq} + X_{al} \tag{3.84}$$

where X_{al} is the armature leakage reactance. The salient pole synchronous motor always $X_d > X_q$, normally $X_q = (0.5 \sim 0.8)X_d$.

Considering the d and q axes synchronous reactances, and referring to Eq. (3.75), the voltage equation of the salient pole rotor synchronous motor can be expressed by

$$V_s = I_sR_s + I_djX_d + I_qjX_q + E_f \tag{3.85}$$

From this equation, the equivalent circuit of the salient pole rotor synchronous motor is shown in Fig. 3.60.

3.2.2.1 Torque of a salient pole rotor synchronous motor

Now, we will derive the torque of a salient pole rotor synchronous motor. In addition to the torque of a cylindrical rotor, it can be expected that a salient pole rotor synchronous motor has a reluctance torque due to the saliency of the rotor as already discussed in Chapter 1.

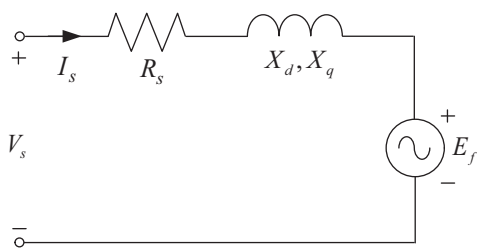


FIGURE 3.60

Equivalent circuit of a salient pole rotor synchronous motor.

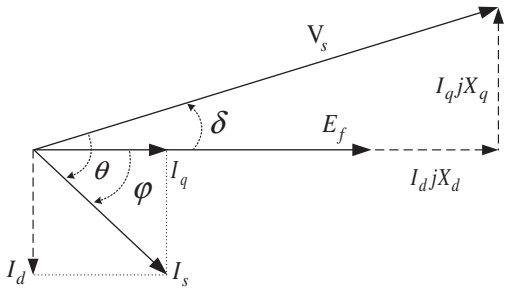


FIGURE 3.61

Phasor diagram of a salient pole synchronous motor.

The input power in terms of *d*-*q* axes currents, I_d and I_q, can be expressed as

$$\begin{aligned} P &= 3V_sI_s\cos\theta = 3V_sI_s\cos(\varphi+\delta) \\ &= 3V_sI_s(\cos\varphi\cos\delta - \sin\varphi\sin\delta) \\ &= 3V_s(I_q\cos\delta - I_d\sin\delta) \end{aligned} \tag{3.86}$$

From Eq. (3.85), assuming that the stator winding resistance is neglected, the phasor diagram can be expressed as Fig. 3.61.

From this phasor diagram, we have

$$V_s\cos\delta = E_f + I_dX_d \tag{3.87}$$

$$V_s\sin\delta = I_qX_q \tag{3.88}$$

Combining Eqs. (3.86)−(3.88), the output power and the torque are given by

$$P = 3\frac{V_sE_f}{X_s}\sin\delta + 3\frac{V_s^2(X_d - X_q)}{2X_dX_q}\sin 2\delta \tag{3.89}$$

$$\text{Torque: } T = \frac{P}{\omega_s} = \underbrace{3\frac{V_s E_f}{\omega_s X_s}\sin\delta}_{\text{Electromagnetic torque } T_f} + \underbrace{3\frac{V_s^2(X_d - X_q)}{2\omega_s X_d X_q}\sin 2\delta}_{\text{Reluctance torque } T_r} \tag{3.90}$$

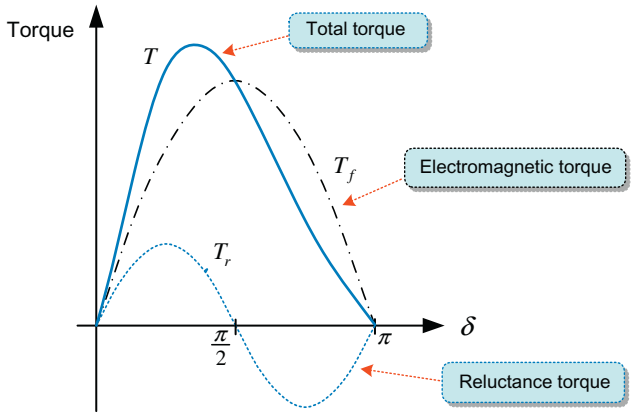


FIGURE 3.62

Torque of a salient pole synchronous motor.

As we can expect, a salient pole synchronous motor has two torque components: *electromagnetic torque* T_f due to the field flux of the rotor (the first term on the right-hand side of Eq. (3.90)) and *reluctance torque* T_r due to the saliency of the rotor (the second term on the right-hand side of Eq. (3.90)). Fig. 3.62 shows the output torque according to the torque angle δ.

Because of this reluctance torque, a synchronous motor with the salient pole rotor can produce more torque than a synchronous motor with the cylindrical rotor. In addition, this motor has the output torque to drive a load even if the field current is zero. Due to the reluctance torque, the torque angle δ at which the pull-out torque occurs is less than 90 electrical degrees.

3.2.3 STARTING OF SYNCHRONOUS MOTORS

Synchronous motors are inherently not able to self-start on an AC power source with the utility frequency of 50 or 60 Hz. As stated in Chapter 1, this is because synchronous motors can develop a torque only when running at the synchronous speed. However, the synchronous speed for the utility frequency is too fast for the rotor to synchronize for starting as shown in Fig. 3.63.

Therefore we need some means for starting synchronous motors. Once the rotor reaches a speed close to the synchronous speed (>95%) through some

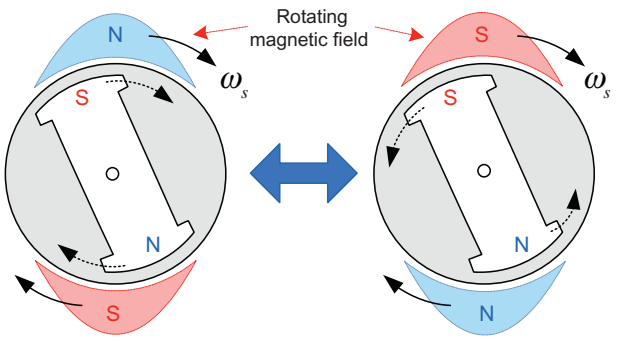


FIGURE 3.63

Synchronization in a synchronous motor.

starting means, the field winding will be excited, so the motor locks into synchronization.

There are some techniques employed to start a synchronous motor. As a simple method, a separate motor is used to drive the rotor to run close to the synchronous speed. A second method is to start the synchronous motor as an induction motor. In this case, the rotor has a special damping winding for the purpose of starting, which is similar to the squirrel-cage arrangements of an induction motor. When the synchronous motor is starting, the torque will be produced by the induced current in the damping winding, so it can start as an induction motor. In addition, the damper winding has another function to help keeping the synchronous motor in synchronism. If the speed of the motor is increased or decreased from the synchronous speed, then a current will be induced in the damper winding and will develop a torque to oppose the change in speed.

As for the starting method of PMSMs used in variable speed drives, we can start the motor slowly at a reduced frequency by using a PWM inverter. In this case, a high starting torque can be developed by using the information of the rotor initial position.

REFERENCES

[1] C.I. Hubert, Electric Machines, Theory, Operation, Applications, Adjustment, and Control, second ed., Prentice Hall, Upper Saddle River, NJ, 2002, p. 135.

[2] P.C. Sen, Principles of Electric Machines and Power Electronics, second ed., John Wiley & Sons, Inc., New York, 1997.

[3] J.F. Funchslocj, W.R. Findley, R.W. Walter, The next generation motor, IEEE Ind. Appl. Mag. 14 (1) (Jan./Feb. 2008) 37–43.

[4] S.J. Chapman, Electric Machinery Fundamentals, third ed., McGrawHill, International editions, Singapore, 1999 (Chapter 7).

CHAPTER

4 Modeling of alternating current motors and reference frame theory

For a proper control of a motor, we need to analyze its dynamic performance as well as steady-state performance. This requires a mathematical model, which describes the behavior of a motor. The motor model can be mainly expressed by the voltage and torque equations. The voltage equation for a motor basically consists of the following components: the voltage drop of the winding resistance R and the induced voltage proportional to the rate of change over time of the winding flux linkage λ as

$$\begin{aligned} v(t) &= Ri(t) + \frac{d\lambda(t)}{dt} \\ &= Ri(t) + \frac{d\left[L(\theta_r)i(t)\right]}{dt} \quad (\theta_r = \omega_r t) \end{aligned} \tag{4.1}$$

As discussed in Chapter 1, the flux linkage can be expressed as the product of inductance and current. For alternating current (AC) motors with windings in the stator and rotor, the mutual-inductance which implies the amount of flux linking between the two windings, is a time-varying parameter. This is because that the mutual-inductance is a function of the rotor position due to the variation in the amount of linking flux with the rotor position. Furthermore, in salient pole synchronous motors, even the self-inductance is a function of the rotor position due to the variation in the air gap according to the rotor position.

As an example, consider the induction motor in Fig. 4.1, in which the stator windings are stationary while the rotor windings are rotating with the rotor. Due to the movement of the rotor, the angular position θ_r between the stator and rotor windings varies over time except for at a standstill. As a result, even if currents (thus, flux) flowing in these two windings remain constant, the amount of the flux linking these windings will vary over time. This results in the mutual-inductance to become time-varying. Due to this time-varying inductance, the voltage equations, which describe the behavior of AC motors, will be expressed by differential equations with time-varying coefficients.

The analysis of such time-varying differential equations will be fairly complex. However, by using the *reference frame transformation*, which will be introduced in this chapter, its complexity can be significantly reduced. This is because the

Electric Motor Control. DOI: http://dx.doi.org/10.1016/B978-0-12-812138-2.00004-0
© 2017 Elsevier Inc. All rights reserved.

Hesai Exhibit 1030, page 156

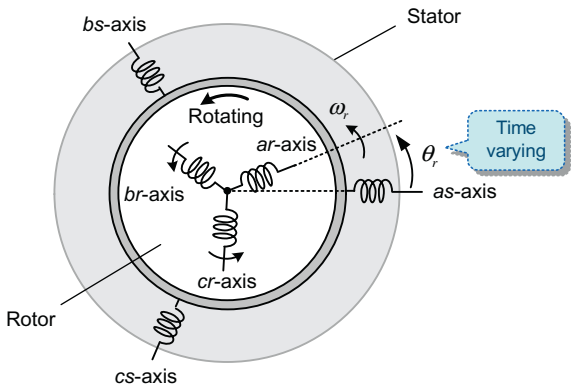


FIGURE 4.1

Angular position between stator and rotor windings.

time-varying inductances can be eliminated in the voltage equations by employing the reference frame transformation. When using this transformation, the three-phase *abc* variables are transformed to *dq* variables in an orthogonal coordinate system. These *dq* orthogonal variables are necessary to employ the *vector control* scheme, which enables a dynamic torque control of AC motors. This scheme will be described in Chapter 5.

In this chapter, we will study the reference frame transformation and introduce the models of AC motors expressed by the *dq* variables in the orthogonal coordinate system. Prior to this, we will start exploring the models of AC motors expressed in the three-phase *abc* variables.

4.1 MODELING OF INDUCTION MOTOR

Unlike the steady-state model of an induction motor shown in Chapter 3, in this section, we will introduce a model to describe the dynamics in the transient-state as well as the steady-state performance.

Consider a three-phase, two-pole induction motor as shown in Fig. 4.2. Assume that the stator windings have a number of effective turns N_s, resistance R_s, leakage inductance L_{ls}, and self-inductance L_s. Similarly, the equivalent rotor windings have a number of effective turns N_r, resistance R_r, leakage inductance L_{lr}, and self-inductance L_r. θ_r is the angular displacement between the stator and rotor axes. Here, we will not consider the nonideal characteristics such as the saturation of iron core, slots effect, and cogging torque. Although these are identical sinusoidal distributed windings, each displaced by 120°, we will consider only the centered coil of each phase for simplicity.

Now, let us derive the voltage equations of an induction motor. Since an induction motor has six windings, we can express it by six voltage equations. The

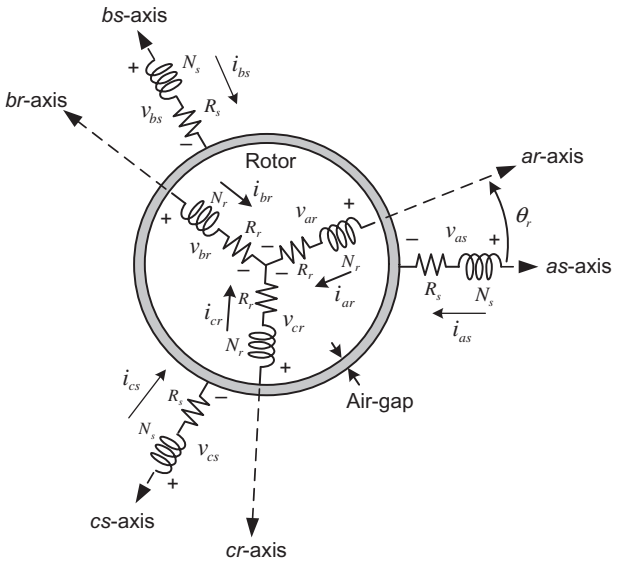


FIGURE 4.2

Stator and rotor windings of an induction motor.

winding voltage is composed of the voltage drop of the winding resistance and the voltage induced by the flux linkage variation of the winding. Thus the six voltage equations for the stator and rotor windings can be written by

$$v_{as} = R_s i_{as} + \frac{d\lambda_{as}}{dt} \tag{4.2}$$

$$v_{bs} = R_s i_{bs} + \frac{d\lambda_{bs}}{dt} \tag{4.3}$$

$$v_{cs} = R_s i_{cs} + \frac{d\lambda_{cs}}{dt} \tag{4.4}$$

$$v'_{ar} = R' i'_{ar} + \frac{d\lambda'_{ar}}{dt} \tag{4.5}$$

$$v'_{br} = R' i'_{br} + \frac{d\lambda'_{br}}{dt} \tag{4.6}$$

$$v'_{cr} = R' i'_{cr} + \frac{d\lambda'_{cr}}{dt} \tag{4.7}$$

where v_{as}, v_{bs}, v_{cs} are the stator voltages, i_{as}, i_{bs}, i_{cs} are the stator currents, v'_{ar}, v'_{br}, v'_{cr} are the rotor voltages, i'_{ar}, i'_{br}, i'_{cr} are the rotor currents, λ_{as}, λ_{bs}, λ_{cs} are the stator flux linkages, and λ_{ar}, λ_{br}, λ_{cr} are the rotor flux linkages. Here, the primed variables denote the rotor variables that are referred to the stator by considering the turns ratio of the two windings. From this point on, we will skip the prime symbol ($'$).

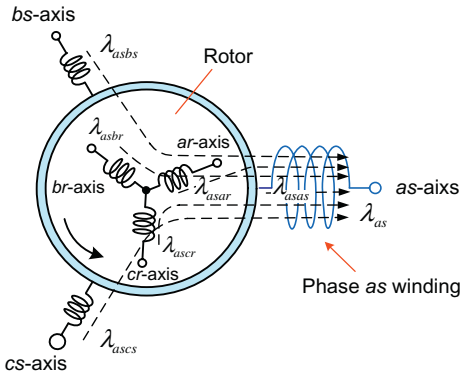


FIGURE 4.3

Flux linkage λ_{as} of the phase *as* winding.

To solve these voltage equations, we need to know the flux linkage of each winding. Since there are six windings, one winding will be linked by not only the flux produced by its own winding current but also the flux produced by the current flowing in the other five windings. For example, the total flux linkage λ_{as} of the phase *as* winding shown in Fig. 4.3 has the following six components.

$$\begin{aligned}\lambda_{as} &= \lambda_{asas} + \lambda_{asbs} + \lambda_{ascs} + \lambda_{asar} + \lambda_{asbr} + \lambda_{ascr} \\ &= L_{asas}i_{as} + L_{asbs}i_{bs} + L_{ascs}i_{cs} + L_{asar}i_{ar} + L_{asbr}i_{br} + L_{ascr}i_{cr}\end{aligned} \tag{4.8}$$

where the flux linkage λ_{xsys} represents the flux, which is produced by the current i_{ys} flowing in the *ys* winding and links the *xs* winding. The flux linkage λ_{xsys} can be expressed as the product of the related current and inductance. In this case inductance L_{xsys} is defined as the ratio of the flux linking the *xs* winding to the current i_{ys} generating the flux, i.e., $L_{xsys} = \lambda_{xsys}/i_{ys}$.

Six flux linkages in the stator and rotor windings can be written by

$$\begin{aligned}\begin{bmatrix}\lambda_{as}\\ \lambda_{bs}\\ \lambda_{cs}\\ \hline \lambda_{ar}\\ \lambda_{br}\\ \lambda_{cr}\end{bmatrix} &= \left[\begin{array}{ccc:ccc} \lambda_{asas} & \lambda_{asbs} & \lambda_{ascs} & \lambda_{asar} & \lambda_{asr} & \lambda_{ascr} \\ \lambda_{bsas} & \lambda_{bsbs} & \lambda_{bscs} & \lambda_{bsar} & \lambda_{bsbr} & \lambda_{bscr} \\ \lambda_{csas} & \lambda_{csbs} & \lambda_{csbs} & \lambda_{csar} & \lambda_{csbr} & \lambda_{cscr} \\ \hline \lambda_{aras} & \lambda_{arbs} & \lambda_{arcs} & \lambda_{arbr} & \lambda_{arbr} & \lambda_{arcr} \\ \lambda_{bras} & \lambda_{brbs} & \lambda_{brcs} & \lambda_{brar} & \lambda_{brbr} & \lambda_{brcr} \\ \lambda_{cras} & \lambda_{crbs} & \lambda_{crcs} & \lambda_{crar} & \lambda_{crbr} & \lambda_{crbcr} \end{array}\right] \\ &= \left[\begin{array}{ccc:ccc} L_{asas} & L_{asbs} & L_{ascs} & L_{asar} & L_{asr} & L_{ascr} \\ L_{bsas} & L_{bsbs} & L_{bscs} & L_{bsar} & L_{bsbr} & L_{bscr} \\ L_{csas} & L_{csbs} & L_{csbs} & L_{csar} & L_{csbr} & L_{cscr} \\ \hline L_{aras} & L_{arbs} & L_{arcs} & L_{arbr} & L_{arbr} & L_{arcr} \\ L_{bras} & L_{brbs} & L_{brcs} & L_{brar} & L_{brbr} & L_{brcr} \\ L_{cras} & L_{crbs} & L_{crcs} & L_{crar} & L_{crbr} & L_{crbcr} \end{array}\right]\begin{bmatrix} i_{as}\\ i_{bs}\\ i_{cs}\\ i_{ar}\\ i_{br}\\ i_{cr}\end{bmatrix}\end{aligned} \tag{4.9}$$

These inductances are largely divided into four groups as

$$\begin{bmatrix} \boldsymbol{\lambda}_{abcs} \\ \boldsymbol{\lambda}_{abcr} \end{bmatrix} = \begin{bmatrix} \boldsymbol{L}_s & \boldsymbol{L}_{sr} \\ (\boldsymbol{L}_{sr})^T & \boldsymbol{L}_r \end{bmatrix} \begin{bmatrix} \boldsymbol{i}_{abcs} \\ \boldsymbol{i}_{abcr} \end{bmatrix} \tag{4.10}$$

where $\boldsymbol{L}_s$ and $\boldsymbol{L}_r$ represent the inductance matrix of the stator and rotor windings, respectively, and $\boldsymbol{L}_{sr}$ represents the mutual-inductance matrix between the stator and rotor windings.

Next, we will determine these inductances.

4.1.1 STATOR WINDINGS

The stator inductance matrix $\boldsymbol{L}_s$ as shown in Fig. 4.4 consists of the self-inductances of each stator winding and the mutual-inductance between the stator windings as

$$\boldsymbol{L}_s = \begin{bmatrix} L_{asas} & L_{asbs} & L_{ascs} \\ L_{bsas} & L_{bsbs} & L_{bscs} \\ L_{csas} & L_{csbs} & L_{cscs} \end{bmatrix} \tag{4.11}$$

Stator self-inductance

Stator mutual-inductance

We can obtain expressions for the self-inductances and the mutual-inductances as follows.

The flux produced by each winding can be separated into two components: the *leakage flux* which links only its own winding and the *magnetizing flux* which links both its own winding and the other windings. These can be expressed

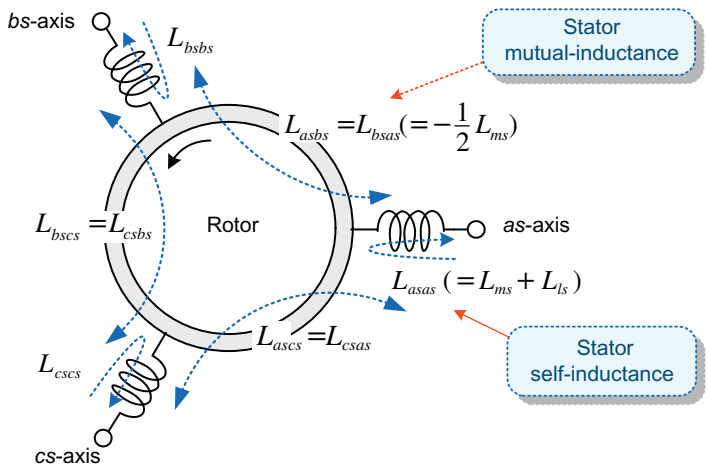


FIGURE 4.4

Stator inductances.

in terms of the leakage inductance and the magnetizing inductance, respectively. Thus the stator self-inductances L_{asas}, L_{bsbs}, L_{cscs} consist of the leakage inductance L_{ls} and the magnetizing inductance L_{ms} as

$$L_{asas} = L_{bsbs} = L_{cscs} = L_{ls} + L_{ms} \tag{4.12}$$

where $L_{ms} = \mu_o N_s^2 (rl/g)(\pi/4)$, μ_o is the permeability of air, l is the axial length of the air gap, and r is the radius to the mean of the air gap [1].

The mutual-inductances L_{asbs}, L_{ascs}, L_{bsas}, L_{bscs}, L_{csas}, L_{csbs} between the two stator windings, which are displaced from each other by 120°, are all the same and are related to the magnetizing inductance as

$$\begin{aligned} L_{asbs} &= L_{ascs} = L_{bsas} = L_{bscs} = L_{csas} = L_{csbs} \\ &= L_{ms} \cos\left(\frac{2\pi}{3}\right) = -\frac{1}{2} L_{ms} \end{aligned} \tag{4.13}$$

Here, the negative sign in the mutual-inductance indicates that each winding produces the flux in a direction opposite to one another. From the inductances of Eqs. (4.12) and (4.13), the inductances of the stator windings are given by

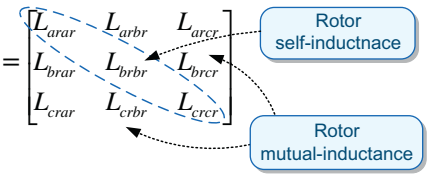
$$\boldsymbol{L}_s = \begin{bmatrix} L_{asas} & L_{asbs} & L_{ascs} \\ L_{bsas} & L_{bsbs} & L_{bscs} \\ L_{csas} & L_{csbs} & L_{cscs} \end{bmatrix} = \begin{bmatrix} L_{ls} + L_{ms} & -\frac{L_{ms}}{2} & -\frac{L_{ms}}{2} \\ -\frac{L_{ms}}{2} & L_{ls} + L_{ms} & -\frac{L_{ms}}{2} \\ -\frac{L_{ms}}{2} & -\frac{L_{ms}}{2} & L_{ls} + L_{ms} \end{bmatrix} \tag{4.14}$$

Because the length of the air gap is constant, these inductances become a constant value, irrespective of the rotor position.

4.1.2 ROTOR WINDINGS

The rotor inductance matrix $\boldsymbol{L}_r$ as shown in Fig. 4.5 consists of the self-inductances of each rotor windings and the mutual-inductance between these windings as

$$\boldsymbol{L}_r = \begin{bmatrix} L_{arar} & L_{arbr} & L_{arcr} \\ L_{brar} & L_{brbr} & L_{brcr} \\ L_{crar} & L_{crbr} & L_{crcr} \end{bmatrix} \tag{4.15}$$



Similar to the stator self-inductances, the rotor self-inductances L_{arar}, L_{brbr}, L_{crcr} consist of the leakage inductance L_{lr} and the magnetizing inductance L_{mr} as

$$L_{arar} = L_{brbr} = L_{crcr} = L_{lr} + L_{mr} \tag{4.16}$$

where $L_{mr} = \mu_o N_r^2 (rl/g)(\pi/4) = (N_r/N_s)^2 L_{ms}$.

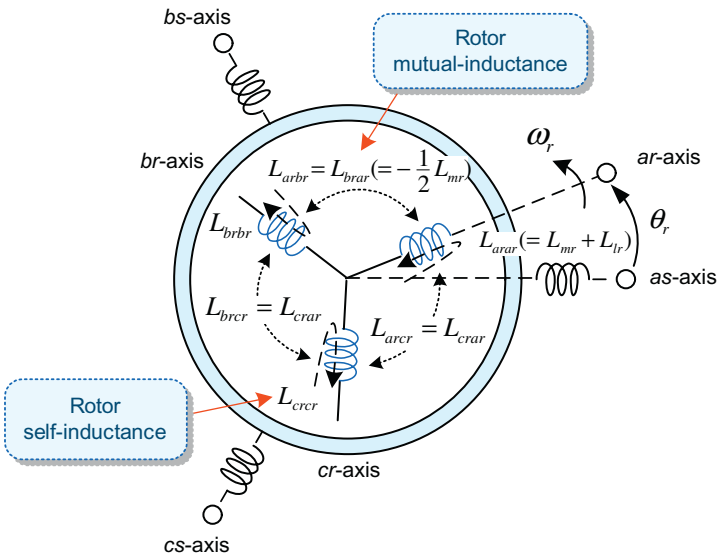


FIGURE 4.5

Inductances of the rotor windings.

The mutual-inductances L_{arbr}, L_{arcr}, L_{brar}, L_{brcr}, L_{crar}, L_{crbr} between the two rotor windings, which are displaced from each other by 120°, are all the same and related to the magnetizing inductance as

$$L_{arbr} = L_{arcr} = L_{brar} = L_{brcr} = L_{crar} = L_{crbr} = L_{mr}\cos\left(\frac{2\pi}{3}\right) = -\frac{1}{2}L_{mr} = -\frac{1}{2}\left(\frac{N_r}{N_s}\right)^2 L_{ms} \tag{4.17}$$

where N_r/N_s is the turns ratio of the stator and rotor windings. With these inductances, the inductances of the rotor windings are given by

$$\boldsymbol{L}_r = \begin{bmatrix} L_{arar} & L_{arbr} & L_{arcr} \\ L_{brar} & L_{brbr} & L_{brcr} \\ L_{crar} & L_{crbr} & L_{crcr} \end{bmatrix} = \begin{bmatrix} L_{ls} + n^2 L_{ms} & -n^2\frac{L_{ms}}{2} & -n^2\frac{L_{ms}}{2} \\ -\frac{L_{ms}}{2} & L_{ls} + n^2 L_{ms} & -n^2\frac{L_{ms}}{2} \\ -n^2\frac{L_{ms}}{2} & -n^2\frac{L_{ms}}{2} & L_{ls} + n^2 L_{ms} \end{bmatrix}, \quad n = \left(\frac{N_r}{N_s}\right) \tag{4.18}$$

These inductances are a constant value, irrespective of the rotor position.

4.1.3 INDUCTANCE BETWEEN THE STATOR AND ROTOR WINDINGS

Next, let us examine the mutual-inductance of the stator and rotor windings. First, we will explore the mutual-inductance matrix $\boldsymbol{L}_{sr}$. This is related to the amount of flux, which is produced by the rotor windings and links the stator windings. The mutual-inductance consists of nine components as

$$\boldsymbol{L}_{sr} = \begin{bmatrix} L_{asar} & L_{asbr} & L_{ascr} \\ L_{bsar} & L_{bsbr} & L_{bscr} \\ L_{csar} & L_{csbr} & L_{cscr} \end{bmatrix} \tag{4.19}$$

As an example, examine the mutual-inductance L_{asar}, which represents the ratio of the flux linking in the stator *as* winding to the rotor *ar* winding current generating the flux. If the rotor winding is rotating at a speed ω_r, the relative position θ_r between the two windings will vary over time. Thus the mutual-inductance vary sinusoidally with respect to the displacement angle θ_r of the rotor as shown in Fig. 4.6.

Considering the turns ratio between the two windings, L_{asar} is given by

$$L_{asar} = L_{mr}\left(\frac{N_s}{N_r}\right)\cos\theta_r = L_{ms}\left(\frac{N_r}{N_s}\right)\cos\theta_r \quad \left(\theta_r = \int \omega_r dt\right) \tag{4.20}$$

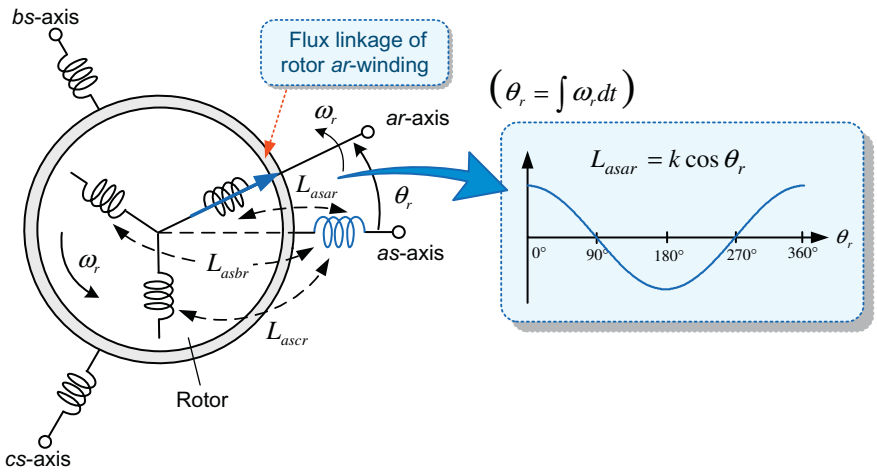


FIGURE 4.6

Mutual-inductance between the stator *as* winding and the rotor *ar* winding.

Likewise, the other mutual-inductances are given by

$$L_{asar} = L_{bsbr} = L_{cscr} = \left(\frac{N_r}{N_s}\right) L_{ms} \cos\theta_r \tag{4.21}$$

$$L_{asbr} = L_{bscr} = L_{csar} = \left(\frac{N_r}{N_s}\right) L_{ms} \cos\left(\theta_r + \frac{2\pi}{3}\right) \tag{4.22}$$

$$L_{ascr} = L_{bsar} = L_{csbr} = \left(\frac{N_r}{N_s}\right) L_{ms} \cos\left(\theta_r - \frac{2\pi}{3}\right) \tag{4.23}$$

With these inductances, the mutual-inductance matrix $\boldsymbol{L}_{sr}$ is given by

$$\boldsymbol{L}_{sr} = \begin{bmatrix} L_{asar} & L_{asbr} & L_{ascr} \\ L_{bsar} & L_{bsbr} & L_{bscr} \\ L_{csar} & L_{csbr} & L_{cscr} \end{bmatrix} = nL_{ms} \begin{bmatrix} \cos\theta_r & \cos\left(\theta_r + \frac{2\pi}{3}\right) & \cos\left(\theta_r - \frac{2\pi}{3}\right) \\ \cos\left(\theta_r - \frac{2\pi}{3}\right) & \cos\theta_r & \cos\left(\theta_r + \frac{2\pi}{3}\right) \\ \cos\left(\theta_r + \frac{2\pi}{3}\right) & \cos\left(\theta_r - \frac{2\pi}{3}\right) & \cos\theta_r \end{bmatrix} \tag{4.24}$$

From Eq. (4.24), we can readily see that the mutual-inductances are a function of the rotor position and thus vary over time except for at a standstill. Consequently, the time-varying coefficients will appear in the stator voltage equations of Eqs. (4.2)−(4.4).

The flux linkage of the stator windings, from Eqs. (4.14) and (4.24), is given by

$$\boldsymbol{\lambda}_{abcs} = \boldsymbol{L}_s \boldsymbol{i}_{abcs} + \boldsymbol{L}_{sr} \boldsymbol{i}_{abcr}$$

$$= \begin{bmatrix} L_{ls} + L_{ms} & -\frac{L_{ms}}{2} & -\frac{L_{ms}}{2} \\ -\frac{L_{ms}}{2} & L_{ls} + L_{ms} & -\frac{L_{ms}}{2} \\ -\frac{L_{ms}}{2} & -\frac{L_{ms}}{2} & L_{ls} + L_{ms} \end{bmatrix} \begin{bmatrix} i_{as} \\ i_{bs} \\ i_{cs} \end{bmatrix} \tag{4.25}$$

$$+ nL_{ms} \begin{bmatrix} \cos\theta_r & \cos\left(\theta_r + \frac{2\pi}{3}\right) & \cos\left(\theta_r - \frac{2\pi}{3}\right) \\ \cos\left(\theta_r - \frac{2\pi}{3}\right) & \cos\theta_r & \cos\left(\theta_r + \frac{2\pi}{3}\right) \\ \cos\left(\theta_r + \frac{2\pi}{3}\right) & \cos\left(\theta_r - \frac{2\pi}{3}\right) & \cos\theta_r \end{bmatrix} \begin{bmatrix} i_{ar} \\ i_{br} \\ i_{cr} \end{bmatrix}$$

Next, examine the mutual-inductance $\boldsymbol{L}_{rs}$. This is related to the amount of flux, which is produced by the stator windings and links the rotor windings. This mutual-inductance $\boldsymbol{L}_{rs}$ is equal to the transpose of $\boldsymbol{L}_{rs}$ as

$$\boldsymbol{L}_{rs} = \boldsymbol{L}_{sr}^{T} = \begin{bmatrix} L_{aras} & L_{arbs} & L_{arcs} \\ L_{bras} & L_{brbs} & L_{brcs} \\ L_{cras} & L_{crbs} & L_{crcs} \end{bmatrix}$$

$$= nL_{ms} \begin{bmatrix} \cos\theta_r & \cos\left(\theta_r - \frac{2\pi}{3}\right) & \cos\left(\theta_r + \frac{2\pi}{3}\right) \\ \cos\left(\theta_r + \frac{2\pi}{3}\right) & \cos\theta_r & \cos\left(\theta_r - \frac{2\pi}{3}\right) \\ \cos\left(\theta_r - \frac{2\pi}{3}\right) & \cos\left(\theta_r + \frac{2\pi}{3}\right) & \cos\theta_r \end{bmatrix} \tag{4.26}$$

Like $\boldsymbol{L}_{sr}$, the mutual-inductance $\boldsymbol{L}_{rs}$ also becomes time-varying except at a standstill. Therefore the time-varying coefficients will appear in the voltage equations of the rotor windings.

The flux linkage of the rotor windings, from Eqs. (4.18) and (4.26), is given by

$$\boldsymbol{\lambda}_{abcr} = \boldsymbol{L}_r \boldsymbol{i}_{abcr} + \boldsymbol{L}_{rs} \boldsymbol{i}_{abcs}$$

$$= \begin{bmatrix} L_{ls} + n^2 L_{ms} & -n^2 \frac{L_{ms}}{2} & -n^2 \frac{L_{ms}}{2} \\ -\frac{L_{ms}}{2} & L_{ls} + n^2 L_{ms} & -n^2 \frac{L_{ms}}{2} \\ -n^2 \frac{L_{ms}}{2} & -n^2 \frac{L_{ms}}{2} & L_{ls} + n^2 L_{ms} \end{bmatrix} \begin{bmatrix} i_{ar} \\ i_{br} \\ i_{cr} \end{bmatrix}$$

$$+ nL_{ms} \begin{bmatrix} \cos\theta_r & \cos\left(\theta_r - \frac{2\pi}{3}\right) & \cos\left(\theta_r + \frac{2\pi}{3}\right) \\ \cos\left(\theta_r + \frac{2\pi}{3}\right) & \cos\theta_r & \cos\left(\theta_r - \frac{2\pi}{3}\right) \\ \cos\left(\theta_r - \frac{2\pi}{3}\right) & \cos\left(\theta_r + \frac{2\pi}{3}\right) & \cos\theta_r \end{bmatrix} \begin{bmatrix} i_{as} \\ i_{bs} \\ i_{cs} \end{bmatrix} \tag{4.27}$$

Finally, from Eqs. (4.25) and (4.27), the total flux linkages of the induction motor are given by

$$\begin{bmatrix} \lambda_{as} \\ \lambda_{bs} \\ \lambda_{cs} \\ \hline \lambda_{ar} \\ \lambda_{br} \\ \lambda_{cr} \end{bmatrix} = \left[\begin{array}{ccc:ccc} L_{ls}+L_{ms} & -\frac{L_{ms}}{2} & -\frac{L_{ms}}{2} & nL_{ms}\cos\theta_r & nL_{ms}\cos\left(\theta_r+\frac{2\pi}{3}\right) & nL_{ms}\cos\left(\theta_r-\frac{2\pi}{3}\right) \\ -\frac{L_{ms}}{2} & L_{ls}+L_{ms} & -\frac{L_{ms}}{2} & nL_{ms}\cos\left(\theta_r-\frac{2\pi}{3}\right) & nL_{ms}\cos\theta_r & nL_{ms}\cos\left(\theta_r+\frac{2\pi}{3}\right) \\ -\frac{L_{ms}}{2} & -\frac{L_{ms}}{2} & L_{ls}+L_{ms} & nL_{ms}\cos\left(\theta_r+\frac{2\pi}{3}\right) & nL_{ms}\cos\left(\theta_r-\frac{2\pi}{3}\right) & nL_{ms}\cos\theta_r \\ \hdashline nL_{ms}\cos\theta_r & nL_{ms}\cos\left(\theta_r-\frac{2\pi}{3}\right) & nL_{ms}\cos\left(\theta_r+\frac{2\pi}{3}\right) & L_{lr}+n^2L_{ms} & -\frac{1}{2}n^2L_{ms} & -\frac{1}{2}n^2L_{ms} \\ nL_{ms}\cos\left(\theta_r+\frac{2\pi}{3}\right) & nL_{ms}\cos\theta_r & nL_{ms}\cos\left(\theta_r-\frac{2\pi}{3}\right) & -\frac{1}{2}n^2L_{ms} & L_{lr}+n^2L_{ms} & -\frac{1}{2}n^2L_{ms} \\ nL_{ms}\cos\left(\theta_r-\frac{2\pi}{3}\right) & nL_{ms}\cos\left(\theta_r+\frac{2\pi}{3}\right) & nL_{ms}\cos\theta_r & -\frac{1}{2}n^2L_{ms} & -\frac{1}{2}n^2L_{ms} & L_{lr}+n^2L_{ms} \end{array}\right] \begin{bmatrix} i_{as} \\ i_{bs} \\ i_{cs} \\ \hline i_{ar} \\ i_{br} \\ i_{cr} \end{bmatrix} \tag{4.28}$$

By substituting these flux linkages into Eqs. (4.2)–(4.7), the voltage equations of the induction motor are completed.

4.2 MODELING OF PERMANENT MAGNET SYNCHRONOUS MOTOR

The stator configuration of a synchronous motor is the same as that of an induction motor. The stator windings are connected to a three-phase AC source to generate a rotating magnetic field. However, unlike an induction motor having three-phase windings, the rotor of a synchronous motor has a field winding or a permanent magnet to generate a magnetic field flux on it. In recent years the magnetic field for synchronous motors has been generated mostly by using a permanent magnet rather than a field winding.

In addition to the electromagnetic torque produced by the magnetic fields of the stator and rotor, synchronous motors with a salient rotor can exploit reluctance torque. Synchronous motors can be divided into several categories according to the ratio of electromagnet torque to reluctance torque as shown in Fig. 4.7 [2].

In this book we will limit the scope of our study only to permanent magnet synchronous motors (PMSMs) except for synchronous reluctance motors, which only exploit reluctance torque.

PMSMs offer many advantages over other motors. They have a higher efficiency than induction motors because there are no copper losses by the rotor. In addition, they exhibit a high power density, high torque-to-volume ratios, and a fast dynamic response because of the availability of cost-effective powerful permanent magnet materials such as NdFeB.

Besides these advantages, PMSMs with magnetic rotor saliency use reluctance torque as well as magnet torque. Owing to these attractive characteristics, PMSMs are gaining more attention for a wide variety of residential and industrial drive applications, ranging from general-purpose drives to high-performance drives.

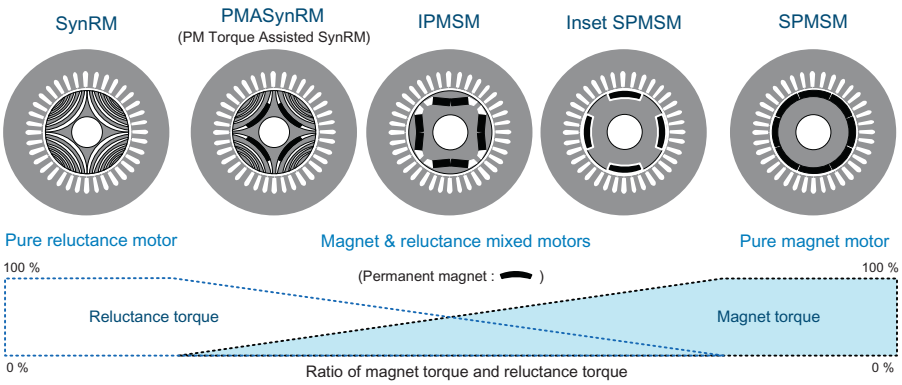


FIGURE 4.7

Several categories of synchronous motors.

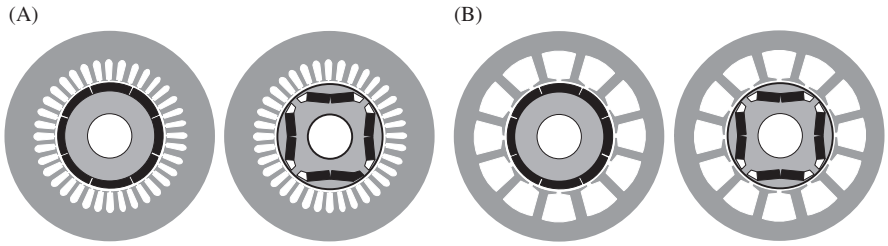


FIGURE 4.8

Different structures for the stator and rotor of PMSMs. (A) Distributed winding and (B) concentrated winding.

4.2.1 STRUCTURE OF PERMANENT MAGNET SYNCHRONOUS MOTORS

4.2.1.1 Stator structure

A distributed winding has been typically used as a three-phase stator winding configuration to produce a sinusoidal flux in the air gap as shown in Fig. 4.8A. However, recently, a concentrated winding has been increasingly used in PMSMs as shown in Fig. 4.8B.

Although a concentrated winding gives less sinusoidal magnetomotive force distribution compared to a distributed winding, this type of winding can provide several advantages such as high power density, high efficiency, short end turns, high slot-fill factor, low manufacturing costs by segmented stator structures, low cogging torque, flux-weakening capability, and fault tolerance [3].

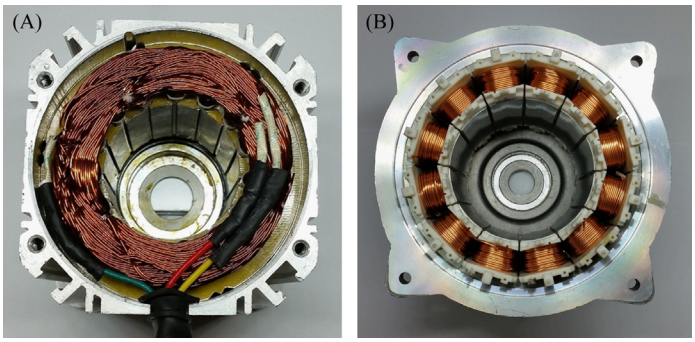


FIGURE 4.9

Comparison of distributed and concentrated windings. (A) Distributed winding and (B) concentrated winding.

Fig. 4.9 compares the distributed winding and concentrated winding in the stator of a PMSM. There are two main types of a concentrated winding: *single-layer winding* configuration, where each slot is occupied by the coil sides of one phase, and *double-layer winding* configuration, where each slot is occupied equally by the coil sides of two phases [4].

4.2.1.2 Rotor structure

The rotor of PMSMs has a permanent magnet to generate a magnetic field flux on it. The characteristics of PMSMs such as the power density, torque density, weight, and size may vary according to the chosen permanent magnet material. These days, a neodymium magnet (also known as NdFeB) is the most commonly employed for PMSMs due to its excellent magnetic characteristics and low cost. Even though we use the same permanent magnet material, many characteristics of PMSMs are heavily dependent on rotor configurations involving the shape and arrangement of the permanent magnets.

PMSMs can be divided into two types according to the direction of the magnetic flux produced from the permanent magnets as shown in Fig. 4.10: *radial-flux type* and *axial-flux type*. In the radial-flux type, the rotor which is cylindrical in shape rotates inside the stator and the magnetic flux crosses the air gap in a radial direction. On the other hand, in the axial-flux type, the rotor which resembles a pancake rotates beside the stator and the magnetic flux crosses the air gap in an axial direction [5].

Out of these two types, the radial-flux type is more commonly used in many applications. The radial-flux type PMSMs can also be further classified into two

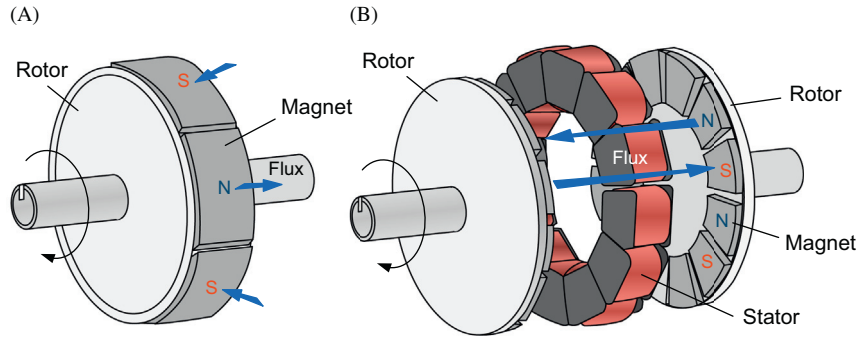


FIGURE 4.10

PMSM configurations. (A) Radial-flux type and (B) axial-flux type.

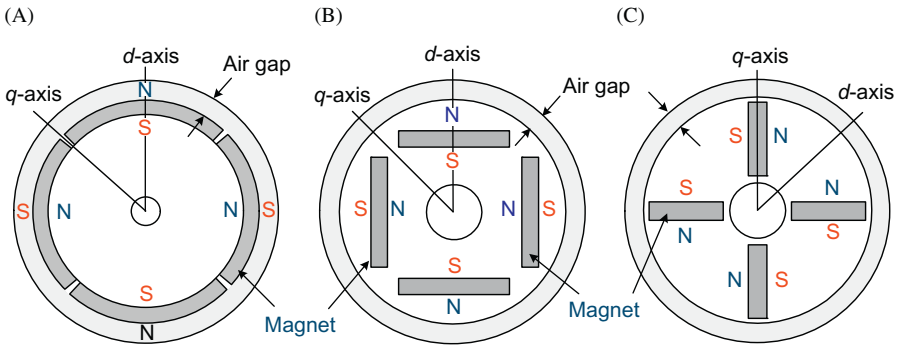


FIGURE 4.11

Rotor topologies of PMSMs (four-pole). (A) Surface mounted, (B) interior (parallel), and (C) interior (perpendicular).

categories based on the position of the permanent magnets as shown in Fig. 4.11: *surface-mounted permanent magnet synchronous motor* (SPMSM) with magnets mounted on the surface of the rotor and *interior permanent magnet synchronous motor* (IPMSM) with magnets buried inside the rotor iron core.

As for IPMSM, there are two topologies according to the arrangement of the permanent magnets: *parallel topology*, in which the magnetic poles are located parallel to the circumference of the rotor as shown in Fig. 4.11B and *perpendicular topology* (also called *spoke type*), in which the magnetic poles are located perpendicularly to the circumference as shown in Fig. 4.11C.

IPMSMs with the parallel topology are more commonly used. The perpendicular topology can concentrate the magnetic flux of the magnets and achieve a high pole number, so that the flux density in the air gap can be higher than the flux density of the magnet itself. Thus although low cost and low flux density magnet

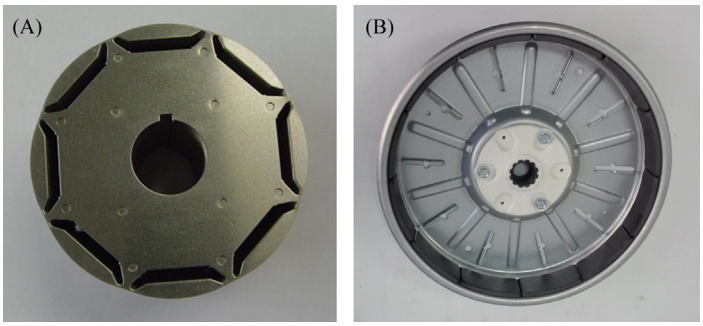


FIGURE 4.12

Rotor configurations of IPMSMs. (A) Inner rotor type and (B) outer rotor type.

material such as ferrite is employed, the motor can exhibit a high torque density. However, due to the flux concentration at the pole edges, there may be a high harmonic distortion in the air-gap flux density near the pole tips and thereby in the back-EMF profile. This also leads to a high ripple in the developed torque.

The rotor can also be constructed as an *inner rotor type* rotating inside the stator windings or an *outer rotor type* rotating outside the stator windings as shown in Fig. 4.12. The inner rotor type has lower inertia, and thus, results in a quick speed response. On the other hand, the outer rotor type has relatively high inertia and, thus, is favorable for constant speed operations.

PERMANENT MAGNETS USED IN ELECTRIC MOTORS

The permanent magnet used in motors can be mainly divided into the following three categories according to the type of magnetic materials: *Alnico, Ferrite, and Rare-earth* (SmCo, NdFeB).

1. Alnico magnets
   Alnico gives a high residual flux density (known as *remanence*) but a low coercivity. It also has a low temperature coefficient of remanence. However, due to a low coercivity, its magnetization is easily reduced by applied external magnetic field (this is called *demagnetization*).
2. Ferrite (or ceramic) magnets
   Ferrite offers a higher coercivity but a lower residual flux density than Alnico. Because of their cheap and moderate magnetic property, Ferrite magnets are widely used in low-performance applications.
3. Rare-earth magnets
   a. Samarium−cobalt (SmCo) magnets
      SmCo gives a higher energy product (BH_{max}) caused by its high residual flux density and coercivity. The Sm-Co magnets have higher Curie temperature (at which the material loses its magnetism) and a low temperature coefficient of coercivity and remanence but are very expensive and brittle.

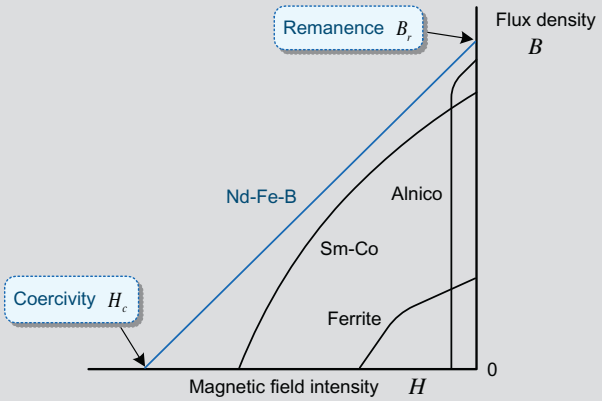
(*Continued*)

PERMANENT MAGNETS USED IN ELECTRIC MOTORS (CONTINUED)

b. Neodymium−iron−boron (NdFeB) magnets

NdFeB is considered as one of the best magnetic materials at present since it gives a much higher residual flux density and coercivity. However, Neodymium magnets are sensitive to temperature and can even lose magnet properties at a high temperature. This drawback is steadily improving.

Among these, NdFeB is the most commonly employed permanent magnet material for PMSMs due to its excellent magnetic characteristics and its recent price reductions. The following figure shows $B-H$ characteristic curves of these magnetic materials.



- Remanence B_r and coercivity H_c

  Remanence or residual flux density indicates the magnetic flux density remaining in a magnetic material after an external magnetic field is removed. Magnetic materials with a large residual flux density are desirable for strong permanent magnets. Coercivity indicates the intensity of the magnetic field required to reduce the magnetization of the material to zero. Magnetic materials with high coercivity are commonly used to make permanent magnets for electric motors.

- Temperature effects on permanent magnets

  The permanent magnets are sensitive to temperature. The residual flux density decreases with the increase in temperature. For example, NdFeB has the temperature coefficient of about 0.1% per degree celsius. The initial flux of the magnet can be restored when it returns to the original temperature. However, if the magnet is exposed to temperatures above the maximum working temperature and experiences a big loss of magnetism, irreversible changes may occur and its original flux level cannot be restored when it returns to the original temperature. Therefore it is advisable to operate magnets below the maximum working temperature. This limits the maximum torque capability of motors because the maximum current should be limited to avoid the demagnetization of magnets.

All the rotors shown in Fig. 4.11 are cylindrical in shape, and thus the physical air gap is constant. However the effective air gap may vary with the arrangement of the magnets. Since the permeability of a magnet approximates to that of air, the magnets placed in the flux path may be regarded as air. Thus, from the viewpoint of the magnetic field, the effective air gap will be the sum of the actual air-gap length and the radial thickness of the magnets.

For SPMSMs, which have magnets of uniform thickness on the surface of the rotor, the effective air gap is increased by the radial thickness of the magnets. Thus SPMSMs have a small stator winding inductance, and the d-axis inductance equals the q-axis inductance.

For IPMSMs, the $d-q$ axes inductances may be different depending on the arrangement of the magnets. On the one hand, in parallel topology IPMSMs the magnets are placed along with the d-axis so that the q-axis inductance becomes higher than the d-axis inductance. On the other hand, in perpendicular topology IPMSMs, the q-axis inductance is smaller than the d-axis inductance. Because of the magnetic saliency resulting from the inductance difference between the d- and q-axes, IPMSMs can exploit the reluctance torque.

The SPMSMs are unsuitable for high-speed operations producing a lager centrifugal force because of the magnets stuck on the surface of the rotor. Furthermore, because of the small inductance resulting from the increased effective air gap, SPMSMs have a relatively limited flux-weakening capability for high-speed operations. On the other hand, IPMSMs have more mechanical strength for high-speed operations because the magnets are inserted inside the rotor. Furthermore, the d-axis inductance of IPMSMs is high compared to that of an equivalent SPMSMs, and this is of a great advantage to IPMSMs for flux-weakening operation, which will be discussed in Chapter 8. Therefore IPMSMs are appropriate for high-speed operations.

As explained above, SPMSMs and IPMSMs are different in their characteristics, requiring different control methods. Now, we will find the model of the PMSMs. Initially, we will introduce the model of an IPMSM with a rotor that has a magnetic saliency. The model of an SPMSM can be derived easily from the IPMSM model. As stated earlier, an IPMSM has parallel and perpendicular topologies. These two topologies can be expressed as the same models but are different in the values of their $d-q$ axes inductances. In this section the most commonly used parallel topology IPMSM will be discussed.

4.2.2 MODEL OF PERMANENT MAGNET SYNCHRONOUS MOTORS

For a parallel topology IPMSM, the q-axis inductance is higher than the d-axis inductance because of the magnets placed along with the d-axis. Although the rotor of an IPMSM is cylindrical in shape, we will express it as a magnetic equivalent salient rotor as shown in Fig. 4.13 to simplify the analysis of the IPMSM.

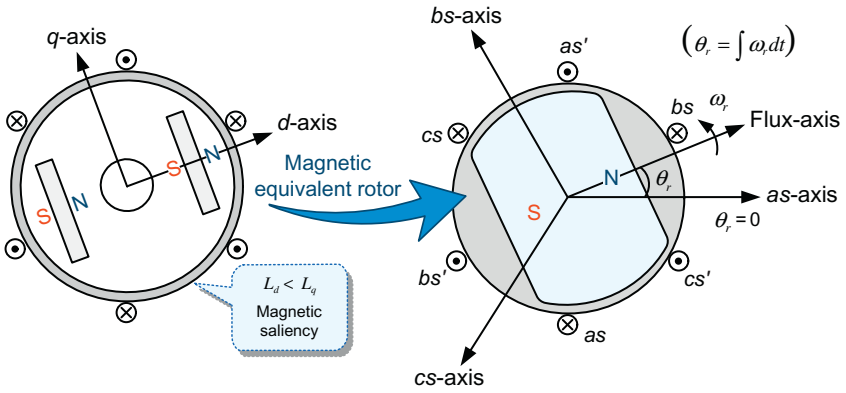


FIGURE 4.13

Rotor and its equivalent of an IPMSM.

As a PMSM has no rotor circuits, we can consider only the voltage equations for the stator windings. The stator windings of a synchronous motor are the same as those of an induction motor. Thus the stator voltage equations will be

$$\boldsymbol{v}_{abcs} = \boldsymbol{R}_s \boldsymbol{i}_{abcs} + \frac{d\boldsymbol{\lambda}_{abcs}}{dt} \tag{4.29}$$

where $\boldsymbol{v}_{abcs} = [v_{as} v_{bs} v_{cs}]^T$, $\boldsymbol{i}_{abcs} = [i_{as} i_{bs} i_{cs}]^T$, $\boldsymbol{\lambda}_{abcs} = [\lambda_{as} \lambda_{bs} \lambda_{cs}]^T$.

Since a synchronous motor has a different rotor configuration from that of an induction motor, the components of the flux linkage of the stator windings are different.

The flux linkage of an IPMSM has the following four components: the flux linkages due to the stator currents and the flux linkage due to the permanent magnet as

$$\lambda_{as} = \lambda_{asas} + \lambda_{asbs} + \lambda_{ascs} + \phi_{asf} \tag{4.30}$$

$$\lambda_{bs} = \lambda_{bsas} + \lambda_{bsbs} + \lambda_{bscs} + \phi_{bsf} \tag{4.31}$$

$$\lambda_{cs} = \lambda_{csas} + \lambda_{csbs} + \lambda_{cscs} + \phi_{csf} \tag{4.32}$$

These flux linkages can be expressed as the product of the related current and inductance as

$$\lambda_{as} = L_{asas} i_{as} + L_{asbs} i_{bs} + L_{ascs} i_{cs} + L_{asf} I_f \tag{4.33}$$

$$\lambda_{bs} = L_{bsas} i_{as} + L_{bsbs} i_{bs} + L_{bscs} i_{cs} + L_{bsf} I_f \tag{4.34}$$

$$\lambda_{cs} = L_{csas} i_{as} + L_{csbs} i_{bs} + L_{cscs} i_{cs} + L_{csf} I_f \tag{4.35}$$

Here, the flux linkages ϕ_{asf}, ϕ_{bsf}, ϕ_{csf} due to the permanent magnet are expressed as the product of the equivalent field current I_f and the related inductance L_{asf} , L_{bsf}, L_{csf}.

Now, we will determine the stator inductances of

$$\boldsymbol{L}_s = \begin{bmatrix} L_{asas} & L_{asbs} & L_{ascs} \\ L_{bsas} & L_{bsbs} & L_{bscs} \\ L_{csas} & L_{csbs} & L_{cscs} \end{bmatrix} \tag{4.36}$$

As can be seen in Section 4.1.1, the stator inductances consist of the self-inductances of the stator windings and the mutual-inductances between the stator windings. Furthermore, the stator self-inductances L_{asas}, L_{bsbs}, L_{cscs} consist of the leakage inductance and the magnetizing inductance.

The self-inductance of an IPMSM, unlike an induction motor, may be different depending on the angular position of the rotor because the effective air gap may vary with the position of the rotor. Consider an example of the phase *as* winding as shown in Fig. 4.14. In this case, the self-inductance becomes the maximum value at the rotor positions of both 90° and 270° (the smallest reluctance position), where the flux produced by the phase *as* current becomes the maximum value. This, in turn, makes the flux linking its own winding to become the maximum value. On the other hand, the self-inductance becomes the minimum value at the rotor positions of both 0 and 180° (the largest reluctance position).

Thus, the self-inductances vary sinusoidally with respect to the rotor angle θ_r and can be expressed as

$$L_{asas} = L_{ls} + L_A - L_B \cos 2\theta_r \tag{4.37}$$

$$L_{bsbs} = L_{ls} + L_A - L_B \cos 2\left(\theta_r - \frac{2}{3}\pi\right) \tag{4.38}$$

$$L_{cscs} = L_{ls} + L_A - L_B \cos 2\left(\theta_r + \frac{2}{3}\pi\right) \tag{4.39}$$

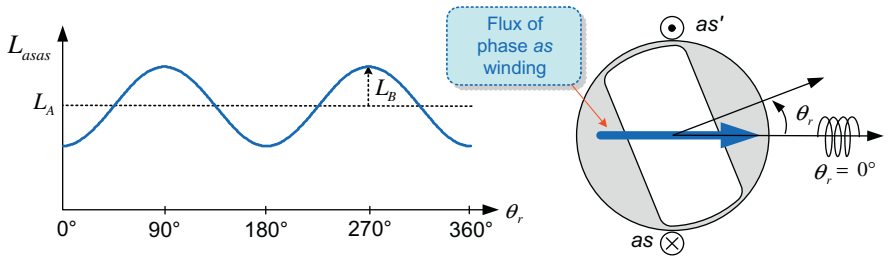


FIGURE 4.14

Self-inductance of phase *as* winding with respect to rotor positions.

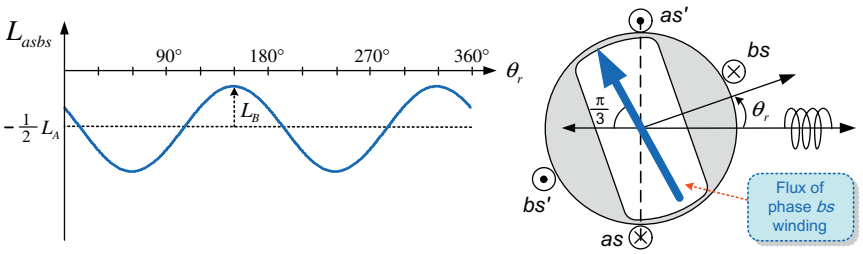


FIGURE 4.15

mutual-inductance between the phase *as* and *bs* stator windings.

where L_{ls} represents the leakage inductance, L_A represents the average value of the magnetizing inductance, and L_B represents the variation in value of the magnetizing inductance.

Similar to those of an induction motor, the mutual-inductances between the stator windings also vary sinusoidally with respect to the angle θ_r as shown in Fig. 4.15.

Thus they are given by

$$L_{asbs} = L_{bsas} = -\frac{1}{2}L_A - L_B\cos 2\left(\theta_r - \frac{\pi}{3}\right) \tag{4.40}$$

$$L_{ascs} = L_{csas} = -\frac{1}{2}L_A - L_B\cos 2\left(\theta_r + \frac{\pi}{3}\right) \tag{4.41}$$

$$L_{bscs} = L_{csbs} = -\frac{1}{2}L_A - L_B\cos 2\theta_r \tag{4.42}$$

With these inductances, the stator inductance is given by

$$\boldsymbol{L}_s = \begin{bmatrix} L_{ls}+L_A-L_B\cos 2\theta_r & -\frac{1}{2}L_A-L_B\cos 2\left(\theta_r-\frac{\pi}{3}\right) & -\frac{1}{2}L_A-L_B\cos 2\left(\theta_r+\frac{\pi}{3}\right) \\ -\frac{1}{2}L_A-L_B\cos 2\left(\theta_r-\frac{\pi}{3}\right) & L_{ls}+L_A-L_B\cos 2\left(\theta_r-\frac{2}{3}\pi\right) & -\frac{1}{2}L_A-L_B\cos 2\theta_r \\ -\frac{1}{2}L_A-L_B\cos 2\left(\theta_r+\frac{\pi}{3}\right) & -\frac{1}{2}L_A-L_B\cos 2\theta_r & L_{ls}+L_A-L_B\cos 2\left(\theta_r-\frac{4}{3}\pi\right) \end{bmatrix} \tag{4.43}$$

Next, let us determine the mutual-inductances L_{asf} L_{bsf} L_{csf} relevant to the amount of the permanent magnet flux linking the stator windings. These mutual-inductance are different depending on the position of the rotor because the magnet flux linking to the stator windings varies with the position of the rotor. As an example of the phase *as* winding, from Fig. 4.16, the mutual-inductance becomes a maximum value at the rotor position of 0°, while it becomes a minimum value at the rotor position of 180°.

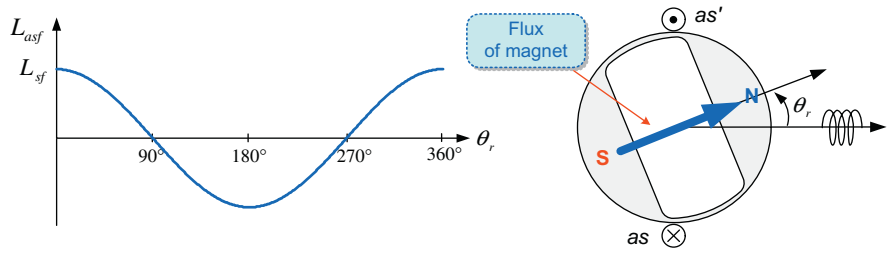


FIGURE 4.16

Mutual-inductance between stator *as* winding and magnet.

Unlike self-inductances, the mutual-inductances vary by $\cos\theta_r$ per one mechanical revolution of the rotor. So we have

$$L_{asf} = L_{sf}\cos\theta_r \tag{4.44}$$

$$L_{bsf} = L_{sf}\cos\left(\theta_r - \frac{2}{3}\pi\right) \tag{4.45}$$

$$L_{csf} = L_{sf}\cos\left(\theta_r + \frac{2}{3}\pi\right) \tag{4.46}$$

where L_{sf} depends on the amplitude of the flux linkage established by the permanent magnet.

From these inductances, the total flux linkages of an IPMSM are given by

$$\boldsymbol{\lambda}_{abcs} = \boldsymbol{L}_s\boldsymbol{i}_{abcs} + \boldsymbol{L}_f I_f$$

$$= \begin{bmatrix} L_{ls}+L_A-L_B\cos 2\theta_r & -\frac{1}{2}L_A-L_B\cos 2\left(\theta_r-\frac{\pi}{3}\right) & -\frac{1}{2}L_A-L_B\cos 2\left(\theta_r+\frac{\pi}{3}\right) \\ -\frac{1}{2}L_A-L_B\cos 2\left(\theta_r-\frac{\pi}{3}\right) & L_{ls}+L_A-L_B\cos 2\left(\theta_r-\frac{2}{3}\pi\right) & -\frac{1}{2}L_A-L_B\cos 2\theta_r \\ -\frac{1}{2}L_A-L_B\cos 2\left(\theta_r+\frac{\pi}{3}\right) & -\frac{1}{2}L_A-L_B\cos 2\theta_r & L_{ls}+L_A-L_B\cos 2\left(\theta_r-\frac{4}{3}\pi\right) \end{bmatrix} \begin{bmatrix} i_{as} \\ i_{bs} \\ i_{cs} \end{bmatrix}$$

$$+ L_{sf}\begin{bmatrix} \cos\theta_r \\ \cos\left(\theta_r-\frac{2}{3}\pi\right) \\ \cos\left(\theta_r-\frac{4}{3}\pi\right) \end{bmatrix} I_f \tag{4.47}$$

All the inductances in the flux linkages of an IPMSM are time varying except for at a standstill of the motor. Therefore the time-varying coefficients will appear in the voltage equations of an IPMSM. In the case of an SPMSM, we can easily obtain the flux linkages by letting $L_B = 0$ in Eq. (4.47).

From the discussion so far, we can see that the voltage equations of an induction motor and a synchronous motor are expressed as the differential equations with time-varying coefficients. Fortunately, by employing the reference frame transformation, these time-varying inductances in the voltage equations can be eliminated. Now, we will study the reference frame transformation and the AC motor models expressed by the *dq* variables.

4.3 REFERENCE FRAME TRANSFORMATION

Reference frame transformation refers to a transformation of the three-phase *abc* variables commonly used in AC systems to *dqn* variables orthogonal to each other. This transformation is often known as *d−q transformation*. Fig. 4.17 compares these variables. Here, the direction of the *abc* variables is considered to be the direction of the magnetic axes of their windings.

The direction of *d*, *q*, and *n* axes in orthogonal coordinates will be defined as the following.

- *d*-axis (direct axis)

  The direction of the *d* variable, which is called the *d*-axis, is normally chosen as the direction of the magnetic flux in the AC motor. In the vector control for AC motors, the *d*-axis is regarded as the reference axis, and the flux-producing component of motor current is aligned along the *d*-axis.

- *q*-axis (quadrature axis)

  The direction of the *q* variable, which is called the *q*-axis, is defined as the direction 90° ahead of the *d*-axis. In the vector control for AC motors,

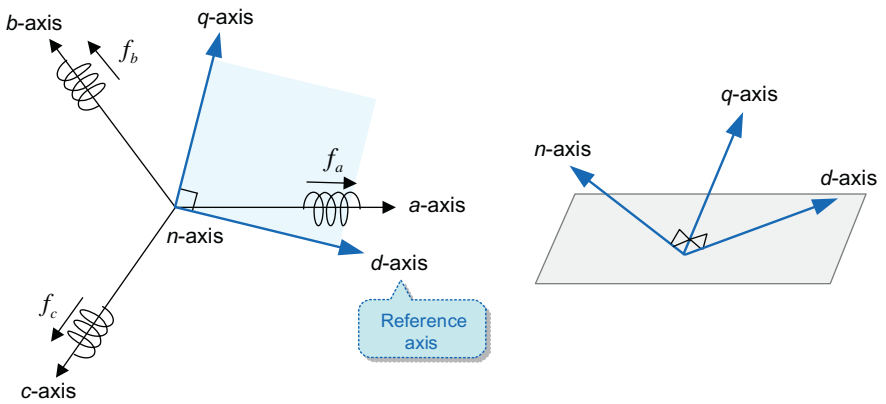


FIGURE 4.17

abc coordinate and *d−q* axes coordinate.

the torque-producing component of motor current or the back-EMF is aligned along the q-axis.

- n-axis (neutral axis)

  The direction of the n variable, which is called the n-axis, is defined as the direction that is orthogonal to both the d- and q-axes. The n-axis has nothing to do with the mechanical output power of the AC motor but is related to the losses.

4.3.1 TYPES OF THE $d-q$ REFERENCE FRAME

The frame of reference, consisting of d, q, and n axes, may rotate at any speed or remain stationary. Therefore, it can be mainly divided into *stationary reference frame* and *rotating reference frame* according to whether or not it will rotate as shown in Fig. 4.18.

- Stationary reference frame

  This frame of reference remains stationary. In other words, in the stationary reference frame, the $d-q$ coordinate system does not rotate. In this book, this will be denoted by $d^s - q^s$ axes. Normally, in AC motor drives, d^s-axis is chosen as the axis of phase *as*. This reference frame is also called *stator reference frame*.

- Rotating reference frame

  This frame of reference rotates at an angular speed ω. In other words, in the rotating reference frame, the $d-q$ coordinate system rotates at a speed ω. The speed of rotation can be chosen arbitrarily. In this book this reference frame will be denoted by $d^\omega - q^\omega$ axes.

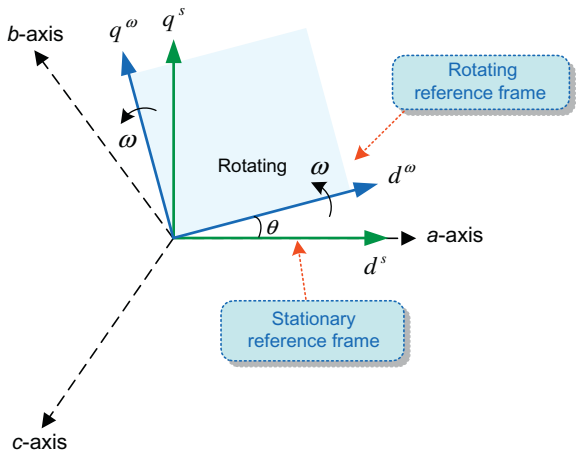


FIGURE 4.18

$d-q$ axes stationary reference frame and rotating reference frame.

Although the rotation of the $d-q$ coordinate system can be arbitrarily set to any speed, there are two widely used speeds or reference frames. The first one is a *synchronously rotating reference frame* or *synchronous reference frame*, which rotates at the speed of the rotating magnetic field and will be denoted by $d^e - q^e$ axes. The second one is a *rotor reference frame*, which rotates at the speed of the rotor and will be denoted by $d^r - q^r$ axes.

The angle between the rotating reference frame and the stationary reference frame may vary over time. This angle θ is given by an integral of the angular velocity ω of the rotating reference frame as

$$\theta = \int \omega(\tau) d\tau + \theta(0) \tag{4.48}$$

where $\theta(0)$ means the initial angle at time $t = 0$, and commonly, $\theta(0) = 0$.

In this book we will use the notation "f_{AB}^{ω}" to represent the variables employed in various reference frames. Here, "f" represents variables such as voltage, current, and flux linkage. A superscript "ω" denotes the angular speed of the reference frame. First, the subscript "A" denotes the type of the axis. $A = d, q, n$ for dqn variables, and $A = a, b, c$ for abc variables. Second, the subscript "B" denotes where the variable is. $B = s$ for the stator, and $B = r$ for the rotor. For example, "i_{ds}^{e}" represents the d-axis stator current in the synchronously rotating reference frame.

The reference frame transformation was originally proposed by R.H. Park in the late 1920s. This transformation is used only for synchronous machines in the rotor reference frame, which is commonly known as *Park's transformation*. Since then, several reference frame transformations have been developed for induction and synchronous machines. Later, it was found that all known types of reference frames can be obtained from arbitrary reference frames by simply changing the rotation speed. This arbitrary reference frame transformation is referred to as the *generalized rotating transformation* [1].

As mentioned earlier, the reference frame transformation to eliminate the time-varying coefficients refers to the transformation of the three-phase abc variables to dqn variables. The reference frame transformation can be easily carried out by using the *matrix forms* or *complex vectors*. First, let us take a look at the reference frame transformation by the matrix equations.

4.3.2 REFERENCE FRAME TRANSFORMATION BY MATRIX EQUATIONS

Fig. 4.19 demonstrates the transformation of the three-phase abc variables into dqn variables in the stationary reference frame.

The reference frame transformation can be simply considered as the orthogonal projection of the three-phase abc variables f_a, f_b, f_c onto the $d-q$ axis

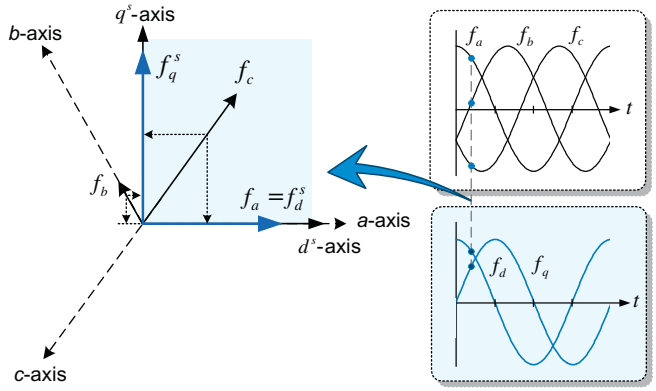


FIGURE 4.19

Transformation into the stationary reference frame.

in the stationary reference frame ($d^s - q^s$ axes). For the example in Fig. 4.19, using trigonometric relationships, the d- and q-axes variables becomes

$$f_d^s = k\left[f_a \cos(0) + f_b \cos\left(-\frac{2}{3}\pi\right) + f_c \cos\left(\frac{2}{3}\pi\right)\right] \tag{4.49}$$

$$f_q^s = k\left[f_a \sin(0) + f_b \sin\left(-\frac{2}{3}\pi\right) + f_c \sin\left(\frac{2}{3}\pi\right)\right] \tag{4.50}$$

Here, the coefficient k can be chosen arbitrarily.

The frame of reference can rotate at an angular velocity ω. So, the transformation of the three-phase stationary abc variables into dqn variables in the arbitrary reference frame rotating at a speed ω can be generally formulated as

$$\boldsymbol{f}_{dqn}^{\omega} = \boldsymbol{T}(\theta)\boldsymbol{f}_{abc} \tag{4.51}$$

where $\boldsymbol{f}_{dqn} = \left[f_d f_q f_n\right]^T$, $\boldsymbol{f}_{abc} = [f_a f_b f_c]^T$, and $[]^T$ denotes the transpose of a matrix. f_x can represent the variables of an AC motor such as voltage, current, and flux linkage.

The transformation matrix $\boldsymbol{T}(\theta)$ is defined as

$$\boldsymbol{T}(\theta) = \frac{2}{3}\begin{bmatrix} \cos\theta & \cos\left(\theta - \frac{2}{3}\pi\right) & \cos\left(\theta + \frac{2}{3}\pi\right) \\ -\sin\theta & -\sin\left(\theta - \frac{2}{3}\pi\right) & -\sin\left(\theta + \frac{2}{3}\pi\right) \\ \frac{1}{2} & \frac{1}{2} & \frac{1}{2} \end{bmatrix} \tag{4.52}$$

where the angular displacement $\theta = \int \omega(\tau)d\tau + \theta(0)$.

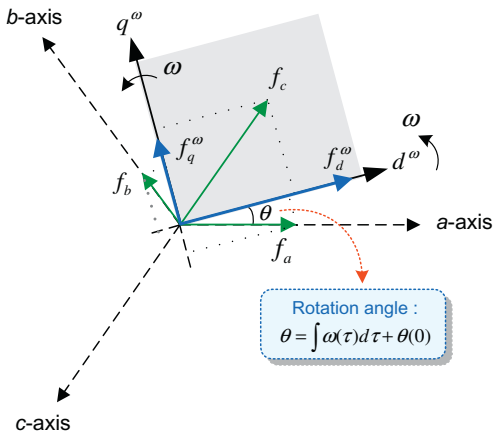


FIGURE 4.20

Transformation into the arbitrary rotating reference frame.

From Eq. (4.52), it can be seen that the f_n variable is independent of the reference frame but is related arithmetically to the *abc* variables. Fig. 4.20 demonstrates the resolution of the three-phase *abc* variables f_a, f_b, f_c into the *d*- and *q*-axes in the stationary reference frame ($d^s - q^s$ axes).

As mentioned previously, when transforming, the coefficient k can be chosen arbitrarily. In the transformation matrix $\boldsymbol{T}(\theta)$ of Eq. (4.52), the coefficient k is chosen as 2/3. In this case the magnitude of the *dq* variables is exactly identical to that of the *abc* variables, so, this transformation is called *magnitude invariance transformation*. However, the power and the torque evaluated in the *dqn* variables become 2/3 less than those evaluated in the *abc* variables, which will be shown later. On the other hand, when using the coefficient of $\sqrt{2/3}$, the power remains the same value in the two reference frames, i.e., $P_{dqn} = P_{abc}$. So, this transformation is called *power invariance transformation*. However, the magnitude of the *dq* variables is not equal to the magnitude of the *abc* variables. The coefficient of 2/3 is normally used when applying the transformation to motor variables. So, in this book, we always use the coefficient of 2/3 for magnitude invariance transformation.

4.3.2.1 *Transformation of* abc *variables into* dqn *variables in the stationary reference frame*

From setting $\theta = 0$ in Eq. (4.51), the transformation of the three-phase *abc* variables into *dqn* variables in the stationary reference frame is given by

$$\boldsymbol{f}_{dqn}^{s} = \boldsymbol{T}(0)\boldsymbol{f}_{abc} = \frac{2}{3}\begin{bmatrix} 1 & -\frac{1}{2} & -\frac{1}{2} \\ 0 & \frac{\sqrt{3}}{2} & -\frac{\sqrt{3}}{2} \\ \frac{1}{\sqrt{2}} & \frac{1}{\sqrt{2}} & \frac{1}{\sqrt{2}} \end{bmatrix}\begin{bmatrix} f_a \\ f_b \\ f_c \end{bmatrix} \tag{4.53}$$

This is known as *Clark's transformation*.

Eq. (4.53) can be disassembled as the following.

- Transformation of *abc* variables into *dqn* variables in the stationary reference frame

$$f_d^s = \frac{2f_a - f_b - f_c}{3} \tag{4.54}$$

$$f_q^s = \frac{1}{\sqrt{3}}(f_b - f_c) \tag{4.55}$$

$$f_n^s = \frac{2(f_a + f_b + f_c)}{3} \tag{4.56}$$

In the stationary reference frame, the *dqn* variables are arithmetically related to the *abc* variables. In particular, if the sum of the *abc* variables in a balanced three-phase system with no neutral connection is zero, i.e., $f_a + f_b + f_c = 0$, then the *n*-axis variable is zero, i.e., $f_n^s = 0$. Thus, $f_d^s = f_a$, i.e., the d^s-axis variable is always equal to the phase *a*-axis variable. In this case the *dq* variables are reduced as following.

$$f_d^s = f_a \quad (f_n^s = 0) \tag{4.57}$$

$$f_q^s = \frac{1}{\sqrt{3}}(f_b - f_c) \tag{4.58}$$

The inverse transformation of the *dqn* variables in the stationary reference frame into the *abc* variables is as following.

- Inverse transformation ($f_n^s = 0$)

$$f_a = f_d^s \tag{4.59}$$

$$f_b = -\frac{1}{2}f_d^s + \frac{\sqrt{3}}{2}f_q^s \tag{4.60}$$

$$f_c = -\frac{1}{2}f_d^s - \frac{\sqrt{3}}{2}f_q^s \tag{4.61}$$

4.3.2.2 Transformation between reference frames

Consider a transformation between reference frames. For the analysis of AC motors, it is often required to transform the variables in one reference frame to variables in another reference frame as shown in Fig. 4.21.

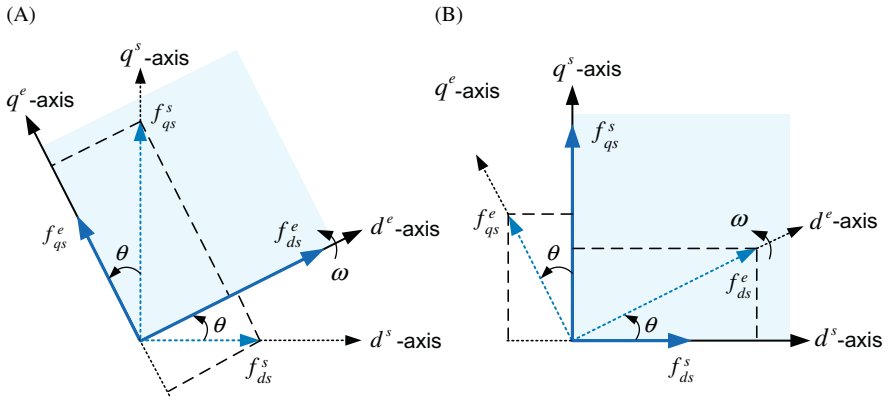


FIGURE 4.21

Transformation between reference frames. (A) Stationary into rotating frame and (B) rotating into stationary frame.

As a widely used transformation, the transformation of the stationary reference frame into the rotating reference frame can be formulated as

$$\boldsymbol{f}^e_{dqn} = \boldsymbol{R}(\theta)\boldsymbol{f}^s_{dqn} = \begin{bmatrix} \cos\theta & \sin\theta & 0 \\ -\sin\theta & \cos\theta & 0 \\ 0 & 0 & 1 \end{bmatrix} \begin{bmatrix} f^s_d \\ f^s_q \\ f^s_n \end{bmatrix} \tag{4.62}$$

The angular displacement $\theta = \int \omega(\tau)d\tau + \theta(0)$.

This is known as *Park's transformation*.

In the case where the n variable is zero, i.e., $f^s_n = 0$, Eq. (4.62) can be separated into Eqs. (4.63) and (4.64).

- Transformation of stationary reference frame into rotating reference frame

$$f^e_d = f^s_d\cos\theta + f^s_q\sin\theta \tag{4.63}$$

$$f^e_q = -f^s_d\sin\theta + f^s_q\cos\theta \tag{4.64}$$

Likewise, for the inverse transformation, it will be Eqs. (4.65) and (4.66).

- Inverse transformation of stationary reference frame into rotating reference frame

$$f^s_d = f^e_d\cos\theta - f^e_q\sin\theta \tag{4.65}$$

$$f^s_q = f^e_d\sin\theta + f^e_q\cos\theta \tag{4.66}$$

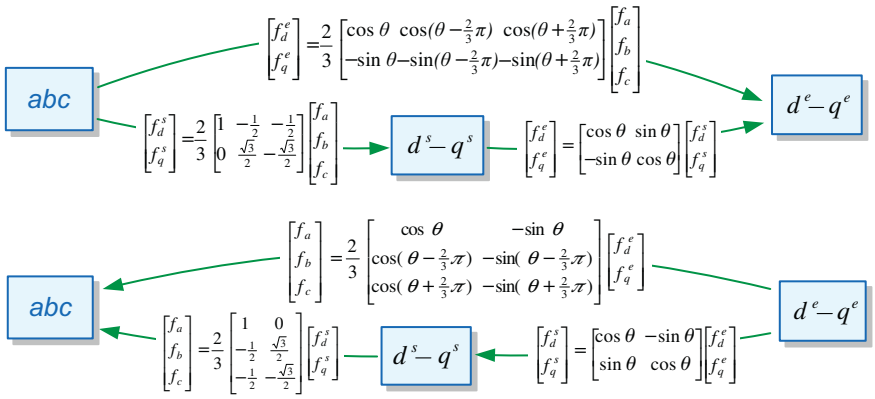


FIGURE 4.22

Reference frame transformations.

The procedure for all the transformations just mentioned is summarized in Fig. 4.22.

Next, we will find the instantaneous power expressed in *dqn* variables. The instantaneous power may be expressed in *abc* variables as

$$P = v_a i_a + v_b i_b + v_c i_c = \boldsymbol{V}_{abc}^T \boldsymbol{I}_{abc} \tag{4.67}$$

where $\boldsymbol{V}_{abc}^T = [v_a v_b v_c]^T$, $\boldsymbol{I}_{abc} = [i_a i_b i_c]$.

By transforming the above equation into the arbitrary reference frame rotating at any angular velocity ω, the instantaneous power is given by

$$\begin{aligned} P = \boldsymbol{V}_{abc}^T \boldsymbol{I}_{abc} &= \left[\boldsymbol{T}^{-1}(\theta)\boldsymbol{V}_{dqn}^{\omega}\right]^T \left[\boldsymbol{T}^{-1}(\theta)\boldsymbol{I}_{dqn}^{\omega}\right] \\ &= \frac{3}{2}(\boldsymbol{V}_{dqn}^{\omega})^T \boldsymbol{I}_{dqn}^{\omega} = \frac{3}{2}(v_d^{\omega} i_d^{\omega} + v_q^{\omega} i_q^{\omega} + v_n^{\omega} i_n^{\omega}) \end{aligned} \tag{4.68}$$

where $\boldsymbol{V}_{dqn}^{\omega} = \left[v_d^{\omega} v_q^{\omega} v_n^{\omega}\right]^T$, $\boldsymbol{I}_{dqn}^{\omega} = \left[i_d^{\omega} i_q^{\omega} i_n^{\omega}\right]^T$, $\boldsymbol{T}^{-1}(\theta) = \frac{3}{2}\boldsymbol{T}^T(\theta)$.

Although the power of Eq. (4.68) has a 3/2 factor due to the choice of the constant used in the transformation matrix $\boldsymbol{T}(\theta)$, it is expressed as the sum of the product of the voltage and the current in each axis like the power expression in the three-phase system. The waveforms of the voltage, current, and flux linkage vary according to the angular velocity of the reference frame, whereas the waveform of the power remains unchanged.

EXAMPLE 1

Transform the following balanced three-phase *abc* voltages into *dqn* voltages in the stationary and rotating reference frames.

$$v_{as} = V_m \cos \omega_e t, \quad v_{bs} = V_m \cos(\omega_e t - 120^\circ), \quad v_{cs} = V_m \cos(\omega_e t - 240^\circ),$$

Solution

From Eq. (4.53), *dqn* voltages in the stationary reference frame are given as

$$v_{ds}^s = \frac{2v_{as} - v_{bs} - v_{cs}}{3} = v_{as} = V_m \cos \omega_e t$$

$$v_{qs}^s = \frac{1}{\sqrt{3}}(v_{bs} - v_{cs}) = V_m \sin \omega_e t$$

$$v_{ns}^s = \frac{\sqrt{2}(v_{as} + v_{bs} + v_{cs})}{3} = 0$$

Therefore, the three-phase *abc* variables, each displaced by 120°, are transformed into two-phase *dq* variables, each displaced by 90°, in the stationary reference frame. These amplitudes are equal to each other but the variable of *d*-axis is ahead of the variable of *q*-axis by 90°.

From Eq. (4.62), *dq* voltages in the synchronously rotating reference frame ($d^e - q^e$ axes) are given as

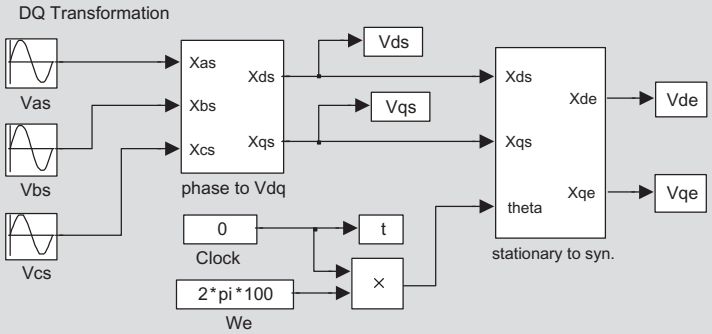
$$\begin{aligned} v_{ds}^e &= v_{ds}^s \cos \theta_e + v_{qs}^s \sin \theta_e \\ &= V_m \cos \omega_e t \cos \theta_e + V_m \sin \omega_e t \sin \theta_e = V_m \end{aligned}$$

$$\begin{aligned} v_{qs}^e &= -v_{ds}^s \sin \theta_e + v_{qs}^s \cos \theta_e \\ &= -V_m \cos \omega_e t \sin \theta_e + V_m \sin \omega_e t \cos \theta_e = 0 \end{aligned}$$

Here, the initial position of the reference frame is set to zero, thus $\theta_e = \omega_e t$. It should be noted that the three-phase *abc* variables are expressed as steady-state direct current (DC) values in the *dq* reference frame rotating at the angular velocity ω_e same as that of *abc* variables. The amplitude of the DC value is equal to the peak value of the *abc* variables.

MATLAB/SIMULINK SIMULATION: REFERENCE FRAME TRANSFORMATIONS

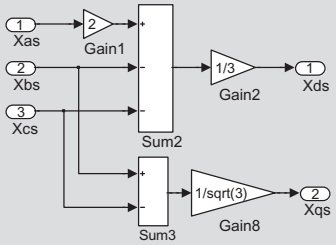
- Simulation conditions: $V_m = 100$ V, frequency = 100 Hz,
  Phase *as* voltage $v_{as} = V_m \cos \omega_e t = 100 \cos(2\pi 100t)$
- Whole simulation block diagram



- Transformation of the three-phase *abc* variables into *dq* variables in the stationary reference frame (phase to V_{dq} block)

$$f_d^s = \frac{2f_a - f_b - f_c}{3}$$

$$f_q^s = \frac{1}{\sqrt{3}}\left(f_b - f_c\right)$$



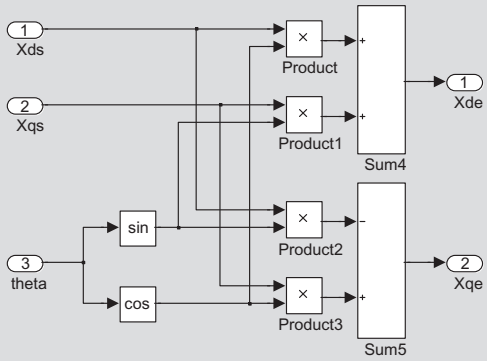
- Transformation of the stationary reference frame into the rotating reference frame (stationary to syn. block)

$$f_d^e = f_d^s \cos\theta + f_q^s \sin\theta, \quad f_q^e = -f_d^s \sin\theta + f_q^s \cos\theta$$

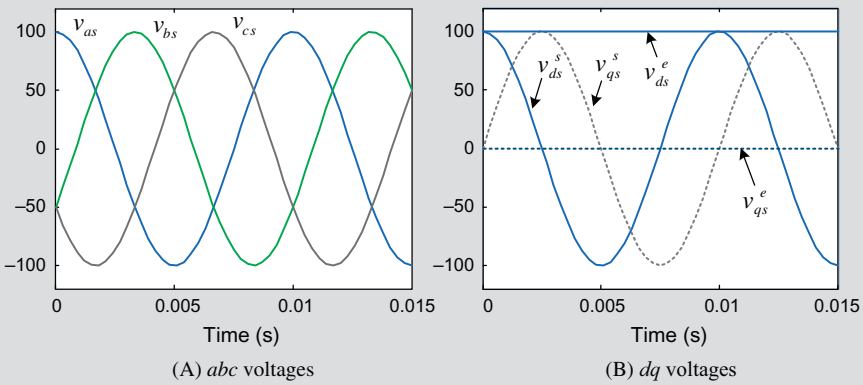
  - Angular displacement: $\theta = \int \omega_e(t)dt = \int (2\pi f)dt = 2\pi 100t = 2\pi 100t$

(*Continued*)

MATLAB/SIMULINK SIMULATION: REFERENCE FRAME TRANSFORMATIONS (CONTINUED)



- Simulation results



(A) *abc* voltages (B) *dq* voltages

We have just studied the reference frame transformation by the matrix equations. We can carry out this transformation more efficiently by using a complex vector, which is a representation of the three quantities in the three-phase system as one quantity. Moreover, by treating three-phase AC motor quantities as complex vectors, the work required in the calculations for a three-phase AC motor can be simplified. Now, we will take a look at the reference frame transformation by the complex vector.

4.3.3 REFERENCE FRAME TRANSFORMATION BY COMPLEX VECTOR

Any three-phase quantity can be represented by a vector $\boldsymbol{f}_{abc}$ in the complex plane as shown in Fig. 4.23.

This vector is called the *complex space vector*, or in short, *space vector*. The complex vector representation allows us to analyze the three-phase system as a whole instead of looking at each phase individually. A space vector is different from a *phasor*, which is a representation of the amplitude and phase for a sine wave in the steady-state condition.

A complex space vector is defined as

$$\boldsymbol{f}_{abc} \equiv \frac{2}{3}(f_a + af_b + a^2 f_c) \quad \left(a = e^{j(2\pi/3)},\ a^2 = e^{j(4\pi/3)}\right) \tag{4.69}$$

This space vector rotates at the same angular velocity ω_e as that of the three-phase quantities as shown in Fig. 4.24.

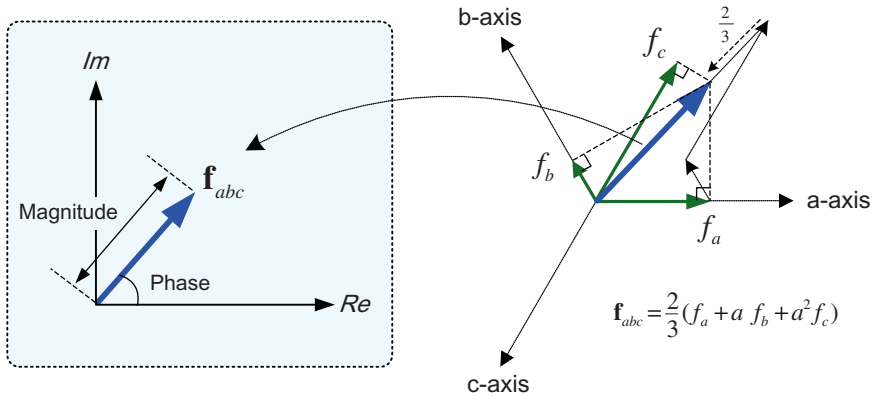


FIGURE 4.23

Complex space vector.

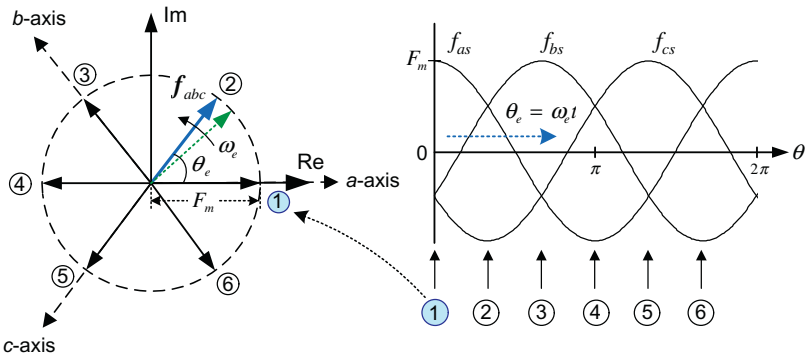


FIGURE 4.24

Three-phase quantities and complex space vector.

The amplitude of a space vector is equal to the peak value of the phase quantity. One example of a space vector is the rotating magnetic field as mentioned in Chapter 3. The rotating magnetic field is identical to the space vector of magnetic fields produced by currents flowing in three-phase windings.

Example 2

Find the space vector representation of three-phase voltages as

$$v_{as} = V_m \cos \omega_e t, \quad v_{bs} = V_m \cos(\omega_e t - 120^\circ), \quad v_{cs} = V_m \cos(\omega_e t - 240^\circ)$$

Solution

According to the definition, voltage space vector $\boldsymbol{V}_{abc}$ is given as

$$\boldsymbol{V}_{abc} = \frac{2}{3}(v_{as} + a v_{bs} + a^2 v_{cs})$$

From Euler formula $e^{j\theta} = \cos\theta + j \sin\theta$, we have $\cos \omega_e t = (e^{j\omega_e t} + e^{-j\omega_e t})/2$, $\sin \omega_e t = (e^{j\omega_e t} - e^{-j\omega_e t})/2j$. Thus,

$$\boldsymbol{V}_{abc} = \frac{2V_m}{3}\left(\frac{e^{j\omega_e t} + e^{-j\omega_e t}}{2} + a\frac{e^{j(\omega_e t - 2\pi/3)} + e^{-j(\omega_e t - 2\pi/3)}}{2} + a^2\frac{e^{j(\omega_e t - 4\pi/3)} + e^{-j(\omega_e t - 4\pi/3)}}{2}\right)$$

$$= \frac{V_m}{3}(3e^{j\omega_e t} + e^{-j\omega_e t}(1 + a + a^2)) = V_m e^{j\omega_e t}$$

where $a = e^{j(2\pi/3)} = \cos\frac{2}{3}\pi + j \sin\frac{2}{3}\pi = -\frac{1}{2} + j\frac{\sqrt{3}}{2}$,

$$a^2 = e^{j(4\pi/3)} = \cos\tfrac{4}{3}\pi + j \sin\tfrac{4}{3}\pi = -\tfrac{1}{2} - j\tfrac{\sqrt{3}}{2}$$

$$\therefore \quad \boldsymbol{V}_{abc} = V_m e^{j\omega_e t} = V_m e^{j\theta_e} \quad \left(\theta_e = \int \omega_e(t)dt + \theta(0)\right)$$

Inversely, the quantities of a three-phase system from the space vector $\boldsymbol{f}_{abc}$ are given by

$$f_a = \mathrm{Re}[\boldsymbol{f}_{abc}] + f_n^{\omega}$$

$$= \mathrm{Re}\left[\frac{2}{3}(f_a + a f_b + a^2 f_c)\right] + \frac{1}{3}(f_a + f_b + f_c) = f_a \tag{4.70}$$

$$f_b = \mathrm{Re}[a^2 \boldsymbol{f}_{abc}] + f_n^{\omega} \tag{4.71}$$

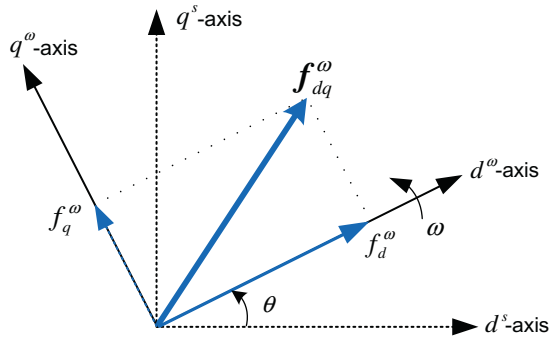


FIGURE 4.25

Vector $\boldsymbol{f}^{\omega}_{dq}$ in the arbitrary reference frame rotating at an angular velocity.

$$f_c = \mathrm{Re}[a\boldsymbol{f}_{abc}] + f^{\omega}_n \tag{4.72}$$

where "Re" represents the real part of the complex vector.

When comparing the complex plane with the $d-q$ coordinate system mentioned in the previous section, we can see that these two systems have similar orthogonal coordinates, that is, the real-axis and the imaginary-axis correspond to the d-axis and the q-axis in the stationary reference frame, respectively. Thus, we can consider that the space vector $\boldsymbol{f}_{abc}$ equals to the vector $\boldsymbol{f}^{s}_{dq}$ in the stationary reference frame, which has the d- and q-axes components of Eqs. (4.49) and (4.50) as

$$\boldsymbol{f}^{s}_{dq} = f^{s}_{d} + jf^{s}_{q} \tag{4.73}$$

However, since the $d-q$ axis may rotate at any angular velocity, we need to take a look at the relationship between a space vector and a vector in the $d-q$ axes rotating at an angular velocity. A vector $\boldsymbol{f}^{\omega}_{dq}$ in the arbitrary reference frame rotating at a speed ω in Fig. 4.25 can be expressed as

$$\boldsymbol{f}^{\omega}_{dq} = f^{\omega}_{d} + \mathrm{j}f^{\omega}_{q} \tag{4.74}$$

Here, from Eqs. (4.49) and (4.50), the d- and q-axes components of this vector are given by

$$f^{\omega}_{d} = \frac{2}{3}\left[f_a\cos\theta + f_b\cos\left(\theta - \frac{2}{3}\pi\right) + f_c\cos\left(\theta - \frac{4}{3}\pi\right)\right]$$

$$f^{\omega}_{q} = -\frac{2}{3}\left[f_a\sin\theta + f_b\sin\left(\theta - \frac{2}{3}\pi\right) + f_c\sin\left(\theta - \frac{4}{3}\pi\right)\right]$$

Using Euler formula, Eq. (4.74) becomes

$$\begin{aligned}\boldsymbol{f}_{dq}^{\omega} &= \frac{2}{3}\left[f_a(\cos\theta - \mathrm{j}\sin\theta) + f_b\left(\cos\left(\theta-\frac{2}{3}\pi\right) - \mathrm{j}\sin\left(\theta-\frac{2}{3}\pi\right)\right)\right.\\ &\quad \left. + f_c\left(\cos\left(\theta-\frac{4}{3}\pi\right) - \mathrm{j}\sin\left(\theta-\frac{4}{3}\pi\right)\right)\right]\\ &= \frac{2}{3}\left[f_a e^{-\mathrm{j}\theta} + f_a e^{-\mathrm{j}\left(\theta-\frac{2}{3}\pi\right)} + f_a e^{-\mathrm{j}\left(\theta-\frac{4}{3}\pi\right)}\right] = \frac{2}{3}\left[f_a + af_a + a^2 f_a\right]e^{-\mathrm{j}\theta}\\ &= \boldsymbol{f}_{abc}e^{-\mathrm{j}\theta}\end{aligned} \tag{4.75}$$

From Eq. (4.75), we can see that there is only a phase difference of θ between $\boldsymbol{f}_{abc}$ and $\boldsymbol{f}_{dq}^{\omega}$. This phase difference comes from the angular displacement between the complex plane and the $d-q$ axes rotating at an angular velocity.

By letting $\theta = 0$ in Eq. (4.75), we can identify that the space vector $\boldsymbol{f}_{abc}$ equals to the vector $\boldsymbol{f}_{dq}^{s}$ in the $d-q$ axis of the stationary reference frame as

$$\boldsymbol{f}_{dq}^{s} = \boldsymbol{f}_{abc}e^{-\mathrm{j}0} = \boldsymbol{f}_{abc} \tag{4.76}$$

A vector $\boldsymbol{f}_{dq}^{\omega}$ in the rotating reference frame with the angular velocity $\omega = \omega_e$ can be expressed as

$$\boldsymbol{f}_{dq}^{e} = \boldsymbol{f}_{abc}e^{-\mathrm{j}\theta_e} = \boldsymbol{f}_{dq}^{s}e^{-\mathrm{j}\theta_e} \quad \left(\theta_e = \int \omega_e(t)dt + \theta(0)\right) \tag{4.77}$$

The instantaneous power is expressed in terms of the complex vector as

$$P = \frac{3}{2}\mathrm{Re}\left[\boldsymbol{V}_{abc}\boldsymbol{I}_{abc}^{*}\right] = \frac{3}{2}\mathrm{Re}\left[\boldsymbol{V}_{dq}^{\omega}\boldsymbol{I}_{dq}^{\omega *}\right] \tag{4.78}$$

where $\boldsymbol{I}_{abc}^{*}$, $\boldsymbol{I}_{dq}^{*}$ are the complex conjugates of $\boldsymbol{I}_{abc}$, $\boldsymbol{I}_{dq}$, respectively.

We have just studied the transformation changing the reference frame of variables. Now, we are going to find out the model of AC motors expressed in the $d-q$ reference frame. Then, it will be found that the time-varying inductances in the voltage equations of AC motors can be eliminated by employing the reference frame transformation. First, let us find out the $d-q$ axes model for an induction motor.

4.4 $d-q$ AXES MODEL OF AN INDUCTION MOTOR

From Eqs. (4.2)–(4.7), the voltage equations for the stator and rotor windings of an induction motor and the flux linkages are rewritten as

$$\boldsymbol{v}_{abcs} = \boldsymbol{R}_s\boldsymbol{i}_{abcs} + \frac{d\boldsymbol{\lambda}_{abcs}}{dt} \tag{4.79}$$

$$\boldsymbol{v}_{abcr} = \boldsymbol{R}_r \boldsymbol{i}_{abcr} + \frac{d\boldsymbol{\lambda}_{abcr}}{dt} \tag{4.80}$$

$$\begin{bmatrix} \boldsymbol{\lambda}_{abcs} \\ \boldsymbol{\lambda}_{abcr} \end{bmatrix} = \begin{bmatrix} \boldsymbol{L}_s & \boldsymbol{L}_{sr} \\ (\boldsymbol{L}_{sr})^T & \boldsymbol{L}_r \end{bmatrix} \begin{bmatrix} \boldsymbol{i}_{abcs} \\ \boldsymbol{i}_{abcr} \end{bmatrix} \tag{4.81}$$

Combining Eqs. (4.79) and (4.80) with (4.81), we have the voltage equations expressed in currents and inductances as

$$\begin{bmatrix} \boldsymbol{v}_{abcs} \\ \boldsymbol{v}_{abcr} \end{bmatrix} = \begin{bmatrix} R_s + p\boldsymbol{L}_s & \boldsymbol{L}_{sr} \\ p(\boldsymbol{L}_{sr})^T & R_r + p\boldsymbol{L}_r \end{bmatrix} \begin{bmatrix} \boldsymbol{i}_{abcs} \\ \boldsymbol{i}_{abcr} \end{bmatrix} \tag{4.82}$$

where p is the time derivative operator d/dt

Now, let us transform these equations expressed as abc variables into the $d-q$ coordinate system.

4.4.1 VOLTAGE EQUATIONS IN THE $d-q$ AXES

The transformation of the stator voltage equations of Eq. (4.79) into the $d-q$ axes rotating at an arbitrary speed ω is as follows:

$$\boldsymbol{v}_{abcs} = \boldsymbol{R}_s \boldsymbol{i}_{abcs} + \frac{d\boldsymbol{\lambda}_{abcs}}{dt}$$

$$\rightarrow \boldsymbol{T}(\theta)\boldsymbol{v}_{abcs} = \boldsymbol{T}(\theta)\boldsymbol{R}_s \boldsymbol{i}_{abcs} + \boldsymbol{T}(\theta)\frac{d\boldsymbol{\lambda}_{abcs}}{dt} \quad (\text{where } \boldsymbol{T}(\theta)\boldsymbol{R}_s\,\boldsymbol{T}(\theta)^{-1} = \boldsymbol{R}_s)$$

$$\rightarrow \boldsymbol{v}^{\omega}_{dqns} = \boldsymbol{R}_s \boldsymbol{i}^{\omega}_{dqns} + \boldsymbol{T}(\theta)\frac{d\boldsymbol{T}(\theta)^{-1}}{dt}\boldsymbol{\lambda}^{\omega}_{dqns} + \boldsymbol{T}(\theta)\boldsymbol{T}(\theta)^{-1} \quad \left(\text{where } \boldsymbol{T}(\theta)\frac{d\boldsymbol{T}(\theta)^{-1}}{dt} = \begin{bmatrix} 0 & -\omega & 0 \\ \omega & 0 & 0 \\ 0 & 0 & 0 \end{bmatrix}\right)$$

$$\rightarrow \boldsymbol{v}^{\omega}_{dqns} = \boldsymbol{R}_s \boldsymbol{i}^{\omega}_{dqns} + \begin{bmatrix} 0 & -\omega & 0 \\ \omega & 0 & 0 \\ 0 & 0 & 0 \end{bmatrix} \boldsymbol{\lambda}^{\omega}_{dqns} + \frac{d\boldsymbol{\lambda}^{\omega}_{dqns}}{dt}$$

This can be resolved into as

$$v^{\omega}_{ds} = R_s i^{\omega}_{ds} + \frac{d\lambda^{\omega}_{ds}}{dt} - \omega\lambda^{\omega}_{qs} \tag{4.83}$$

$$v^{\omega}_{qs} = R_s i^{\omega}_{qs} + \frac{d\lambda^{\omega}_{qs}}{dt} + \omega\lambda^{\omega}_{ds} \tag{4.84}$$

$$v^{\omega}_{ns} = R_s i^{\omega}_{ns} + \frac{d\lambda^{\omega}_{ns}}{dt} \tag{4.85}$$

Comparing the voltage equations in the abc coordinate system, we can see that there are *speed voltage* terms, $\omega\lambda^{\omega}_{qs}$ and $\omega\lambda^{\omega}_{ds}$, in the $d-q$ coordinate system due to the rotation of the axes. In addition, it should be noted that the flux linkages in these speed voltages are cross-coupled.

Next, we will transform the rotor voltage equations of Eq. (4.80) into $d-q$ axes rotating at an arbitrary speed ω. In this case we should be careful when selecting the angle used in the transformation. From the standpoint of the rotor, which rotates at the speed ω_r, the $d-q$ axes will rotate at the difference speed

$\omega - \omega_r$. Thus the angle used in the transformation should be $\theta - \theta_r (= \beta)$. Here, $\theta\left(= \int \omega_e(t)dt\right)$ is the displacement angle of the $d-q$ axes and $\theta_r\left(= \int \omega_r(t)dt\right)$is the displacement angle of the rotor.

With the angle β, we can transform the rotor voltage equations into the $d-q$ axes rotating at an arbitrary speed ω as

$$\boldsymbol{v}_{abcr} = \boldsymbol{R}_r \boldsymbol{i}_{abcr} + \frac{d\boldsymbol{\lambda}_{abcr}}{dt}$$

$$\rightarrow \boldsymbol{T}(\beta)\boldsymbol{v}_{abcr} = \boldsymbol{T}(\beta)\boldsymbol{R}_r \boldsymbol{i}_{abc} + \boldsymbol{T}(\beta)\frac{d\boldsymbol{\lambda}_{abcr}}{dt}$$

$$\rightarrow \boldsymbol{v}^{\omega}_{dqnr} = \boldsymbol{T}(\beta)\boldsymbol{R}_r(\boldsymbol{T}(\beta)^{-1}\boldsymbol{i}^{\omega}_{dqnr}) + \boldsymbol{T}(\beta)\frac{d[\boldsymbol{T}(\beta)^{-1}\boldsymbol{\lambda}^{\omega}_{dqnr}]}{dt} \quad \text{where } (\boldsymbol{T}(\beta)\boldsymbol{R}_s\boldsymbol{T}(\beta)^{-1} = \boldsymbol{R}_r)$$

$$\rightarrow \boldsymbol{v}^{\omega}_{dqnr} = \boldsymbol{R}_r \boldsymbol{i}^{\omega}_{dqnr} + \boldsymbol{T}(\beta)\frac{d\boldsymbol{T}(\beta)^{-1}}{dt}\boldsymbol{\lambda}^{\omega}_{dqnr} + \boldsymbol{T}(\beta)\boldsymbol{T}(\beta)^{-1}\frac{d\boldsymbol{\lambda}^{\omega}_{dqnr}}{dt}$$

$$\rightarrow \boldsymbol{v}^{\omega}_{dqnr} = \boldsymbol{R}_r \boldsymbol{i}^{\omega}_{dqnr} + \begin{bmatrix} 0 & -(\omega-\omega_r) & 0 \\ \omega-\omega_r & 0 & 0 \\ 0 & 0 & 0 \end{bmatrix}\boldsymbol{\lambda}^{\omega}_{dqrs} + \frac{d\boldsymbol{\lambda}^{\omega}_{dqnr}}{dt}$$

This can be resolved into

$$v^{\omega}_{dr} = R_r i^{\omega}_{dr} + \frac{d\lambda^{\omega}_{dr}}{dt} - (\omega - \omega_r)\lambda^{\omega}_{qr} \tag{4.86}$$

$$v^{\omega}_{qr} = R_r i^{\omega}_{qr} + \frac{d\lambda^{\omega}_{qr}}{dt} + (\omega - \omega_r)\lambda^{\omega}_{dr} \tag{4.87}$$

$$v^{\omega}_{nr} = R_r i^{\omega}_{nr} + \frac{d\lambda^{\omega}_{nr}}{dt} \tag{4.88}$$

For squirrel-cage rotor induction motors, since the rotor bars are short-circuited by the end rings, the rotor voltage is zero, and thus, $v^{\omega}_{dr} = 0,\ v^{\omega}_{qr} = 0,\ v^{\omega}_{nr} = 0$.

To complete these stator and rotor voltage equations, we need the flux linkages expressed as dq variables.

4.4.2 FLUX LINKAGE EQUATIONS IN THE $d-q$ AXES

The transformation of the stator flux linkage of Eq. (4.81) into the $d-q$ axes rotating at an arbitrary speed ω is as follows:

$$\boldsymbol{\lambda}_{abcs} = \boldsymbol{L}_s \boldsymbol{i}_{abcs} + \boldsymbol{L}_{sr}\boldsymbol{i}_{abcr}$$

$$\rightarrow \boldsymbol{T}(\theta)\boldsymbol{\lambda}_{abcs} = \boldsymbol{T}(\theta)\boldsymbol{L}_s \boldsymbol{i}_{abcs} + \boldsymbol{T}(\theta)\boldsymbol{L}_{sr}\boldsymbol{i}_{abcr}$$

$$\rightarrow \boldsymbol{\lambda}^{\omega}_{dqns} = \boldsymbol{T}(\theta)\boldsymbol{L}_s(\boldsymbol{T}^{-1}(\theta)\boldsymbol{i}^{\omega}_{dqns}) + \boldsymbol{T}(\theta)\boldsymbol{L}_{sr}(\boldsymbol{T}^{-1}(\beta)\boldsymbol{i}^{\omega}_{dqnr})$$

$$\rightarrow \boldsymbol{\lambda}^{\omega}_{dqns} = \begin{bmatrix} L_{ls} + \frac{3}{2}L_{ms} & 0 & 0 \\ 0 & L_{ls} + \frac{3}{2}L_{ms} & 0 \\ 0 & 0 & L_{ls} \end{bmatrix}\boldsymbol{i}^{\omega}_{dqns} + \begin{bmatrix} \frac{3}{2}L_{ms} & 0 & 0 \\ 0 & \frac{3}{2}L_{ms} & 0 \\ 0 & 0 & 0 \end{bmatrix}\boldsymbol{i}^{\omega}_{dqnr}$$

where

$$\boldsymbol{T}(\theta)\boldsymbol{L}_s\boldsymbol{T}^{-1}(\theta)=\begin{bmatrix} L_{ls}+\frac{3}{2}L_{ms} & 0 & 0 \\ 0 & L_{ls}+\frac{3}{2}L_{ms} & 0 \\ 0 & 0 & L_{ls} \end{bmatrix},\quad \boldsymbol{T}(\theta)\boldsymbol{L}_{sr}\boldsymbol{T}^{-1}(\beta)=\begin{bmatrix} \frac{3}{2}L_{ms} & 0 & 0 \\ 0 & \frac{3}{2}L_{ms} & 0 \\ 0 & 0 & 0 \end{bmatrix}$$

By letting $L_m=\frac{3}{2}L_{ms}$, $L_s=L_{ls}+L_m$ in the above equations, we will have the stator flux linkages in the $d-q$ axes as

$$\lambda_{ds}^{\omega}=L_{ls}i_{ds}^{\omega}+L_m(i_{ds}^{\omega}+i_{dr}^{\omega})=L_s i_{ds}^{\omega}+L_m i_{dr}^{\omega} \tag{4.89}$$

$$\lambda_{qs}^{\omega}=L_{ls}i_{qs}^{\omega}+L_m(i_{qs}^{\omega}+i_{qr}^{\omega})=L_s i_{qs}^{\omega}+L_m i_{qr}^{\omega} \tag{4.90}$$

$$\lambda_{ns}^{\omega}=L_{ls}i_{ns}^{\omega} \tag{4.91}$$

Next, we transform the rotor flux linkage of Eq. (4.81) into the $d-q$ axes rotating at an arbitrary speed ω as follows.

$$\boldsymbol{\lambda}_{abcr}=\boldsymbol{L}_r\boldsymbol{i}_{abcr}+\boldsymbol{L}_{rs}\boldsymbol{i}_{abcs}$$

$$\rightarrow \boldsymbol{T}(\beta)\boldsymbol{\lambda}_{abcr}=\boldsymbol{T}(\beta)\boldsymbol{L}_r\boldsymbol{i}_{abcr}+\boldsymbol{T}(\beta)\boldsymbol{L}_{sr}^{T}\boldsymbol{i}_{abcs}$$

$$\rightarrow \boldsymbol{\lambda}_{dqnr}^{\omega}=\boldsymbol{T}(\beta)\boldsymbol{L}_r(\boldsymbol{T}^{-1}(\beta)\boldsymbol{i}_{dqnr}^{\omega})+\boldsymbol{T}(\beta)\boldsymbol{L}_{sr}^{T}(\boldsymbol{T}^{-1}(\theta)\boldsymbol{i}_{dqns}^{\omega})$$

$$\rightarrow \boldsymbol{\lambda}_{dqnr}^{\omega}=\begin{bmatrix} L_{ls}+\frac{3}{2}L_{mr} & 0 & 0 \\ 0 & L_{ls}+\frac{3}{2}L_{mr} & 0 \\ 0 & 0 & L_{ls} \end{bmatrix}\boldsymbol{i}_{dqnr}^{\omega}+\begin{bmatrix} \frac{3}{2}L_{ms} & 0 & 0 \\ 0 & \frac{3}{2}L_{ms} & 0 \\ 0 & 0 & 0 \end{bmatrix}\boldsymbol{i}_{dqns}^{\omega}$$

Assuming the turns ratio $N_s/N_r=1$ and letting $L_m=\frac{3}{2}L_{mr}=\frac{3}{2}L_{ms}$, $L_r=L_{lr}+L_m$ in the above equations, we will have rotor flux linkages in the $d-q$ axes as

$$\lambda_{dr}^{\omega}=L_{lr}i_{dr}^{\omega}+L_m(i_{dr}^{\omega}+i_{ds}^{\omega})=L_r i_{dr}^{\omega}+L_m i_{ds}^{\omega} \tag{4.92}$$

$$\lambda_{qr}^{\omega}=L_{lr}i_{qr}^{\omega}+L_m(i_{qr}^{\omega}+i_{qs}^{\omega})=L_r i_{qr}^{\omega}+L_m i_{qs}^{\omega} \tag{4.93}$$

$$\lambda_{nr}^{\omega}=L_{lr}i_{nr}^{\omega} \tag{4.94}$$

From the flux linkage expressions of the stator and rotor in the $d-q$ axes, it is found that the main purpose of the transformation has been achieved. In other words, by employing the reference frame transformation, the time-varying mutual-inductances due to the relative motion between the stator and rotor windings become constant in the $d-q$ reference frame. This result can be valid regardless of the rotating speed of the reference frame. Furthermore, the flux linkages become magnetically decoupled between the d- and q-axes. Fig. 4.26 shows the $d-q$ axes equivalent circuits.

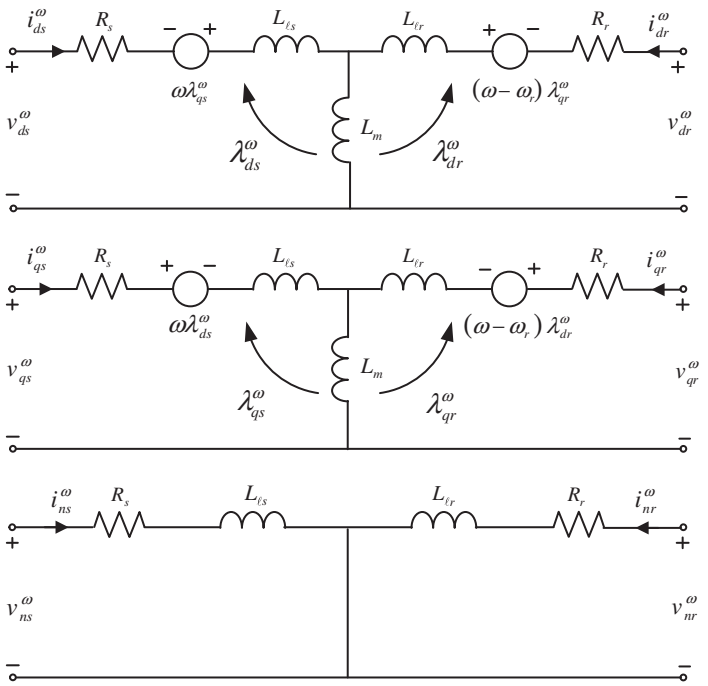


FIGURE 4.26

d–q axes equivalent circuit of an induction motor.

We can obtain voltage and flux linkage equations in the different reference frames by setting $\omega = 0$ for the stationary reference frame, $\omega = \omega_e$ for synchronously rotating reference frame, and $\omega = \omega_r$ for rotor reference frame.

- Stationary reference frame ($\omega = 0$)

$$v^s_{ds} = R_s i^s_{ds} + p\lambda^s_{ds} \qquad \lambda^s_{ds} = L_s i^s_{ds} + L_m i^s_{dr}$$
$$v^s_{qs} = R_s i^s_{qs} + p\lambda^s_{qs} \qquad \lambda^s_{qs} = L_s i^s_{qs} + L_m i^s_{qr}$$
$$0 = R_r i^s_{dr} + p\lambda^s_{dr} + \omega_r \lambda^s_{qr} \qquad \lambda^s_{dr} = L_r i^s_{dr} + L_m i^s_{ds}$$
$$0 = R_r i^s_{qr} + p\lambda^s_{qr} - \omega_r \lambda^s_{dr} \qquad \lambda^s_{qr} = L_r i^s_{qr} + L_m i^s_{qs}$$

- Synchronously rotating reference frame ($\omega = \omega_e$)

$$v^e_{ds} = R_s i^e_{ds} + p\lambda^e_{ds} - \omega_e \lambda^e_{qs} \qquad \lambda^e_{ds} = L_s i^e_{ds} + L_m i^e_{dr}$$
$$v^e_{qs} = R_s i^e_{qs} + p\lambda^e_{qs} + \omega_e \lambda^e_{ds} \qquad \lambda^e_{qs} = L_s i^e_{qs} + L_m i^e_{qr}$$

$$0 = R_r i_{dr}^e + p\lambda_{dr}^e - (\omega_e - \omega_r)\lambda_{qr}^e \qquad \lambda_{dr}^e = L_r i_{dr}^e + L_m i_{ds}^e$$
$$0 = R_r i_{qr}^e + p\lambda_{qr}^e + (\omega_e - \omega_r)\lambda_{dr}^e \qquad \lambda_{qr}^e = L_r i_{qr}^e + L_m i_{qs}^e$$

- Voltage equations of an induction motor in the $d-q$ axes

$$v_{ds}^\omega = R_s i_{ds}^\omega + \frac{d\lambda_{ds}^\omega}{dt} - \omega\lambda_{qs}^\omega$$

$$v_{qs}^\omega = R_s i_{qs}^\omega + \frac{d\lambda_{qs}^\omega}{dt} + \omega\lambda_{ds}^\omega$$

$$v_{ns}^\omega = R_s i_{ns}^\omega + \frac{d\lambda_{ns}^\omega}{dt}$$

$$v_{dr}^\omega = R_r i_{dr}^\omega + \frac{d\lambda_{dr}^\omega}{dt} - (\omega - \omega_r)\lambda_{qr}^\omega$$

$$v_{qr}^\omega = R_r i_{qr}^\omega + \frac{d\lambda_{qr}^\omega}{dt} + (\omega - \omega_r)\lambda_{dr}^\omega$$

$$v_{nr}^\omega = R_r i_{nr}^\omega + \frac{d\lambda_{nr}^\omega}{dt}$$

- Flux linkages of an induction motor in the $d-q$ axes

$$\lambda_{ds}^\omega = L_{ls} i_{ds}^\omega + L_m(i_{ds}^\omega + i_{dr}^\omega) = L_s i_{ds}^\omega + L_m i_{dr}^\omega$$

$$\lambda_{qs}^\omega = L_{ls} i_{qs}^\omega + L_m(i_{qs}^\omega + i_{qr}^\omega) = L_s i_{qs}^\omega + L_m i_{qr}^\omega$$

$$\lambda_{ns}^\omega = L_{ls} i_{ns}^\omega$$

$$\lambda_{dr}^\omega = L_{lr} i_{dr}^\omega + L_m(i_{dr}^\omega + i_{ds}^\omega) = L_r i_{dr}^\omega + L_m i_{ds}^\omega$$

$$\lambda_{qr}^\omega = L_{lr} i_{qr}^\omega + L_m(i_{qr}^\omega + i_{qs}^\omega) = L_r i_{qr}^\omega + L_m i_{qs}^\omega$$

$$\lambda_{nr}^\omega = L_{lr} i_{nr}^\omega$$

4.4.3 TORQUE EQUATION IN THE $d-q$ AXES

As it can be seen in Chapter 1, the torque of double-fed machines such as induction motors is given by

$$T_e = \left(\frac{P}{2}\right)(\boldsymbol{i}_{abcs})^T \frac{\partial \boldsymbol{L}_{sr}}{\partial \theta_r} \boldsymbol{i}_{abcr} \tag{4.95}$$

The transformation of this torque into the $d-q$ axes rotating at an arbitrary speed ω is as follows:

$$\begin{aligned} T_e &= \left(\frac{P}{2}\right)(\boldsymbol{i}_{abcs})^T \frac{\partial \boldsymbol{L}_{sr}}{\partial \theta_r} \boldsymbol{i}_{abcr} \\ &= \left(\frac{P}{2}\right)(T(\theta)^{-1}\boldsymbol{i}^{\omega}_{dqns})^T \frac{\partial \boldsymbol{L}_{sr}}{\partial \theta_r}(T(\beta)^{-1}\boldsymbol{i}^{\omega}_{dqnr}) \\ &= \left(\frac{P}{2}\right)(\boldsymbol{i}^{\omega}_{dqns})^T \left(\frac{3}{2}T(\theta)\frac{\partial \boldsymbol{L}_{sr}}{\partial \theta_r}T(\beta)^{-1}\right)\boldsymbol{i}^{\omega}_{dqnr} \\ &= \left(\frac{P}{2}\right)(\boldsymbol{i}^{\omega}_{dqns})^T \frac{3}{2}\begin{bmatrix} 0 & \frac{3}{2}L_{ms} & 0 \\ -\frac{3}{2}L_{ms} & 0 & 0 \\ 0 & 0 & 0 \end{bmatrix}\boldsymbol{i}^{\omega}_{dqnr} \end{aligned} \tag{4.96}$$

where $\boldsymbol{T}^{-1}(\theta) = \frac{3}{2}\boldsymbol{T}(\theta)^T$.

This torque can be resolved into

$$\therefore \quad T_e = \frac{3}{2}\frac{P}{2}L_m(i^{\omega}_{qs}i^{\omega}_{dr} - i^{\omega}_{ds}i^{\omega}_{qr}) \tag{4.97}$$

where $L_m = \frac{3}{2}L_{ms}$.

The torque can be also expressed in terms of different motor variables but is independent of the speed of the reference frame as following.

$$T_e = \frac{3}{2}\frac{P}{2}L_m \mathrm{Im}\left[i^*_{dqr}i_{dqs}\right] = \frac{3}{2}\frac{P}{2}L_m(i_{qs}i_{dr} - i_{ds}i_{qr}) \tag{4.98}$$

$$= \frac{3}{2}\frac{P}{2}\frac{L_m}{L_r}\mathrm{Im}\left[\lambda^*_{dqr}i_{dqs}\right] = \frac{3}{2}\frac{P}{2}\frac{L_m}{L_r}(\lambda_{dr}i_{qs} - \lambda_{qr}i_{ds}) \tag{4.99}$$

$$= \frac{3}{2}\frac{P}{2}\mathrm{Im}\left[\lambda^*_{dqm}i_{dqs}\right] = \frac{3}{2}\frac{P}{2}(\lambda_{dm}i_{qs} - \lambda_{qm}i_{ds}) \tag{4.100}$$

$$= \frac{3}{2}\frac{P}{2}\mathrm{Im}\left[\lambda^*_{dqs}i_{dqs}\right] = \frac{3}{2}\frac{P}{2}(\lambda_{ds}i_{qs} - \lambda_{qs}i_{ds}) \tag{4.101}$$

$$= \frac{3}{2}\frac{P}{2}\mathrm{Im}\left[i^*_{dqr}\lambda^*_{dqm}\right] = \frac{3}{2}\frac{P}{2}(i_{dr}\lambda_{qm} - i_{qr}\lambda_{dm}) \tag{4.102}$$

$$= \frac{3}{2}\frac{P}{2}\mathrm{Im}\left[i^*_{dqr}\lambda^*_{dqs}\right] = \frac{3}{2}\frac{P}{2}(i_{dr}\lambda_{qr} - i_{qr}\lambda_{dr}) \tag{4.103}$$

$$= \frac{3}{2}\frac{P}{2}\frac{L_m}{L_r}\mathrm{Im}\left[i^*_{dqr}\lambda_{dqs}\right] = \frac{3}{2}\frac{P}{2}\frac{L_m}{L_r}(i_{dr}\lambda_{qs} - i_{qr}\lambda_{ds}) \tag{4.104}$$

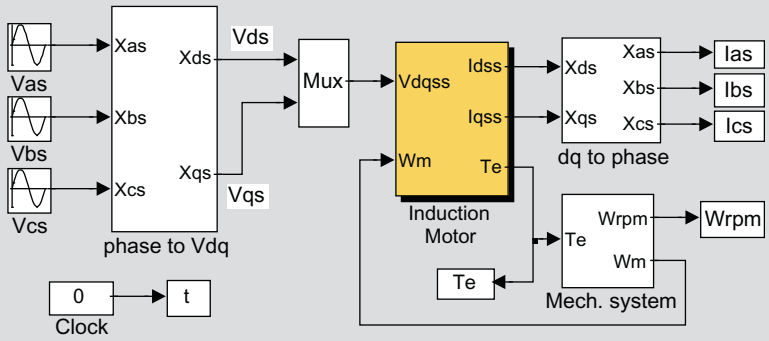
$$= \frac{3}{2}\frac{P}{2}\frac{L_m}{L_\sigma L_r}\mathrm{Im}\left[\lambda^*_{dqr}\lambda_{dqs}\right] = \frac{3}{2}\frac{P}{2}\frac{L_m}{L_\sigma L_r}(\lambda_{dr}\lambda_{qs} - \lambda_{qr}\lambda_{ds}) \tag{4.105}$$

Among these, the torque of Eq. (4.99) is widely used for the vector control, especially the rotor flux oriented control.

MATLAB/SIMULINK SIMULATION: AN INDUCTION MOTOR

With the model of an induction motor in the d–q axes, a 3-hp, 4-pole, 220 V, 60 Hz, three-phase induction motor will be simulated for acceleration characteristics when a full voltage is applied at a standstill.

- Overall diagram for simulation



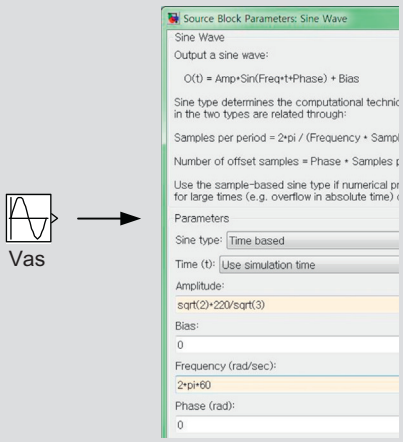
- Applied voltages

$$v_{as} = V_m \cos \omega_e t$$

$$v_{bs} = V_m \cos(\omega_e t - 120^\circ)$$

$$v_{cs} = V_m \cos(\omega_e t - 240^\circ)$$

$$\left(V_m = \sqrt{2}\frac{220}{\sqrt{3}}, \quad \omega_e = 2\pi 60 \right)$$



(*Continued*)

MATLAB/SIMULINK SIMULATION: AN INDUCTION MOTOR (CONTINUED)

- Induction motor $d-q$ equations in the stationary reference frame

$$v_{ds}^s = R_s i_{ds}^s + p\lambda_{ds}^s \rightarrow \lambda_{ds}^s = \int (v_{ds}^s - R_s i_{ds}^s)dt$$

$$v_{qs}^s = R_s i_{qs}^s + p\lambda_{qs}^s \rightarrow \lambda_{qs}^s = \int (v_{qs}^s - R_s i_{qs}^s)dt$$

$$0 = R_r i_{dr}^s + p\lambda_{dr}^s + \omega_r \lambda_{qr}^s \rightarrow \lambda_{dr}^s = \int (-R_r i_{dr}^s - \omega_r \lambda_{qr}^s)dt$$

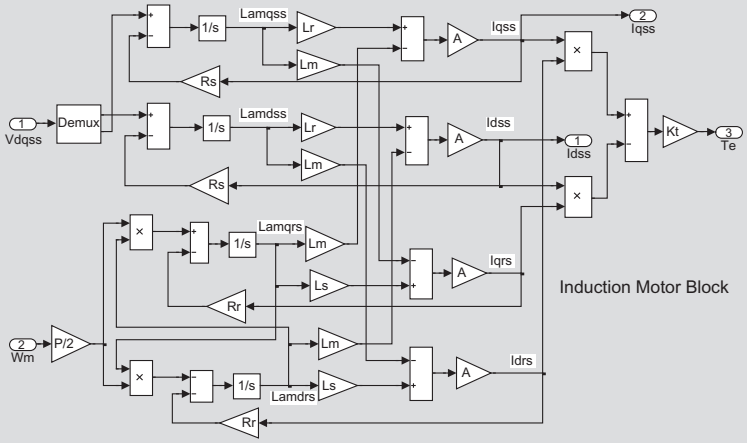
$$0 = R_r i_{qr}^s + p\lambda_{qr}^s - \omega_r \lambda_{dr}^s \rightarrow \lambda_{qr}^s = \int (-R_r i_{qr}^s + \omega_r \lambda_{dr}^s)dt$$

$$i_{ds}^s = \frac{L_r \lambda_{ds}^s - L_m \lambda_{dr}^s}{L_s L_r - L_m^2}, \quad i_{qs}^s = \frac{L_r \lambda_{qs}^s - L_m \lambda_{qr}^s}{L_s L_r - L_m^2}$$

$$i_{dr}^s = \frac{L_s \lambda_{dr}^s - L_m \lambda_{ds}^s}{L_s L_r - L_m^2}, \quad i_{qr}^s = \frac{L_s \lambda_{qr}^s - L_m \lambda_{qs}^s}{L_s L_r - L_m^2}$$

$$T_e = \frac{3}{2}\frac{P}{2} L_m (i_{qs}^s i_{dr}^s - i_{ds}^s i_{qr}^s)$$

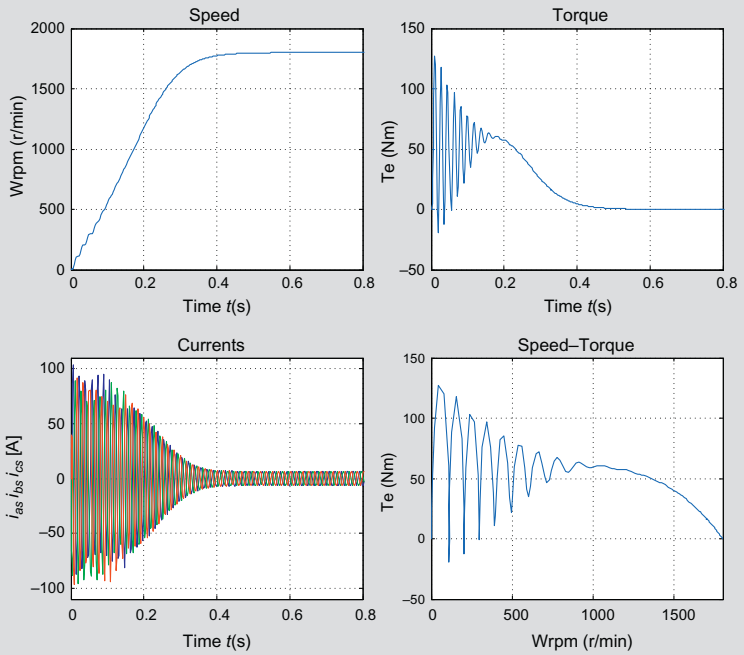
- Induction motor block diagram (Induction Motor Block)



(*Continued*)

MATLAB/SIMULINK SIMULATION: AN INDUCTION MOTOR (CONTINUED)

- Simulation results



At a standstill the input impedance of an induction motor is small and the back-EMF is zero. Thus, when starting with a full voltage, the starting current becomes large, even more than several times the rated value as can be seen the simulation result.

We can see that, from the speed result, the induction motor reaches the final speed without oscillations. However, in the case of higher power induction motors, there may be large overshoots and oscillations in speed and torque. This depends on the parameters of the motor.

4.5 $d-q$ AXES MODEL OF A PERMANENT MAGNET SYNCHRONOUS MOTOR

Now, let us transform the model of an IPMSM expressed as *abc* variables into the $d-q$ coordinate system.

4.5.1 VOLTAGE EQUATIONS IN THE $d-q$ AXES

The stator windings of a PMSM are the same as those of an induction motor. Thus, they can be expressed by the same the $d-q$ axes stator voltage equations, Eqs. (4.83)−(4.85), of an induction motor, and are rewritten as

$$v_{ds}^{\omega} = R_s i_{ds}^{\omega} + \frac{d\lambda_{ds}^{\omega}}{dt} - \omega\lambda_{qs}^{\omega} \tag{4.106}$$

$$v_{qs}^{\omega} = R_s i_{qs}^{\omega} + \frac{d\lambda_{qs}^{\omega}}{dt} + \omega\lambda_{ds}^{\omega} \tag{4.107}$$

$$v_{ns}^{\omega} = R_s i_{ns}^{\omega} + \frac{d\lambda_{ns}^{\omega}}{dt} \tag{4.108}$$

However the flux linkages of a PMSM are different from those of an induction motor. Now, let us find out the flux linkages in the $d-q$ axes required to complete the above voltage equations.

4.5.2 FLUX LINKAGE EQUATIONS IN THE $d-q$ AXES

The transformation of the stator flux linkage of an IMPSM (Eq. 4.47) into the $d-q$ axes rotating at an arbitrary speed ω is as follows:

$$\boldsymbol{\lambda}_{abcs} = \boldsymbol{L}_s \boldsymbol{i}_{abcs} + \boldsymbol{L}_f \boldsymbol{i}_f$$

$$\rightarrow \boldsymbol{T}(\theta)\boldsymbol{\lambda}_{abcs} = \boldsymbol{T}(\theta)\boldsymbol{L}_s \boldsymbol{i}_{abcs} + \boldsymbol{T}(\theta)\boldsymbol{L}_f \boldsymbol{i}_f$$

$$\rightarrow \boldsymbol{\lambda}_{dqns}^{\omega} = \boldsymbol{T}(\theta)\boldsymbol{L}_s(\boldsymbol{T}^{-1}(\theta)\boldsymbol{i}_{dqns}^{\omega}) + \boldsymbol{T}(\theta)\boldsymbol{L}_f \boldsymbol{i}_f$$

Transformations of inductances needed by the above equation are as follows. From the following stator inductance

$$\boldsymbol{L}_s = \begin{bmatrix} L_{ls}+L_A & -\frac{1}{2}L_A & -\frac{1}{2}L_A \\ -\frac{1}{2}L_A & L_{ls}+L_A & -\frac{1}{2}L_A \\ -\frac{1}{2}L_A & -\frac{1}{2}L_A & L_{ls}+L_A \end{bmatrix} - L_B \begin{bmatrix} \cos 2\theta_r & \cos 2(\theta_r - \frac{\pi}{3}) & \cos 2(\theta_r + \frac{\pi}{3}) \\ \cos 2(\theta_r - \frac{\pi}{3}) & \cos 2(\theta_r - \frac{2}{3}\pi) & \cos 2\theta_r \\ \cos 2(\theta_r + \frac{\pi}{3}) & \cos 2\theta_r & \cos 2(\theta_r - \frac{4}{3}\pi) \end{bmatrix}$$

we have

$$\boldsymbol{T}(\theta)\boldsymbol{L}_s\boldsymbol{T}^{-1}(\theta) = \begin{bmatrix} L_{ls}+\frac{3}{2}L_A & 0 & 0 \\ 0 & L_{ls}+\frac{3}{2}L_A & 0 \\ 0 & 0 & L_{ls} \end{bmatrix} + \frac{3}{2}L_B \begin{bmatrix} -\cos 2(\theta-\theta_r) & \sin 2(\theta-\theta_r) & 0 \\ \sin 2(\theta-\theta_r) & \cos 2(\theta-\theta_r) & 0 \\ 0 & 0 & 0 \end{bmatrix}$$

From the inductance

$$\boldsymbol{L}_f = L_{sf}\begin{bmatrix} \cos\theta_r \\ \cos(\theta_r - \frac{2}{3}\pi) \\ \cos(\theta_r - \frac{4}{3}\pi) \end{bmatrix}$$

we have

$$\boldsymbol{T}(\theta)\boldsymbol{L}_f = L_{sf}\begin{bmatrix} \cos(\theta - \theta_r) \\ -\sin(\theta - \theta_r) \\ 0 \end{bmatrix}$$

Thus the stator flux linkage in the $d-q$ axes rotating at an arbitrary speed ω is given as

$$\boldsymbol{\lambda}^{\omega}_{dqs} = \begin{bmatrix} L_{ls} + \frac{3}{2}(L_A - L_B\cos 2(\theta - \theta_r)) & \frac{3}{2}\sin 2(\theta - \theta_r) & 0 \\ \frac{3}{2}\sin 2(\theta - \theta_r) & L_{ls} + \frac{3}{2}(L_A + L_B\cos 2(\theta - \theta_r)) & 0 \\ 0 & 0 & L_{ls} \end{bmatrix} \boldsymbol{i}^{\omega}_{dqs} + \begin{bmatrix} \cos(\theta - \theta_r) \\ -\sin(\theta - \theta_r) \\ 0 \end{bmatrix} \phi_f \tag{4.109}$$

where $\phi_f = L_{sf} i_f$.

By letting $L_{ds} = L_{ls} + \frac{3}{2}(L_A - L_B)$, $L_{qs} = L_{ls} + \frac{3}{2}(L_A + L_B)$, Eq. (4.109) becomes

$$\boldsymbol{\lambda}^{\omega}_{dqs} = \begin{bmatrix} \frac{L_{ds} + L_{qs}}{2} + \frac{L_{ds} - L_{qs}}{2}\cos 2(\theta - \theta_r) & \frac{L_{ds} - L_{qs}}{2}\sin 2(\theta - \theta_r) & 0 \\ \frac{L_{ds} - L_{qs}}{2}\sin 2(\theta - \theta_r) & \frac{L_{ds} + L_{qs}}{2} - \frac{L_{ds} - L_{qs}}{2}\cos 2(\theta - \theta_r) & 0 \\ 0 & 0 & L_{ls} \end{bmatrix} \boldsymbol{i}^{\omega}_{dqs} + \begin{bmatrix} \cos(\theta - \theta_r) \\ -\sin(\theta - \theta_r) \\ 0 \end{bmatrix} \phi_f \tag{4.110}$$

This stator flux linkage can be expressed in the stationary reference frame ($\theta = 0$) as

$$\boldsymbol{\lambda}^{s}_{dqs} = \begin{bmatrix} \frac{L_{ds} + L_{qs}}{2} + \frac{L_{ds} - L_{qs}}{2}\cos 2\theta_r & \frac{L_{ds} - L_{qs}}{2}\sin 2\theta_r & 0 \\ \frac{L_{ds} - L_{qs}}{2}\sin 2\theta_r & \frac{L_{ds} + L_{qs}}{2} - \frac{L_{ds} - L_{qs}}{2}\cos 2\theta_r & 0 \\ 0 & 0 & L_{ls} \end{bmatrix} \boldsymbol{i}^{s}_{dqs} + \begin{bmatrix} \cos\theta_r \\ -\sin\theta_r \\ 0 \end{bmatrix} \phi_f \tag{4.111}$$

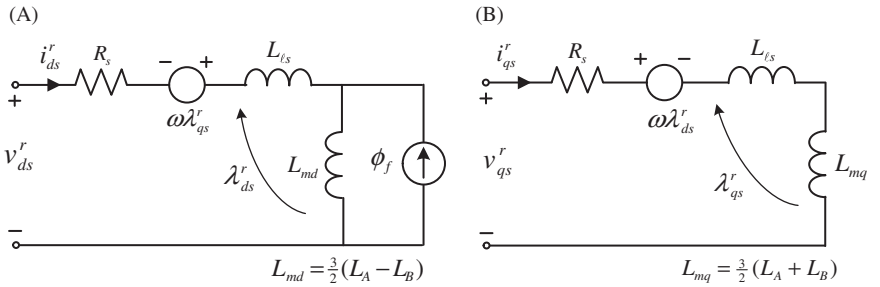


FIGURE 4.27

$d^r - q^r$ axes equivalent circuit of an IPMSM. (A) d^r-axis and (B) q^r-axis.

In this case it is found that there are still time-varying inductances in the flux linkages. Unlike the case of an induction motor, it should be noted that the time-varying inductances of an IPMSM can be eliminated by employing the transformation into only the rotor reference frame ($d^r - q^r$ axes) rotating at the rotation speed ω_r of the rotor. Thus, letting $\theta = \theta_r$ in Eq. (4.110), we have the stator flux linkages with a constant inductance in the rotor reference frame as

$$\boldsymbol{\lambda}^r_{dqn} = \begin{bmatrix} L_{ds} & 0 & 0 \\ 0 & L_{qs} & 0 \\ 0 & 0 & L_{ls} \end{bmatrix} \begin{bmatrix} i^r_{ds} \\ i^r_{qs} \\ i^r_{ns} \end{bmatrix} + \begin{bmatrix} \phi_f \\ 0 \\ 0 \end{bmatrix} \tag{4.112}$$

This can be resolved into

$$\lambda^r_{ds} = L_{ds} i^r_{ds} + \phi_f \tag{4.113}$$

$$\lambda^r_{qs} = L_{qs} i^r_{ds} \tag{4.114}$$

$$\lambda^r_{ns} = L_{ls} i^r_{ns} \tag{4.115}$$

By letting $L_{ds} = L_{qs}$ in the above equations, we can obtain the flux linkages of an SPMSM with a cylindrical rotor. Fig. 4.27 shows the $d^r - q^r$ axes equivalent circuit of an IPMSM.

4.5.3 TORQUE EQUATION IN THE $d-q$ AXES

We can obtain the output torque of an IPMSM from its output power. As we can see from Eq. (4.68), the input power may be expressed in the $d-q$ axes as

$$P_{in} = \frac{3}{2}(v^r_{ds} i^r_{ds} + v^r_{qs} i^r_{qs}) \tag{4.116}$$

By substituting the voltages and flux linkages into Eq. (4.116), we have

$$P_{in} = \frac{3}{2}\left(\left(R_s i_{ds}^r + \frac{d\lambda_{ds}^r}{dt} - \omega_r \lambda_{qs}^r\right) i_{ds}^r - \left(R_s i_{qs}^r + \frac{d\lambda_{qs}^r}{dt} + \omega_r \lambda_{ds}^r\right) i_{qs}^r\right)$$

$$= \frac{3}{2}\left(R_s(i_{ds}^{r2} + i_{qs}^{r2}) + i_{ds}^r \frac{d\lambda_{ds}^r}{dt} + i_{qs}^r \frac{d\lambda_{qs}^r}{dt} + \omega_r \phi_f i_{qs}^r + \omega_r (L_{ds} - L_{qs}) i_{ds}^r i_{qs}^r\right) \quad (4.117)$$

Stator copper losses | Variation of magnetic energy | Mechanical output power P_{out}

The first term on the right-hand side of Eq. (4.117) represents the stator copper losses. The second two terms represent the variation in the magnetic energy. Thus the last two terms represent the mechanical output power that develops the output toque. The output torque is obtained by dividing the output power by the rotor speed ω_r as

$$T_e = \frac{P}{2}\frac{3}{2}\left[\phi_f i_{qs}^r + (L_{ds} - L_{qs}) i_{ds}^r i_{qs}^r\right] \quad (4.118)$$

Magnet torque | Reluctance torque

This equation implies that the developed torque of an IPMSM consists of two components. The first term represents the magnet torque produced by the permanent magnet, and the second term represents the reluctance torque due to a saliency.

For the torque of an SPMSM with a cylindrical rotor, by letting $L_{ds} = L_{qs} = L_s$ in Eq. (4.118), we can obtain

$$T_e = \frac{P}{2}\frac{3}{2}\phi_f i_{qs}^r \quad (4.119)$$

- Voltage and flux linkage equations of an IPMSM in the $d^r - q^r$ axes

$$v_{ds}^r = R_s i_{ds}^r + \frac{d\lambda_{ds}^r}{dt} - \omega_r \lambda_{qs}^r$$

$$v_{qs}^r = R_s i_{qs}^r + \frac{d\lambda_{qs}^r}{dt} + \omega_r \lambda_{ds}^r$$

$$\lambda_{ds}^r = L_{ds} i_{ds}^r + \phi_f$$

$$\lambda_{qs}^r = L_{qs} i_{ds}^r$$

$$T_e = \frac{P}{2}\frac{3}{2}\left[\phi_f i_{qs}^r + (L_{ds} - L_{qs}) i_{ds}^r i_{qs}^r\right]$$

REFERENCES

[1] P.C. Krause, et al., Analysis of Electric Machinery and Drive System, second ed., Wiley-Interscience, New York, NY, 2002.
[2] S. Morimoto, Trend of permanent magnet synchronous machines, IEEJ Trans. Electr. Electron. Eng. 2 (2007) 101–108.
[3] A.M. EL-Refaie, Fractional-slot concentrated-windings synchronous permanent magnet machines: opportunities and challenges, IEEE Trans. Ind. Electron. 57 (1) (2010) 107–121.
[4] F. Magnussen, C. Sadrangani, Winding factors and joule losses of permanent magnet machines with concentrated windings, in: Conf. Rec. IEEE IEMDC'03, 2003, pp. 333–339.
[5] T.J. Woolmer, M.D. McCulloch, Analysis of the yokeless and segmented armature machine, in: Conf. Rec. IEEE IEMDC'07, 2007, pp. 704–708.

CHAPTER

Vector control of alternating current motors

5

The output torque of a motor is the primary control object in motor drive systems. This is because the position or speed of loads can be controlled by controlling the torque of the driving motor. There are two methods of the torque control of alternating current (AC) motors: *average torque control* and *instantaneous torque control*.

The average torque control is a cost-effective variable speed control solution for general-purpose applications, such as fans, blowers, and pump drives, which do not require an accurate speed or torque control. In these applications the main objective for control is the average speed of the motor/load, which is usually regulated by controlling the average torque of the motor. A typical example of the average torque control technique (also called the *scalar control method*) is the constant *V/f* control in the induction motor drives, which was stated in Chapter 3. However, this method can control the motor torque only in the steady-state condition and thus cannot be used to control the dynamic behavior of the motor.

On the other hand, the instantaneous torque control is needed for high-performance applications such as robots, elevators, CNC machine tools, and automation line drives. In these applications a precise speed/torque control and a fast dynamic response are required. To achieve these, it is necessary to control the instantaneous torque of the motor. For direct current (DC) motors, the instantaneous torque control can be readily achieved through the control of the armature current as discussed in Chapter 2. However, for AC motors, a complicated technique called the *vector control method* is required. The *field-oriented control technique* is a typical vector control method. The direct torque control is also another method for the instantaneous torque. This technique is less complicated than the vector control method, but is not as popular.

A scalar control method based on the control of the average current can control the average torque of a motor in the steady-state condition. On the other hand, a vector control method based on the control of both the magnitude and the direction (phase) of the motor current can control its dynamics at the transient condition as well as the torque of a motor in the steady-state condition.

Electric Motor Control. DOI: http://dx.doi.org/10.1016/B978-0-12-812138-2.00005-2
© 2017 Elsevier Inc. All rights reserved.

Hesai Exhibit 1030, page 206

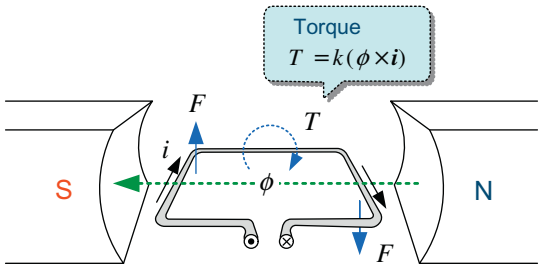


FIGURE 5.1

Torque production in the motor.

In this chapter we will explain the vector control method of AC motors in detail. Prior to this, we need to understand the instantaneous torque. As shown in Fig. 5.1, the instantaneous torque T of a motor is expressed as the cross-product of the magnetic flux vector $\mathbf{\Phi}$ and current vector $\boldsymbol{i}$, and is denoted by

$$T = k(\mathbf{\Phi} \times \boldsymbol{i}) \tag{5.1}$$

$$T = k|\phi||i|\sin\theta \tag{5.2}$$

From this, it can be seen that the instantaneous torque of a motor depends on not only the magnitude of both the magnetic flux and current vectors but also the space angle θ between two vectors. Hence, to control the instantaneous torque, we need to control the directions of the flux and the current as well as their magnitudes. In general, the direction of the current vector is controlled based on the flux vector $\mathbf{\Phi}$. Such method for the instantaneous torque control of AC motors is called *vector control* or *field-oriented control*.

To understand the vector control of AC motors, first, we need to take a close look at the principle of torque production in a separately excited DC motor. This is because the vector control of AC motors imitates the torque control of a separately excited DC motor. A separately excited DC motor has a desirable mechanical structure, which makes it possible to control its instantaneous torque by controlling only its armature current without using any special control technique. Thus a separately excited DC motor can be considered as a role model for the instantaneous torque control of AC motors.

5.1 CONDITIONS FOR INSTANTANEOUS TORQUE CONTROL OF MOTORS

As we discussed in Chapter 2, in DC motors, the field flux ϕ_f is produced by a field winding or a permanent magnet in the stator. Under this field flux, a torque on the conductors of the armature winding carrying the current i_a is produced. A separately excited DC motor has a special mechanical structure, as shown in

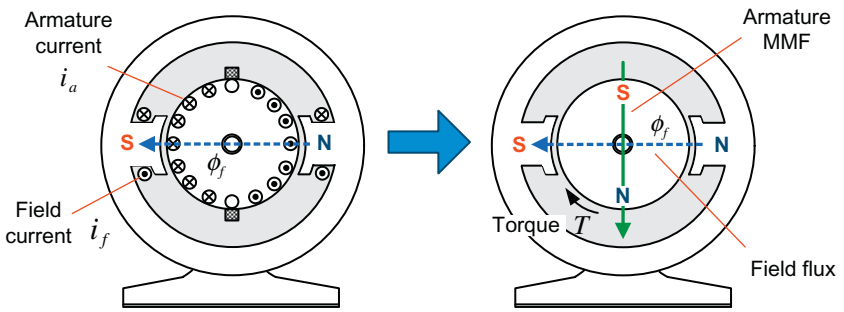


FIGURE 5.2

Separately excited DC motor.

Fig. 5.2, where the direction of the armature current i_a (i.e., magnetomotive force (mmf)) is always 90 electrical degrees with regard to the field flux ϕ_f regardless of rotor rotation.

Like this, since the space angle between the armature current and the field flux always remains at 90 electrical degrees without using any particular control technique, the developed torque can be maximized under a given flux and current. Moreover, as a result of this orthogonality, there is no mutual coupling between the field flux and the armature current, though there is an effect of armature reaction.

In addition, this orthogonality makes the instantaneous torque of Eq. (5.2) for a separately excited DC motor to be expressed simply as

$$T = k|\phi_f||i_a| \tag{5.3}$$

In this condition, if we can control the magnitudes of the field flux and the current independently, the instantaneous torque control will become simpler. When using a permanent magnet or making the field flux constant with a separate DC voltage source, the torque of Eq. (5.3) becomes

$$T = k'|i_a|, \quad k' = k|\phi_f| \tag{5.4}$$

This implies that it is possible to control the instantaneous torque of a DC motor by controlling only the magnitude of the armature current $|i_a|$. If the armature current can be controlled rapidly, the instantaneous torque can also be controlled rapidly to that extent. By using a power electronic converter such as H-bridge circuit with a current controller as stated in Chapter 2, the armature current can be controlled fast enough with a control bandwidth up to several hundred Hertz. Alternatively, we can consider regulating the field flux to control the instantaneous torque under a constant armature current. This, however, may result in a sluggish response and cause a saturation problem. Thus it is desirable to not use the field flux control except in high-speed operations.

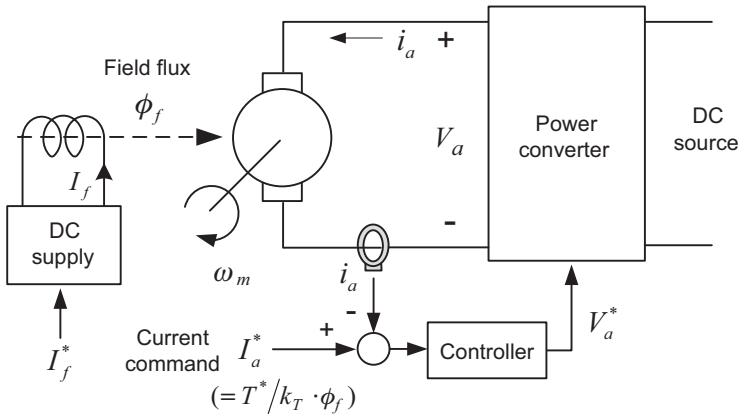


FIGURE 5.3

Torque control system of a DC motor.

On the basis of the analysis stated earlier, we can find out the following requirements for the instantaneous torque control of a DC motor.

The requirements for the instantaneous torque of a DC motor:

1. The space angle between the field flux and the armature current (i.e., mmf) always has to be 90 electrical degrees.
2. Both the field flux and the armature current should be controlled independently.
3. The armature current can be controlled instantaneously.

When the above three requirements are satisfied instantaneously, the instantaneous torque control for a DC motor can be achieved. Separately excited DC motors inherently satisfy the requirements 1 and 2 due to their special mechanical structure. Thus only the requirement 3 remains to be met.

A typical system for the torque control of a DC motor is shown in Fig. 5.3. In such a system, the field flux ϕ_f is usually controlled constantly and the instantaneous torque is controlled by the armature current i_a. The armature current command I_a^* is given from the torque command T_e for driving the load. If the armature current i_a is instantaneously controlled to follow the current command by using a power electronic converter such as H-bridge circuit, the instantaneous torque of the DC motor can follow the command torque.

5.2 VECTOR CONTROL OF AN INDUCTION MOTOR

Even though the output torque of induction motors is not easy to control, it can be controlled instantaneously like DC motors. In induction motors, unlike DC

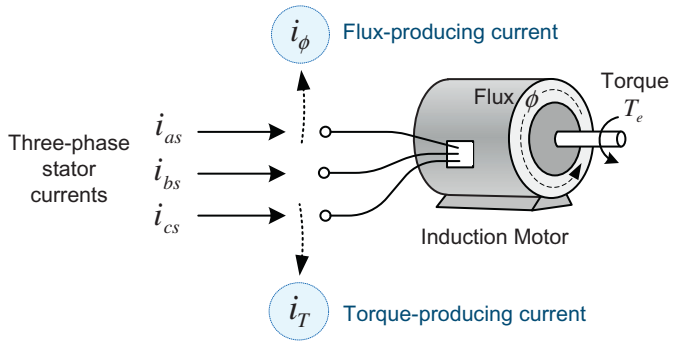


FIGURE 5.4

Currents of an induction motor.

motors, the field flux−producing current and the torque-producing current (equivalent to armature current) are provided all together through the three-phase stator windings as shown in Fig. 5.4.

Therefore it appears that the instantaneous torque control of an induction motor is not as simple as that of a DC motor. The three requirements for controlling the instantaneous torque of a DC motor as mentioned earlier can also be applied to an induction motor as follows:

1. The space angle between the flux-producing current (or the field flux) and the torque-producing current has to be always be 90 degrees.
2. Both the flux-producing current (or the field flux) and the torque-producing current should be controlled independently.
3. The torque-producing current can be controlled instantaneously.

Now we will take a close look at how we can meet these three requirements for the instantaneous torque control of an induction motor.

5.2.1 INSTANTANEOUS TORQUE CONTROL OF AN INDUCTION MOTOR

In an induction motor the currents for producing both the field flux and the torque are provided through the three-phase stator windings. Thus before applying the above three requirements, we first need to know how much the field flux- and torque-producing components are included in the three-phase stator currents i_{as}, i_{bs}, i_{cs}.

This knowledge can be obtained by resolving the three-phase currents into two orthogonal currents, which are utilized as flux-producing current and torque-producing current. This resolution can be easily achieved by using the reference frame transformation as mentioned in Chapter 4. When we transform the

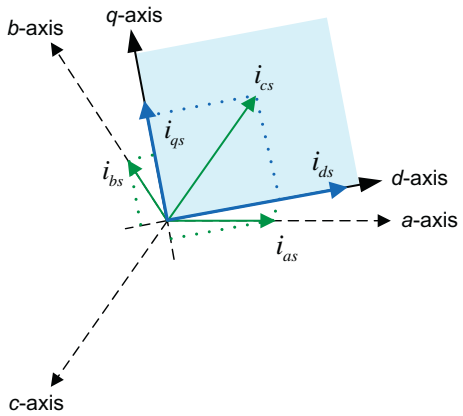


FIGURE 5.5

Reference frame transformation for currents.

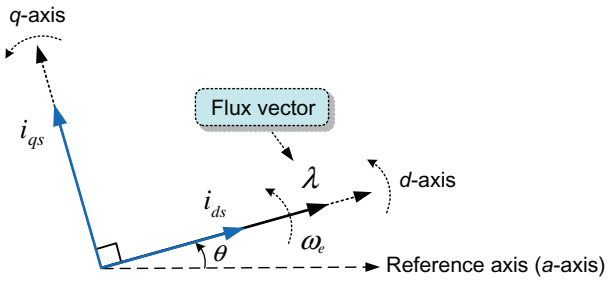


FIGURE 5.6

Assignment of $d-q$ axes based on the flux vector λ.

three-phase *abc* stator currents of an induction motor into the $d-q$ axes currents by using the transformation as shown in Fig. 5.5, we need to designate which of the two currents is the flux- or the torque-producing current. Commonly, the *d*-axis stator current is assigned as the flux-producing current, whereas the *q*-axis stator current is assigned as the torque-producing current. By obtaining these orthogonal currents, the requirement 1 can be fulfilled.

In this case it should be noted that in order for the assigned *d*-axis stator current to become the true flux-producing current, the *d*-axis should be located at the actual position of the flux vector λ in the induction motor as shown in Fig. 5.6.

Here, the flux vector λ in the induction motor is the rotating magnetic field generated by the three-phase currents as mentioned in Chapter 3. Unlike the

stationary field flux of a DC motor, the field flux of an induction motor is rotating at the synchronous speed ω_e corresponding to the supply frequency. Thus we have to use the transformation into the synchronous reference frame rotating at the synchronous speed ω_e. The d-axis will then be located at the actual position of the flux vector. Through this process, the d-axis stator current i_{ds}^e in the synchronous reference frame becomes the true flux-producing current, and then can be used for controlling the magnitude of the flux. This d-axis stator current i_{ds}^e corresponds to the field current of a DC motor.

Moreover, in this case, since the field flux exists only on the d-axis, the torque equation of Eq. (4.99) for an induction motor becomes similar to that of a DC motor as

$$\begin{aligned} T_e &= \frac{3}{2}\frac{P}{2}\frac{L_m}{L_r}(\lambda_{dr}^e i_{qs}^e - \lambda_{qr}^e i_{ds}^e) \\ &= k|\lambda| i_{qs}^e \quad \left(\lambda_{dr}^e = |\lambda|,\ \lambda_{qr}^e = 0,\ k = \frac{3}{2}\frac{P}{2}\frac{L_m}{L_r}\right) \end{aligned} \tag{5.5}$$

The flux used in Eq. (5.5) is assumed to be the flux linkage of the rotor.

In this condition, if the magnitude of the flux vector is kept constant by controlling i_{ds}^e, Eq. (5.5) becomes as

$$T_e = k' i_{qs}^e \quad (k' = k|\lambda|) \tag{5.6}$$

This torque equation is similar to that of a DC motor. We can see easily that the q-axis current acts like the armature current of a DC motor. The torque can be directly controlled by the q-axis current i_{qs}^e, so the q-axis current is considered as the torque-producing current.

There is no cross-coupling between the d-axis stator current (thus, the flux vector) and the q-axis stator current because they are orthogonal to each other. In other words, i_{qs}^e is not influenced by i_{ds}^e and vice versa. Thus the flux-producing current and the torque-producing current can be controlled independently. In this case the magnitude of the flux vector can be controlled independently by the d-axis stator current i_{ds}^e, while the torque can be controlled independently by the q-axis stator current i_{qs}^e. This indicates that the requirement 2 can be fulfilled.

Finally, the torque-producing current can be controlled instantaneously by means of the current regulator as will be described in Chapter 6, and thus the requirement 3 can also be fulfilled. Likewise, through these three processes, the torque of an induction motor can be controlled instantaneously as in the separately excited DC motors.

In summary, to control the instantaneous torque of an induction motor, first, the three-phase stator currents are separated into d- and q-axes stator currents by using the synchronous reference frame transformation in which the d-axis is assigned to the position of the flux vector. Then, the flux can be controlled by

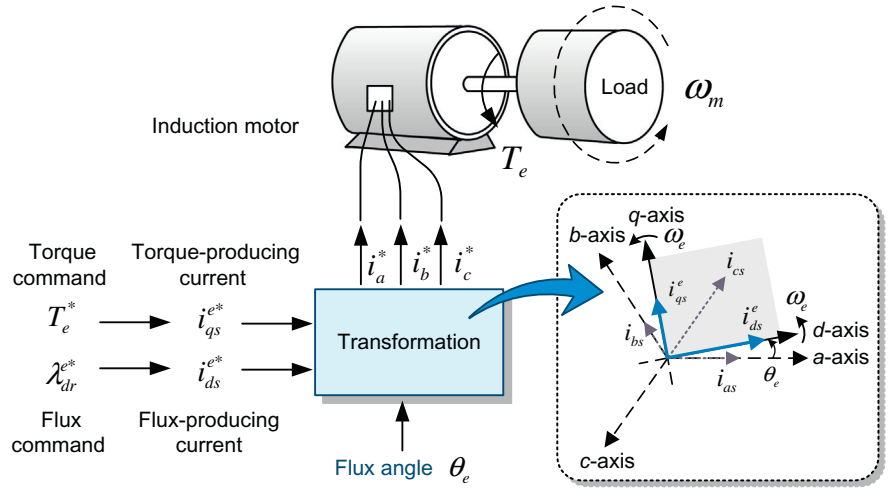


FIGURE 5.7

Instantaneous torque control method of an induction motor.

the d-axis stator current i_{ds}^e while the instantaneous torque can be controlled by the q-axis stator current i_{qs}^e independently. Finally, the instantaneous torque control can be achieved by controlling these currents instantaneously. This instantaneous torque control method for an induction motor is called the *vector control* or *field-oriented control*.

The actual implementation process of the vector control is demonstrated in Fig. 5.7.

In the vector control of an induction motor, the magnitude of the flux remains normally at a constant level of the rated value except for high-speed operations above the rated speed. Based on the rated flux command λ_{ds}^{e*}, the required flux-producing current command i_{ds}^{e*} is calculated. On the other hand, the torque-producing current command i_{qs}^{e*} is calculated based on the output torque command T_e^* required for driving a given load. These command currents i_{ds}^{e*} and i_{qs}^{e*} are given in the synchronous rotating reference frame. Thus we need to obtain the three-phase stator current commands through the inverse transformation into these $d-q$ current commands. Here, it should be noted that this transformation requires the knowledge of the angular position of the flux vector, so called the *flux angle*. Finally, by making the three-phase stator currents of the induction motor to follow these current commands fast enough, the output torque of the induction motor can be controlled to the required torque command T_e^* instantaneously.

5.2.1.1 Important information for vector control: flux angle θ

It was mentioned that for the vector control, we should make the d-axis to be located at the actual position of the flux vector $\boldsymbol{\lambda}$. In an induction motor, this flux

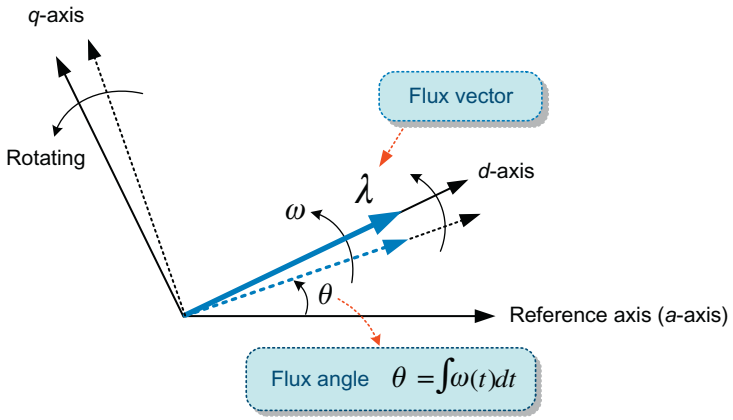


FIGURE 5.8

Rotating flux vector in the $d-q$ axes.

vector $\boldsymbol{\lambda}$ is the rotating magnetic field generated by the three-phase stator currents. Thus the position of the flux vector $\boldsymbol{\lambda}$ varies over time as shown in Fig. 5.8.

Consider that the flux vector $\boldsymbol{\lambda}$ is rotating at a speed ω. In order for the d-axis to be always located at the position of the rotating flux vector $\boldsymbol{\lambda}$, the d-axis should rotate along with the flux vector, i.e., the d-axis has to be moved by the flux angle $\theta\left(=\int \omega(t)dt\right)$, which is the amount of movement of the flux vector. For this purpose, it is necessary to use the synchronous $d-q$ reference frame, which rotates at the same speed as that of the flux vector $\boldsymbol{\lambda}$, i.e., the synchronous speed. Therefore, to accomplish the vector control, the flux angle θ is an inevitable information.

The vector control of an induction motor can be classified into *direct vector control* and *indirect vector control* depending on how the information about the flux angle is obtained. In the direct vector control the flux angle is obtained directly from the flux itself, which can be either measured or estimated. On the other hand, in the indirect vector control, the flux is not used to obtain the flux angle. Instead, it uses the slip angular velocity, which is needed to separate the stator currents into the flux- and the torque-producing currents at the desired values. From this slip angular velocity and the rotor angular velocity, the flux angle can be obtained.

An induction motor has three fluxes available for reference: *stator flux*, *rotor flux*, and *air-gap flux*. The vector control of an induction motor can be classified according to the reference flux as

- Rotor flux−oriented (RFO) control
- Stator flux−oriented (SFO) control
- Air-gap flux−oriented (AFO) control